Volume 31 DECEMBER, 1961 Number 4

FEB 5 1962

Journal of Sedimentary Petrology

A Publication of the Society of Economic Paleontologists and Mineralogists
a Division of
The American Association of Petroleum Geologists

« CONTENTS »

Reef petrography in the Beaverhill Lake Formation, Upper Devonian, Swan Hills area, Alberta, Canada ..... *Albert V. Carozzi* 497
Distinction between dune, beach, and river sands from their textural characteristics ..... *Gerald M. Friedman* 514
Discriminating between refractory and non-refractory quartzite by quantitative petrography ..... *G. V. Wood* 530
Submarine geology of the Santa Rosa-Cortes ridge ..... *E. Uchupi* 534
Phosphatic pebbles from the Brightseat Formation of Maryland ..... *John K. Adams, Johan J. Groot, and N. William Hiller, Jr.* 546
Genesis of primary structures in anhydrite ..... *Charles M. Riley and John V. Byrne* 553
Colloid phenomena in sedimentation of argillaceous rocks ..... *W. Arthur White* 560
Mechanical analysis and heavy minerals, Morrison and Cloverly formations, southern Big Horn Mountains, Wyoming ..... *Arthur Mirsky* 571
Post-Sangamonian (?) calcareous spring deposits, Wellsville area, Colorado ..... *C. C. Reeves, Jr.* 586
Genetic relationship among Tertiary blue sandstones in central California ..... *J. F. Lerbekmo* 594
Backset beds in the Coso Formation, Inyo County, California .. *W. Robert Power, Jr.* 603

NOTES

Note on measurement of grain size in Phi units ..... *G. C. Grender* 608
A simple drilling tool for orienting cores at shallow depth ..... *Carlton R. Johnson and Othar M. Kiel* 609
Regenerated anhydrite redefined ..... *Marcus I. Goldman* 611
Comments on Teodorovich's "Structural classification of limestones and dolomites" and Shvetsov's "Genetic classification of limestones" ..... *Harold J. Bissell and George V. Chilingar* 611
Axiometer—a mechanical device for locating and measuring pebble and cobble axes for macrofabric studies .... *Henry R. Schmoll and Richard H. Bennett* 617
Method of solution of calcareous materials using the complexing agent, EDTA ..... *Everett D. Glover* 622
Occurrence of *Rangia cuneata* Gray and *Crassostrea virginica* (Gmelin) in Sabine Lake, Texas-Louisiana ..... *Henry E. Kane* 627
The free-corer: sediment sampling without wire and winch ..... *David G. Moore* 627
Field method for sieve analysis of sand ..... *Emanuel Azmon* 631
Clay and peat boulders ..... *William F. Tanner* 634

EVIEWS 637

NDEX TO VOLUME 31 641

NOTICE OF PAGE CHARGE AUTHORIZATION

The editor wishes to call to the attention of prospective authors a ruling by the S.E.P.M. council authorizing the application of page charges to articles offered for publication in the *Journal of Sedimentary Petrology*. Application of the charges is left to the judgment of the editor and will be applied at the rate of $20.00 per page.

Charges will be applied to manuscripts considered excessive in length or of a nature requiring special treatment. In addition, authors of articles that have been supported by grants that include funds for publication costs, or whose organizations are in a position to pay page charges, will be asked to subsidize publication of their articles to the degree that their funds allow. Authors are further urged to include allowances for publication costs in any future grant proposals.

Inability to pay assessed charges will in no way prejudice publication of an article, but authors are reminded that publication delays of prohibitive length lie in the near future if the size of the *Journal* cannot be increased through subsidies.

Lewis M. Cline

Editor

Journal of Sedimentary Petrology

A Publication of the Society of Economic Paleontologists and Mineralogists
a Division of
The American Association of Petroleum Geologists

EDITOR

LEWIS M. CLINE, University of Wisconsin, Madison, Wisconsin.

MANAGING EDITOR

DONALD B MACURDA, JR., University of Wisconsin, Madison, Wisconsin.

ASSOCIATE EDITORS

STURGES W. BAILEY, University of Wisconsin, Madison, Wisconsin
ROBERT N. GINSBURG, Shell Development Company, Coral Gables, Florida
RALPH E. GRIM, University of Illinois, Urbana, Illinois
K. JINGHWA HSU, Shell Development Company, Houston, Texas
WILLIAM C. KRUMBEIN, Northwestern University, Evanston, Illinois
HEINZ A. LOWENSTAM, California Institute of Technology, Pasadena, California
JOHN SANDERS, Yale University, New Haven, Connecticut
RAYMOND SIEVER, Harvard University, Cambridge, Massachusetts
THEODORE R. WALKER, University of Colorado, Boulder, Colorado

The *Journal of Sedimentary Petrology* is published in March, June, September, and December of each year.

Annual membership dues of the Society of Economic Paleontologists and Mineralogists are as follows:

including the Journal of Sedimentary Petrology	$ 7.00
including the Journal of Paleontology	10.00
including both journals	17.00

The subscription prices of the journals, to non-members of the Society, are as follows:

Journal of Sedimentary Petrology	$11.00
Journal of Paleontology	15.00

Postage is included in these prices, for all addresses in the United States. An additional charge of 40 cents on annual subscriptions is made for addresses in all other countries.

The price of single numbers of the *Journal of Sedimentary Petrology* is $1.50 to members and $3.00 to non-members of the Society.

Communications about *Journal* subscriptions, rates, memberships, change of address, and non-receipt of preceding number should be addressed to Society of Economic Paleontologists, and Mineralogists, P.O. Box 979, Tulsa, Oklahoma. Claims for non-receipt of preceding numbers must be sent in within three months of the date of publication in order to be filled gratis.

Communications regarding manuscripts and purely editorial matters should be addressed to The Editor, *Journal of Sedimentary Petrology*, Department of Geology, University of Wisconsin, Madison, Wisconsin.

NOTICE

Articles submitted for publication in the *Journal of Sedimentary Petrology* should be original pages, typewritten double-spaced on 8½ by 11-inch white paper. A prefatory abstract is required for all papers, exclusive of short notes and discussions. The mechanical details of the manuscript should conform with usage in recent issues of the *Journal*, particularly in regard to capitalization and citation of references. Tables and illustrations should be separate from the text, and originals of illustrations are preferred. Detailed instructions and suggestions are given in the March, 1958 issue of the *Journal* (v. 28, p. 102–107).

Second-class postage paid at MENASHA, WISCONSIN, and at additional mailing office.

GEORGE BANTA COMPANY, INC., MENASHA, WISCONSIN
PRINTED IN THE U.S.A.

SOCIETY OF ECONOMIC PALEONTOLOGISTS AND MINERALOGISTS

A Division of
The American Association of Petroleum Geologists

OFFICERS FOR THE YEAR ENDING MARCH, 1962

President: L. L. Sloss, Evanston, Illinois.
Past-President: William M. Furnish, Jr., Iowa City, Iowa.
Vice-President: Kenneth E. Lohman, Washington, D. C.
Secretary-Treasurer: Lloyd C. Pray, Littleton, Colorado.
Councilor (Paleontology): Lyman D. Toulmin, Tallahassee, Florida.
Councilor (Mineralogy): Albert L. Kidwell, Tulsa, Oklahoma.
Co-Editors, Journal of Paleontology: M. L. Thompson and C. W. Collinson, Urbana, Illinois.
Editor, Journal of Sedimentary Petrology: Lewis M. Cline, Madison, Wisconsin.

The foregoing officers constitute the Council of the Society.

REPRESENTATIVES AND COMMITTEES

REPRESENTATIVE TO NATIONAL RESEARCH COUNCIL
John C. Frye (for the term ending 1964)

REPRESENTATIVES ON BOARD OF DIRECTORS OF THE AMERICAN GEOLOGICAL INSTITUTE
William M. Furnish, Jr., Senior Representative
L. L. Sloss, Junior Representative

REPRESENTATIVE TO THE GOVERNMENT RELATIONS COMMITTEE OF THE AMERICAN GEOLOGICAL INSTITUTE
Norman S. Hinchey

REPRESENTATIVES TO AMERICAN ASSOCIATION FOR THE ADVANCEMENT OF SCIENCE
Francis J. Pettijohn (for term ending 1962)
W. D. Keller (for the term ending 1964)

EDITOR, TREATISE ON INVERTEBRATE PALEONTOLOGY
Raymond C. Moore

S.E.P.M. VICE-CHAIRMAN FOR 1962 SAN FRANCISCO CONVENTION
William F. Barbat

RESEARCH COMMITTEE

R. N. Ginsburg 62	A. T. Cross (Chairman) 63	J. M. Forgotson, Jr. 64
H. N. Frenzel 62	D. J. McLaren 63	W. K. Hamblin 64
M. L. Natland 62	F. J. Beales 63	E. H. Rainwater 64
E. J. Guzman 62	J. M. Schopf 63	Gene A. Rusnak 64
John L. Wray 62	B. H. Burma 63	John Sanders (V. Chairman) 64

NOMINATING COMMITTEE

A. Rodger Denison (Chairman)	W. C. Krumbein
Marcus A. Hanna	R. Dana Russell
John C. Hazzard	

PUBLICATIONS COMMITTEE

Jack L. Hough (Chairman) 63	W. Frank Scott 62
Bob Perkins 63	Weldon Rau 62
A. T. Cross 62	

MEMBERSHIP COMMITTEE

Lyman D. Toulmin 62	A. L. Kidwell 62

COMMITTEE TO SELECT BEST PAPER AT 1961 DENVER CONVENTION

F. W. Cropp (Chairman)	Richard L. Jodry
R. L. Batten	W. B. N. Berry
John B. Droste	C. H. Summerson

PACIFIC SECTION S.E.P.M. OFFICERS (1961–1962)

President: Joseph J. Graham, Stanford, California
Vice-President: Richard Pierce, Bakersfield, California
Secretary-Treasurer: Keith Berry, Oildale, California

GULF COAST SECTION S.E.P.M. OFFICERS (1961–1962)

President: H. V. Andersen, Baton Rouge, Louisiana
Vice-President: Theodore D. Cook, Corpus Christi, Texas
Secretary: Ben J. Petrusek, Houston, Texas
Treasurer: A. D. Warren, Bellaire, Texas

PERMIAN BASIN SECTION S.E.P.M. OFFICERS (1961–1962)

President protem: Richard D. Jons
Second Vice-President: Leo Hendricks, Fort Worth, Tex.
Secretary: Kenneth R. Etter, Midland, Tex.
Treasurer: David S. Holland, Midland, Tex.

Volume 31 DECEMBER, 1961 Number 4

Journal of Sedimentary Petrology

A Publication of the Society of Economic Paleontologists and Mineralogists
a Division of
The American Association of Petroleum Geologists

CONTENTS

Reef petrography in the Beaverhill Lake Formation, Upper Devonian, Swan Hills area, Alberta, Canada ... *Albert V. Carozzi* 497
Distinction between dune, beach, and river sands from their textural characteristics ... *Gerald M. Friedman* 514
Discriminating between refractory and non-refractory quartzite by quantitative petrography ... *G. V. Wood* 530
Submarine geology of the Santa Rosa-Cortes ridge ... *E. Uchupi* 534
Phosphatic pebbles from the Brightseat Formation of Maryland ... *John K. Adams, Johan J. Groot, and N. William Hiller, Jr.* 546
Genesis of primary structures in anhydrite ... *Charles M. Riley and John V. Byrne* 553
Colloid phenomena in sedimentation of argillaceous rocks ... *W. Arthur White* 560
Mechanical analysis and heavy minerals, Morrison and Cloverly formations, southern Big Horn Mountains, Wyoming ... *Arthur Mirsky* 571
Post-Sangamonian (?) calcareous spring deposits, Wellsville area, Colorado ... *C. C. Reeves, Jr.* 586
Genetic relationship among Tertiary blue sandstones in central California ... *J. F. Lerbekmo* 594
Backset beds in the Coso Formation, Inyo County, California ... *W. Robert Power, Jr.* 603

NOTES

Note on measurement of grain size in Phi units ... *G. C. Grender* 608
A simple drilling tool for orienting cores at shallow depth ... *Carlton R. Johnson and Othar M. Kiel* 609
Regenerated anhydrite redefined ... *Marcus I. Goldman* 611
Comments on Teodorovich's "Structural Classification of limestones and dolomites" and Shvetsov's "Genetic classification of limestones" ... *Harold J. Bissell and George V. Chilingar* 611
Axiometer—a mechanical device for locating and measuring pebble and cobble axes for macrofabric studies ... *Henry R. Schmoll and Richard H. Bennett* 617
Method of solution of calcareous materials using the complexing agent, EDTA ... *Everett D. Glover* 622
Occurrence of *Rangia cuneata* Gray and *Crassostrea virginica* (Gmelin) in Sabine Lake, Texas-Louisiana ... *Henry E. Kane* 627
The free-corer: sediment sampling without wire and winch ... *David G. Moore* 627
Field method for sieve analysis of sand ... *Emanuel Azmon* 631
Clay and peat boulders ... *William F. Tanner* 634

REVIEWS ... 637
INDEX TO VOLUME 31 ... 641

PAPERS IN PRESS FOR FORTHCOMING ISSUES

Plant-baffle entrapment as an origin for Mississippian bioherms. By Arthur R. Troell, Jr.

Primary structures produced by tadpoles. By Stuart W. Maher.

A quick field or laboratory staining scheme for the differentiation of the major carbonate minerals. By S. St. J. Warne.

Petrography of Mississippian (Borden) crinoidal limestones at Stobo, Indiana. By Albert V. Carozzi and J. G. Soderman.

Detrital dolomite in central Texas. By David L. Amsbury.

The Runn of Cutch. By Lucian B. Platt.

Determination of surface areas of sediments. By F. Conrad Greer, Carrol M. Beeson, Richard Main, and George V. Chilingar.

Possible loss of magnesium from fossils to the surrounding sediments. By George V. Chilingar.

Flysch and associated beds of the Martinsburg Formation (Ordovician), central Appalachians. By Earle F. McBride.

Petrology of some Pennsylvanian sedimentary rocks. By John C. Ferm.

Quantitative petrographic study of Paleozoic carbonate rocks, Caballo Mountains, New Mexico. By Karl W. Stauffer.

A squeezer for extracting interstitial water from modern sediments. By Raymond Siever.

Laminites: a structure of flysch-type sediments. By Augustin Lombard.

Computing mineral compositions of sedimentary rocks from their chemical analyses. By A. T. Miesch.

Comparison of moment measures for sieving and thin-section data in sedimentary petrological studies. By Gerald M. Friedman.

Electron microscopy of sand surface texture. By John P. Porter.

Distinction of shoreline environments in New Jersey. By Edwin W. Biederman, Jr.

X-Ray techniques for study of structures in homogeneous sediments. By Wm. Kenneth Hamblin.

Cyclic deposits in the Cretaceous Ocozocuautla Formation of central Chiapas, Mexico. By H. G. Richards.

High-angle beach stratification, Sapelo Island, Georgia. By John H. Hoyt.

Observations on slickolites. By Matthew H. Nitecki.

Zircon-tourmaline-rutile heavy mineral maturity index for sandstones. By John F. Hubert.

JOURNAL OF SEDIMENTARY PETROLOGY, VOL. 31, No. 4, pp. 497–513
FIGS. 1–9, DECEMBER, 1961

REEF PETROGRAPHY IN THE BEAVERHILL LAKE FORMATION, UPPER DEVONIAN, SWAN HILLS AREA, ALBERTA, CANADA[1]

ALBERT V. CAROZZI
University of Illinois, Urbana, Illinois

ABSTRACT

Statistical measurements of organic and inorganic parameters in thin sections reveal that the Swan Hills Member of the Beaverhill Lake Formation in the Shell Swan Hills 10–17 well is made up by the rhythmical alternation of eight carbonate microfacies. These rock-types are closely related and interpreted as a continuous sequence representing fore-reef, reef and back-reef conditions. The fore-reef environment shows dark-colored calcarenites whereas the reef itself consists of dark-colored bio-constructed limestones made up by cabbage-type stromatoporoids followed in shallower water by branching colonies of *Amphipora*. With these two organically constructed deposits are associated several types of biocalcarenites. The back-reef environment is represented by light-colored calcilutites containing scattered colonies of *Amphipora* and of mat-type stromatoporoids.

The vertical superposition of these microfacies displays seven rhythms of sedimentation during which an *Amphipora*-stromatoporoid reef community was established over a carbonate platform, developed and eventually disappeared. The rhythms seem to correspond to tectonically controlled phases of depth decrease.

INTRODUCTION

The object of the present investigation has been the petrographic description and environmental interpretation of the microfacies forming the Swan Hills Member of the Beaverhill Lake Formation in the Shell Swan Hills 10–17 well located in Twp. 64, Rge 13W 5th.

In the investigated locality, the Beaverhill Lake Formation has a thickness of 473 ft of which 438 ft were cored from the contact with the Middle Devonian Elk Point Formation upward through a large development of the Swan Hills Member as defined by Fong (1960), which here seems to occupy almost the entire Beaverhill Lake interval. In these organically constructed limestones and associated bioclastics 400 thin sections approximately at 1-ft intervals have been investigated with a total number of about 7000 statistical measurements. In spite of the fact that a fairly detailed knowledge has been obtained along a vertical line, the horizontal characteristics of these reef build-ups are not well established, and their paleogeographic relations are still under discussion (Andrichuk, 1958 a,b; Edie, 1959; Illing, 1959).

[1] Manuscript received August 15, 1960.

METHOD OF INVESTIGATION

The author's method (Carozzi, 1950, 1958) can be designated as a statistical investigation of the microscopic components of carbonate rocks. It is based on the measurements of the apparent maximum grain size (or clasticity index) and of the frequency of the detrital components. These values are expressed as curves of variation drawn alongside the stratigraphic column and interpreted on the basis of their relations to the frequencies of benthonic and pelagic microfaunas. After completion of all the measurements, average values for the different parameters are computed for each of the microfacies distinguished in the investigated section. These average values appear characteristic to a varying degree of each of the microfacies and allow their classification acccording to a relative bathymetrical scale. Such a scale is used as a basis for drawing the relative bathymetrical curve which indicates the successive changes of depth which took place at the location of the investigated section. The relative bathymetrical curve is always located at the extreme right of the diagrams; it shows depth decrease from left to right and represents the final interpretation.

Curves of "main trend" (fig. 5 to 7) are presented here for the first time. Their func-

tion is to express the general evolution of the variation curve of a given parameter; this is particularly useful whenever the local fluctuations complicate the overall picture. The curves of main trend are of pure interpretative nature in contrast to the variation curves which express graphically the measurements of the microscopic parameters.

APPLICATION OF METHOD TO BEAVERHILL LAKE FORMATION

The term "reef" and related adjectives will be used in the discussion of the environment of deposition of the Beaverhill Lake Formation as a convenient designation for emphasizing the fact that constructive organisms such as stromatoporoids and *Amphipora* played a predominant role in the sedimentation.

In such a reef environment, detrital minerals are absent with the exception of the shale breaks R2 and R3 which display some angular grains of detrital quartz. The agitation and depth variations of this environment can nevertheless be expressed by measuring the maximum apparent grain size of the inorganic pellets of cryptocrystalline calcite. The measurements must be restricted to pellets entirely devoid of any organic fragments because the presence of the latter affects their size to a high degree. Such a value may be called *index of general clasticity*. It has the same significance as the clasticity of any detrital mineral grains as demonstrated in cases where quartz grains and pellets are associated (Carozzi, 1958).

Under reef conditions the organic growths of all sorts introduce numerous factors of perturbation in the distribution of detrital particles in relation to depth. In other words, it is expected that sometimes depth conditions will be expressed more by ecological relations of benthonic organisms than by the absolute values of the index of general clasticity. For instance, along channels protected by irregular ridges of stromatoporoids, the detrital particles may grade very quickly from calcarenites to calcilutites under practically similar depth conditions. In the present investigation, the following organic parameters have been computed:

Benthonic components.—The frequency of stromatoporoids, *Amphipora*, and bryozoans has been determined over a thin section surface of 450 mm². The frequency of gastropods, brachiopods, and pelecypods (grouped together because of frequent lack of internal structure caused by recrystallization) has not been determined by actual counting but by a visual estimation resulting from the combination of binocular core description and thin section observation. This combination was necessary because most of these organisms are of megascopic character and also because the effect of fragmentation would increase frequency values in an erroneous way.

Presence or absence has been reported for accessory components such as sponge spicules, Dasycladaceae, arenaceous foraminifera, solitary corals, crinoids, and *Chara* stems which are not present in sufficient number to allow statistical measurements.

Pelagic components.—The frequency of ostracods and calcispheres has been determined over a thin section surface of 60 mm². It may be pointed out that the ostracods were originally benthonic elements but their tests have been floated by the currents and hence their behavior becomes that of pelagic components.

DESCRIPTION OF THE MICROFACIES

Eight microfacies form by their rhythmic alternations the investigated sequence. Five of them are basic types and three subtypes which may be missing locally. To this succession of eight carbonate microfacies must be added an argillaceous one forming the shale breaks R2 and R3.

Microfacies 1 (*fig. 1 A*).—It is a dark to light-colored medium-grained calcarenite with a well-developed secondary cement of largely crystallized anhedral calcite. The abundant pellets have an average size of 0.494 mm; they are sub-rounded to well rounded and fairly well sorted locally. The pellets, which may be of accretionary origin, are predominantly composed of structureless cryptocrystalline calcite stained brown by bituminous matters and pyrite pigments. A few pellets contain fragments of smooth ostracods, echinoderms, and calcispheres. The recrystallization of the cement is demonstrated by indented pellets and residual ghost structures; however, the largely crystallized calcite may contain some per-

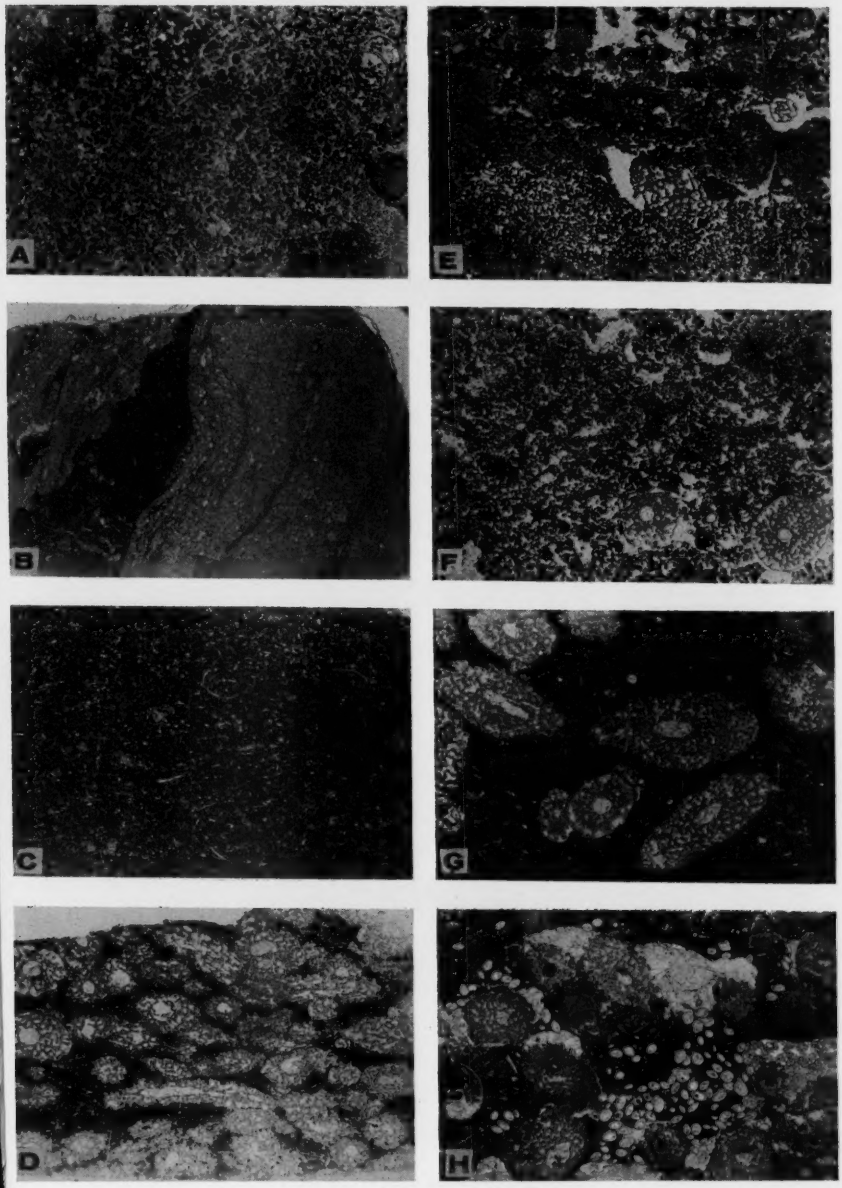

FIG. 1.—Typical microfacies of the Beaverhill Lake Formation, Nicols not crossed, ×3. A: microfacies 1; B: microfacies 2; C: microfacies 2a; D: microfacies 3; E: microfacies 3a; F: microfacies 4; G: microfacies 4a; H: microfacies 5.

fectly preserved ostracod and gastropod tests. In some instances, the pellets appear to be surrounded by a thin layer of fibro-radiated calcite simulating a superficial oolite texture. Such a layer, however, may join several pellets to one another, indicating that it is a form of recrystallization of the cement.

Microfacies 2 (*fig. 1 B*).—It is a dark-colored stromatoporoid-constructed limestone with an interstitial fine-grained matrix of calcarenite. The organic framework consists predominantly of cabbage-type stromatoporoids with which are associated a few *Amphipora*. The interstitial calcarenitic matrix is made up of unsorted particles reaching an average grain-size of 0.185 mm which are predominantly angular fragments of stromatoporoids and *Amphipora* associated with a few reciprocally deformed pellets of dark cryptocrystalline calcite. Large zones of the organic framework may be recrystallized in a calcite mosaic. Dark stylolitic zones are concentrated along the boundaries between cabbages and the interstitial matrix.

Microfacies 2a (*fig. 1 C*).—It is a dark-colored fine-grained and unsorted calcarenite with a very reduced amount of detrital matrix. The average diameter of the particles is 0.225 mm. The particles are either angular fragments of stromatoporoids or subrounded pellets of cryptocrystalline calcite, closely packed and reciprocally deformed. Calcispheres are very abundant and a few broken ostracod tests may be noticed locally. The thin stylolitic zones display concentrations of bituminous matter and pyrite.

Microfacies 3 (*fig. 1 D*).—It is a dark-colored *Amphipora*-constructed limestone with an interstitial medium-grained matrix of calcarenite. The organic framework consists predominantly of branching types of *Amphipora* either complete or broken and oriented parallel to the bedding; their internal cavities and interstitial areas appear almost always filled by secondary calcite. The calcarenitic matrix consists of unsorted to incipiently sorted particles which have an average size of 0.307 mm. The particles are either angular fragments of *Amphipora* or subrounded to irregular pellets of cryptocrystalline calcite deeply stained by bituminous matters and pyrite pigments; local concentrations of calcispheres may be noticed. Numerous stylolites are present along the boundaries between the matrix and the *Amphipora* fragments and also between the different components of the matrix itself.

Microfacies 3a (*fig. 1 E*).—It is a dark to light-colored, coarse-grained calcarenite with a moderate amount of fine-grained matrix locally recrystallized in clear secondary calcite. The constituting particles, unsorted to slightly sorted, have an average grain size of 0.540 mm and are predominantly irregular to subrounded pellets of cryptocrystalline calcite. Scattered among them are larger fragments of *Amphipora* and concentrations of calcispheres.

Microfacies 4 (*fig. 1 F*).—It is a light colored, very coarse-grained calcarenite with a matrix largely recrystallized in clear secondary calcite. The constituting particles, which have an average size of 1.680 mm, appear unsorted to moderately sorted but in an irregular fashion. They consist again of *Amphipora* fragments and irregular to subrounded pellets of cryptocrystalline calcite. Among these particles are scattered numerous larger fragments of branching *Amphipora* filled with secondary calcite.

Microfacies 4a (*fig. 1 G*).—It is a light colored, medium-grained calcarenite with a very reduced amount of matrix. The constituting particles, which have an average size of 0.387 mm, appear unsorted to moderately sorted but in an irregular manner. They consist of *Amphipora* fragments and irregular to subrounded pellets of cryptocrystalline calcite. Among these particles are scattered numerous larger fragments of branching *Amphipora* filled with secondary calcite as well as concentrations of calcispheres and ostracod tests.

Microfacies 5 (*fig. 1 H*).—It is a light colored, very fine-grained calcarenite to calcilutite with the average diameter of the particles ranging from 0.104 mm to beneath the resolution power of the petrographic microscope. In the calcarenitic zones, angular organic fragments are associated with very small and well-rounded pellets of cryptocrystalline calcite which may be of faecal and algal origin. In the calcilutitic matrix are scattered large fragments of *Amphipora* and abundant mat-type colonies of stroma-

toporoids. Gastropods and local concentrations of entire shells of smooth ostracods, sponge spicules, and calcispheres may be noticed. Appreciable surfaces of the thin sections appear as mosaics of coarsely crystalline clear calcite of secondary origin; the latter replaces also organic fragments and fills original cavities between branching *Amphipora* and stromatoporoidal mats.

Table 1 summarizes the essential characteristics of the eight microfacies. Their identity is demonstrated not only by the organic parameters but also by their average values of the index of general clasticity which are remarkably characteristic for a reef environment where local anomalies are to be expected (fig. 2).

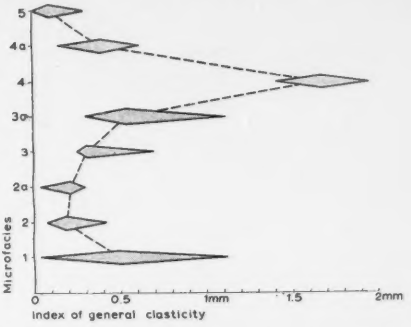

FIG. 2.—Position of maxima and range of variation of the index of general clasticity in the succession of microfacies.

VERTICAL SUCCESSION OF THE MICROFACIES

The succession of the eight microfacies described above corresponds to an ideal sequence expressing a gradual shallowing of the environment of deposition. Such a succession has been indeed almost perfectly realized between 9884.5 and 10,001.5 ft. The variation of its microscopic parameters will now be described as a key for the interpreta-

TABLE 1.—*Characteristic parameter values of microfacies*

Microfacies	Average Index of General Clasticity in mm	Variation Range of Index of General Clasticity in mm	Freq. Strom.	Freq. Amphip.	Freq. Bryoz.	Freq. Brah. & Pelec.	Freq. Gast.	Freq. Ostracods	Freq. Calcispheres
5	0.104	0.310–0.010	20	10	0	rare	common to abundant	100	375
4a	0.387	0.630–0.165	15	15	0	rare	rare to common	50	300
4	1.680	1.950–1.410	10	17	0	rare	rare	25	250
3a	0.540	1.125–0.310	5	20	0	rare	0 to rare	10	200
3	0.307	0.690–0.255	5	35	0	rare	0	2	50
2a	0.225	0.300–0.045	15	20	0	rare	0 to rare	25	500
2	0.185	0.420–0.075	25	10	0	rare to common	0 to rare	35	300
1	0.494	1.120–0.040	5	3	23	common to abundant	rare	60	100

tion of the entire Beaverhill Lake Formation. Here will be only a description of the pattern of evolution of the curves, reserving the main interpretation for the discussion of the horizontal juxtaposition of the microfacies.

During the vertical superposition of microfacies 1 to 5, through 2, 2a, 3, 3a, 4 and 4a, the following features appear characteristic (fig. 3).

The index of general clasticity starts with a medium value in microfacies 1 and decreases to a first minimum in microfacies 2. The index then gradually increases upward until its maximum in microfacies 4; a rapid decrease follows until a second minimum is reached in microfacies 5.

The frequency of the stromatoporoids starts at a minimum in microfacies 1 and increases to its maximum in microfacies 2. It reaches a second minimum zone in microfacies 3 and 3a and then gradually increases toward a medium value in microfacies 5.

The frequency of *Amphipora* begins at a minimum in microfacies 1 and gradually increases to its maximum in microfacies 3. Then a very gradual decrease occurs upward until a medium value is reached in microfacies 5.

The frequency of bryozoans reaches its maximum in the upper portion of microfacies 1 and gradually decreases to zero in microfacies 2.

The frequency of gastropods starts with a medium value in microfacies 1 and decreases through 2 and 2a to almost zero in microfacies 3. It increases again upward until it reaches its maximum in microfacies 5.

The frequency of brachiopods and pelecypods displays its maximum value in microfacies 1. It gradually decreases to its minimum in microfacies 3a and remains constant until microfacies 5.

The frequency of the smooth ostracods begins with a medium value in microfacies 1 and gradually decreases to almost zero in microfacies 3 and 3a. It then increases rapidly to its maximum in microfacies 5.

The frequency of the calcispheres starts with a relatively low value in microfacies 1 and increases rapidly towards its maximum in microfacies 2a. This peak is followed upward by a rapid decrease leading to a minimum in microfacies 3. The frequency then gradually increases to a relatively high and stable value in microfacies 5. The accessory components are represented by floated *Chara* stems which are found in all microfacies; by Dasycladaceae in microfacies 1 to 4a; by arenaceous foraminifera restricted to microfacies 3 and 3a, and by sponge spicules present only in microfacies 5.

The variations of the index of general clasticity and their relations to the behavior of the benthonic and pelagic parameters appear sufficiently characteristic to allow a good prediction of the evolution of the sedimentation when a minimum of two microfacies are investigated statistically in a complete vertical succession as illustrated in figure 3.

HORIZONTAL JUXTAPOSITION OF THE MICROFACIES

The same pattern of evolution which has been described during a shallowing of the environment for a given point and during a certain span of time (fig. 3) applies also when the changes of sedimentation are studied laterally during an instant of time (fig. 4). The latter approach is well suited for a more thorough interpretation of the general environment of deposition. However, first the final conclusions must be anticipated by stating that the horizontal juxtaposition of microfacies 1 to 5 corresponds to a generalized section extending from fore-reef to back-reef conditions. This section displays a first group of dark-colored microfacies (1 to 3a) deposited in a reducing environment. In this group microfacies 1 represents the fore-reef zone, microfacies 2 a ridge of cabbage-type stromatoporoids and microfacies 3 a ridge of *Amphipora*, both of which built the predominant part of the reef zone. Microfacies 2a and 3a are deposits which were laid down in relatively quiet conditions under the protection of the organically constructed ridges. The section shows a second group of light-colored microfacies (3a to 5) deposited in oxidizing environment. Microfacies 4 corresponds to the wave breaking zone, microfacies 4a is transitional toward 5 representing back-reef conditions where scattered mat-like colonies of stromatoporoids were growing in association with *Amphipora*.

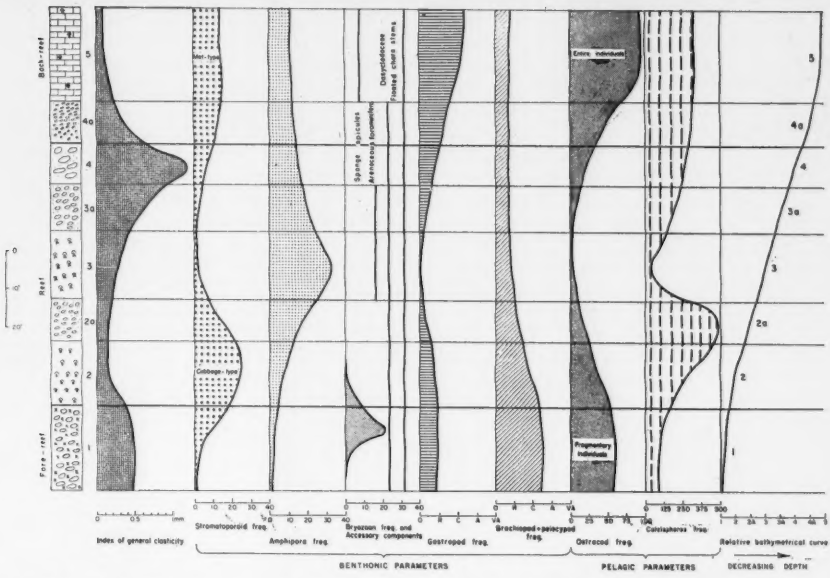

FIG. 3.—Schematic representation of a typical rhythm of sedimentation of the Beaverhill Lake Formation based on interval 9884.5 to 10,001.5 ft.

ENVIRONMENTAL INTERPRETATION

The environmental significance of each computed parameter in relation to the horizontal juxtaposition of the microfacies will now be discussed (fig. 4).

The relatively high value of the index of general clasticity in microfacies 1 is rather surprising as one would expect a minimum size of the clastic components in the deepest environment. This microfacies is also the only one in the sequence displaying a fair sorting of its pellets; it is suggested that both features could result from an accretionary or faecal origin of the pellets. The index of general clasticity increases through microfacies 2, 2a, 3 and 3a until it reaches its maximum in microfacies 4 corresponding to the wave breaking point. Such an increase is consistent with the fact that *Amphipora* is known to live in shallower water than cabbage-type stromatoporoids and also with the transition from a deeper reducing environment to a shallower and oxidizing one. Microfacies 4a has a smaller value of the index of general clasticity because it was deposited in quiet waters in the back of the ridge built up by wave-accumulated larger fragments. Microfacies 5, extremely fine-grained, is a typical expression of protected back-reef lagoonal conditions.

The frequency curve of the stromatoporoids actually combines two stromatoporoidal communities living in different environments. A first community is of cabbage-type; it reaches its maximum development in the open sea reducing conditions of microfacies 2. This group is very well limited in space by rapid decreases in frequency both toward deeper conditions (microfacies 1) and shallower conditions (microfacies 2a, 3, and 3a). The second community is of a mat-type; it reaches its maximum development in the back-reef oxidizing conditions of microfacies 4a and 5. However, its frequency never reaches the high values of the first community.

The main development of branching *Amphipora* colonies takes place in open sea reducing conditions but at a shallower level than the stromatoporoids and in complete

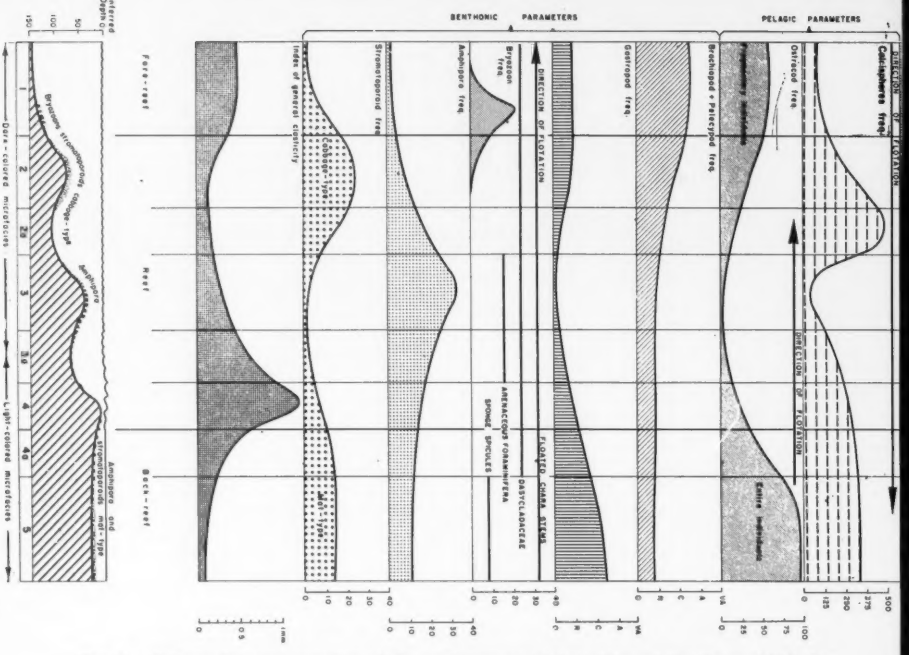

FIG. 4.—Schematic representation of the environment of deposition of the Beaverhill Lake Formation based on interval 9884.5 to 10,001.5 ft.

opposition to the latter. After its maximum in microfacies 3, the frequency of the *Amphipora* decreases very slowly across microfacies 3a, 4, 4a, and 5. In these microfacies there is apparently an association of broken fragments and of individuals living in place. Wave action, particularly in microfacies 4, was probably very effective in moving many *Amphipora* from their position of growth and accumulating them in selected spots; consequently their present distribution in these microfacies may not be representative of their growth density.

The bryozoans have a very narrow zone of distribution. They reach their maximum frequency in microfacies 1 (that is, in fore-reef conditions) and disappear very rapidly as soon as the cabbage-type stromatoporoids begin to develop. In other words, they build the deepest organic zone of the investigated sequence.

The sponge spicules are typically monaxonic types which are concentrated mainly in the back-reef environment of microfacies 5 with some rare occurrences in microfacies 4a. The quiet conditions of lagoonal waters are known to be favorable to their development.

Arenaceous foraminifera of relatively small size and thick shell have been observed only in microfacies 3 and 3a. They are considered to be rather typical of agitated conditions immediately below the zone of wave breaking and they do appear in such a position in the investigated section.

Fragments of large Dasycladaceae stems are scattered in very small number in all the microfacies except 5. Such conditions of occurrence indicate, as will be discussed later, that all the microfacies were deposited in the zone of photosynthesis.

Floated *Chara* stems are present in all the microfacies but in badly preserved condi-

tions indicating extensive floatation. Since they develop only in fresh-water to slightly brackish environments, their origin should be looked for in emerged portions enclosing fresh water ponds which would occur in back-reef conditions. From these zones, the *Chara* stems would be carried out to sea. A similar mechanism will be assumed later also to explain the distribution of the smooth ostracods.

The frequency curve of the gastropods combines actually two communities living in different environments in a similar way to the stromatoporoids. A first community, however not very abundant, reaches its maximum development in open sea reducing conditions, mainly in microfacies 1 to 2. This group is fairly well separated by a zone of low frequency (microfacies 2a, 3, and 3a) from the second community which reaches its maximum in the back-reef oxidizing conditions of microfacies 5. This second group always displays a greater frequency than the first one.

The frequency of the association brachiopod-pelecypod reaches its maximum in microfacies 1 in agreement with the fact that thick-shelled brachiopods are characteristic of fore-reef conditions. A gradual decrease of frequency is apparent across the reef environment, reaching complete stability from microfacies 3a on to the back-reef (microfacies 5).

The frequency curve of the smooth ostracods expresses two different environments. In the first one the ostracods have developed as benthonic components; in the second, they have been distributed passively by wave and current actions and behave as pelagic components. The conditions of preservation and the frequency relations to other parameters allow a fair discrimination of the origin of frequency maxima. Ostracods are extremely abundant in the quiet back-reef environment of microfacies 5 where they occur as perfectly preserved complete individuals indicating ideal conditions of development and preservation. Their frequency gradually decreases toward a minimum in microfacies 3; it may be pointed out that from microfacies 4 on, fragmentary individuals predominate over entire ones. The frequency increases and reaches a second peak in microfacies 1 where all the individuals are broken and often form the nuclei of accretionary pellets. This second maximum, always smaller than the first one, may be interpreted as a result of mechanical concentration of floated tests in the fore-reef environment away from the agitated conditions surrounding the constructed ridges. Such an interpretation implies a flotation of the ostracod shells from the back-reef toward the open sea as considered previously for the distribution of the floated *Chara* stems.

The frequency curve of the pelagic calcispheres appears to be entirely opposed to the curve of the index of general clasticity. The frequency is very low in microfacies 1 and increases toward its maximum in microfacies 2a which corresponds to a fairly protected environment in the back of the stromatoporoidal ridge where the index of general clasticity is very low. The frequency of the calcispheres decreases rapidly in microfacies 3 and then increases gradually toward a medium value in microfacies 5. This last trend can be interpreted by the assumption that the calcispheres did not accumulate in the agitated conditions where the *Amphipora* developed but were gradually washed into the back-reef as some pelagic foraminifera (*Globigerina*) are trapped today in atoll lagoons. Phases of transportation in such a direction probably alternated with others during which ostracods and *Chara* were floated in an opposite direction.

BATHYMETRICAL INTERPRETATION

A bathymetrical comparison between Mesozoic reefs and present ones is possible only in a very broad manner (Carozzi, 1955a). When a similar comparison is attempted for Paleozoic reefs, the problem becomes quite difficult because of the lack of data concerning the bathymetrical distribution of stromatoporoids and *Amphipora* which are the predominant colonial organisms.

The only information in our possession is a relative one corresponding to the fact that in order of decreasing depth, one finds successively a bryozoan, a stromatoporoid, and an *Amphipora* belt before reaching the wave breaking zone and back-reef conditions. However, one absolute fact is known, it is

the depth distribution of the Dasycladaceae which stops at 135 ft depth, the lower limit of the photosynthesis zone. The presence of Dasycladaceae even in microfacies 1 indicates that the latter was still deposited above 135 ft. The distribution of the arenaceous foraminifera in microfacies 3 and 3a is also consistent with such a relation (Carozzi, 1954, 1955b). In conclusion, the sequence of microfacies 1 to 5 was deposited in an environment which did not reach more than 150 ft in depth as far as can be assumed from the present stage of our knowledge of Paleozoic reefs.

DESCRIPTION OF THE RHYTHMS OF SEDIMENTATION

The Beaverhill Lake Formation of the investigated section can be subdivided into seven well defined rhythms of sedimentation on the basis of the succession of microfacies and of their microscopic parameters (figs. 5–7).

Rhythm 1, 10,050′–10,001.5′ (fig. 5).—Its sequence starts with microfacies 1 followed by an alternation of 2 and 2a; the rhythm ends with several thin alternations of microfacies 1 and 3. The general trend of the sedimentary evolution is 1, 2, 2a, 3 in an upward direction. Such an evolution is clearly displayed by the organic components; indeed frequency peaks of bryozoans, cabbage-type stromatoporoids, and *Amphipora* follow each other. Brachiopod, pelecypod, and gastropod frequencies decrease gradually upwards as do also the fragments of ostracods. The frequency of the calcispheres reaches a peak in microfacies 2a before decreasing upward. The index of general clasticity decreases in the middle portion of the rhythm before increasing again near the top.

Rhythm 1 is clearly a gradual decrease of depth during which the sedimentary trend extends from microfacies 1 to 3. It should be noticed that the bryozoan maximum is unique in the investigated section as if such colonies represented the first organic growth on the carbonate platform. This growth was then completely eliminated when stromatoporoids and *Amphipora* sprang to predominance.

Rhythm 2, 10,001.5′–9,884.5′, (fig. 5, 6).—This rhythm is a complex association of microfacies in which, however, the general trend of sedimentary evolution is very apparent on closer examination. It starts with a zone in which 1, 2, and 2a predominate; then microfacies 3 appears and expands, eliminating 2a. Upward, 3a and 4 appear and upon elimination of 3, microfacies 4 becomes predominant until microfacies 5 which forms the top. The organic parameters of this rhythm have an almost ideal behavior. They have been used in establishing our schematic representations (fig. 2) and do not need to be described again. This also applies to the index of general clasticity.

Rhythm 2 starts by a subsidence during which its basal microfacies 1 is deposited on top of the shallowest microfacies 3 of the first rhythm. The succession is then a gradual and complete depth decrease through microfacies 2, 2a, 3, 3a, 4, 4a, and 5. For the first time in our sequence, the depth decrease has overpassed the wave-breaking zone (microfacies 4) and reached back-reef conditions.

Rhythm 3, 9884.5′–9825.5′ (fig. 6).—This rhythm is relatively simple. It starts with a rather symmetrical portion in which microfacies 3 is preceded and followed by 4a; it ends with another symmetrical portion in which microfacies 4a is preceded and followed by 5. The organic parameters have a normal behavior; the *Amphipora* maximum related to microfacies 3 is well realized; matlike stromatoporoids are very abundant in microfacies 5, as well as important concentrations of whole ostracods and calcispheres. Among the accessory components, a few solitary cup corals are present and sponge spicules are locally concentrated in the lower part of microfacies 5. The index of general clasticity reaches a maximum in microfacies 3a and decreases gradually throughout 5 until the top of the rhythm.

The lower part of this rhythm is a subsidence period during which the back-reef conditions developed on top of rhythm 2 were interrupted by an increase of depth which temporarily re-established the environment favorable to *Amphipora* colonies (microfacies 3). The upper half of the rhythm is a new depth decrease during which the back-reef environment again became predominant. It may be pointed out

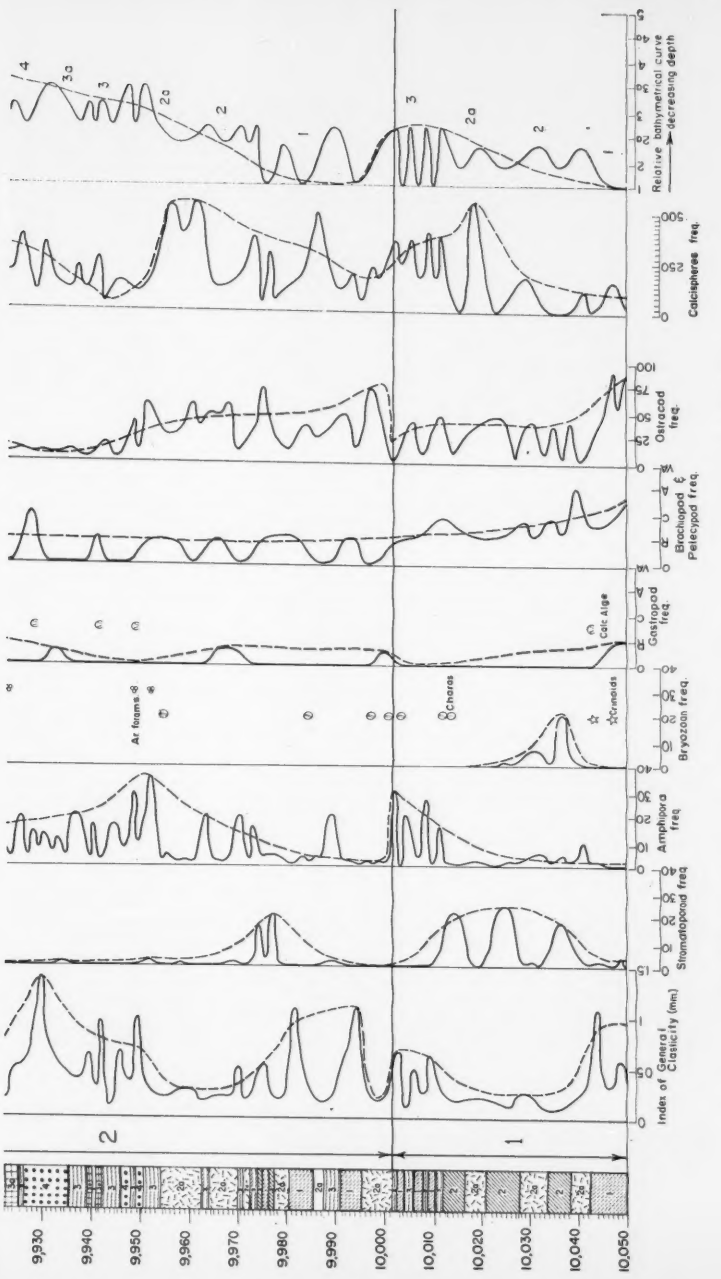

FIG. 5.—Variation curves of microscopic paramters in the Beaverhill Lake Formation (rhythms 1 and 2).

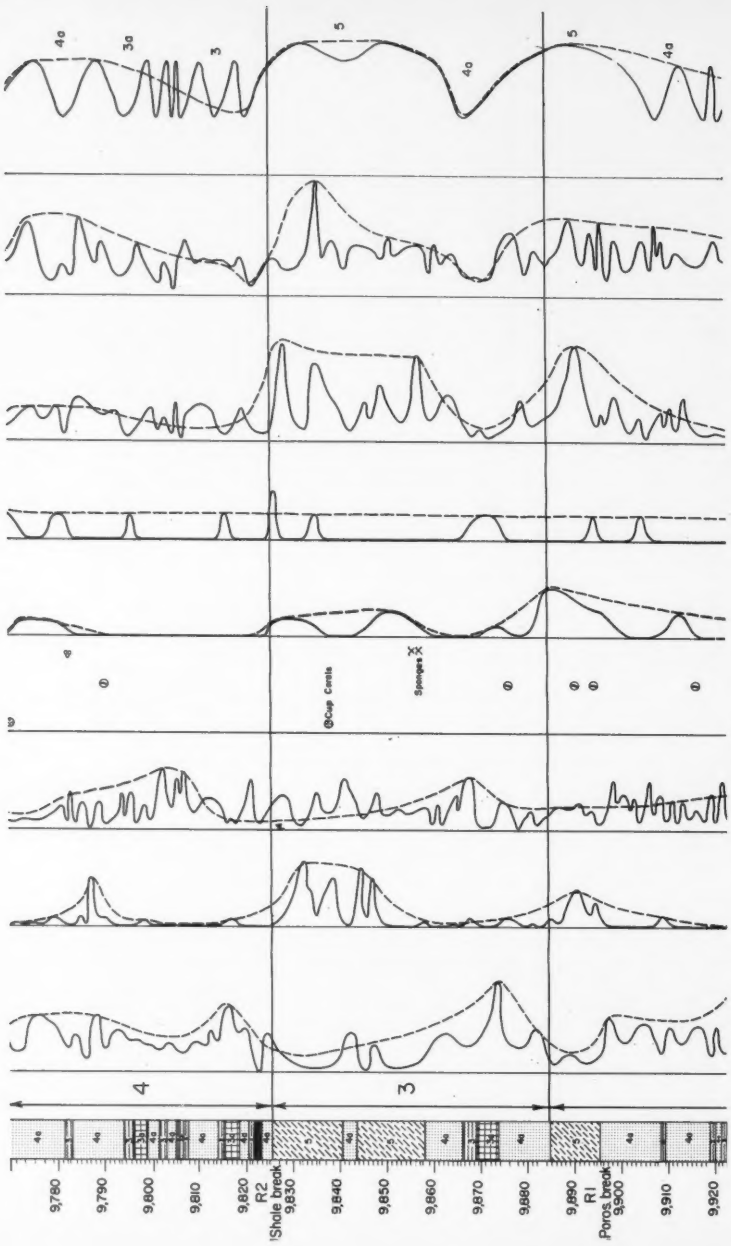

FIG. 6.—Variation curves of microscopic parameters in the Beaverhill Lake Formation (rhythms 2, 3, and 4).

that microfacies 5 of the upper half of this rhythm corresponds to the last presence of back-reef conditions in the investigated sequence.

Rhythm 4, 9825.5′–9769.5′ (fig. 6).—This rhythm is a complex association of microfacies 3, 3a, and 4a in which the general trend of sedimentary evolution shows a sequence 3, 3a, to 4a upward. The rhythm shows in its lower portion a shale break (R2) after which microfacies 3 becomes predominant, until it is replaced at the top of the sequence by a large development of microfacies 4a.

The organic parameters follow the lithological evolution; the maximum of *Amphipora* is well displayed in the middle of the rhythm and followed upwards by that of mat-type stromatoporoids. The frequency of the ostracods and calcispheres increases upward. The index of general clasticity does not vary much because the difference of indexes between microfacies 3, 3a, and 4a is not very significant.

Rhythm 4 starts with a subsidence which definitely ends back-reef conditions and establishes again an environment favorable to *Amphipora* growth (microfacies 3), this subsidence is accompanied by the shale break R2. The middle and upper portions of this rhythm correspond to a depth decrease during which *Amphipora* becomes predominant followed by microfacies 4a, indicating a tendency toward back-reef conditions which were never fully realized. In other words, after the shale break R2, depth decreased and organic growth started again.

Rhythm 5, 9769.5′–9717′ (fig. 7).—This sequence is again an association of microfacies 3, 3a, and 4a similar to the preceding one but without any basal shale break. The general trend of sedimentary evolution is also 3, 3a, to 4a upwards with a large predominance of the latter microfacies.

The organic parameters of this rhythm are fairly well displayed; the *Amphipora* maximum occupies the lower half of the sequence whereas the mat-like stromatoporoid maximum appears in the upper half. The ostracod frequency normally increases slightly upwards but the calcispheres have an abnormal behavior by steadily decreasing in frequency upward; such erratic conditions are to be expected occasionally with pelagic components. The index of general clasticity does not vary much, as in the preceding rhythm, because the indexes of 3, 3a, and 4a are not very different from one another.

Rhythm 5 starts with a slight subsidence during which microfacies 3 and 3a are deposited on top of microfacies 4a, forming the top of the preceding rhythm. Depth decreases upwards and rapidly reaches microfacies 4a which builds the last thick unit in the described sequence, indicating a tendency toward back-reef conditions.

Rhythm 6, 9717′–9657.5′ (fig. 7).—It is a rather complex sequence starting at the bottom with a thick shale break (R3) and consisting of an association of microfacies 1, 2, 2a, 3, and 3a. However, the general trend of sedimentary evolution shows a predominance of microfacies 3 and 3a in the lower portion of the rhythm, of microfacies 2 in the middle, and of microfacies 1 in the upper portion.

The variations of the organic parameters are entirely in agreement with the microfacies distribution. The *Amphipora* maximum in the lower part of the rhythm is followed by that of the cabbage-type stromatoporoids which re-appear here again after their last occurrence in the lower part of rhythm 2. Gastropod, brachiopod, and pelecypod frequencies increase upward; the fragments of ostracods vary in the same way. The calcispheres, after having reached a peak in microfacies 2a, decrease gradually upward in frequency. The index of general clasticity oscillates in a somewhat irregular way.

This rhythm is the first one of the investigated section during which depth increases gradually upward through a sequence 3a, 3, 2a, 2, and 1. Such an evolution is separated from microfacies 4 of the preceding rhythm by the shale break R3, indicating by itself a rupture of equilibrium in the carbonate deposition.

Rhythm 7, 9657.5′–9612′ (fig. 7).—This probably incomplete rhythm has a symmetrical appearance. Its lower and upper portions are constituted by microfacies 2, whereas the center displays an alternation of microfacies 1 and 3.

Among the organic parameters two maxima of cabbage-type stromatoporoids

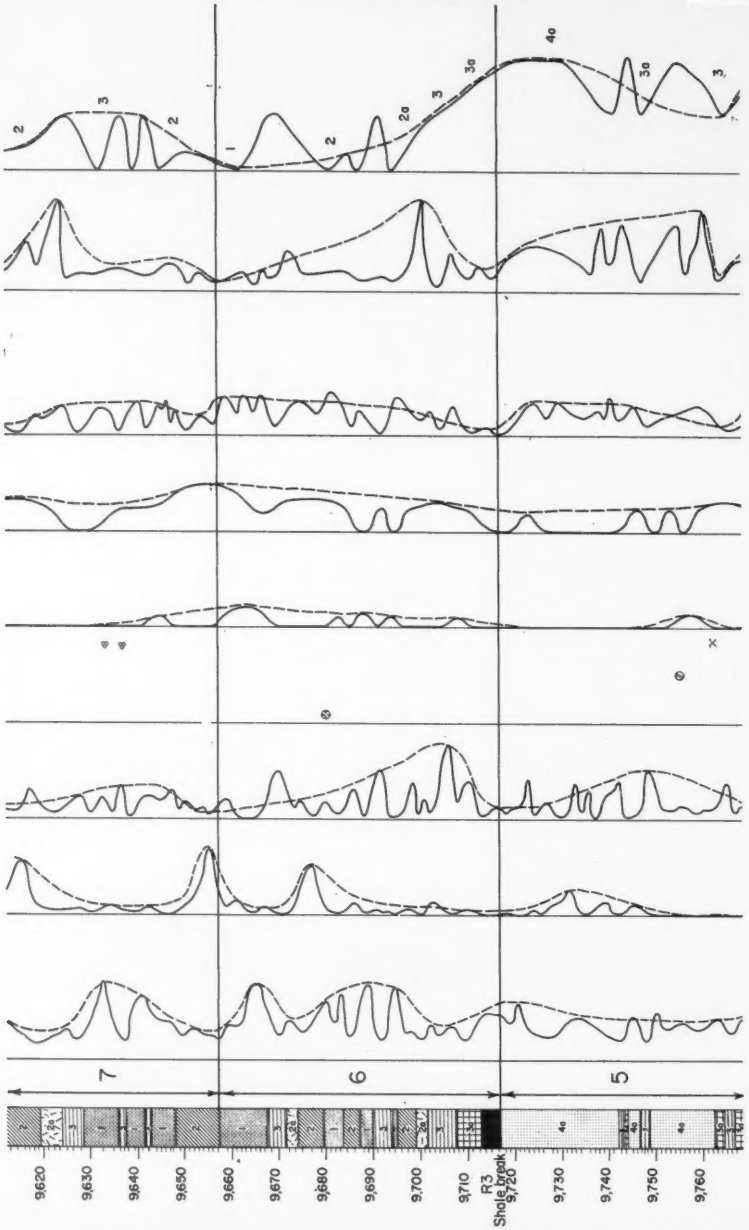

FIG. 7.—Variation curves of microscopic parameters in the Beaverhill Lake Formation (rhythms 5, 6, and 7).

surround a central maximum of *Amphipora* indicating a predominant influence of microfacies 3 against 1. The behavior of the ostracods is abnormal whereas the calcispheres display a very strong maximum only in the upper part of the rhythm where microfacies 2a is present. The index of general clasticity shows a peak in the middle of the sequence.

Rhythm 7 which is probably only a fraction of a larger unit extending beyond the investigated core is a simple oscillation reaching by depth decrease microfacies 3, starting and ending in microfacies 2.

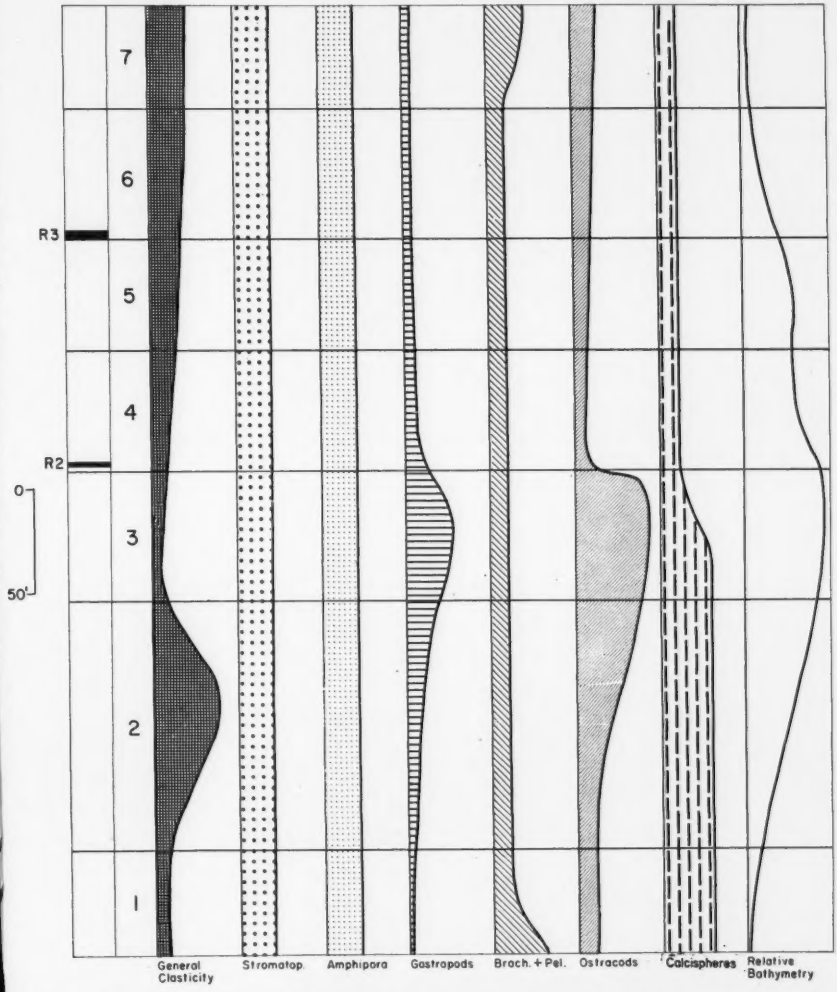

FIG. 8.—General schematic evolution of the microscopic parameters in relation to relative depth (amplitudes of curves not to scale, compare with figs. 5 to 7).

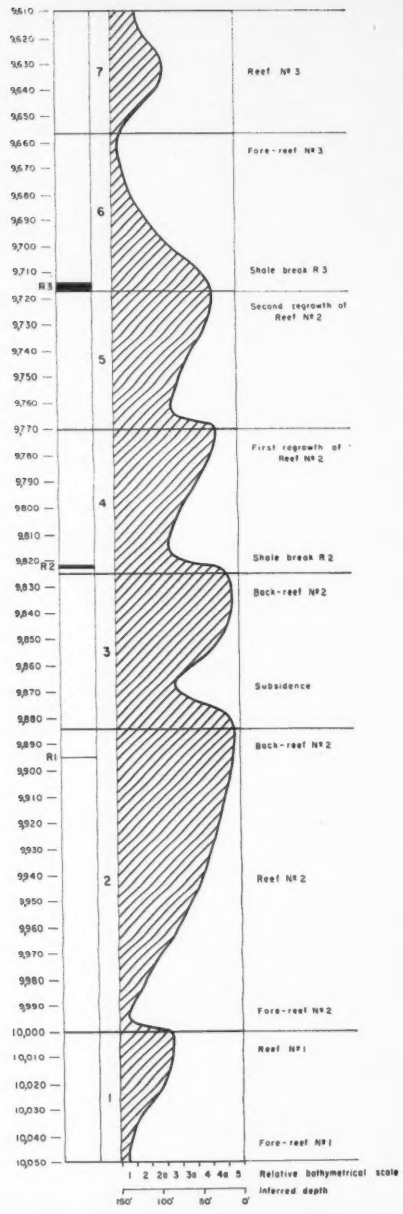

FIG. 9.—General bathymetrical interpretation of the Beaverhill Lake Formation.

GENERAL EVOLUTION OF THE MICROSCOPIC PARAMETERS

It appears interesting to point out that during the depositional history of the investigated core, most of the microscopic components display a general evolution which is superposed as a larger scale mechanism on the rhythmic patterns described above. This corresponds actually to the determination of the large scale trend of the different curves of main trend (compare fig. 8 with figs. 5–7).

The overall evolution of the index of general clasticity indicates an increase until the middle of rhythm 2 where microfacies 4 is reached for the first time. A minimum is apparent during rhythm 3 and relatively low values predominate in the rest of the sequence with a slight increase upwards. In other words, the index of general clasticity shows lower values during rhythms 3 to 7 than during 1 to 2.

This upward decrease of the index of general clasticity can be readily explained by the fact that rhythms 4 to 7 and particularly 4 and 5 do not display microfacies 4 (wave-breaking zone) but 4a. Such conditions indicate that the upper portion of the investigated sequence was deposited in a generally less agitated environment than the lower one during which the reefs were established. It seems as if the organic constructions had influenced the sedimentary history in an irreversible way.

The frequency curves of the stromatoporoids and *Amphipora* do not show any general evolution. The general evolution of the frequency of the gastropods indicates an increase until rhythm 3 followed by a decrease in the rest of the section. There is a tendency for the gastropods to be less abundant in the upper half of the sequence than in the lower one. The general evolution of the frequency curve of brachiopods and pelecypods shows stability over most of the sequence with increases toward top and bottom.

The overall evolution of the frequency of the ostracods displays an increase until rhythm 3 after which there is a general decrease. However, a slight increase may be noted within the upper field of low values. In other words, the ostracods are definitely less abundant during rhythms 4 to 7 than during 1 to 3. This decrease of general fre-

quency starts with the disappearance of the typical back-reef microfacies 5 from which the ostracods seem to have originated. The general evolution of the frequency of the calcispheres shows a gradual decrease upwards. Here again, the values are lower during rhythms 4 to 7 than during 1 to 3. This decrease is difficult to understand because increasing open sea conditions should give rise to an increased frequency of these pelagic organisms. It is possible that one faces here an effect of dispersal whereas during the ascending phase of the reef (rhythms 1 to 3) the calcispheres were concentrated by waves and currents in the immediate vicinity of the growing colonies which had wave breaking effects.

GENERAL BATHYMETRICAL INTERPRETATION

The general bathymetrical history of the investigated sequence is definitely an asymmetrical one comprising seven rhythms of sedimentation which are also themselves predominantly of asymmetrical character (fig. 9).

Rhythm 1 is a gradual depth decrease starting in fore-reef environment and ending with reef no. 1. An abrupt subsidence starts rhythm 2, bringing back fore-reef conditions. A gradual depth decrease leads then to the development of reef no. 2 followed by its back-reef facies.

Rhythm 3 is actually an interruption of back-reef conditions by a subsidence reestablishing an open sea environment rapidly followed by a return of the back-reef facies. The latter is abruptly interrupted by a subsidence during which clay materials (shale break R2) are brought into the carbonate environment. In spite of this unfavorable foreign inflow, colonial organisms grew up again, apparently in a more quiet environment than before, during the gradual depth decrease which forms most of rhythm 4. A rapid subsidence inaugurates rhythm 5 during which another depths decrease corresponds to a second regrowth of organic colonies.

Rhythm 6 is in itself a continuous depth increase bringing back fore-reef conditions. It was certainly a major rupture of equilibrium since it begins with a second and very important inflow of clay materials (shale break R3). Rhythm 7 is a simple oscillation corresponding to a relatively short-lived reef no. 3. The asymmetrical character of most of these sedimentary rhythms which seems to correspond to a gradual decrease of depth followed by a rapid subsidence (provided constant sedimentation rates are admitted) appears as a typical feature of tectonically controlled oscillations (Carozzi, 1950). In spite of the fact that such a pattern has not yet received a satisfactory explanation, it leads to six natural breaks in the Beaverhill Lake Formation among which two correspond to the deposition of argillaceous material brought from outside the carbonate environment.

ACKNOWLEDGMENTS

The writer is grateful to Shell Oil Company of Canada Limited for making the core available for study.

REFERENCES

ANDRICHUK, J. M., 1958a, Stratigraphy and facies analysis of Upper Devonian reefs in Leduc, Stettler, and Redwater areas, Alberta: Am. Assoc. Petroleum Geol. Bull., v. 42, p. 1–93.

———, 1958b, Cooking Lake and Duvernay (Late Devonian) sedimentation in the Edmonton area of Central Alberta: Am. Assoc. Petroleum Geol. Bull., v. 42, p. 2189–2222.

CAROZZI, A., 1950, Contribution à l'étude des rythmes de sédimentation: Archives des Sciences, Genève, v. 3, p. 1–76.

———, 1954, Sédimentation rythmique en milieu corallien, le Jurassique supérieur du Grand-Salève, France: Archives des Sciences, Genève, v. 7, p. 65–93.

———, 1955a, Le Jurassique supérieur récifal du Grand-Salève, essai de comparaison avec les récifs coralliens actuels: Eclogae Geol. Helv., v. 47, p. 373–376.

———, 1955b, Sédimentation récifale rythmique dans le Jurassique supérieur du Grand Salève: Geol. Rundschau, v. 43, p. 433–446.

———, 1958, Micro-mechanisms of sedimentation in the epicontinental environment: Jour. Sedimentary Petrology, v. 28, p. 133–150.

EDIE, R. W., 1959, Middle Devonian sedimentation and oil possibilities, Central Saskatchewan, Canada: Am. Assoc. Petroleum Geologists Bull., v. 43, p. 1026–1057.

FONG, G., 1960, Geology of Devonian Beaverhill Lake Formation, Swan Hills area, Canada: Am. Assoc. Petroleum Geologists Bull., v. 44, p. 195–209.

ILLING, L. V., 1959, Deposition and diagenesis of some Upper Paleozoic carbonate sediments in Western Canada: Fifth World Petr. Congr. Proc. New York, Section I, p. 23–52.

JOURNAL OF SEDIMENTARY PETROLOGY, VOL. 31, NO. 4, PP. 514–529
FIGS. 1–8, DECEMBER, 1961

DISTINCTION BETWEEN DUNE, BEACH, AND RIVER SANDS FROM THEIR TEXTURAL CHARACTERISTICS

GERALD M. FRIEDMAN[1]
Pan American Petroleum Corporation, Research Center, P.O. Box 591, Tulsa, Oklahoma

ABSTRACT

Criteria for the recognition of the depositional environment of sandstones are important in the reconstruction of paleoenvironments. Petrographic characteristics of recent sands from dune, beach, and river environments have been studied to determine if there are mineralogical or textural characteristics which will permit diagnosing the environment of deposition. At present satisfactory depositional petrographic criteria are nonexistent. Since near-shore sands are shifted from one environment to the other, it is necessary to relate the petrographic characteristics to the terminal environment.

The mineralogy of clastic sediments for the most part seems to reflect the nature of the source rock, whereas textural parameters are chiefly related to the mode of transportation and the energy conditions of the transporting medium. Grain-size distribution analyses represent a plot of abundance or frequency against grain-size. Dune sands commonly can be distinguished from beach sands on the basis of such plots. The distinction between the sand types can be numerically stated by computing the third moment (skewness) of the distribution curve. On the phi scale the third moment (skewness) for dune sands is generally positive, whereas that of beach sands is generally negative. This seems to hold whether the dune samples are from barrier islands, coasts, lakes, rivers, or deserts. Beach sands of positive skewness occur on Padre Island, Texas, near the delta of the Rio Grande River, and on Horn Island, Mississippi. Sporadic positively-skewed beach sands have been found elsewhere, but for medium- to fine- and very fine-grained sands these appear to be relatively uncommon. Within the widely scattered samples a number of dune samples with slight negative skewness (-0.28 or less) have also been found. A plot of mean grain-size against third moment (skewness) results in an almost complete separation of the fields representing dune sands and beach sands. The sign of the skewness is not affected by the mineralogy of the sample. Sands of quartz, carbonate, gypsum, and olivine all follow the same general rule.

The distribution curves of river sands like those of dune sands are generally positively skewed, but a number of exceptions to this rule have been noted. Within limitations, medium- to fine- and very fine-grained river sands can be distinguished from beach sands on the basis of plots of third moment (skewness) against standard deviation (sorting). The third moment (skewness) of coarse-grained sand is inconclusive as an indicator of depositional environment. Dune sands can commonly be distinguished from river sands by their sorting characteristics; dune sands tend to be better sorted than river sands. Since dune and river sands are skewed in the same direction, a further criterion is needed for distinguishing river from dune sands which have overlapping sorting characteristics. This has been found by separating the light mineral grains from those of the heavy minerals and determining the mean grain-size ratio of quartz and that of a specific heavy mineral in the same sand, such as garnet or magnetite. The ratio of the radius of quartz to that of a specific heavy mineral is usually larger for river sands than for dune sands. For one Mid-Continent drainage system (Arkansas River and tributaries), plots of ratio of mean grain-size of heavy to light minerals (using the phi system) against the ratio of sorting (standard deviation) of heavy to light minerals show points representing river sands to lie in a different area of the graph from those for dunes.

Transportation of dune and river sands represents, for the most part, unidirectional flow. The upper size range of grains carried in suspension or by saltation is governed by the competency of the transporting medium. Such limitation does not affect fine particles in transport. The result of this limiting competency is reflected at the coarse-grained end of the frequency distribution curve by the lack of a "tail" usually present in a normal curve, resulting in positive skewness.

In beach sands the fine-grained particles of sand are removed by winnowing. The distribution curve of a winnowed sand appears to have a "chopped off" tail at the fine-grained end in comparison to a normal curve, thus indicating negative skewness.

INTRODUCTION

Criteria for recognition of the environments of deposition of ancient sands are of considerable importance in connection with the search for stratigraphic oil traps. However, reliable criteria have proved elusive. Even attempts to distinguish between sands of such widely different origin as beach, dune, and river sands have generally been ineffective. A useful criterion for distin-

[1] Manuscript received October 31, 1960

guishing between beach and dune sands and between beach and river sands and between some dune and river sands has recently been developed and is reported here. A method proposed by von Engelhardt (1940) can be used to distinguish river from dune sands.

A number of workers have tried to distinguish beach from dune sands and beach from river sands (Alimen and Bender, 1960; Beal and Shepard, 1956; Bradley, 1957; von Engelhardt, 1940; Nanz, 1954; Schneider and Cailleux, 1959; Guggenmoos, 1934; Shepard and Moore, 1955; Shepard, 1960; Zimdars, 1958).

Methods which have been proposed in the literature for distinguishing these types of environment by studying the texture or morphology of sand or sand grains are not satisfactory. A method reported by Rogers and Strong (1959) proved useful in distinguishing some Texas river and beach sands. Mason and Folk (1958) showed how it is possible to distinguish dune from beach sands on Mustang Island, Texas. The F:C ratio study of Keller (1945) indicated that dune sands can be distinguished from beach sands on the basis of shape of size-frequency curves.

In a near-shore environment sands may be transported from beaches to dunes and back again to the beaches. Each sand grain may have been deposited many times either by water or by wind. These movements may recur again and again for a considerable period of time, perhaps millions of years. To determine the environment of deposition from the petrographic characteristics of sands and sandstones, one must relate these characteristics to the terminal environment.

Textural parameters have been selected for study which reflect the mode of transportation and the energy conditions of the transporting medium.

Samples for this project have been obtained through the cooperation of the following persons and institutions: Mlle. Henriette Alimen (Centre National de la Recherche Scientifique, France), Tj. H. van Andel (Scripps Institution of Oceanography), William S. Cooper and C. O. Morgan, Wakefield Dort (University of Kansas), Richard H. Durrell and Ronald G. Schmidt (University of Cincinnati), William M. Fairley and Erhard M. Winkler (Notre Dame University), Oswalt C. Farquhar (University of Massachusetts), Gordon A. Macdonald and Robert M. Moberly, Jr. (University of Hawaii), Robert M. Norris (University of California), William Odynsky (Research Council of Alberta), and John J. W. Rogers (Rice University).

PROCEDURE

Samples were collected from dunes, rivers, ocean beaches, and Great Lakes beaches. One sample was obtained from a large lake which is not part of the Great Lakes system. Table 1 (*see* APPENDIX) indicates the location of the samples studied.

A total of 267 samples was studied from widely scattered locations in the United States, Canada, Mexico, the Bahamas, Bermuda, Hawaii, and North Africa. Of this total, 114 samples were collected from dunes, 80 from ocean beaches, 18 samples from lake beaches, and 55 from rivers.[2] The several dune types sampled include barrier island dunes, coastal dunes, lake dunes, river dunes, and desert dunes. Quartz sands, carbonate sands, gypsum sands, and olivine sands were investigated. Carbonate sands were represented by 18 samples (16 beach sands and 2 dune sands) from Bermuda, North Bimini and Andros Islands in the Bahamas, and the Islands of Hawaii. A total of seven gypsum dune sands was collected at White Sands National Monument near Alamogordo, New Mexico, and at Salt Flat, West Texas. Four samples of olivine beach sands were obtained from the islands of Hawaii. Most of the sands examined (240 samples) are composed of quartz. In the field, samples were taken parallel to the bedding, where possible, to avoid mixing of populations. Beach sands were sampled from the swash zone or close to the swash zone.

In the laboratory, grain-size determinations were made on these samples by con-

[2] The 55 river sand samples are medium-, fine- and very fine-grained sands with a size range comparable to that of the dune and beach sands studied. In addition, coarse-grained sands, gravelly sands, and gravels were collected from rivers (refer to Table 1 under hearding of "River Sands").

ventional sieving methods, using $\frac{1}{4}\phi$ sieve intervals. On some of the river and dune sands, the heavy minerals were separated out, and grain-size analyses were made on the heavy mineral fractions. The first, third, and fourth moments (mean, skewness and kurtosis) of the grain-size distribution curve were computed for each sample.

The first moment (mean) is defined by the equation $\bar{x}_\phi = 1/100\ \Sigma f m_\phi$, where $\bar{x}_\phi$ is the mean grain-size (in phi), f is the frequency or abundance of the different grain-size grades present in the sediment, and m_ϕ is the midpoint of each grain-size grade in phi values. The third moment (skewness) which describes the symmetry of the grain-size distribution curve is defined statistically as the average of the cubed deviations from the mean divided by the cube of the standard deviation[3] and is expressed by the equation

$$\alpha_{3\phi} = (1/100)\sigma_\phi^{-3}\Sigma f(m_\phi - \bar{x}_\phi)^3$$

where $\alpha_{3\phi}$ is the skewness and σ_ϕ is the standard deviation in phi values. The fourth moment (kurtosis) which measures the peakedness of the grain-size distribution curve is expressed by the equation

$$\alpha_{4\phi} = (1/100)\sigma_\phi^{-4}\Sigma f(m_\phi - \bar{x}_\phi)^4$$

where $\alpha_{4\phi}$ is the kurtosis.

RESULTS

In figure 1 the third moment (skewness) for dune sands and for ocean and lake beach sands is plotted against the first moment (mean grain-size) for these samples using the phi (ϕ) scale. Between the dune sands and the ocean beach sands a nearly complete separation is found for the two depositional environments, the dune sands being for the most part positively skewed, and the ocean beach sands generally negatively skewed. Lake beach sands, like the ocean beach sands, are mostly negatively skewed. However, four of the lake beach samples overlap into the field of the dune sand samples. Dune sands generally are positively-skewed, irrespective of whether the dunes are barrier island, coastal, lake, river, or desert dunes. Of the 114 sand samples collected from dunes only eight samples are slightly negatively skewed (-0.28 or less). In the widely scattered sampling, one area was discovered where beacn sands show positive skew. This area is located on southern Padre Island, Texas, opposite the Rio Grande delta.[4] It is believed that the beach sands in that area have "inherited" the positive skew of river sands and have apparently not yet come to equlibrium with the new environment. Sporadic positively-skewed beach sands have been found elsewhere, but for medium to fine and very fine-grained sands these appear to be relatively uncommon. Coarse-grained beach sands may be either positively or negatively skewed. One anomalous beach sand sample with a high positive skewness was collected on Andros Island in the Bahamas. A second sample taken 40 feet away from it showed "normal" negative skewness.

The mineralogy of the sands does not affect the tendency for sand dunes to be positively-skewed or beach sands to be negatively-skewed. Quartz, carbonate, and gypsum dune sands and quartz, carconate and olivine beach sands were studied. The skewness for all the sands reflects the environment of deposition and is not altered by the mineralogy of the sand.

In figure 2 the third moment (skewness) for beach and dune sands is plotted against the mean (first moment) using the millimeter scale. The points representing beach sands lie for the most part in a different area of the graph from those for dunes.

The lower limit of mean grain-size of the dune sand samples studied is 1.49ϕ. In contrast 40 percent of the beach sand samples have mean grain-size values lower than 1.49ϕ. Newell and Boyd (1955) describe very coarse eolian sands of the Ica Desert of Peru which may have mean grain-size values considerably below 1.49ϕ.

[3] The standard deviation is the square root of the mean of the squared deviations from the mean and is expressed by the equation

$$\sigma_\phi = (\Sigma f(m_\phi - \bar{x}_\phi)^2/100)^{1/2}.$$

[4] Since this study has been completed, a second area of positively skewed beach sands has been found. This area appears to include all of Horn Island, Miss., in the Gulf of Mexico. The anomalous skewness of the sands collected along Horn Island may be the effect of proximity to the mouth of the Mobile River, or some unknown factor such as exceptionally strong longshore currents.

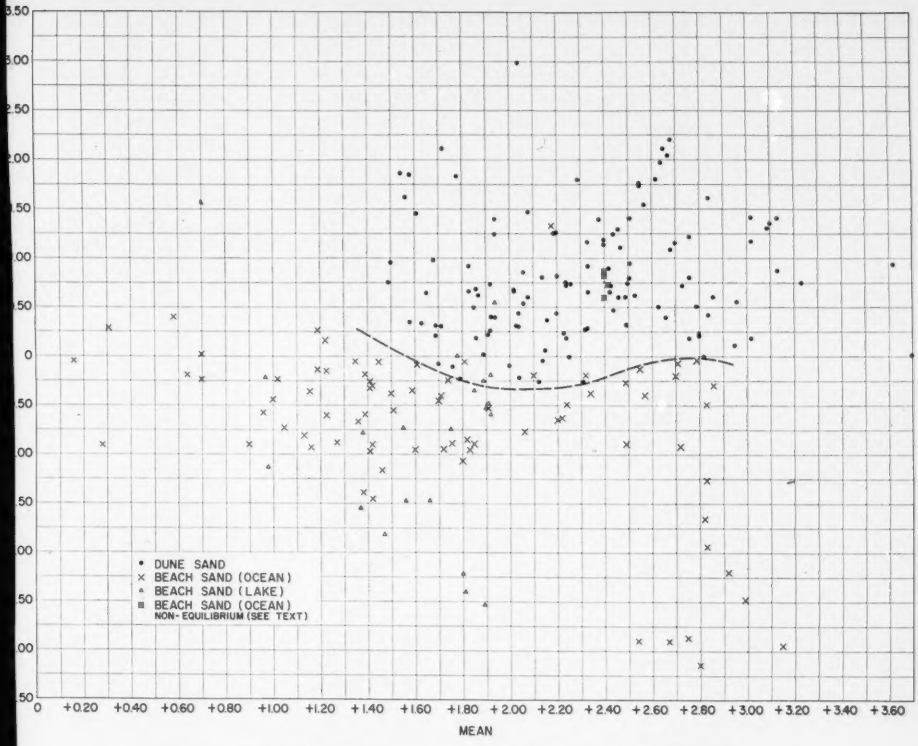

FIG. 1.—Plot of first moment (mean) and third moment (skewness), using phi (ϕ) scale, for beach and dune sands.

In figure 3 third moment (skewness) is plotted against the fourth moment (kurtosis) for beach and river sands using the phi (ϕ) scale. The kurtosis provides a second dimension for the plot, but is not diagnostic of depositional environment. A plot of skewness against mean could have been employed, but kurtosis was found to provide a wider spread of the points for the river data and the points were thus less crowded. River sands are generally positively skewed, as are dune sands; but a number of exceptions were found. Skewness is environment-sensitive, whereas kurtosis is not.[5]

In figure 4 the third moment (skewness) is plotted against the standard deviation, a measure of the degree of sorting, for beach and river sands in which less than 5 percent of the grains are larger than 0.500 mm. ($<+1.00\phi$). This figure indicates that the degree of sorting is of help in distinguishing beach from river sands. Beach sands of positive skewness, such as the sand samples from southern Padre Island, Texas, opposite the Rio Grande delta, have a low numerical value for the standard deviation and, as indicated in figure 4, can be distinguished from

[5] River sand samples with more than 5 percent of the grains in excess of 0.500 mm. ($<+1.00\phi$) size were not plotted in figure 2. River sands of coarse sand to gravel size can be either positively or negatively skewed and no predictable relationship could be determined.

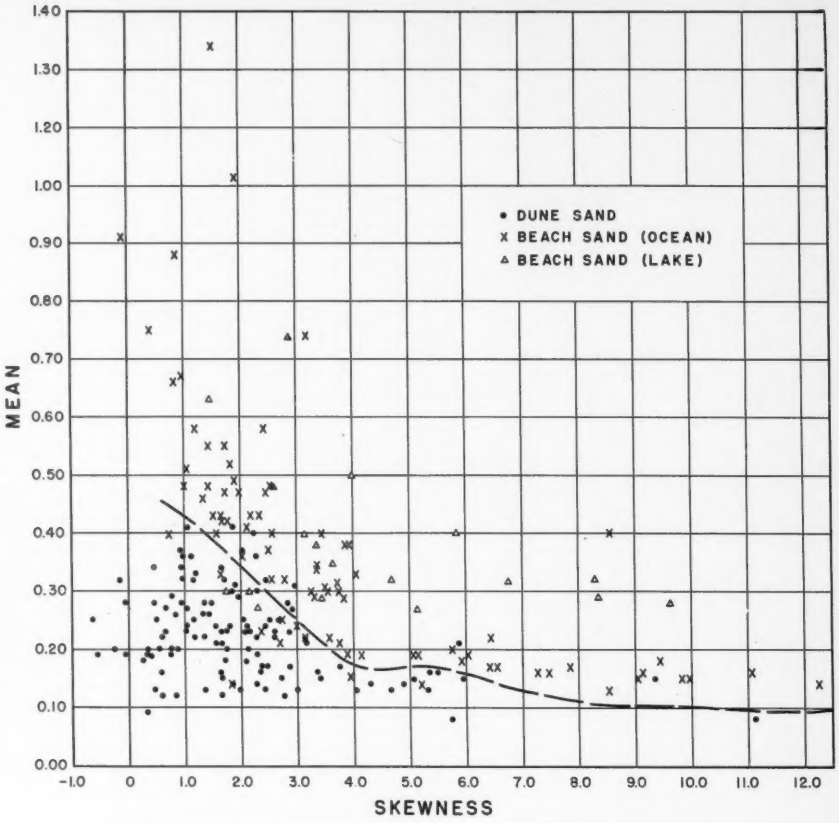

FIG. 2.—Plot of first moment (mean) and third moment (skewness), using millimeter scale, for beach and dune sands.

river sands.[6] Similarly some of the negatively-skewed river sands can be distinguished from beach sands on the basis of their high numerical value for the standard deviation. Two of the positively skewed beach sands which were considered "exceptions" in figure 3, since their points lie in the field of the river sands, fall in the field of the beach sands in figure 4, where the third moment (skewness) has been plotted against the standard deviation. Of the 108 points plotted in figure 4, which represent sands from twenty-nine different rivers and from beaches of the Atlantic and Pacific Oceans, Gulfs of Mexico and California, and the Great Lakes, only two samples of river sands were found to lie outside their field.

A plot of third moment (skewness) against another parameter, such as the standard deviation, for beach and river sands on the millimeter scale does not provide a good separation between two fields representing

[6] In figure 4 the southern Padre Island samples are represented by an x inside a square. The positively-skewed beach sands from Horn Island, Mississippi, referred to in footnote 4 fall within the field of the beach sands of figure 4.

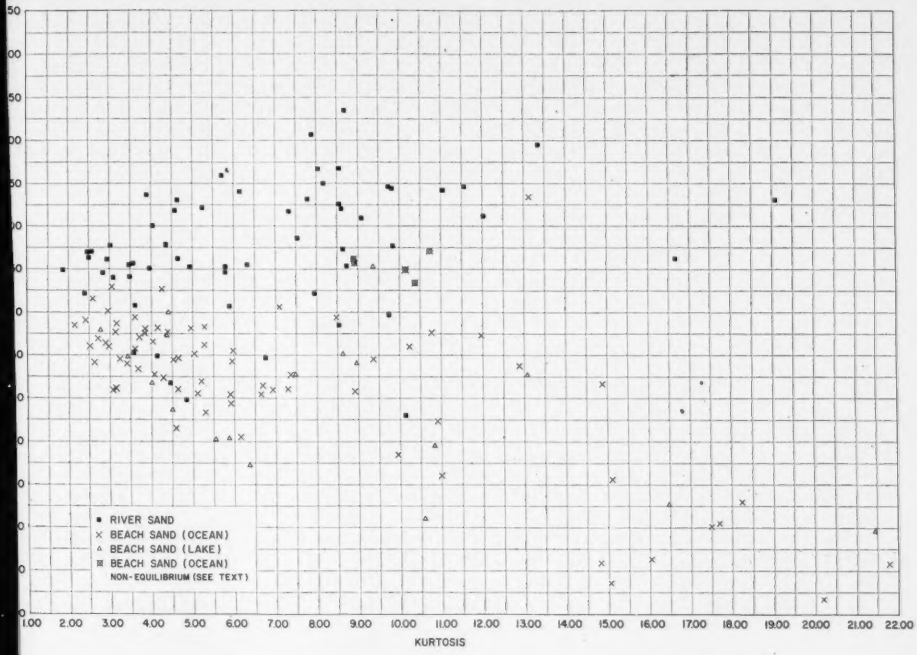

FIG. 3.—Plot of third moment (skewness) and fourth moment (kurtosis), using phi (ϕ) scale, for beach and river sands.

two different depositional environments. On the millimeter scale the third moment (skewness) apparently is not effective in distinguishing beach from river sands, and plots of moment measures for these environments using this scale are therefore not reproduced in this study.

Beach sands commonly may be distinguished from river sands and from dune sands primarily on the basis of textural parameters, chiefly third moment (skewness). However, river sands cannot often be distinguished from dune sands on the basis of the textural properties of the bulk sediments, since both types of sand exhibit positive skewness. Dune sands tend to be better sorted than river sands, and a plot of standard deviation (sorting) against mean grain-size (fig. 5) indicates three fields, one for river sands, one for dune sands (in which one exceptional river sand point is represented), and a third field of overlap. Only medium to fine and very fine-grained river sands have been plotted in figure 5. This figure points out that many river sands can be distinguished from dune sands and vice versa on the basis of their textural parameters but that a wide field of overlap exists. In practice this field of overlap is not necessarily a serious matter, since most coastal, barrier bar, and lake dune sands have a standard deviation of less than 0.40 and many desert and inland dune sands do not exceed 0.50, whereas most river sands have a standard deviation in excess of 0.50. Many of the dune sands in the field of overlap of figure 5 are from inland dunes, some of them stable dunes which may have been texturally modified since deposition.

In figure 6 the ratio of mean grain-size of heavy and light minerals has been plotted against the ratio of sorting (standard deviation) for heavy and light minerals. A separation of the fields representing river

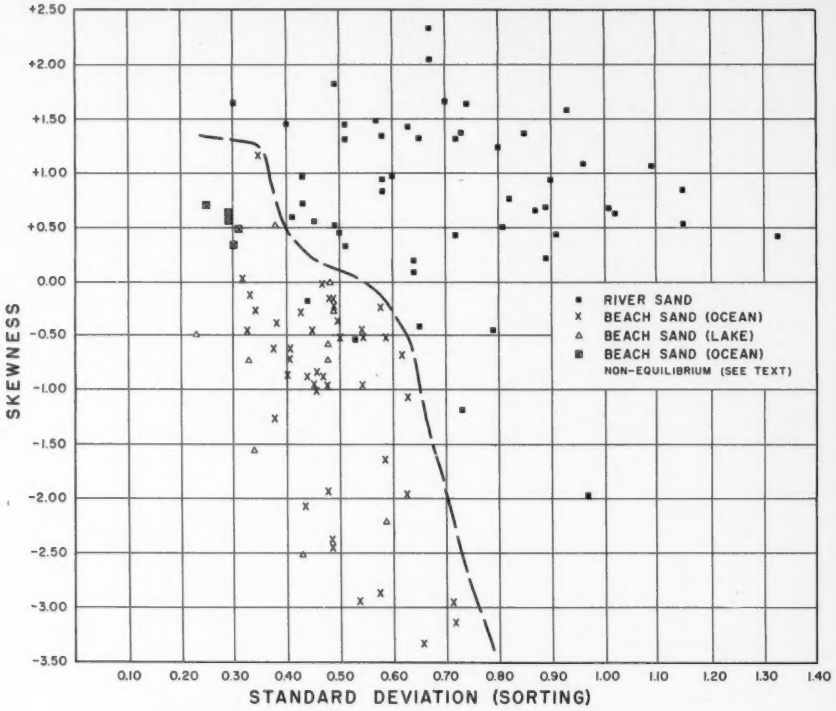

FIG. 4.—Plot of third moment (skewness) and standard deviation, using phi (ϕ) scale, for beach and river sands.

and dune sands results. These samples have been obtained from a Mid-Continent drainage system (Arkansas River and tributaries) and are only characteristic for the river and dune sands of that system. Dune and river sands from other drainage systems which have a different heavy mineral assemblage may give their own characteristic plot, although there is no certainty that for other drainage systems the distribution may not be random.

DISCUSSION OF RESULTS

The textural parameters of sands reflect the mode of transportation and the energy of the transporting medium. The waves which deposit sand on the beach have a greater competency than the wind transporting sand onto dunes or eolian flats. This difference in competency between water and wind explains why none of the dune sand samples studied show mean phi values of less than 1.49ϕ, whereas many beach sand samples do.

Wind and river transportation results from unidirectional flow and may be responsible for the generally positive skewness of dune and river sands. The grain-size distribution of a sand in transport is not known. The upper size limits of grains carried in suspension or by saltation are governed by the competency of the transporting medium. Such limitation does not affect fine particles in transport. This limiting competency may be graphically illustrated. Figure 7 illustrates three dif-

ferent curves of size frequency distribution. Figure 7a is a positively skewed distribution; figure 7b is a symmetrical distribution; and figure 7c is a negatively skewed distribution. The positively skewed curve (fig. 7a) illustrates the limiting competency of dune and river transportation. At the coarse-grained end of the frequency distribution curve the "tail" of the curve is "chopped off" in comparison with a normal distribution curve (figs. 7, a and b).

On a marine beach, sand is exposed to two forces of unequal strength acting in opposite directions. The incoming waves and outgoing wash remove the fine-grained particles. Such winnowing is characteristic of a beach environment. The frequency distribution curve of a winnowed sand lacks the "tail" at the fine-grained end of the curve, and the sand is negatively skewed (fig. 7c).

Accurate third moment (skewness) calculations are tedious and time-consuming to make. For rapid calculations of the sign of skewness, reference should be made to figure 7. In figure 7a, a positively-skewed

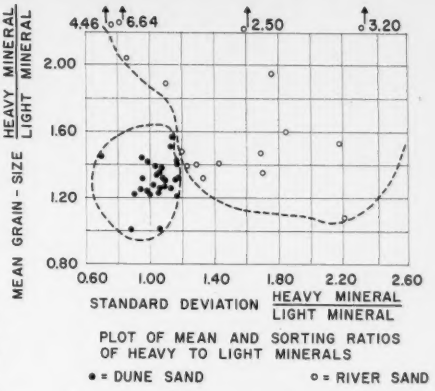

FIG. 6.—Distinction between river and dune sands.

distribution, the mean has a larger phi value than the median, and the difference (mean minus median) is positive. In figure 7b, mean and median are the same, and the difference is zero. In figure 7c, mean minus median results in a negative sign, and a sample which shows this type of distribution is negatively skewed. Since the median value can be obtained rapidly from a cumulative curve and the mean is not too time-consuming to compute, determination of median and mean constitutes a rapid method of obtaining the sign of the skew. This rapid method, however, is not very sensitive.

Mason and Folk (1958) have proposed a formula for obtaining a measure of symmetry of the distribution curve. This measure, which they term skewness (SK_I) (p. 217), is useful since it can be determined rapidly and for the most part indicates correctly the direction of skewness, whether positive or negative; but it lacks the sensitivity of the true third moment.[7]

The bulk properties of the sands, such as the grain-size distribution or measures derived from the grain-size distribution, are ineffective in distinguishing some river sands from dune sands. The fact that river

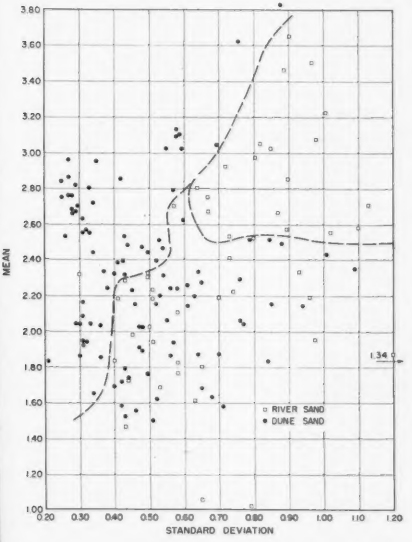

FIG. 5.—Plot of mean and standard deviation, using phi (ϕ) scale, for dune and river sands.

[7] Mason and Folk's skewness formula:

$$SK_I = \frac{\phi 16 + \phi 84 - 2\phi 50}{2(\phi 84 - \phi 16)} + \frac{\phi 5 + \phi 95 - 2\phi 50}{2(\phi 95 - \phi 5)}$$

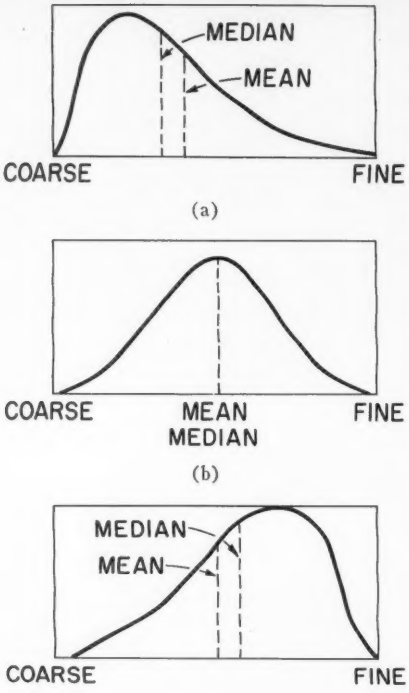

FIG. 7.—Curves showing positively skewed (7a), symmetrical (7b), and negatively skewed (7c) distributions.

and dune sands are skewed in the same direction came as a surprise, since the physical characteristics of the media (viscosity and density) depositing the two types of sand are greatly different. To develop a method which will distinguish between dune and river sands, it is necessary to select properties which reflect the fundamentally different physical characteristics of the two media.

Von Engelhardt (1940) has studied the ratios of the grain-size of quartz to magnetite and quartz to garnet and concludes that it is possible to distinguish dune sands from river and beach sands by this method. On a theoretical basis the ratio of the mean grain-size of heavy to light minerals will differ in wind- and water-laid deposits. The relationship between grain-sizes of different minerals under water transportation can be expressed as follows (Gaudin, 1939, p. 186):

$$\frac{r_1}{r_2} = \frac{D_2 - K}{D_1 - K}$$

where r_1 and r_2 are the radii of particles (spheres) for minerals 1 and 2 (quartz and any heavy mineral), D_1 and D_2 are the specific gravities of the two minerals, and K is the specific gravity of the medium (water). Since the specific gravity of air is negligible in comparison with that of the minerals, it can be neglected and the following equation holds for windlaid materials:

$$\frac{r_1}{r_2} = \frac{D_2}{D_1}.$$

For quartz and magnetite, one of the most abundant of the heavy minerals in sands and sandstone, the following relationship holds:

Settling in water:

$$\frac{r(\text{quartz})}{r(\text{magnetite})} = \frac{5.18 - 1.00}{2.65 - 1.00} = 2.56$$

Settling in air:

$$\frac{r(\text{quartz})}{r(\text{magnetite})} = \frac{5.18}{2.65} = 1.96$$

The ratio $r(\text{quartz})/r(\text{magnetite})$ is much greater for water than for wind. The same kind of relationship can be shown for other heavy minerals (table 2).[8]

To effectively distinguish river sands from dune sands which fall within the field of overlap in figure 5, it is necessary to determine the mean grain-size ratio of quartz and a specific heavy mineral, such as garnet or magnetite. The heavy minerals are separated by conventional techniques, and the grain-size distribution of one or several heavy minerals is determined under the petrographic microscope. The grain-size distribution of quartz can be obtained

[8] These ratios have reference to the movement of quartz and heavy minerals that can be rolled along by water and wind at the same velocity. A second equation which is of importance in comparing water- and wind-laid sands governs the settling velocity of minerals. This equation, which is the Oseen modification of Stokes Law, is more complex than the equation for rolling particles, but it also shows that the ratio $r(\text{quartz})/r(\text{magnetite})$ is much greater for water than for wind.

TABLE 2.—*Ratios of Radii of Quartz and Heavy Minerals of Equal Rolling Velocity*

Mineral	Ratio in Water $\left(\frac{r(\text{quartz})}{r(\text{heavy mineral})}\right)$	Ratio in Air $\left(\frac{r(\text{quartz})}{r(\text{heavy mineral})}\right)$
Magnetite	2.56	1.96
Pyrite	2.39	1.87
Garnet (Almandite)	1.94	1.58
Zircon	2.24	1.78
Tourmaline	1.26	1.16

by sieving, in thin-section according to the method described by Friedman (1958, in press), or by size analysis under the petrographic microscope.

It should be noted that in figure 6 the size ratio of quartz and heavy minerals seems reversed from that given in table 2. In table 2 the size of the heavy mineral is given in the denominator, whereas in figure 6 it is shown in the numerator. This is explained by the fact that the phi (ϕ) system has been employed in figure 6.

If the heavy mineral assemblage in a given drainage system does not vary greatly, a graph of the type shown in figure 6 may be useful in distinguishing dune from river sands. The mean grain-size for the heavy minerals in figure 6 takes in the entire heavy mineral suite and does not discriminate between the mean grain-size of the different mineral species. The same applies to the ratio of the standard deviation. This type of analysis is rapid but crude and is not reliable where there are significant changes in the heavy mineral suite. A more useful method of distinguishing dune from river sands employs the size ratios of quartz and a specific heavy mineral. Von Engelhardt (1940) has shown that for water-laid sands which he studied the r (quartz) $/r$ (garnet) ratio varied between 1.67 and 2.03, whereas in dune sands it ranged from 1.41 to 1.54. For quartz and magnetite, the respective values are 2.14 to 2.38 for water-laid sands and 2.00 to 2.08 for wind-laid sands. Von Engelhardt employed the mode of the grain-size distribution instead of the mean. Figure 8 presents a diagram which indicates how water- and wind-laid sands can be distinguished with the aid of heavy minerals. This figure suggests that the grain-size distribution of the light fraction is of importance in distinguishing between the two types of sand.

CONCLUSIONS

1. Mean grain-size for dune and beach sands is plotted against the third moment (skewness) for these samples. For dune and beach sands, an almost complete separation of the fields representing the two depositional environments results.

2. The grain-size distribution of dune sands is for the most part positively-skewed, whereas that of beach sands is for the most part negatively-skewed, if the phi (ϕ) scale is used in computation.

3. The third moment (skewness) for beach and river sands is plotted against fourth moment (kurtosis) for these samples.

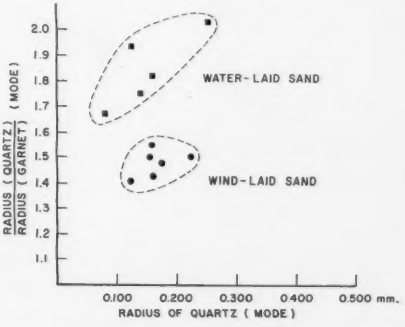

FIG. 8.—Distinction between water- and wind-laid sands (modified from v. Engelhardt).

River sands, like dune sands, are generally positively-skewed, but a number of exceptions to this rule have been observed. The kurtosis is employed to provide a second dimension for the plot, but does not contribute information diagnostic of depositional environment. Skewness is environment-sensitive, whereas kurtosis is not.

Within limitations, river sands can be distinguished from beach sands on the basis of plots of third moment (skewness) against standard deviation (sorting). Beach sands tend to be better sorted than river sands, and thus tend to have lower numerical standard deviation values. Only medium to fine and very fine-grained sands have been employed in this plot since the third moment (skewness) of coarse-grained river sands is inconclusive as an indicator of depositional environment.

4. The positive skewness of dune sands and the negative skewness of beach sands is independent of the mineralogy of the sands. Quartz, carbonate, and gypsum dune sands have been studied as well as quartz, carbonate, and olivine beach sands. For all these sands, the sign of the skewness tends to reflect the environment and does not change with the mineralogy of the sands.

5. None of the dune sand samples studied shows a mean grain-size value lower than 1.49ϕ, whereas almost 40 percent of the beach sand samples have mean values lower than this amount.

6. The fact that wind and river transportation results from unidirectional flow is believed to provide an explanation for the generally positive skewness of dune and river sands. The grain size distribution of the sand that is being transported is not known. However, the upper size limits of the grains that are carried in suspension or by saltation are governed by the competency of the medium, whereas no such limitation affects the fine particles in transport. The result of this limiting competency at the coarse-grained end of the frequency distribution curve is the lack of a "tail," and the "chopped off" appearance at the coarse end in comparison with a normal distribution.

On a marine beach, sand is exposed to two forces of unequal strength acting in opposite directions. These forces are the incoming waves and outgoing wash. They cause the removal of fine-grained particles by winnowing, which is characteristic of the beach environment. Comparison of a normal curve with the distribution curve of a sand that has been winnowed suggests that the "tail" at the fine-grained end of the distribution curve of the sand has been "chopped off" resulting in negative skewness.

7. Dune sands tend to be better sorted than river sands and a plot of standard deviation (sorting) against mean grain-size indicates three fields, one for river sands, one for dune sands, and a third field of overlap. This figure points out that many river sands can be distinguished from dune sands and vice versa on the basis of their textural parameters but that a wide field of overlap exists. In practice this field of overlap is not necessarily a serious matter, since most coastal, barrier bar, and lake dune sands have a standard deviation of less than 0.40 and many desert and inland dune sands do not exceed 0.50, whereas most river sands have a standard deviation in excess of 0.50.

To distinguish river sands from dune sands which fall within the field of overlap, it is necessary to determine the mean grain-size ratio of quartz and a specific heavy mineral, such as garnet or magnetite. A plot of the ratio of mean grain-size of heavy to light minerals against the ratio of sorting (standard deviation) for heavy and light minerals has been found satisfactory to distinguish between dune and river sands of several Mid-Continent rivers.

REFERENCES

ALIMEN, HENRIETTE, AND BEUCHER, FRANCOISE, 1960, Premiers résultats d'une étude statistique de la forme des grains de quartz dans des sables d'origines diverses: Compt. Rend., v. 250, p. 165–167.

BEAL, M. A., AND SHEPARD, F. P., 1956, A use of roundness to determine depositional environments: Jour. Sedimentary Petrology, v. 26, p. 49–60.

BRADLEY, J. S., 1957, Differentiation of marine and sub-aerial sedimentary environments by volume percentage of heavy minerals, Mustang Island, Texas: Jour. Sedimentary Petrology, v. 27, p. 116–125.

ENGELHARDT, WOLF VON, 1940, Die Unterscheidung wasser-und wind-sortierter Sande auf Grund der Korngrössenverteilung ihrer leichten und schweren Gemengteile: Chemie der Erde, v. 12, p. 445–465.

FRIEDMAN, G. M., 1958, Determination of sieve-size distribution from thin-section data for sedimentary petrological studies: Jour. Geology, v. 66, p. 394–416.

———, in press, Comparison of moment measures for sieving and thin-section data in sedimentary petrological studies: Jour. Sedimentary Petrology.

GAUDIN, A. M., 1939, Principles of mineral dressing: McGraw-Hill Book Co., New York, 554 p.

GUGGENMOOS, TH., 1934, Uber Korngroessen-und Kornformenverteilung von Sanden verschiedener geologischer Entstehung: Neues Jb. Miner. etc., Beilage-B., (B), v. 72, p. 429–487.

KELLER, W. D., 1945, Size distribution of sand in some dunes, beaches, and sandstones: American Assoc. Petroleum Geologists Bull., v. 29, p. 215–221.

MASON, C. C., AND FOLK, R. L., 1958, Differentiation of beach, dune, and aeolian flat environments by size analysis, Mustang Island, Texas: Jour. Sedimentary Petrology, v. 28, p. 211–226.

NANZ, R. H., 1954, Genesis of Oligocene sandstone reservoir, Seeligson field, Jim Wells and Kleberg Counties, Texas: Am. Assoc. Petroleum Geologists Bull., v. 38, p. 96–107.

NEWELL, N. D., AND BOYD, D. W., 1955, Extraordinarily coarse eolian sand of the Ica Desert, Peru: Jour. Sedimentary Petrology, v. 25, p. 226–228.

ROGERS, J. J. W., AND STRONG, CYRUS, 1959, Textural differences between two types of shoestring sands: Transactions, Gulf Coast Geol. Societies, v. 9, p. 167–170.

SCHNEIDER, H. E., AND CAILLEUX, ANDRE, 1959, Signification geomorphologique des formes des grains de sables des Etats Unis: Zeitschr. Geomorphologie, v. 3, p. 114–125.

SHEPARD, F. P., 1960, Gulf coast barriers, *in* Recent sediments, Northwest Gulf of Mexico: Am. Assoc. Petroleum Geologists, Tulsa, Okla., p. 197–220.

SHEPARD, F. P., AND MOORE, D. G., 1955, Central Texas Coast sedimentation: Characteristics of sedimentary environment, recent history and diagenesis: Am. Assoc. Petroleum Geologists Bull., v. 39, p. 1463–1593.

APPENDIX

TABLE 1.—*Location of sample*

BEACH SANDS (OCEAN)

Sample No.	Location
	Massachusetts
1	Nauset Beach, Cape Cod, Massachusetts
	New York
2	Fire Island, So. of Mastic Beach, Long Island, N. Y.
3	Fire Island, So. of Mastic Beach, Long Island, N. Y.
4	Fire Island, So. of Mastic Beach, Long Island, N. Y.
5	Westhampton Beach, Long Island, N. Y.
6	Westhampton Beach, Long Island, N. Y.
7	Captree State Park, Long Island, N. Y.
8	Captree State Park, Long Island, N. Y.
9	West Tobay Beach, South Oyster Bay, Long Island, N. Y.
10	West Tobay Beach, South Oyster Bay, Long Island, N. Y.
11	Jones Beach, Jones Beach State Park, Long Island, N. Y.
12	Jones Beach, Jones Beach State Park, Long Island, N. Y.
13	Ocean Parkway and Brighton Beach, Brooklyn, Long Island, N. Y.
14	Coney Island and Brighton Beach, Brooklyn, Long Island, N. Y.
15	Brighton Beach, Brooklyn, Long Island, N. Y.
16	Brighton Beach, Brooklyn, Long Island, N. Y.

TABLE 1.—(*Continued*)

Sample No.	Location
	New Jersey
17	Sandy Hook, N. J.
18	Sandy Hook, N. J.
19	Long Branch, N. J.
20	Belmar, N. J.
21	Pt. Pleasant, N. J.
22	Spring Lake, N. J.
23	Mantoloking, N. J.
24	Normandy Beach, N. J.
25	Seaside Park, N. J.
26	Asbury Park, N. J.
27	Ship Bottom, N. J.
	Florida
28	Miami Beach, Florida
29	Miami Beach, Florida
30	Miami Beach, Florida
31	Miami Beach, Florida
32	Dania, Florida
33	Dania, Florida
34	Coral Gables, Florida
	Alabama
35	Dauphin Island, Alabama
36	Dauphin Island, Alabama
37	Dauphin Island, Alabama
38	Dauphin Island, Alabama
39	Dauphin Island, Alabama
40	Dauphin Island, Alabama
	Louisiana
41	Holly Beach, Louisiana

TABLE 1.—(*Continued*)

Sample No.	Location
	Texas
42	High Island Beach, High Island, Texas
43	Galveston Beach, Galveston Island, Texas
44	Galveston Beach, Galveston Island, Texas
45	Mustang Island, Texas
46	Mustang Island, Texas
47	Mustang Island, Texas
48	Mustang Island Texas
49	Mustang Island, Texas
50	Mustang Island, Texas
51	Northern Padre Island, Texas
52	Northern Padre Island, Texas
53	Northern Padre Island, Texas
54	Northern Padre Island, Texas
55	Southern Padre Island, Texas
56	Southern Padre Island, Texas
57	Southern Padre Island, Texas
58	Southern Padre Island, Texas
59	Del Mar and Boca Chica Beach, Brazos Island, Texas
60	Del Mar and Boca Chica Beach, Brazos Island, Texas
	Bermuda
61	Long Beach, Fort St. Catherine, St. George's Island, Bermuda
62	John Smith's Beach, Bermuda
63	Marley Beach, Bermuda
64	Church Bay, Bermuda
65	Somerset Island, Bermuda
66	Ireland Island, Bermuda
	Bahamas
67	North Bimini Island (west shore)
68	North Bimini Island (west shore)
69	North Bimini Island (west shore)
70	Andros Island (east shore)
71	Andros Island (east shore)
	Mexico
72	Eldesemboque del Rio Concepcion, Gulf of California, Baja, California, Mexico
73	Eldesemboque del Rio Concepcion, Gulf of California, Baja, California, Mexico
	Hawaii
74	Waimanalo Beach, Oahu, Hawaii
75	Diamond Head Beach, Oahu, Hawaii
76	Kahuku Beach, Oahu, Hawaii
77	Makua Beach, Oahu, Hawaii
78	Hanauma Bay near Koko Head, Oahu, Hawaii
79	Hanauma Bay near Koko Head, Oahu, Hawaii
80	Puu Mahana Beach, 3 miles northeast of South Point, Hawaii Island, Hawaii

TABLE 1.—(*Continued*)

BEACH SANDS (LAKE)

Sample No.	Location
	Lake Michigan
1	Straits of Mackinac, Mackinac City, Michigan
2	Straits of Mackinac, Mackinac City, Michigan
3	Indiana Dunes State Park, Indiana
4	Indiana Dunes State Park, Indiana
	Lake Erie
5	Toledo, Ohio
6	Toledo, Ohio
7	Toledo, Ohio
8	Pelee Point National Park, Ontario Canada
9	Pelee Point National Park, Ontario, Canada
	Lake Ontario
10	Hamilton, Ontario, Canada
11	Hamilton, Ontario, Canada
12	Selkirk Shores State Park, Pulaski, New York
13	Selkirk Shores State Park, Pulaski, New York
	Lake Huron
14	Georgian Bay, Parry Sound, Ontario, Canada
15	Georgian Bay, Parry Sound, Ontario, Canada
	Lake Superior
16	Point des Chenes, Sault Ste. Marie, Ontario, Canada
17	Point des Chenes, Sault Ste. Marie, Ontario, Canada
	Lake Simcoe
18	Barrie, Ontario, Canada

DUNE SANDS
(COASTAL AND BARRIER BAR DUNES)

	New York
1	Fire Island, South of Mastic Beach, N. Y.
2	Fire Island, South of Mastic Beach, N Y.
	New Jersey
3	Between Mantoloking and Normandy Beach, N. J.
4	Between Mantoloking and Normandy Beach, N. J.
	North Carolina
5	Between Nag's Head and Kitty Hawk, North Carolina
	Alabama
6	Dauphin Island, Alabama
7	Dauphin Island, Alabama
8	Dauphin Island, Alabama

TABLE 1.—(*Continued*)

Sample No.	Location
	Texas
9	Galveston Beach, Galveston Island, Texas
10	Galveston Beach, Galveston Island, Texas
11	Mustang Island, Texas
12	Mustang Island, Texas
13	Mustang Island, Texas
14	Mustang Island, Texas
15	Mustang Island, Texas
16	Northern Padre Island, Texas
17	Northern Padre Island, Texas
18	Northern Padre Island, Texas
19	Northern Padre Island, Texas
20	Southern Padre Island, Texas
21	Southern Padre Island, Texas
22	Southern Padre Island, Texas
23	Del Mar and Boca Chica Beach, Brazos Island, Texas
24	Del Mar and Boca Chica Beach, Brazos Island, Texas
25	Del Mar and Boca Chica Beach, Brazos Island, Texas
	Oregon
26	Winchester Bay, Oregon
27	Winchester Bay, Oregon
28	Winchester Bay, Oregon
29	Winchester Bay, Oregon
	Bermuda
30	Elbow Beach, Bermuda
31	Elbow Beach, Bermuda
	Mexico
32	Eldesemboque del Rio Concepcion, Gulf of California, Baja, California, Mexico
	LAKE DUNES
	New York
33	Selkirk Beach, near Port Ontario, N. Y.
34	Selkirk Beach, near Port Ontario, N. Y.
35	Selkirk Beach, near Port Ontario, N. Y.
	Michigan
36	Straits of Mackinac, Mackinac City, Michigan
37	Straits of Mackinac, Mackinac City, Michigan
	Indiana
38	Gary, Indiana
39	Michigan City, Indiana
40	Mt. Tom, Indiana Dunes State Park, Indiana
41	Mt. Tom, Indiana Dunes State Park, Indiana
42	Mt. Tom, Indiana Dunes State Park, Indiana
43	Mt. Tom, Indiana Dunes State Park, Indiana

TABLE 1.—(*Continued*)

INLAND DUNES
(RIVER DUNES, DESERT DUNES, ETC.)

Sample No.	Location
	Oklahoma
44	Guthrie, Oklahoma
45	Guthrie, Oklahoma
46	Gate, Oklahoma
47	Gate, Oklahoma
48	Gate, Oklahoma
49	Gate, Oklahoma
50	May, Oklahoma
51	Near Beaver Creek, Cimarron County, Oklahoma
52	Near Beaver Creek, Cimarron County, Oklahoma
53	Near Canton, Oklahoma
54	Bixby, Oklahoma
55	Bixby, Oklahoma
	Texas
56	Monahans Sand Hills State Park, Texas
57	Salt Flat, West Texas
58	Salt Flat, West Texas
	Wyoming
59	Muddy Creek, So. of Rawlins, Wyoming
	New Mexico
60	Cienequilla Creek, near Seneca, New Mexico
61	White Sands National Monument, near Alamogordo, N. M.
62	White Sands National Monument, near Alamogordo, N. M.
63	White Sands National Monument, near Alamogordo, N. M.
64	White Sands National Monument, near Alamogordo, N M.
65	White Sands National Monument, near Alamogordo, N. M.
	Colorado
66	Near Holly, Colorado
67	Great Sand Dunes National Monument, San Luis Valley, Colo.
68	Great Sand Dunes National Monument, San Luis Valley, Colo.
	Kansas
69	Near Garden City, Kansas
70	Near Garden City, Kansas
71	Kendall, Kansas
72	Kendall, Kansas
73	Kendall, Kansas
74	Syracuse, Kansas
75	Syracuse, Kansas
76	Syracuse, Kansas
77	Syracuse, Kansas
	Idaho
78	Near Terreton and Mud Lake, Snake River Plain, Idaho

TABLE 1.—(*Continued*)

Sample No.	Location
79	Near Hamer, Snake River Plain, Idaho
80	Near St. Anthony, Snake River Plain, Idaho
	California
81	Algodones Dunes, Imperial County, California
82	Algodones Dunes, Imperial County, California
83	Algodones Dunes, Imperial County, California
84	Algodones Dunes, Imperial County, California
85	Algodones Dunes, Imperial County, California
86	Algodones Dunes, Imperial Count California
87	Algodones Dunes, Imperial County, California
88	Algodones Dunes, Imperial County, California
	Canada
89	Ft. Vermilion, Tsp. 107, R14W of 5, Alberta, Canada
90	Ft. Vermilion, Tsp. 108, R14W of 5, Alberta, Canada
91	Culp, Tsp. 77, R23W of 5, Alberta, Canada
92	Iosegun Lake, Tsp. 64, R20 W of 5, Alberta, Canada
93	Nestow, Tsp. 60, R24W of 4, Alberta, Canada
94	Winterburn, Tsp. 52, R26W of 4, Alberta, Canada
95	Wainwright, Tsp. 43, R6W of 4, Alberta, Canada
96	Hays, Tsp. 12, R13W of 4, Alberta, Canada
97	Hays, Tsp. 12, R13W of 4, Alberta, Canada
98	Bindloss, Tsp. 20, R2W of 4, Alberta, Canada
99	Medicine Hat, Tsp. 12, R4W of 4, Alberta, Canada
100	Grande Prairie, Tsp. 70, R6W of 6, Alberta, Canada
101	Smith, Tsp. 70, R27W of 5, Alberta, Canada
102	Whitecourt, Tsp. 61, R13W of 5, Alberta, Canada
103	Jasper, Tsp. 45, R1W of 6, Alberta, Canada
104	Bickerdike, Tsp. 51, R19W of 5, Alberta, Canada
105	Morningside, Tsp. 42, R26W of 4, Alberta, Canada
106	Red Deer, Tsp. 38, R27W of 4, Alberta, Canada
107	Rocky Mountain House, Tsp. 40, R8W of 5, Alberta, Canada

TABLE 1.—(*Continued*)

Sample No.	Location
108	Retlaw, Tsp. 13, R19W of 4, Alberta, Canada
	Sahara Desert, French North Africa
109	Foum Seiada, Valée de la Saoura, French North Africa
110	Foum Seiada, Valée de la Saoura, French North Africa
111	Foum Seiada, Valée de la Saoura, French North Africa
112	Foum Seiada, Valée de la Saoura, French North Africa
113	Erg Djemel, French North Africa
114	Erg Djemel, French North Africa
	RIVER SANDS[9]
	Alabama
1	Mobile River, ¼ mile downstream from Tombigbee River, Ala.
2	Alabama River, south of Gainestown, Alabama
3	Alabama River, about ½ mile west of Clairborne, Alabama
4	Styx River, about 5 miles ENE of Rosinton, Alabama
	Arkansas
5	Arkansas River, Fort Smith, Arkansas
6	Arkansas River, Fort Smith, Arkansas
	Florida
7	Escambia River, on State Highway 184 about 4 miles east of junction with U. S. Highway 29, Florida
8	Escambia River, about 2 miles east of Century, Florida
9	Yellow River, about 7 miles SE of Milton, Florida
10	Shoal River, about 4 miles south of Crestview, Florida
	Georgia
11	Coosa River at Coosa, Georgia
12	Tallapoosa River at Tallapoosa, Georgia
	Illinois
13	Illinois River, Havana, Illinois
14	Illinois River, Havana, Illinois

[9] The 55 river sand samples listed in this table are comparable in size range to the dune and beach sands studied. In addition samples of coarse-grained sand, gravelly sand, and gravel were collected from the Hudson River in New York, Arkansas River in Colorado, and Kansas, and Ohio and Little Miami Rivers in Ohio. These coarse-grained river sands and gravels had variable, unpredictable skewness characteristics and could not be employed in characterizing the terminal environment. They are therefore not included in this table.

TABLE 1.—(*Continued*)

Sample No.	Location
15	Quiver Beach, 2½ miles north of Havana, Illinois
16	Mississippi River, Hamilton, Illinois
17	Mississippi River, Hamilton, Illinois
18	Mississippi River, Hamburg, Illinois
19	Mississippi River, Hamburg, Illinois
	Kentucky
20	Ohio River, Ghent, Kentucky
21	Ohio River, Ghent, Kentucky
22	Ohio River, Carrollton, Kentucky
23	Ohio River, Carrollton, Kentucky
	Louisiana
24	Bogue Chitto River, 6 miles east of McComb, Mississippi
25	Bogue Chitto River, 1 mile west of Clifton Louisiana
	Mississippi
26	Tohoutacatouffa River, north of Biloxi, Mississippi
27	Pascagoula River, about 2 miles east of Benndale, Mississippi
28	Pearl River, 2 miles west of Columbia, Mississippi
	Missouri
29	Mississippi River, near Boschertown, Missouri
30	Mississippi River, near Boschertown, Missouri
31	Missouri River, Dutzow, Missouri
32	Missouri River, Dutzow, Missouri
33	Missouri River, Dutzow, Missouri

TABLE 1.—(*Continued*)

Sample No.	Location
	Oklahoma
34	Arkansas River, Jenks, Oklahoma
35	Arkansas River, Jenks, Oklahoma
36	Small creek flowing into Arkansas River, 6 miles south of Sallisaw, Oklahoma
37	Arkansas River, Webbers Fall, Oklahoma
38	Arkansas River, Webbers Fall, Oklahoma
39	Cimarron River, Oilton, Oklahoma
40	Cimarron River, Oilton, Oklahoma
41	Cimarron River, 2 to 3 miles north of Guthrie, Oklahoma
42	Beaver Creek, 3½ miles south of Gate, Oklahoma
43	North Canadian River, near Eufaula, Oklahoma
44	North Canadian River, Oklahoma City, Oklahoma
45	North Canadian River, Oklahoma City, Oklahoma
46	Small Creek, near Broken Arrow, Oklahoma
47	Small Creek, near Broken Arrow, Oklahoma
48	Small Creek, near Broken Arrow, Oklahoma
	Texas
49	Brazos River, Texas
50	San Antonio River, Texas
51	Nueces River, Texas
52	Frio River (tributary of Nueces River), Texas
53	Guadalupe River, Texas
54	Colorado River, Texas
	Virginia
55	North River, near Stokesville, Virginia

JOURNAL OF SEDIMENTARY PETROLOGY, VOL. 31, NO. 4, PP. 530–533
FIG. 1, DECEMBER, 1961

DISCRIMINATING BETWEEN REFRACTORY AND NON-REFRACTORY QUARTZITE BY QUANTITATIVE PETROGRAPHY[1]

G. V. WOOD
Pennsylvania State University, University Park, Pa.[2]

ABSTRACT

The Tuscarora Quartzite is the most important source of silica refractory raw material in Pennsylvania. Quantitative estimations of quartz %, silica cement %, Fe_2O_3 and mean length of quartz grains, when applied in the form of a discriminant function, are found to differentiate between the refractory and non-refractory occurrences.

INTRODUCTION

The discriminant function as first described by Fisher (1936) may be viewed as the definition of a hyperplane which best separates two populations in "p" dimensional space, where p = the number of variables under consideration.

Emery (1954) was the first to use this technique in discriminating between the oil-bearing Berea Sandstone in Ohio and the barren Pocono Sandstone of Pennsylvania. It was later used by Hulbe (1957), Griffiths (1957), and Stanonis (1958).

This paper is concerned with a method for discriminating between the refractory and non-refractory portions of the Tuscarora Quartzite (Lower Silurian) of Pennsylvania. Stratigraphically the Tuscarora Quartzite is underlain by the Juniata Red Beds (Upper Ordovician) and overlain by the Castanea Sandstone (and Rose Hill Shale). The outcrop forms the crest of the dominant ridges in the Valley and Ridge physiographic province in Pennsylvania and is characteristically masked by a mantle of white quartzite boulders.

SAMPLING LOCALITIES

The two populations under investigation were:

T-1.—Refractory Tuscarora Quartzite, Harbison-Walker Quarry, Port Matilda, Centre Co., Pennsylvania (20 samples).

T-2.—Non-Refractory Tuscarora Quartzite.

i.—Rt. 22, Mt. Union, Huntingdon Co., Pennsylvania (10 samples).

ii.—Rt. 30, Cove Summit, Franklin Co., Pennsylvania (10 samples).

(T-2) is a composite population selected to provide a range of the Tuscarora Quartzite not used as refractory raw materal. The actual sampling was done in such a way that a complete range of the available grain size was included with an emphasis on the extremes, as recommended by Mood (1950, p. 296) to give a stable multiple regression estimate. It is emphasized that no selective procedure was used in the sampling of T-1 and a certain degree of overlap with T-2 is to be expected.

GENERAL PETROGRAPHY

T-1 is a well indurated fine-grained quartzite which has a silica cement. In hand specimen it exhibits a conchoidal-type fracture and ranges in color from reddish-brown to dark grey.

The quartz grains are well rounded, well sorted, and essentially lie within the fine sand category. Quartz with normal extinction is dominant while grains with undulose extinction are rare. Finely divided flakes of sericite-illite are the dominant micaceous element and rarely comprise more than 5 percent of the total volume. This mica has two habits: (1) lying along the margin of the quartz grains and bound to them by silica cement, and (2) occurring in intergranular pockets, sometimes intimately intermixed with cement. The first habit is the principal mode of occurrence. Ferruginous dust also serves to emphasize the outlines of the quartz grains. Composite rock fragments, either quartzose or micaceous, are rare.

Within population T-2 no apparent differ-

[1] College of Mineral Industries Contribution No. 60-14, Pennsylvania State University, University Park, Pa., U.S.A.

[2] Present address: The British Petroleum Co. Ltd., BP Research Centre, Chertsey Road, Sunbury-on-Thames, Middlesex, England.

ences were observed between exposure i and the Port Matilda samples except for the absence of ferruginous staining in the former. Exposure ii was more friable and coarser grained than the quartzite from the other outcrops. Except for a small increase in the proportion of micaceous rock fragments and kaolinite clots, no mineralogical differences could be detected.

SELECTION OF VARIABLES

The physical specifications for refractory silica brick raw materials were set out by Davies (1952). It was said that the rock should be a quartzite that possesses an even grain size and compact texture which should fracture independently of grain size on crushing. The chemical specifications were outlined by Moore and Taylor (1926) who, using the Tuscarora Quartzite as the type rock, gave the following permissible values:

	Maximum (%)	*Minimum* (%)
SiO_2	98.76	96.78
Al_2O_3	1.14	0.78
Fe_2O_3	1.78	0.70
CaO	0.14	0.05
TiO_2	0.16	0.02

The modern requirements are much more stringent, especially as to the percent of Al_2O_3 allowable.

The Al_2O_3 and Fe_2O_3 content of populations T-1 and T-2 was determined by emission spectroscopy and the following results were obtained (values shown as $\log_{10}$ parts per million):

	Fe_2O_3		Al_2O_3	
	$\bar{X}$	S	$\bar{X}$	S
T–1	3.745	0.383	3.957	0.322
T–2	2.985	0.274	3.919	0.290

$\bar{X}$ = mean value and S = standard deviation.

The subsequent analysis of variance shows a significant difference at the .01 probability level in the Fe_2O_3 content of the two populations but no significant difference exists in the Al_2O_3 content. The Fe_2O_3 content (X4) must be considered in discriminating between the two populations.

The other variables were selected arbitrarily from those making the principal contributions to the multiple regression relationship, using bulk density as the dependent variable. They were:

X_1[3] = Quartz content (%)
X_2[3] = Silica cement content (%)
X_3[4] = Length of the long axis ("a") of quartz in phi units (as defined by Griffiths and Rosenfeld, 1950).

The first two moments of these variables are:

	X_1 (Quartz)		X_2 (Silica cement)		X_3 ($\bar{X}_{a\phi}$)	
	$\bar{X}$%	S%	$\bar{X}$%	S%	$\bar{X}$	S
T-1	77.86	3.31	14.51	3.38	1.948	0.532
T-2	82.06	4.16	12.59	4.16	1.836	0.454

STATISTICAL BACKGROUND

The calculation of the discriminant function is analogous to that used for multiple regression analysis (see Rao, 1952, table 7B), except that the dependent variable is now the differences between the means of the selected variables. One of the most important assumptions is that the classification into groups can be made without error (Quenouille, 1952, p. 188).

Goulden (1952, p. 380) has shown that the discriminant function is equally valid when calculated from the correlation coefficients and this method was followed during the present investigation.

RESULTS

The variables were arranged in order of magnitude of the differences between the means of the two populations, which acted as the dependent variable. These were:

X_1 (Quartz %) + 4.20
X_2 (Silica cement %) − 1.92
X_4 (Fe_2O_3 − $\log_{10}$ ppm) − 0.76
X_3 (Size $\bar{X}a\phi$) − 0.112

The obtained discriminant was as follows:

$$Z = 7.519766\ X_1 + 2.506222\ X_2 + 2.200192\ X_4 + 2.481266\ X_3. \quad (1)$$

These coefficients have no absolute value and only their proportions are fixed; therefore, it is customary to reduce the smallest to unity (Griffiths 1957) i.e., $Z = 3.418X_1$

[3] Determined by point-count analysis (see Chayes, 1956).
[4] Determined by direct measurement from a thin section enlarged by a Zeiss "Prado" Projector.

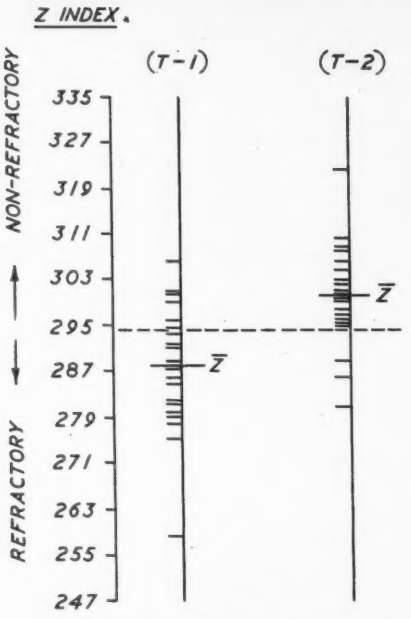

FIG. 1.—*Z* values (and *Z* means) for refractory (T-1) and non-refractory (T-2) outcrops of the Tuscarora Quartzite.

$+1.139\ X_2+X_4+1.128\ X_3$ (2). The mean values for both populations combined were substituted in the equation (2) giving $Z=294.236$ as the Z index best separating the refractory (T-1) from the non-refractory (T-2) populations. The means for each population were then substituted in turn in (2) giving the mean Z values for each population;

$$(T\text{-}1)-Z_1=288.595$$
$$(T\text{-}2)-Z_2=299.877.$$

Fig. 1 shows the distribution of Z values for the individual samples. The refractory (T-1) and the non-refractory (T-2) samples show five and three misclassifications respectively.

By far the most important variable in delimiting refractory raw material in the Tuscarora Quarzite is the quartz content. The Z value decreases for the refractory quartzite and it can be seen that with a decrease in the amount of quartz the sample shifts towards a refractory index. This is contrary to normal expectation.

TABLE 1.—*Model for the analysis of variance testing the significance of the discriminant equation*

S of V.	$H_0: \beta_1=\beta_2=\beta_3=\beta_4=0$		
	d.f.	S.S.	M.S.
Discriminant	p	λ^2R^2	$\lambda^2\frac{R^2}{p}$
Unaccounted for Residual	$N-p-1$	$\lambda^2(1-R^2)$	$\frac{\lambda^2(1-R^2)}{N-p-1}$
Total	$N-1$	λ^2	

$$\text{Where } \lambda^2=\frac{N_1N_2}{N_1+N_2} \text{ and}$$

$$R^2=\frac{N_1N_2\sum b_iQ_i}{N_1+N_2+N_1N_2\Sigma b_iQ_i}$$

To test the effectiveness of the discriminant function, Fisher (1936) set up a test of the null hypothesis, $Ho:\beta_1=\beta_2=\beta_3=\beta_4=0$ in the form of an analysis of variance (table 1). This analysis (table 2) gives an "F" ratio of 2165, which is highly significant at the .01 level and leads to the rejection of the null hypothesis, i.e., the discriminant is highly effective in separating the two populations.

TABLE 2.—*Analysis of variance of discriminant function differentiating refractory and non-refractory Tuscarora Quarztite*

S. of V.	d.f.	S.S.	M.S.	F
Discriminant	4	99.599	24.899	2165**
Residual	35	.401	.0115	
Total	39	100.000		

CONCLUSIONS

The discriminant index has proved to be a powerful tool in differentiating between the refractory and non-refractory Tuscarora Quartzite of Pennsylvania.

However, it must be pointed out that the Al_2O_3 content is usually a critical variable. Unless it can be shown to be related to the

other variables under consideration (in this case the correlation coefficient of Fe_2O_3: Al_2O_3 was positive and significant for both populations), it should be used in any further use of this method for delimiting potentially useful refractory raw material.

ACKNOWLEDGMENTS

I would like to thank Professor J. C. Griffiths for reading the manuscript and for his interest throughout the course of the work. Professor P. Allen kindly read the manuscript.

REFERENCES

CHAYES, F., 1956, Petrographic modal analysis: John Wiley and Sons, New York, 113 p.

DAVIES, W., 1952, Low alumina silica brick raw materials: Trans. Brit. Ceram. Soc., 51, p. 95–171.

EMERY, J. R., 1954, The application of a discriminant function to a problem in petrology: Unpublished M.S. Thesis, Department of Mineralogy, The Pennsylvania State University.

FISHER, R. A., 1950, The use of multiple measurement in taxonomic problems (1936), Paper 32, *in* Contributions to mathematical statistics: John Wiley and Sons, New York, 656 p.

GOULDEN, C. H., 1952, Methods of statistical analysis: 2nd ed., John Wiley and Sons, New York, 467 p.

GRIFFITHS, J. C., 1957, Petrographic investigation of the Salt Wash sediments: United States Atomic Energy Commission RME-3151.

GRIFFITHS, J. C. AND ROSENFELD, M., 1950, Progress in the measurement of grain orientation in the Bradford Sand: Penn. State University Min. Ind. Exp. Sta. Bull., 56, p. 202–236.

HULBE, C. W., 1957, An investigation of the size and shape of quartz grain, Pedro Beach, California: Unpublished M.S. Thesis, Department of Mineralogy, The Pennsylvania State University.

MOOD, H. M., 1950, Introduction to the theory of statistics: McGraw Hill Book Co., New York, 433 p.

MOORE, E. A. AND TAYLOR, T. G., 1926, The silica refractories of Pennsylvania: Pennsylvania Topographic and Geological Survey, Bulletin 113, Harrisburg.

QUENOUILLE, M. H., 1952, Associated measurements: Butterworths Scientific Publications, London, 242 p.

RAO, C. R., 1952, Advanced statistical methods in biometric research: John Wiley and Sons, New York, 390 p.

STANONIS, F. L., 1958, The petrology of the Chipmunk Sand and its relationship to reservoir properties: Unpublished Ph.D. Thesis, Department of Mineralogy , The Pennsylvania State University.

JOURNAL OF SEDIMENTARY PETROLOGY, VOL. 31, NO. 4, PP. 534–545
FIGS. 1–12, DECEMBER, 1961

SUBMARINE GEOLOGY OF THE SANTA ROSA-CORTES RIDGE

E. UCHUPI[1]
University of Southern California

ABSTRACT

The Santa Rosa-Cortes Ridge is located 60 miles west of San Pedro, California in a submerged basin and range province known as the "Continental Borderland." The ridge is flanked by two steep slopes which are believed to be fault scarps, and it is cut by transverse depressions that probably were formed by erosion along fault lines or have a structural origin.

Gravel composed of igneous, metamorphic, and sedimentary materials is present atop the ridge. Several lines of evidence suggest that it was deposited during the Pleistocene. Rocks obtained from the ridge range in age from Eocene to Late Miocene. Middle and Upper Eocene shales, sandstones, and siltstones are limited to the area south of Begg Rock. Miocene shales were recovered from the rest of the ridge.

The present distribution of bottom sediments is believed to be the result of (1) deposition during the Pleistocene of coarse detrital sediments at depths too great to be explained by present-day currents, and (2) post-Pleistocene accumulation of calcareous organic sediments over most of the ridge and medium to very fine sands immediately off the shores of the islands.

INTRODUCTION

The sea floor off southern California is a submerged basin and range province that has been designated as the "Continental Borderland" (Shepard and Emery, 1941). It extends seaward for approximately 150 miles and is terminated on the west by the continental slope. One-fourth of this borderland consists of 13 basins which have a total area of 6550 statute square miles. The remaining three-fourths consists of topographic highs such as shelves, banks, and ridges.

The most prominent of these topographic highs is the Santa Rosa-Cortes Ridge located 60 miles west of San Pedro, California (fig. 1). It extends from Santa Rosa Island on the northwest to Cortes Bank on the southeast, a distance of about 130 miles. The ridge rises 900 feet above sea level on San Nicolas Island and to within 15 feet of sea level on Cortes Bank. Much of the remaining part is shallower than 600 feet with the greatest depth of 1530 feet being found in a transverse saddle midway between the islands of San Nicolas and Santa Rosa.

This report is a detailed study of the section of the Santa Rosa-Cortes Ridge between San Nicolas and Santa Rosa Islands. Although separated from the ridge by Santa Cruz Canyon, the insular shelf of Santa Cruz Island was also included in this study. A total of 50 bottom photographs and 285 samples were available from this area. These include 256 scoop fish and snapper samples collected by F. P. Shepard and K. O. Emery in the course of acoustic studies conducted by the University of California Division of War Research during World War II, and 12 dredge samples secured from the Allan Hancock Foundation collection. The remainder are 17 orange peel grab samples collected aboard the Hancock Foundation oceanographic research vessel "Velero IV" during two sampling expeditions to the Santa Rosa-Cortes Ridge.

The results obtained from the study of the above samples were augmented by data from reports by Trask (1931), Emery and Shepard (1945), Norris (1951) and Menard *et al.* (1954). The sampling stations from the last two reports are restricted to the area south of Begg Rock, and those from the first two to the area near Santa Cruz Canyon. The positions of the sampling stations given by all of these reports and the positions of the samples available to the writer provide a good degree of coverage (fig. 2).

PREVIOUS INVESTIGATIONS

The Santa Rosa-Cortes Ridge has been included in a number of reports dealing with regional investigations of the general sea floor off southern California. However, none

[1] Manuscript received October 11, 1960.

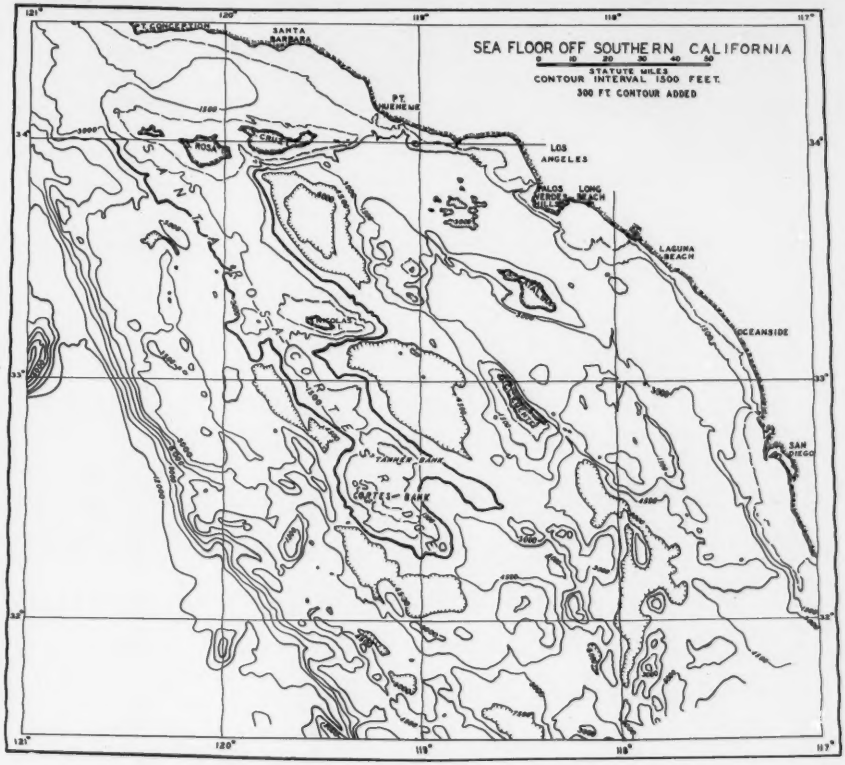

FIG. 1.—Bottom topography off the southern California coast showing the location of the Santa Rosa-Cortes Ridge.

of these reports place any particular emphasis on the ridge. Trask (1931) made a study of the sediments of the Channel Island region and the ridge was included in a discussion of the recent sediments off the coast of southern California by Revelle and Shepard (1939). Shepard and Emery (1941) briefly mentioned the ridge in a report dealing with the topography and structure of the borderland, and they also described rocks from two localities in this area (Emery and Shepard, 1945). Norris (1951) made a study of the recent sediments in the San Nicolas region, and Menard *et al* (1954) made a geological reconnaissance of two square miles of the sea floor north of San Nicolas Island using aqualungs. More recently Resig (1958) included the eastern flank of the ridge in her ecological study of the Foraminifera of the Santa Cruz basin.

BOTTOM TOPOGRAPHY

Information concerning the topography of the Santa Rosa-Cortes Ridge was obtained from photographic copies of 12 original United States Coast and Geodetic Survey field sheets. Contours were drawn on the copies and later reduced to a common scale. The ridge has been contoured at a 10 fathom interval to a depth of 100 fathoms and at a 50 fathom interval beyond this depth (fig. 2).

Two prominent faults flank the ridge on the east and west (Emery, 1960). The faults

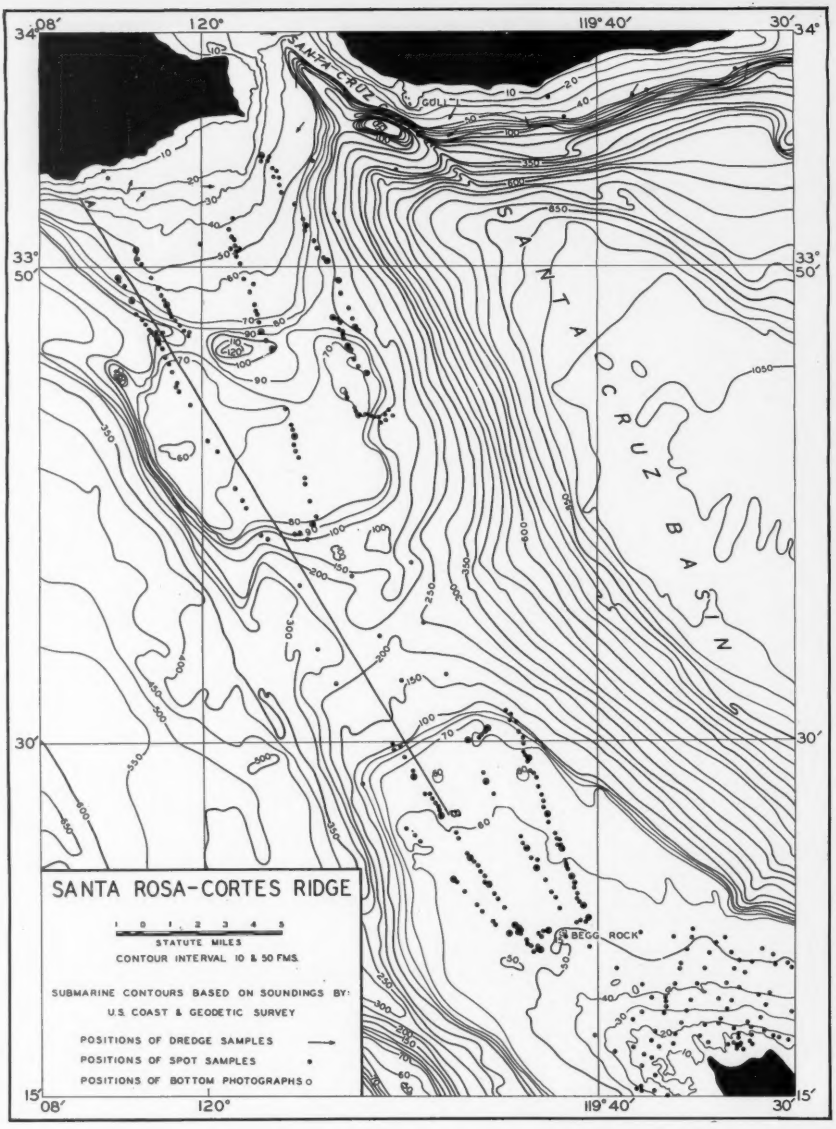

FIG. 2.—Bottom contour chart of the Santa-Rosa-Cortes Ridge. Line AB indicates the location of the echo sounding trace shown in figure 3.

are inferred from the relative straightness and steepness of the ridge which slopes reach a maximum of 12 degrees on the eastern side and 6 degrees on the western side. A deep saddle that transects the ridge in a east-west direction and a small depression south of Santa Rosa Island are the other striking topographic features (fig. 2 and 3). The latter features, in contrast to the slopes flanking the ridge which have a northwest-southeast trend, seem to parallel the east-west alignment of the northern Channel Islands. Consequently, they may have been formed by erosion along a fault line or may have a structural origin.

An echo sounding trace taken with an Edo recorder indicates that the surface of the ridge north of the saddle is rather smooth with small prominences rising above its general surface that may represent rock areas (fig. 3). Six submarine terraces can be recognized in this area. The seaward edges of these features are at depths of 180, 240, 360, 390, 420, and 480 feet. Farther south, within the saddle, a terrace occurs on both sides at a depth of 660 feet. In contrast to the northern area, only three terraces can be observed in the more southerly part of the ridge. Emery (1958), who made a regional study of the submarine terraces of the southern California coast, believed that they are wave cut features carved during the Wisconsin.

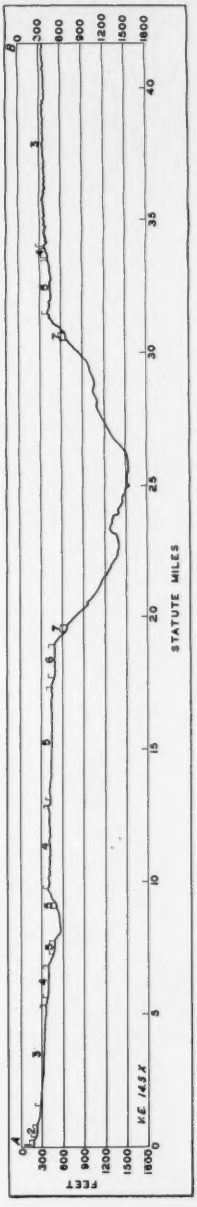

FIG. 3.—Echo sounding trace of the Santa Rosa-Cortes Ridge. Symbols ⌜ and ⌝ bracket inner and outer edges of the terraces. For location of trace see figure 2.

OCEANOGRAPHY

Oceanographic data were not collected during this study and the following brief description of the oceanographic conditions existing over the Santa Rosa-Cortes Ridge is based on a report by Fleming (1938). He reported two currents in the region. A southeasterly current, the eastern portion of the California Current, with a velocity of 0.5 to 0.7 feet per second, is active in the west, whereas the northerly part of the Southern California Counter Current with a velocity of 0.3 to 0.5 feet per second prevails east of the ridge. Vertical distribu-

tion of salinity, temperature, oxygen, and the thickening of the convection layer from the Counter Current zone to the Offshore zone indicate that the interface of these two conflicting currents, the Trough zone located over the ridge, is an area of much turbulence and lateral mixing. This lateral mixing is produced by eddies, some of which reach a diameter of 100 miles.

Throughout the area, the surface waters are saturated with oxygen, but below 600 feet the oxygen decreases rapidly. The ridge is also a zone containing nutrient-rich water which supports a dense crop of phytoplankton. Concentrations greater than 100,000 diatoms per liter of water have been reported from this area (Emery, 1960).

In summary, the Santa Rosa-Cortes Ridge is a zone of conflicting currents that produce eddies and considerable turbulence which may be important in suspending and transporting sediments.

LITHOLOGY

Islands

The sedimentary rocks in Santa Cruz, Santa Rosa, and San Nicolas Islands range in age from Late Cretaceous to Pleistocene (Kew, 1927; Bremner, 1932; Kemnitzer, 1933 and Norris, 1951). Medium to coarse sandstones and light gray shales of Upper Cretaceous age occur only at the southern end of Santa Rosa. Eocene well bedded sandstones, thin beds of sandy shales and occasional lenses of conglomerate of Eocene age are limited to Santa Cruz and San Nicolas. Oligocene rocks appear to be absent from all three islands, and the Miocene rocks cropping out in Santa Rosa and Santa Cruz consist of gray sandstones, tuffaceous and siliceous shales, and local lenses of conglomerate. Buff sands and coarse terrace deposits of Pleistocene age are present in all three islands.

Triassic (?) metamorphic rocks and a fine-grained hornblende diorite of Jurassic (?) age occur within the basement complex of Santa Cruz. Miocene volcanics consisting of rhyolite flows, rhyolite breccias and tuffs, andesite breccias, and olivine basalt flows are found throughout the area of this island. There are no metamorphic rocks on either Santa Rosa or San Nicolas, and the igneous rocks present on Santa Rosa are Upper Miocene agglomerates containing boulders of basalt and rhyolite, rhyolite flows, and basalt intrusions. The only igneous rock on San Nicolas is a small diabase dike on the southeast end of the island.

Santa Rosa-Cortes Ridge

Rock fragments were obtained from 170 samples from the Santa Rosa-Cortes Ridge. They can be divided into three classes: rocks essentially in place, transported rocks, and authigenic rocks. The rocks in place were identified on the basis of angularity, fragility, and similarity in composition (Emery and Shepard, 1945). Well rounded igneous, metamorphic, and sedimentary rocks and fragments of varied lithology that showed no relationship to the adjacent rock samples were considered as having been transported. Authigenic rocks are limited to phosphorite.

Rocks occur in place throughout most of the ridge (figs. 4 and 5). Basalt has been reported by Emery and Shepard (1945) from the Santa Cruz Canyon area, and a greenish buff sandstone was recovered south of Santa

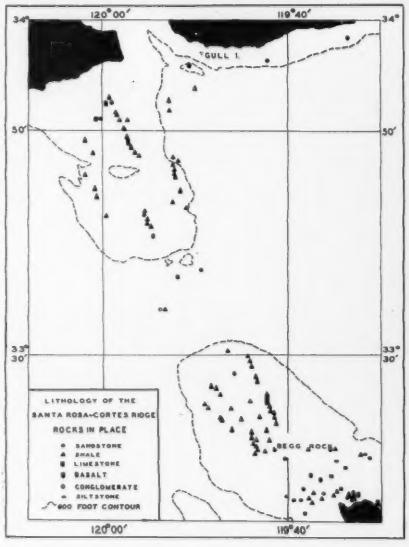

FIG. 4.—Areal distribution of bedrock, Santa Rosa-Cortes Ridge.

Cruz. Because fossiliferous material was not obtained from this area, the age of the rocks is not known. A Miocene age, however, is assigned the basalt on the basis of its lithologic similarity to the Miocene extrusives of Santa Cruz Island (Emery and Shepard, 1945).

The majority of the rock samples from Santa Rosa to Begg Rock are light to gray silty shales. The rest are very fine-grained sandstones, arenaceous limestones, and a poorly cemented conglomerate. Only the shales are fossiliferous and they contain Foraminifera indicative of the Zemorrian, Saucesian, Relizian and Mohnian stages of the Miocene (fig. 6).

Begg Rock, located five miles northwest of San Nicolas Island, is made up of two rocks, a flat rock no more than three feet above sea level, and a pinnacle which rises 15 feet above the surface of the sea (Norris, 1951). The composition of the flat rock is not known, but the pinnacle is composed of a fine grained rhyolite showing value flow structure (Kemnitzer, 1933).

The rocks south of Begg Rock are micaceous, yellow-buff sandstones, and light gray shales and siltstones. They are lithologically similar to the sedimentary rocks exposed on San Nicolas Island (Norris, 1933). Therefore, they are considered as

FIG. 5.—Bottom photograph of a submarine rock outcrop. Loc. : lat. 33° 47.4′ N, long. 119° 52′ W. Depth: 642 feet. Area: 16 square feet.

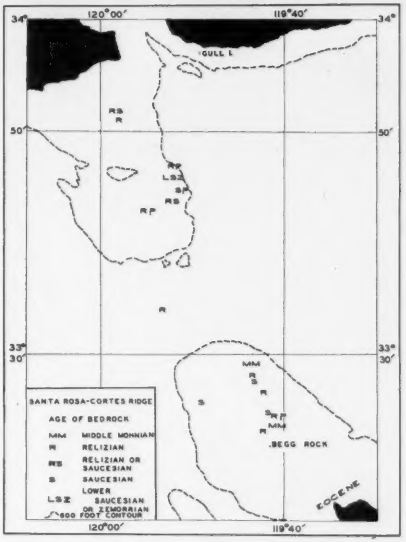

FIG. 6.—Areal distribution and geologic age of fossiliferous material.

Middle to Late Eocene in age.

Some of the samples contain well rounded to subrounded clasts which range in size from granules to cobbles and are believed to have undergone transporation from their outcrops. These fragments are mainly basalt, occasional pebbles of sandstone, shale, siltstone, and andesite, and a few rare granules of metamorphic quartzite (fig. 7).

The transported rocks must have been derived from outcrops in the area, from nearby islands, from past land masses, or from a combination of these sources. The transported rocks immediately northwest of San Nicolas are similar to the sedimentary rocks on the island and those cropping out on the sea floor. Consequently, they must have been derived from one or both of these sources. The basalt on Santa Rosa and Santa Cruz Islands could have been the source of the igneous material off the coast of San Nicolas, but the absence of basalt pebbles from the saddle itself and the area immediately south of it suggests that it was not derived from either of these two sources. It probably originated from the same source as the basalt and quartzite

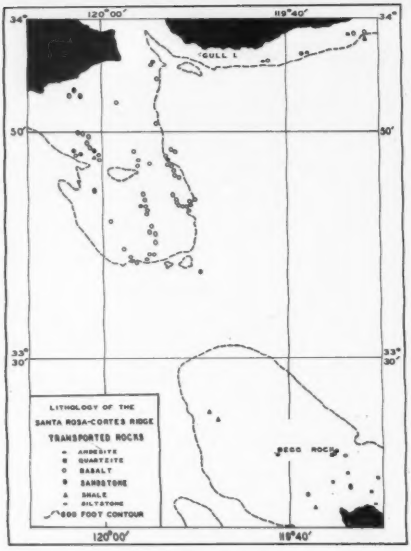

FIG. 7.—Areal distribution of transported rocks.

pebbles that occur in the terraces of San Nicolas Island. The terrace material becomes coarser to the southwest indicating a source to the southwest. That it could have been derived from an earlier land mass to the southwest of San Nicolas was partly verified by Holzman (1952) who collected a number of samples containing basalt on Cortes Bank.

The igneous material from north of the saddle was probably derived from Santa Rosa or Santa Cruz islands or from both of these two sources. The sedimentary rock from this area was probably derived from outcrops nearby or from sedimentary rocks on Santa Rosa and Santa Cruz.

Several lines of evidence suggest that the transported rocks were deposited during the Pleistocene when sea level was lower than today. The transported rocks rest on a series of wave cut terraces and therefore must have been deposited at the same time or after the formation of these surfaces. Zeuner (1945) and Emery (1958) suggested that erosion at such depths may have occurred during the lowering of sea level during the Pleistocene glacial stages. The large size of most of the rocks indicates that they could not have been transported by present-day currents, suggesting further that they were deposited during the Pleistocene.

The only authigenic rock collected from the Santa Rosa-Cortes Ridge was phosphorite. It was found in 42 samples from the Santa Rosa area, in 5 samples from the saddle, and in 33 samples from the San Nicolas area (fig. 8).

The phosphorite occurs as smoothly rounded nodules that range in size from 1 mm to 30 centimeters. Most of the nodules have no internal structure, but a few show concentric layers and include some manganese oxide that indicate discontinuous deposition. Not all of the nodules were pure phosphate; most contain pebbles and granules of clastic material. Detrital sand is a common constituent of most of the nodules.

Dietz, Emery, and Shepard (1942) suggested that the phosphorite off the southern California coast was formed *in situ* by chemical precipitation and an examination of the phosphorite in this area bears their theory out. An *in situ* origin is indicated by (1) the lack of abrasion, (2) the polished

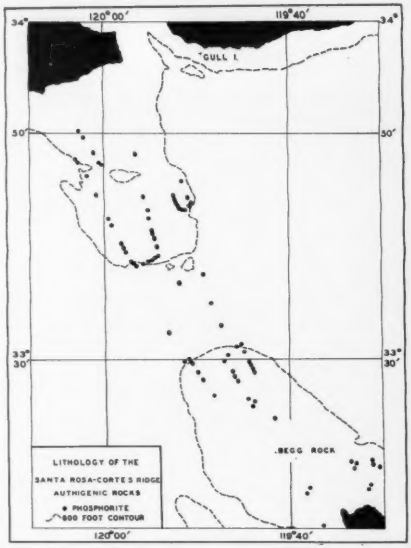

FIG. 8.—Areal distribution of phosphorite.

surfaces, and (3) included clastic material which is similar to that surrounding the phosphorite nodules. Deposition *in situ* is also suggested by the large size of some of the nodules.

A post-Miocene age is indicated for the phosphorite of the Santa Rosa-Cortes Ridge area on the basis of stratigraphic relations between the phosphorite and the surface upon which it rests. If it was formed *in situ* it must be younger than this surface. Because the rocks forming it are of Miocene age, the phosphorite must be younger than Miocene.

UNCONSOLIDATED SEDIMENTS

Knowledge of the unconsolidated sediments blanketing the Santa Rosa-Cortes Ridge is based on examination of all the samples available, on data from a report by Norris (1951), and on bottom notations from the United States Coast and Geodetic Survey field sheets that were used to determine the submarine topography of the ridge.

Mechanical analysis of the unconsolidated sediments were made by two methods. Of the 285 samples available, 128 were analyzed with Emery's settling tube. The remainder were analyzed by the rapid visual method developed by Emery and Gould (1948) using some of the conventional analyzed samples as standards. The carbonate content of 120 samples and the organic carbon of 112 samples were also determined. Carbonate content was measured by leaching with dilute hydrochloric acid and the organic carbon was determined by the potassium dichromate method (Allison, 1935). The heavy and light minerals of 12 samples were separated in acetylene tetrabromide (sp gr 2.96) after treatment with dilute hydrochloric acid. Quartz, orthoclase, and plagioclase of the light fraction were identified using staining techniques (Twenhofel and Tyler, 1941). The minerals of the heavy fraction were identified with a petrographic microscope.

The sediments, excluding the coarse clastics which have been described in the section on lithology, are classified on the basis of composition into the following groups: (1) clastic sediments, and (2) calcareous organic sediments. These two groups are further subdivided on the basis of their median diameter into six sedimentary types, half of which are organic sediments and the rest detrital (fig. 9).

Of the two major groups, the calcareous organic sediments are the most abundant, covering 60 percent of the surface of the ridge. Shell sand, consisting predominantly of shell fragments with occasional bryozoan and coral fragments mixed with them, is for the most part restricted to the turbulent shallow water near shore. The deeper parts of the ridge are blanked by foraminiferal sands which contain glauconite as their most common constituent.

The detrital sediments, medium to very fine sand and sand-silt, are found throughout most of the ridge. The present day detrital sediments are those bordering the shore zone. Those in deeper waters probably represent either residual or relict detrital sediments that were deposited during a lower stand of sea level in the Pleistocene as present day currents are not capable of transporting medium sand so far from shore.

The wide distribution of calcareous sediments and their presence as a component in the detrital sediments lead to a high calcium carbonate content on the ridge. Values greater than 40 percent are characteristic of most of the ridge, and still higher values of 80 percent are common in the saddle (fig. 10).

The ridge is an area of relatively strong currents which results in the winnowing of the finer detrital sediments and the development of ripple marks (fig. 11). As one would expect in an oxygen-rich environment, the organic carbon content is generally low (fig. 12). Average values of less than 0.5 percent occur on most of the ridge. Higher values are associated with the finer sediments in the saddle, depression, and near Santa Cruz Canyon.

The mineralogy of the sediments north of the saddle differs from that of the sediments farther south (table 1). Both areas have a high quartz-feldspar ratio. In the southern area hornblende and biotite are the characteristic heavy minerals, whereas the diagnostic minerals north of the saddle are garnet and epidote. Glauconite is the most abundant authigenic mineral on the ridge. It occurs in three different forms: as

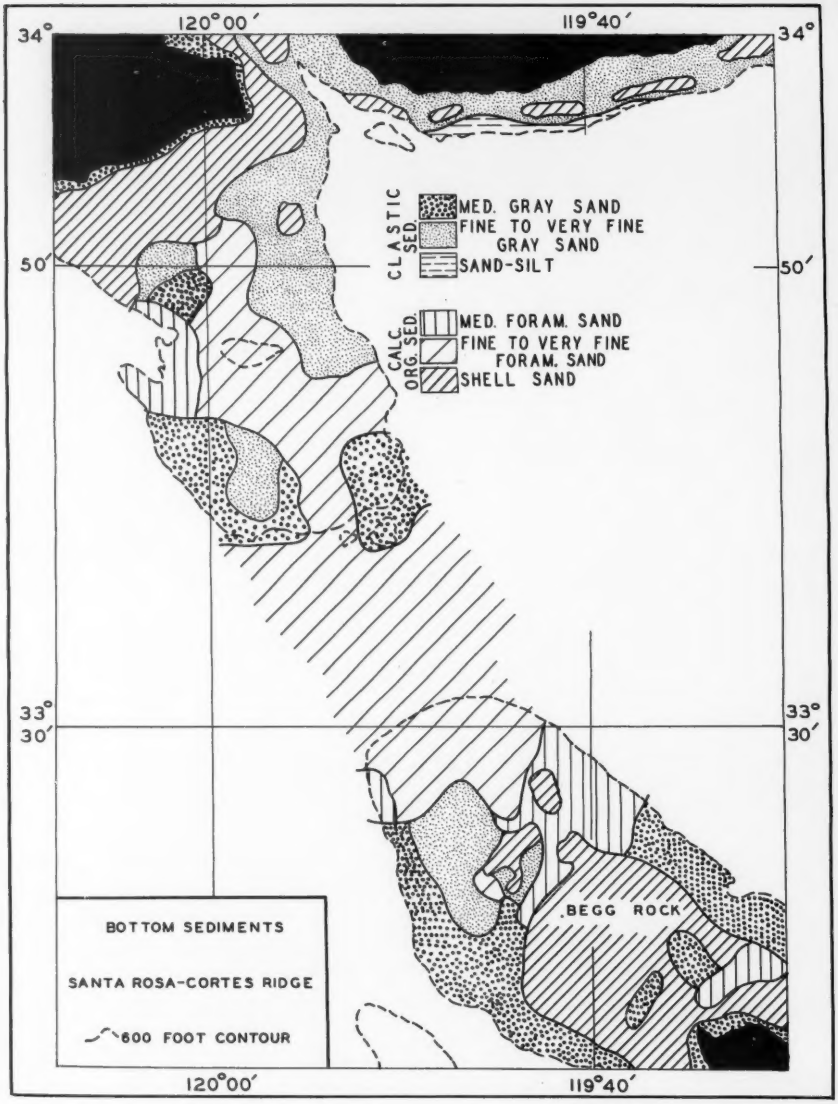

FIG. 9.—Areal distribution of unconsolidated sediments, Santa Rosa-Cortes Ridge.

foraminiferal casts, as dark well rounded and polished grains, and as irregular subangular grains. The greatest concentrations occur in the depression and saddle where it exceeds 10 percent. South of the saddle percentages are rarely higher than 1.0 percent and south of Begg Rock and near Santa Rosa no glauconite was observed in the sediments.

SUMMARY

Knowledge of the structure of a submarine area must usually be based on such indirect evidence as bottom topography, the distribution of lithology, and extrapolation of structures of nearby land.

The dominant features of the Santa Rosa-Cortes Ridge are the two scarps flanking the ridge on the northeast and southwest, the saddle and the small depression southeast of Santa Rosa Island. The slopes on the southwest and northeast are steep, relatively straight and are sites of seismic activity (Clements and Emery, 1947). They probably represent fault scarps. The saddle and depression probably also have a structural origin, but may have been modified by erosion.

The age of the deformation is not known, but inasmuch as the youngest rock collected

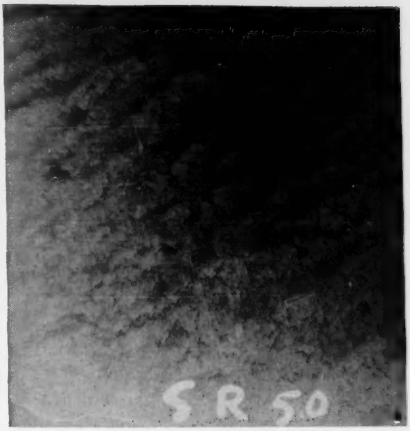

FIG. 11.—Bottom photograph showing ripple marks. Loc.: lat. 33° 21.9′ N, long. 119° 42.7′ W. Depth: 300 feet. Area: 16 square feet.

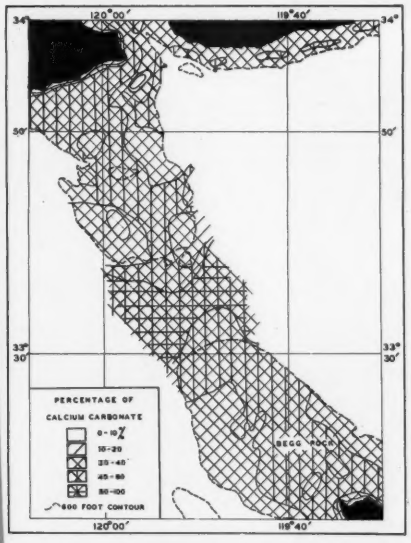

FIG. 10.—Areal distribution of calcium carbonate in ridge sediments.

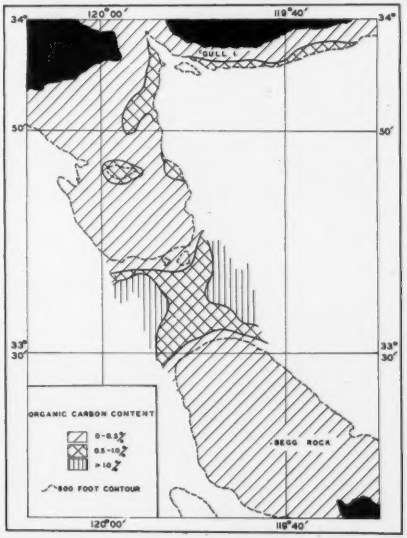

FIG. 12.—Areal distribution of organic carbon in ridge sediments.

TABLE 1 —*Mineral composition of ridge sediments*

Mineral Species	San Nicolas Island Area (Av. of 12 Samples)		Santa Rosa Island Area (Av. of 10 Samples)	
Organic				
Calcite		64.0		51.8
Authigenic				
Glauconite	97.0		99.1	
Collophane	3.0		0.9	
	100.0	8.0	100.0	1.5
Detrital Lights				
Quartz	85.2		84.0	
Plagioclase	11.0		1.1	
Orthoclase	0.0		14.0	
Muscovite	4.8		0.9	
	100.0	27.2	100.0	45.9
Detrital Heavies				
Magnetite	57.4		75.0	
Hornblende	30.2		12.0	
Biotite	8.0		2.3	
Epidote	1.1		4.1	
Garnet	0.9		3.8	
Chlorite	0.6		0.1	
Hypersthene	0.4		0.0	
Hematite	0.1		0.0	
Ilmenite	0.1		0.0	
Olivine	0.1		0.4	
Serpentine	0.1		0.3	
Zircon	0.1		0.9	
Augite	0.0		0.1	
	100.0	0.8	100.0	0.8
		100.0		100.0

from this area is Miocene, the deformation is probably post-Miocene. The presence of a 660 foot terrace on both sides of the saddle suggests that the movement along these faults occurred before the formation of the terrace. If the terrace was formed by wave erosion during the Pleistocene, the faults are also pre-Pleistocene.

An echo sounding record parallel to the axis of the ridge shows the presence of seven terraces, probably wave cut features that were carved during the Pleistocene when sea level was lower.

Bedrock was recovered from most of the ridge. Yellow-buff sandstones, gray shales and siltstones, probably of Middle and Late Eocene age, are restricted to the area south of Begg Rock. The rocks on the rest of the ridge contain Foraminifera indicative of the Mohnian, Relizian, Saucesian, and Zemorrian stages of the Miocene.

Transported rocks that range in size from two millimeters to 10 centimeters are present throughout the ridge. They are predominantly composed of basalt with occasional pebbles of sandstone, shale, siltstone, and a few granules of metamorphic quartzite. The basalt north of the saddle is believed to have been derived from Santa Rosa and Santa Cruz, whereas that found immediately off the coast of San Nicolas was probably derived from an older land mass located to the southwest of the island. The source of the sedimentary rocks was probably local outcrops and the rocks on nearby islands. The transported rocks are believed to have been deposited during the Pleistocene because (1) they rest on wave-cut surfaces which were probably formed during the Pleistocene and (2) they are too large to have been transported by present day currents.

The detrital sediments covering the ridge are thought to represent two periods of deposition. The earliest of these periods is represented by the medium gray sands northeast and southwest of San Nicolas, at the northern flank of the saddle, and the gravel scattered throughout the ridge. Norris (1951) suggested that the sand northeast and southwest of San Nicolas may be a Pleistocene beach that was deposited when the shoreline was located near the 70 fathom contour.

The second period of deposition is represented by the medium to very fine sand restricted to the area immediately off the shores of the islands. The rest of the ridge is covered by calcareous organic sediments where detrital sediments are not accumulating or where their rate of accumulation is very slow.

Today, the Santa Rosa-Cortes Ridge, excluding the areas near the islands, is a non-depositional marine environment where the fine detrital sediments, silts and clays, by-pass the ridge and are deposited in the basins flanking it.

ACKNOWLEDGMENTS

The writer wishes to express his appreciation to Doctors O. L. Bandy and R. H. Merriam of the geology department of the

University of Southern California for their helpful suggestions. For the use of drafting and laboratory facilities, for the loan of 12 dredge samples, and for the opportunity to collect samples from the oceanographic vessel "Velero IV" the writer is indebted to the Allan Hancock Foundation. Appreciation is expressed to Mr. J. R. Grady and members of the micropaleontological laboratory of Richfield Oil Company who kindly identified the Foraminifera in some of the rock samples.

The writer wishes especially to thank Dr. K. O. Emery for providing most of the samples and for his suggestions during the preparation of this report.

REFERENCES

ALLISON, L. E., 1935, Organic carbon by reduction of chromic acid: Soil Science, v. 40, p. 311–320.

BREMNER, C. T., 1932, Geology of Santa Cruz Island, Santa Barbara County, California: Santa Barbara Museum Nat. Hist. Occasional Papers, no. 1, 33 p.

CLEMENTS, T., AND EMERY, K. O., 1947, Seismic activity and topography of the sea floor off southern California: Bull. Seismological Soc. America, v. 37, p. 307–313.

DIETZ, R. S., EMERY, K. O., AND SHEPARD, F. P., 1942, Phosphorite deposits of the sea floor off southern California: Geol. Soc. America Bull., v. 53, p. 815–848.

EMERY, K. O., 1938, A rapid method of mechanical analysis: Jour. Sedimentary Petrology, v. 8, p. 105–111.

———, 1958, Shallow submerged terraces of southern California: Geol. Soc. America Bull., v. 69, p. 39–60.

———, 1960, The sea off southern California: a modern habitat of oil: John Wiley & Sons, Inc., New York, 366 p.

EMERY, K. O., AND GOULD, H., 1948, A code for expressing grain size distribution: Jour. Sedimentary Petrology, v. 18, p. 14–23.

EMERY, K. O., AND SHEPARD, F. P., 1945, Lithology of the sea floor off southern California: Geol. Soc. America Bull., v. 56, p. 431–478.

FLEMING, R. H., 1938, Character of the currents off southern California: 6th Pacific Science Congress, p. 149–160.

HOLZMAN, J. E., 1952, Submarine geology of Cortes and Tanner Bank: Jour. Sedimentary Petrology, v. 22, p. 97–118.

KEW, W. S. W., 1927, Geologic sketch of Santa Rosa Island, Santa Barbara County, California: Geol. Soc. America Bull., v. 38, p. 645–654.

KEMNITZER, L. E., 1933, Geology of San Nicolas and Santa Barbara Islands, southern California: Unpublished thesis, Calif. Institute of Technology, 45 p.

MENARD, H. W., DILL, R. F., HAMILTON, E. L., MOORE, D. G., SHUMWAY, G., SILVERMAN, M., AND STEWART, H. B., 1954, Underwater mapping by diving geologists: Amer. Assoc. Petroleum Geologists Bull., v. 38, p. 129–147.

NORRIS, R. M., 1951, Marine geology of the San Nicolas Island region: Ph.D. dissertation, Univ. of Calif. at Los Angeles, 124 p.

REVELLE, R., AND SHEPARD, F. P., 1939, Sediments off the California coast. *in* Recent marine sediments: Am. Assoc. Petroleum Geologists, Tulsa, Oklahoma, p. 245–272.

RESIG, JOHANNA, M., 1958, Ecology of Foraminifera of the Santa Cruz Basin: Micropaleontology, v. 4, 287–308.

SHEPARD, F. P., AND EMERY, K. O., 1941, Submarine topography off the coast of California; canyons and tectonic interpretation: Geol. Soc. America Spec. Paper 31, 171 p.

TRASK, P. D., 1931, Sediments in the Channel Islands region: Economic Geology Bull., v. 26, p. 24–43.

TWENHOFEL, W. H., AND TYLER, S. A., 1941, Methods of study of sediments. McGraw-Hill Company, Inc., New York and London, 185 p.

ZEUNER, F. E., 1945, Pleistocene period, its climate, chronology, and faunal succession: Ray Society, London, 322 p.

JOURNAL OF SEDIMENTARY PETROLOGY, VOL. 31, NO. 4, PP. 546–552
FIGS. 1–3, DECEMBER, 1961

PHOSPHATIC PEBBLES FROM THE BRIGHTSEAT FORMATION OF MARYLAND[1]

JOHN K. ADAMS, JOHAN J. GROOT, AND N. WILLIAM HILLER, JR.
University of Delaware, Newark, Delaware

ABSTRACT

Phosphate pebbles in the Brightseat Formation of Maryland are composed chiefly of cryptocrystalline apatite (collophane). The pebbles originally were composed largely of calcite which subsequently was partially replaced by collophane. Compositional differences between the pebbles and the sediments in which they occur suggest that the pebbles are allochthonous.

INTRODUCTION

The Brightseat Formation (Paleocene) is known to crop out at 5 localities 1 to 3 miles east of Washington, D. C. In three outcrops phosphatic pebbles have been found in the upper 5 feet of the formation close to the contact with the overlying Aquia Formation (Eocene). The location of the outcrops where phosphatic pebbles were found is shown in figure 1.

The Brightseat Formation was first described by Bennett and Collins (1952). They assigned the formation to the Paleocene on the basis of the foraminifers and the megafossils. The Foraminifera were studied in more detail by Page (1959) who also concluded that the formation is Paleocene.

GENERAL DESCRIPTION OF PHOSPHATE PEBBLES

The phosphate pebbles from the Brightseat Formation have a dark-gray to black, shiny surface. Their interior is dark-brown and dull. They range in size from $\frac{1}{16}$ in to $1\frac{3}{4}$ in and are of various shapes (fig. 2). The pebbles can be roughly classified on the basis of shape into 4 groups: shell-shaped, irregular, cylindrical, and bean-shaped.

The shell-like forms represent internal molds of pelecypod shells that have been replaced by collophane. These forms contain many cavities concentrated in the central portion of the pebble. A thin outer layer, which may represent a replaced portion of the original shell, is composed entirely of collophane and is free of cavities and inclusions. A thin section of a shell-like pebble revealed a fish tooth (fig. 3a), fecal pellets, recrystallized calcite, quartz grains (fig. 3b), and an organic fragment that may be part of an ostracod test (fig. 3b).

The irregular forms are large, cracked, and pitted. They have more detrital material than any of the other forms, and show many cavities, cracks, and borings which are evenly distributed throughout the pebbles. Some of the borings completely penetrate the pebbles and are as large as 3 mm in diameter; most of them contain pyrite, skeletal calcite, and quartz (fig. 3c). Thin sections of the irregular pebbles show recrystallized calcite, Foraminifera (fig. 3d), algal borings (fig. 3e), and fecal pellets in addition to detrital minerals.

The cylindrical pebbles are small and smooth and they contain only a few cracks, and a small amount of detrital material. Some of these forms show circumscribing furrows; they are probably phosphatized coprolites.

The bean-shaped pebbles also are small and smooth and contain only a few cracks, but they have greater amounts of detrital material than the cylindrical specimens. Thin sections of the bean-shaped forms show smooth round cavities that range from 0.1 mm to 0.7 mm in diameter. Some of these cavities are filled with finely disseminated glauconite and pyrite, whereas others are filled with clay, glauconite, and calcite. Additional features which appear in the bean-shaped pebbles are recrystallized calcite, detrital quartz grains, and a small, round body resembling an oolith (fig. 3f).

[1] Manuscript received September 26, 1960.

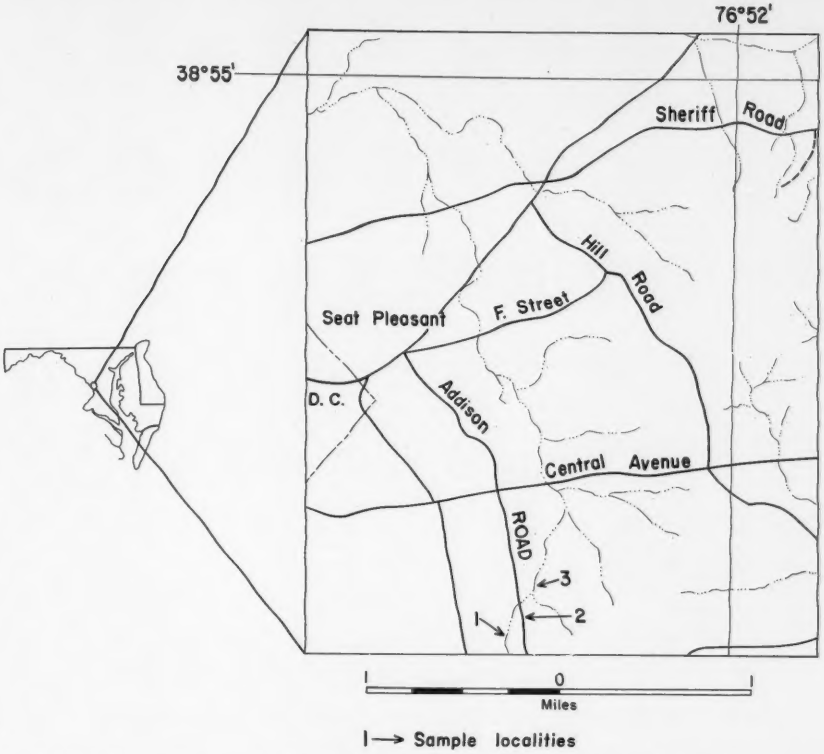

FIG. 1.—Map showing sampling localities. The regional setting is indicated in the map on the left.

Shark teeth also are present in the Brightseat Formation. They are composed of collophane and have the same color and luster as the phosphatic pebbles.

TEXTURE

Some of the pebbles and samples of the matrix surrounding the pebbles were soaked in dilute HCl for 12 to 14 hours. The mechanical composition of the insoluble residues was obtained by sieving and the material finer than $\frac{1}{16}$ mm was discarded. The results of these size analyses are shown in table 1.

The sediments insoluble residue from the sediment that surrounds the pebbles shows much better sorting and contains much larger quantities of material within the $\frac{1}{8}$ to $\frac{1}{16}$ mm size fraction than does the residue from the pebbles. The insoluble residues from the pebbles have higher percentages in the $\frac{1}{2}$ to $\frac{1}{4}$ mm fraction than the insoluble residues from the surrounding sediments. There also is a profound difference between the percentage of insoluble residue contained in the pebbles and that contained in the surrounding sediments. The pebbles have less than 10 percent insoluble material that is coarser than $\frac{1}{16}$ mm, whereas the surrounding sediment contains over 50 percent of insoluble material in this size range.

The differences in the size distribution of the insoluble residues suggests that the pebbles were not formed in material that

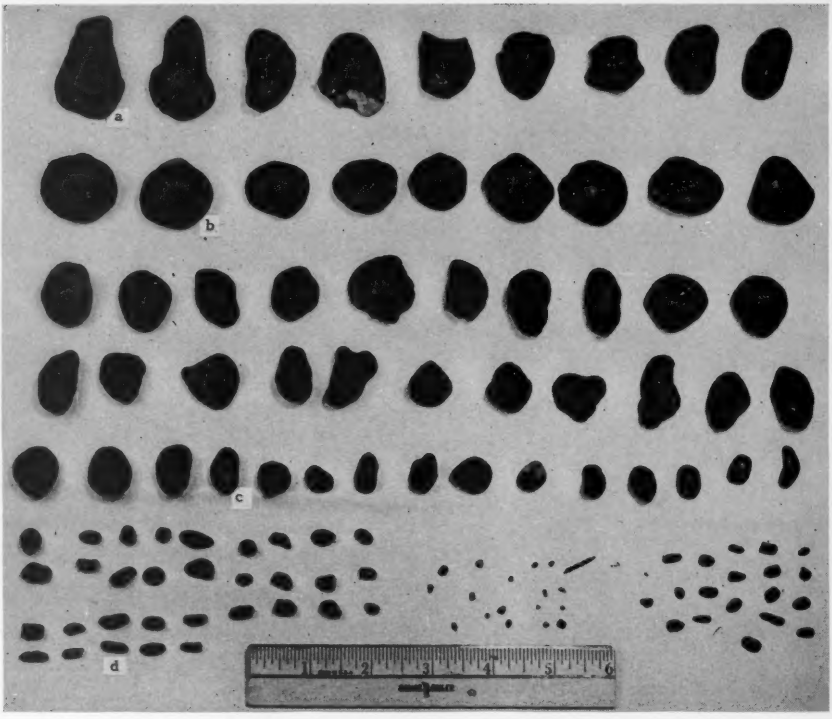

FIG. 2.—Photograph of phosphatic pebbles from the Brightseat Formation showing typical sizes and shapes.
a. —Irregular pebble.
b.—Shell-shaped pebble.
c.—Bean-shaped pebble.
d.—Cylindrical pebble.

had the same texture as that in which the pebbles now occur.

MINERALOGY

Quantitative mineralogical examinations were made of thin sections of an irregular-shaped pebble, a shell-shaped pebble, and a bean-shaped pebble. The important mineral constituents are collophane, finely disseminated calcite, skeletal calcite, quartz, recrystallized calcite, pyrite, glauconite, and clay. The collophane appears to have partially replaced the finely disseminated calcite, but it has not replaced many of the included shell fragments. The pyrite occurs as euhedral grains associated with organic

FIG. 3.—Photomicrographs of thin sections of phosphatic pebbles. All figures ×100.
a.—Fish tooth.
b.—Ostracod carapace (?) and quartz grains.
c.—Crack containing skeletal calcite, pyrite, and quartz.
d.—Section of Foraminifera.
e.—Algal boring (?).
f.—Oolith.

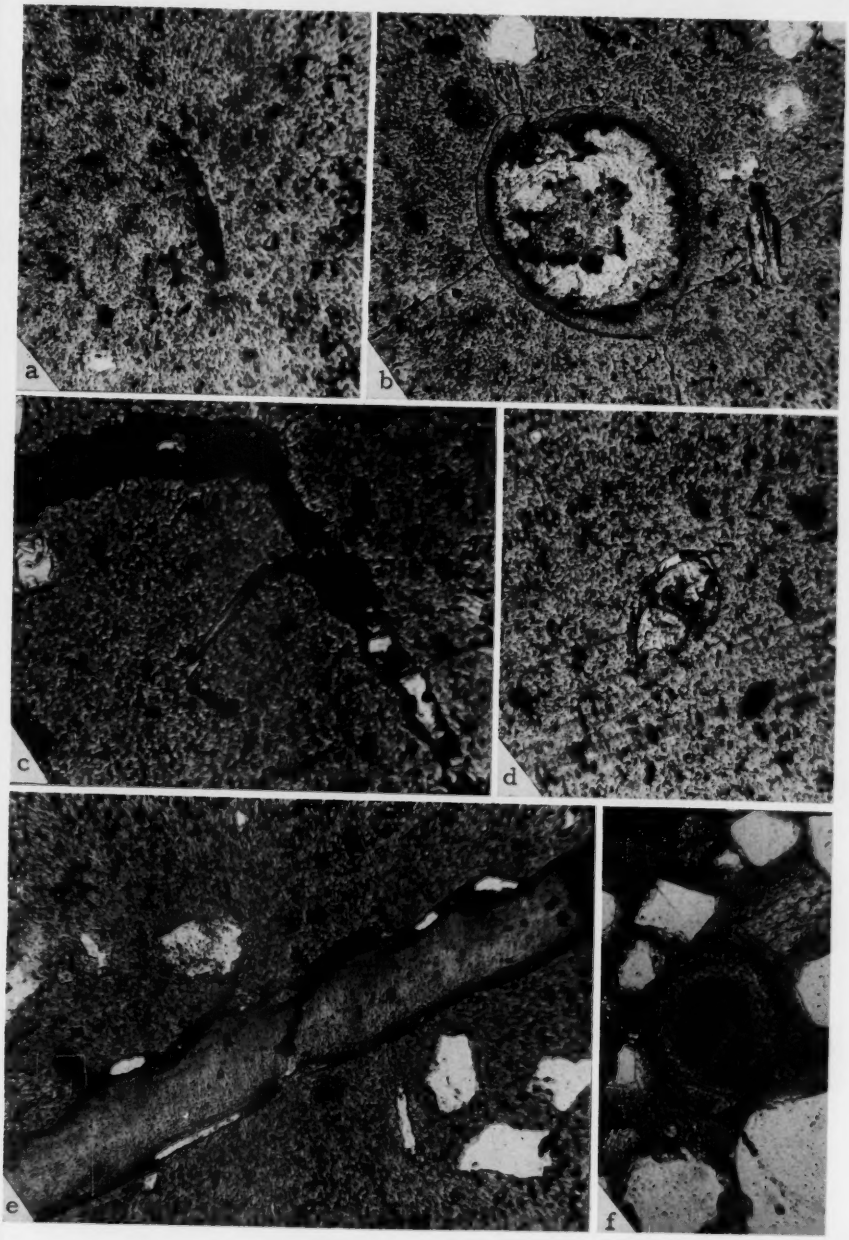
a
b
c
d
e
f

TABLE 1.—*Mechanical composition in weight percentages of insoluble residue*

Sample	A	B	C	D
Total sample				
Weight of sample in gms.	100.0	100.0	100.0	100.0
% insoluble residue	6.8	8.6	56.7	67.0
Insoluble residue				
% coarser than 1 mm	0.0	0.0	0.0	0.3
% between 1 and $\frac{1}{2}$ mm	4.4	1.2	0.2	0.3
% between $\frac{1}{2}$ and $\frac{1}{4}$ mm	27.9	20.9	2.1	3.9
% between $\frac{1}{4}$ and $\frac{1}{8}$ mm	25.1	34.9	32.1	11.9
% between $\frac{1}{8}$ and $\frac{1}{16}$ mm	42.6	43.0	65.1	83.0
	100.0	100.0	99.3	99.4

A Sample of pebbles of various shapes.
B Sample of large pebbles of various shapes.
C Sample of Brightseat Formation from locality 1.
D Sample of Brightseat Formation from locality 2.

borings, cavities, and fecal pellets, suggesting that it formed in areas where organic remains were decomposing. The glauconite and clay commonly are associated with fecal pellets. Some glauconite and quartz occur as isolated grains within the matrix of collophane.

The insoluble residues obtained from the pebbles and the surrounding sediments were separated into light and heavy fractions with tetrabromoethane (sp gr = 2.89). The light fractions from both the pebbles and the surrounding sediments are very similar in composition; both contain from 93 to 95 percent angular to subangular quartz and the remainder is principally orthoclase.

The heavy mineral fractions from the pebbles and from the surrounding sediments differ considerably. The pebbles contain high percentages of pyrite, smaller amounts of non-opaque minerals, and very small amounts of black-opaque minerals. In contrast, the sediment that surrounds the pebbles has a high percentage of black-opaques and non-opaques and only a small amount of pyrite (table 2). However, if the percentages of opaque minerals are recalculated to exclude pyrite, the percentages of black-opaques are similar in the pebbles and in the surrounding sediment.

Differences also occur between the non-opaque heavy mineral fractions in the pebbles and in the surrounding sediments. The important minerals in the non-opaque heavy mineral suite from both the pebbles and the surrounding sediment are: tourmaline, staurolite, epidote, chloritoid, garnet, and zircon. Analyses of the sediments surrounding the pebbles show high percentages of chloritoid and smaller amounts of zircon. In contrast to this, the pebbles yield only small amounts of chloritoid and considerably larger percentages of zircon (table 3). Other heavy mineral analyses have been made of the Brightseat Formation from localities where phosphatic pebbles are absent. Although the heavy mineral suites from the Brightseat Formation are quite variable (i.e. high percentages of rutile occur at some localities), sample E in table 3 shows the lowest percentage of chloritoid and the highest percentage of zircon.

X-ray diffraction analyses also were made

TABLE 2.—*Frequency of opaque heavy minerals by relative percentages of grains*

Sample	A	B	C	D	E
Black opaques	3	9	16	43	55
Leucoxene	11	1	2	7	5
Hematite	–	–	–	T	–
Pyrite	58	73	60	1	T
Non-opaques	28	17	22	48	40

A Sample of an irregular shaped pebble.
B Sample of 100 grams of various shaped pebbles
C Sample of 100 grams of large pebbles.
D Sample of Brightseat Formation from locality 1.
E Sample of Brightseat Formation from locality 2.

TABLE 3.—*Frequency of non-opaque heavy mineral by relative percentage of grains*

Sample	A	B	C	D	E
Tourmaline	12	5	11	9	6
Staurolite	6	12	13	13	7
Epidote	22	35	18	26	29
Zoisite	8	3	3	4	2
Chloritoid	4	6	4	17	13
Garnet	16	14	20	18	22
Sillimanite	3	2	T	3	–
Zircon	22	19	20	5	14
Rutile	–	–	T	1	2
Kyanite	3	–	T	2	–
Sphene	1	T	–	T	1
Andalusite	–	–	T	1	–
Hornblende	3	4	7	1	3
Corundum	–	T	–	–	–
Fluorite	–	–	T	–	–
Monazite	–	–	T	–	–
Brookite	–	–	–	–	T

A Sample of an irregular shaped pebble.
B Sample of 100 grams of various shaped pebbles.
C Sample of 100 grams of large pebbles.
D Sample of Brightseat Formation from locality 1.
E Sample of Brightseat Formation from locality 2.

of the pebbles. These studies confirmed the fact that the collophane in the pebbles is not an amorphous mineral, but is cryptocrystalline apatite. The lattice spacings most closely resemble those of fluorapatite. The analyses indicate that quartz, calcite, and pyrite also are present.

ACID-INSOLUBLE MICROFOSSILS

Fifty grams of phosphatic pebbles and 2 samples from the sediments surrounding the pebbles were examined for acid-insoluble microfossils. All of the samples contained pollen, spores, hystrichosphaerids, and dinoflagellates. The fossils from the pebbles do not differ enough from those in the surrounding sediments to postulate any age or environmental difference, but they do differ in the degree of preservation. The fossils are better preserved in the pebbles than in the surrounding sediments. There are three possibile explanations for the difference in degree of preservation of the fossils. (1) The sediments may have been reworked after the formation of the pebbles, in which case the fossils in the sediment would have been damaged by abrasion with the quartz grains, whereas the fossils in the pebbles would have been protected. (2) There may have been more interstratal weathering of the fossils within the sediments than of those within the pebbles. (3) The pebbles may have originated in an area in which the fossils were in a better state of preservation.

ORIGIN OF BRIGHTSEAT PHOSPHATE PEBBLES

The phosphatic pebbles from the Brightseat Formation are the product of replacement of either calcareous pebbles or concretions by collophane. The original pebbles may have been formed in an environment that was different from the one reflected by the sediments in which they now occur. The replacement may have taken place at another locality as evidenced by the presence of unaltered mollusks, foraminifers, and ostracods which are intimately mixed with the pebbles in the outcrop. After the replacement by collophane, boring organisms penetrated the pebbles and left narrow openings permeating some of them. These borings were then partially lined by pyrite which represents the final stage of mineralization in the history of the pebbles.

Goldberg and Parker (1960) have studied phosphatized wood from the Pacific Ocean. They describe the phosphatization process in the following way:

> "Dissolved oxygen of the sea water reacted with the more readily oxidizable organic components of the wood with a subsequent reduction in Eh. This also leads to a decrease in pH, and this in turn diminishes the carbonate content. Although the hydrogen ion concentration controlling the precipitation of calcium carbonate and calcium phosphate are remarkably similar, the high phosphate content of the water apparently turns the tide in favor of apatite deposition."

The replacement process in the phosphatic pebbles could have occurred under similar conditions. Shell fragments and organic structures within the pebbles suggest that there may have been organic components present which locally used up the dissolved oxygen thus lowering the Eh and pH. Of course, there is a difference between the replacement process which is demonstrated by the pebbles, and the direct precipitation

which took place in the phosphatization of the wood. However, it is plausible to suppose that the physical and chemical conditions were much the same.

Summarizing, the phosphatic pebbles differ from the sediments that surround them in six compositional and textural aspects. These differences are: the size distributions of insoluble residues, the weight percentage of insoluble residues, the percentages of chloritoid and zircon, the percentage of pyrite, the distribution of calcite, and the degree of preservation of the microfossils. The differences strongly suggest that the composition of the pebbles before replacement was unlike the composition of the sediments in which they are now found. However, it is not clear whether the pebbles were formed in place or transported from another locality.

ACKNOWLEDGMENTS

The writers wish to thank Mrs. Catharina R. Groot for her examination of the microfossils, and Mr. Robert R. Jordan who critically reviewed the manuscript.

REFERENCES

BENNETT, R. R., AND COLLINS, G. G., 1952, Brightseat Formation, a new name for sediments of Paleocene age in Maryland: Washington Acad. Sci. Jour., v. 42, p. 114–116.

GOLDBERG, E. D., AND PARKER, R. H., 1960, Phosphatized wood from the Pacific sea floor: Geol. Soc. America Bull., v. 71, p. 631–632.

PAGE, R. A., 1959, Micropaleontology and stratigraphy of the Brightseat Formation: unpublished Ph.D. thesis, Rutgers University, New Brunswick, N. J.

JOURNAL OF SEDIMENTARY PETROLOGY, VOL. 31, NO. 4, PP. 553–559
FIGS. 1–6, DECEMBER, 1961

GENESIS OF PRIMARY STRUCTURES IN ANHYDRITE[1]

CHARLES M. RILEY AND JOHN V. BYRNE[2]
Humble Oil & Refining Company, Houston, Texas

ABSTRACT

Anhydrite, a common evaporite in all systems since the Cambrian, displays a variety of structures which may be classified as layered, mosaic, flocculent, contorted, boudinage, and authiclastic. A primary origin of these structures and of the anhydrite itself is suggested by interbedding of undeformed anhydrite and clastics with layers of disturbed anhydrite. Flowage resulting from differences in density of semifluid anhydrite and unconsolidated nonevaporite sediments during or shortly after deposition seems to explain the origin of the structures observed. Model experiments in which most of the structures were simulated by artificial sedimentation techniques support this conclusion.

INTRODUCTION

Extensive thick sequences of evaporites, commonly deposited during a late stage of basin filling, are represented in every geologic period since the Cambrian. In many of these sequences anhydrite is the principal evaporite, and in others it is second in abundance only to halite. Although anhydrite is extremely common, little is known about its mode of origin or of the environmental conditions which prevailed at the time of its accumulation. Some of the processes of deposition and early diagenesis, however, can be deduced by a study of the structures occurring in the anhydrite. These structures also provide information regarding the fundamental problem of whether anhydrite was laid down as a primary precipitate or whether it formed at some later time by dehydration of gypsum.

Studies of characteristic structures in Jurassic and Cretaceous anhydrite sequences in the Gulf Coast area suggest that many of the structures are primary and, therefore, that much of the anhydrite itself accumulated as a primary precipitate. Laboratory model experiments support this thesis and in addition yield significant information on the genesis of the structures.

CLASSIFICATION OF ANHYDRITE STRUCTURES

Most rock anhydrite occurs as an aggregate of individual masses of acicular crystals which are commonly as much as 0.5 mm in length and rarely exceed 0.03 mm in width. Within the anhydrite masses the crystals are generally aligned in swirls except near the edges where they parallel the boundaries between the anhydrite and adjacent and/or included sediments. The mineral anhydrite also occurs as large lath-like or blocky crystals which are believed to be of secondary origin; these occur as a replacement of other minerals and are not discussed in this paper.

A variety of distinctive structures, which may occur individually or in combination, were observed in the cores of rock anhydrite from the Gulf Coast. These structures are described in the following six-fold classification and are illustrated in figure 1.

Layered (*fig. 1a*).—Most anhydrite sections are made up of laminae and beds ranging in thickness from a few tenths of a millimeter to many tens of feet. Layers of other sediments are commonly intercalated with the anhydrite. A striking example of layered anhydrite with limestone laminae occurs in the Upper Permian Castile Formation of the Delaware basin of west Texas and eastern New Mexico; it has been termed "laminated anhydrite" by Udden (1924).

Mosaic (*fig. 1b*).—Mosaic structure consists of irregular masses of anhydrite, generally less than an inch in diameter, which are separated by thin stringers of dark carbonate, clay, or silt. The edges of each mass are well defined and conform roughly to irregularities of adjacent anhydrite masses. Most anhydrite masses are flattened and oriented with their long axes lying in a horizontal plane but locally they may be inclined or randomly oriented. On any plane surface,

[1] Manuscript received September 9, 1960.
[2] Present address: Department of Oceanography, Oregon State College, Corvallis, Oregon.

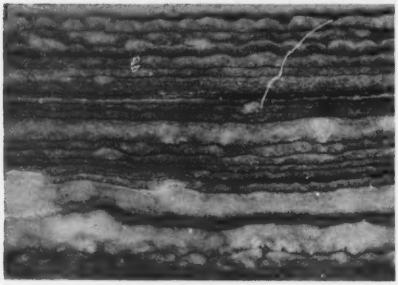

A. LAYERED

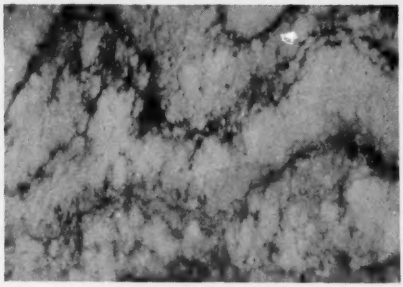

D. CONTORTED

ONE INCH

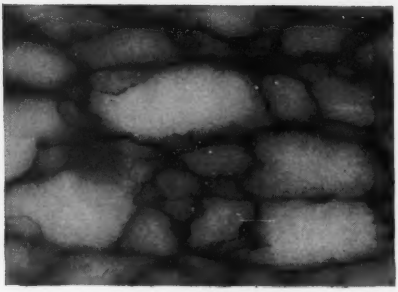

B. MOSAIC

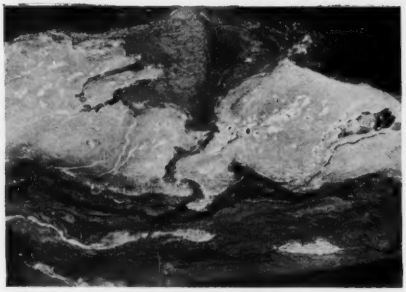

E. BOUDINAGE

C. FLOCCULENT

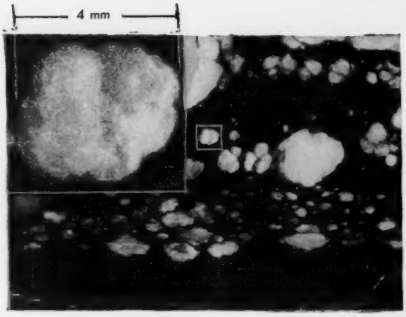

F. AUTHICLASTIC

FIG. 1.—Classification of structures in anhydrite rocks.

the dark stringers separating the anhydrite masses have a netlike pattern which Forgotson (1956) refers to as "chicken-wire" structure.

Flocculent (*fig. 1c*).—Flocculent structure consists of closely packed clumps or floccules of anhydrite which resemble tufts of cotton or wool. The main distinctions between flocculent and mosaic structure are that floccules do not have distinct edges, are more nearly equidimensional, and do not conform to the boundaries of adjacent masses.

Contorted (*fig. 1d*).—Anhydrite structure consisting of layers characterized by small-scale crumpling or folding is termed contorted. Anhydrite within individual layers may display mosaic or flocculent structure.

Boudinage (*fig. 1e*).—This name is proposed for structures resembling the boudinage or "sausage-link" lenses which occur in some metamorphic rocks. Boudinage structures in anhydrite form where individual layers or lenses are locally thinned, or where they are separated by irregular transverse fractures filled with dark nonevaporite sediments. The nonevaporites appear to have flowed into the fractures. Boudinage structure is most prevalent where nonevaporite sediments make up more than one-third of the rock.

Authiclastic (*fig. 1f*).—Discrete, rounded, or irregular masses of anhydrite, ranging in diameter from a fraction of a millimeter to several inches, occur as inclusions in several types of nonevaporite sedimentary rocks. In most occurrences these anhydrite inclusions are confined to distinct layers and locally are so abundant that they grade into nearly pure anhydrite with a mosaic or boudinage structure. Such discrete masses of anhydrite are termed *authiclasts* because they appear to have formed from the disruption in place of newly deposited layers of semiconsolidated anhydrite.

ORIGIN OF ANHYDRITE STRUCTURES

The genesis of anhydrite structures is only part of a greater problem—the origin and diagenetic history of rock anhydrite itself. Forgotson (1956) has postulated that calcium sulfate was originally precipitated from sea water as gypsum and, after burial, was converted to anhydrite as a result of increased heat and pressure. He attributes structures such as mosaic or "chicken wire" to the diagenetic expulsion of molecular water which, according to Pettijohn (1957, p. 479), would result in a 30 to 50 percent shrinkage as the gypsum altered to anhydrite. Much of the expelled water could then saturate the intervening nonevaporite sediments which would become plastic and invade the shrunken and disrupted anhydrite.

Forgotson's theory, however, does not adequately explain the occurrence of undistorted laminated anhydrite, nor does it account for flat-lying nonevaporite layers which are intimately associated with deformed anhydrite structures throughout thick evaporite sequences. Such undeformed sediments could not have remained unaffected during the shrinkage and the expulsion of water attending the conversion of gypsum to anhydrite as proposed in the above theory. It must be concluded, therefore, that no significant shrinkage has taken place and that every lamina of anhydrite was either a primary deposit or was converted from gypsum on the sea bottom before the overlying nonevaporite lamina was deposited. Moreover, the deformation structures in anhydrite beds which lie between undisturbed nonevaporite layers must have been formed in newly deposited sediments before they were buried. The orientation of acicular crystals indicates further that the structures were formed while the sediments were in a semifluid state, probably soon after deposition.

Although wave and current action on the

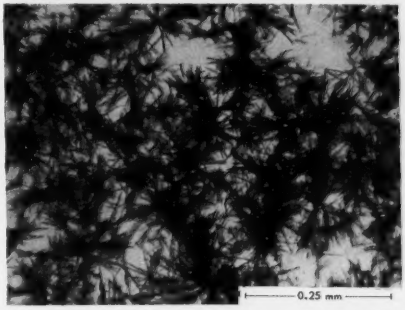

FIG. 2.—Photomicrograph of anhydrite precipitate showing felted interlocking mass of acicular crystals.

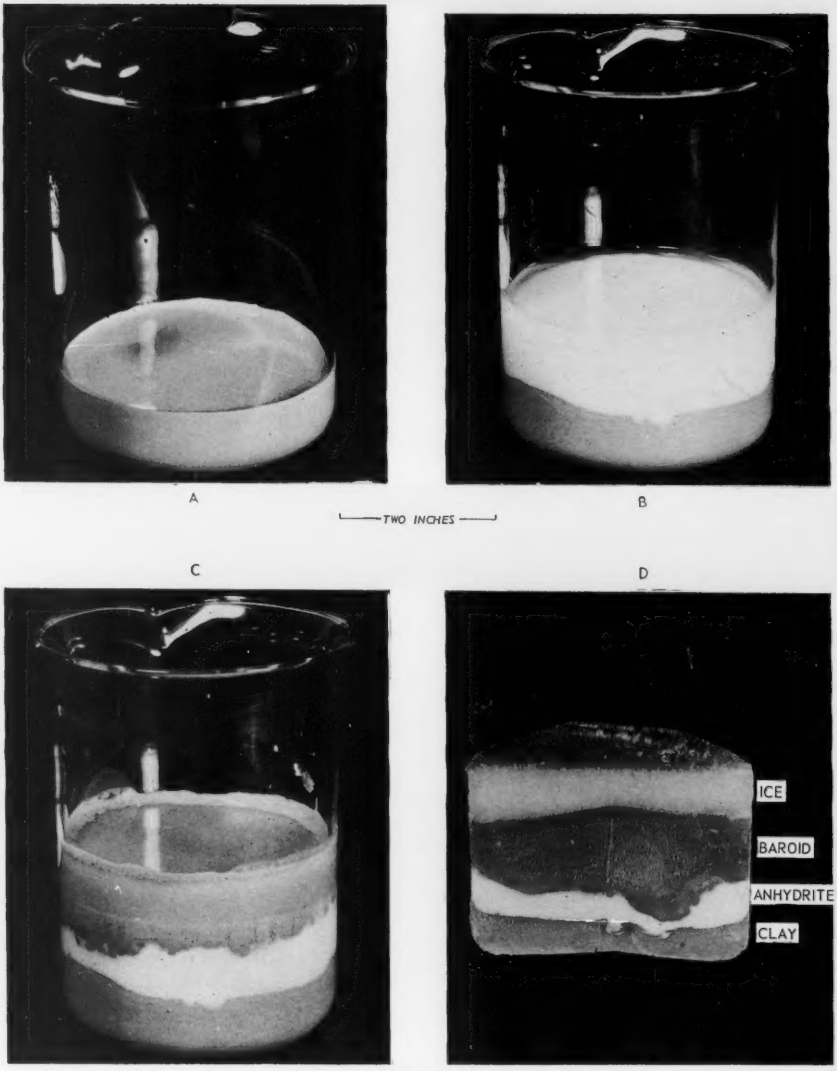

FIG. 3.—Stages in laboratory synthesis of anhydrite structures: A, 600-ml beaker with fluid clay layer; B, layer of anhydrite precipitated above clay; C, baroid layer added, shown settling into and deforming anhydrite; D, sawed surface of frozen model revealing boudinage structure and anhydrite layer.

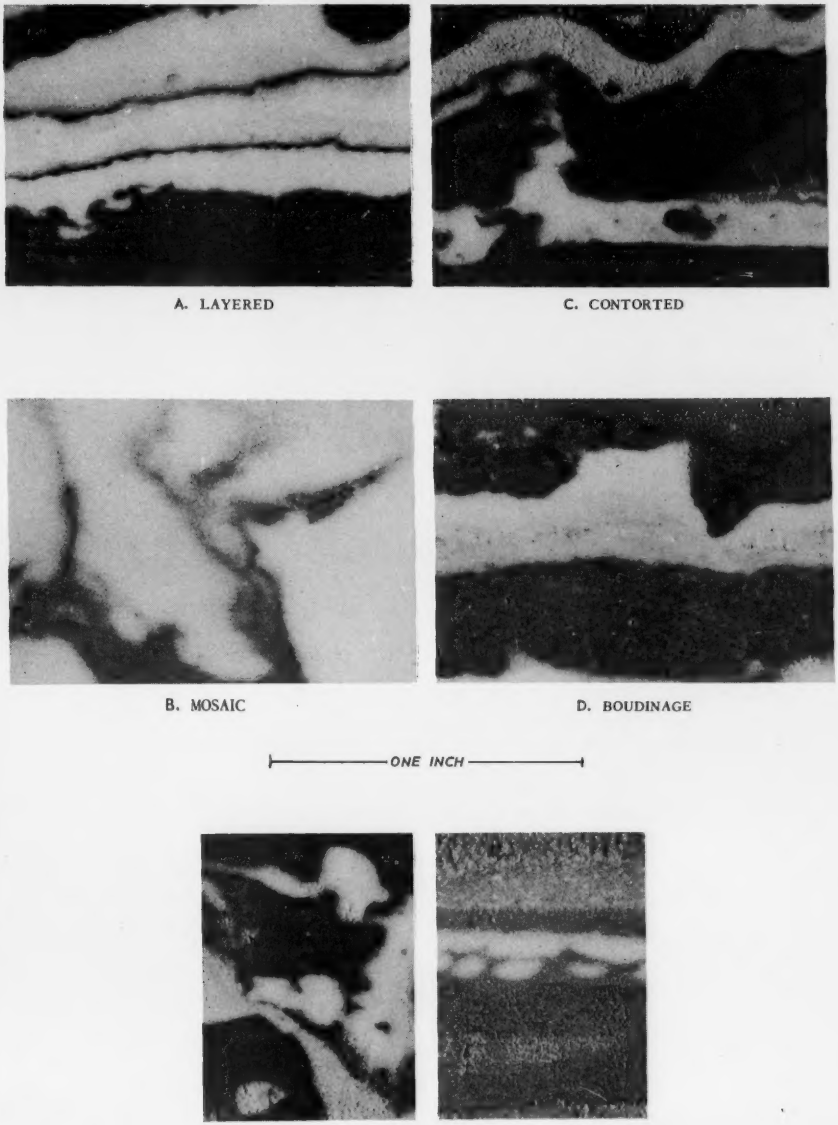

FIG. 4.—Anhydrite structures formed in model experiments.

bottom sediments may have produced some of the structures, most of them probably were formed by flowage caused by differences in density between the light, semifluid anhydrite and the heavier, plastic carbonate and detrital material. This process would account also for their widespread occurrence. It is suggested that the nonevaporite materials either settled directly into the newly precipitated anhydrite or that they accumulated in layers which thickened sufficiently to cause flowage and overturning into the underlying, lighter anhydrite.

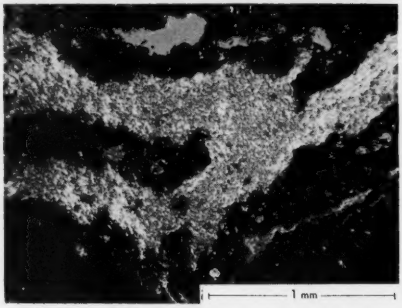

FIG. 5.—Photomicrograph of anhydrite from a deformed layer in a laboratory model, showing alignment of acicular crystals parallel to the anhydrite boundaries. Crossed nicols with accessory plate (550 mμ retardation).

MODEL EXPERIMENTS

To test the thesis that anhydrite structures were formed by flowage caused by density differences, a series of model experiments was devised. In these experiments no attempt was made to determine the different environmental conditions responsible for each type of structural class. Slight variations in experimental procedures, however, and differences in the proportions, thicknesses, and sequences of model materials in the experiments resulted in the formation of a variety of structures.

Natural anhydrite was simulated in the experiments by a flocculent white precipitate made by mixing concentrated solutions of calcium chloride and sodium sulfate. This precipitate formed either as anhydrite[3] or gypsum, depending upon the temperature of the solutions. When warm solutions were used, anhydrite was formed; gypsum was produced when the solutions were mixed cold. The physical characteristics of the two mineral precipitates, however, are essentially the same, and both forms were employed as model materials. For simplicity, this material is referred to in the following discussion as anhydrite. Although neither of these crystalline substances is colloidal, the initial precipitate is gelatinous because of the high percentage of water incorporated within the felted mass of acicular crystals (fig. 2); as the mass gradually compacts, the precipitate becomes less gelatinous.

Baroid mud, flint clay, and mixtures of both were used to simulate the nonevaporite sediments. These were deposited in semifluid suspensions which had bulk densities higher than that of the initial precipitate of anhydrite.

The models were made in 600-ml beakers, in 4-in-diameter cardboard ice-cream cartons, and in a 12-in-square by 2-in-deep galvanized steel tray. In most of the experiments, anhydrite was first precipitated into the containers, and detrital sediments were added slowly and allowed to settle through the overlying solution so as not to disrupt prematurely the underlying anhydrite; steps in the preparation of one of the models are illustrated in figure 3.

After the anhydrite and sediments were deposited, the models were not disturbed until all internal flowage had ceased. They were then quick-frozen by immersing them

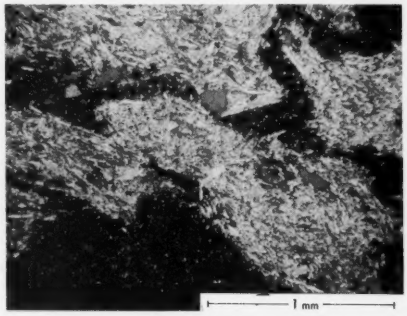

FIG. 6.—Photomicrograph of anhydrite rock, showing alignment of acicular crystals. Crossed nicols with accessory plate (550 mμ retardation).

[3] This may be the hemihydrate ($CaSO_4 \cdot \frac{1}{2}H_2O$).

either in liquid nitrogen (−196° C) or in a slushy mixture of ground dry ice and acetone (−80° C). When the models were completely frozen, the containers were broken away. The models were then sawed into slabs, and the sawed surfaces were scraped clean and photographed. Structures produced in the model experiments are shown in figure 4. All of the structures exhibited by natural anhydrite, with the exception of the flocculent structure, were duplicated to some extent in the experiments.

Several fragments of frozen sediment were allowed to thaw and dry, and, although somewhat shrunken and porous, these pieces were sufficiently coherent to permit thin sectioning. A petrographic study of thin sections made from the model anhydrite (fig. 5) showed that the flowage during the experiments produced swirls and other crystal alignments that closely duplicate similar features noted in thin sections of anhydrite rock (fig. 6).

CONCLUSIONS

The experiments demonstrated that the alignment of acicular crystals and the variety of structures observed in rock anhydrite probably were formed by the flowage of semifluid sediments soon after they were deposited. The flowage was the result, moreover, of density differences between the plastic anhydrite precipitate and subsequently deposited, heavier, nonevaporite sediments. Some flowage might even have been caused by differences in density within the layers of fluid anhydrite precipitate. This analysis of the sedimentary structures and textures gives support to the theory that anhydrite is a primary marine evaporite.

REFERENCES

FORGOTSON, J. M., JR., 1956, A correlation and regional stratigraphic analysis of the formations of the Trinity Group of the Comanchean Cretaceous of the Gulf Coastal Plain and the genesis and petrography of the Ferry Lake Anhydrite: Unpublished thesis, Northwestern University.

PETTIJOHN, F. J., 1957, Sedimentary rocks, 2nd ed.: Harper and Brothers, New York, 718 p.

UDDEN, J. A., 1924, Laminated anhydrite in Texas: Geol. Soc. America Bull., v. 35, p. 347–354.

JOURNAL OF SEDIMENTARY PETROLOGY, VOL. 31, NO. 4, PP. 560–570
PLATES 1–4, FIGS. 1–2, DECEMBER, 1961

COLLOID PHENOMENA IN SEDIMENTATION OF ARGILLACEOUS ROCKS[1]

W. ARTHUR WHITE
Illinois State Geological Survey, Urbana, Illinois

ABSTRACT

Laboratory studies of clay-water systems and field observations of the properties of argillaceous rocks of the Paleozoic systems in the Illinois Basin suggest a close relationship between the environments of deposition of such rocks and the origin of such internal structures such as fissures, slickensides, fissility, and synaeresis cracks. Therefore, the purpose of this report is to suggest a possible origin for fissility, slickensides, synaeresis cracks, and fissures.

Clay minerals in fissile argillaceous rocks, such as shales, are oriented with the longest dimensions more or less parallel to the bedding. The shales generally contain few slickensides, are relatively resistant to disaggregation in water, and generally contain the better-developed crystalline clay minerals.

In contrast, the clay minerals have random orientation in shales that show poor or no fissility. Such rocks commonly contain an abundance of slickensides, break down readily in water, and generally contain a larger percentage of mixed-lattice clay minerals than the fissile shales.

INTRODUCTION

In laboratory experiments with fine-grained sediments, Jüngst (1934, p. 312–25) demonstrated that by varying the salt concentration of his suspensions, he could produce such structures as pits and mounds (resembling rain drop impressions) and cones and craters (suggesting hail impressions) in sediments. He also suggested that some mud cracks might be the result of the environment of deposition. He found that all these structures developed in flocculated suspensions as the result of synaeresis, which is the expulsion of part of the liquid phase from the solid phase in a liquid-solid suspension when internal forces of attraction are greater than internal forces of repulsion between the particles of the solid phase.

In my investigations (White, 1955) of the water-sorption properties of homoionic clay minerals, observations made during preparation of the suspension suggested that certain structures such as synaeresis cracks, fissures, slickensides, and fissility in natural sediments might indicate the environments of deposition. In several different studies (for example, studies of mine roofs, underclay squeezes in coal mines, and petrology of Paleozoic shales and underclays) that were made on shales, clay-shales, and underclays of Paleozoic age, it was observed that the shales that show excellent fissility and have few slickensides have properties quite different from those clays and shales that contain a large number of slickensides and in which fissility was poorly developed or absent. The purpose of this paper is to suggest a possible origin for fissility, synaeresis cracks, and slickensides.

[1] Manuscript received November 30, 1960.

DEFINITIONS USED IN THIS REPORT

Fissility is the characteristic that causes a rock to split into thin layers lying parallel in a particular direction, as, for example, along bedding planes.

Shale is an argillaceous rock that shows varying degrees of fissility.

Fissures, as defined in this paper, are small joints which occur in sediments deposited in the flocculated state and along which no slippage has taken place.

Clay-shale is a shale that has poor fissility and contains slickensides.

Underclay refers to clay that occurs under a coal bed or under the position where a coal bed normally would have developed; an underclay has very little fissility but does contain slickensides.

Slickensides is a term referring to small joints that can be measured in inches or fractions of an inch, and along which there has been some movement, but they do not

cross the boundaries of the rock in which they occur.

Synaeresis cracks are fissures that develop in a suspension where waters are expelled from the clay-water system by internal forces; they may resemble mud cracks in the sediments.

ANALYTICAL PROCEDURE

Preparation of Clay Minerals Suspensions

Clay samples weighing 150 grams were leached with 1 liter of neutral 2N salt solutions of ammonium acetate and potassium, sodium, lithium, calcium, and magnesium chlorides. The batches were then washed free of the salt solutions with distilled water.

Observations in the Preparation of the Homoionic Clay Minerals

Clay mineralogists are aware that when clay minerals are dispersed they will settle with parallel orientation, but if flocculated they will settle randomly. However, the degree of flocculation, and hence randomness of sedimentation, is influenced by the various cations in solution, each of which has different powers of flocculation. For example, trivalent ions generally have a greater flocculating power than the divalent, and divalent ions in turn have greater flocculating power than the monovalent.

When the clay minerals suspended in salt solution were poured onto a filter, the clay flocculated and settled, leaving clear water above. Synaeresis cracks, similar to mud-cracks, developed in the filter cake when it was covered with a considerable thickness of solution. This phenomenon occurred while the samples were being washed with distilled water and it continued until enough of the salts had been removed so that the clay minerals stayed in suspension or until they were dispersed in the water. At such a stage the resulting filter cake did not crack under water. The dried filter cake formed from the flocculated clay minerals was considerably larger than the dried filter cake made from the same clays after they were dispersed. The filter cake made of flocculated clay minerals did not contain laminations whereas the filter cake made of dispersed clay minerals did. When filter cakes made of flocculated clay minerals were put into water, they disintegrated readily with a small amount of agitation, but the aggregates made of dispersed clays required considerable mechanical agitation to get them back into suspension.

When suspensions of clays from cavities and joints in a Silurian limestone were being prepared, synaeresis cracks formed almost immediately on the surface of the clay under water (pl. 1) and along the sides of the beakers. The clays were at once poured into a rectangular glass tank in order to study the development of the cracks and their behavior during sedimentation and compaction. The cracks began to develop within 30 minutes to an hour after sedimentation began, reached their maximum development after two hours, and remained visible (pl. 2) during most of the period of sedimentation.

Plate 2 also shows that the cracks within the suspension have a completely random orientation ranging from vertical to horizontal, and shrinkage by synaeresis therefore takes place in all directions. The plate shows further that as the clay settled, the cracks after maximum development became gradually narrower and finally closed when settling was almost complete. However, the cracks at the surface of the suspension remained open throughout the process of sedimentation. The fact that the cracks of all other orientations, as well as those in the verticle plane, eventually closed indicates that lateral as well as downward movement takes place during sedimentation of the suspension.

The synaeresis cracks can be seen best when the salt concentrations are such that the clay minerals form large open flocs that settle slowly, but even smaller synaeresis cracks also form when salt concentrations are such that the clay minerals form smaller, more compact flocs that settle rapidly. In the latter instance, the minute cracks are more difficult to see.

It might be argued that synaeresis cracks would develop only in undisturbed waters but not in water which was being disturbed, as in nature. Nevertheless, while on a field trip, I observed underwater synaeresis cracks that had formed in a large clay company's thickening tank. The tank is 300 feet in diameter and 18 feet deep. More than 1500 gallons of water, clay, and

PLATE 1.—Showing development of synaeresis cracks under water.

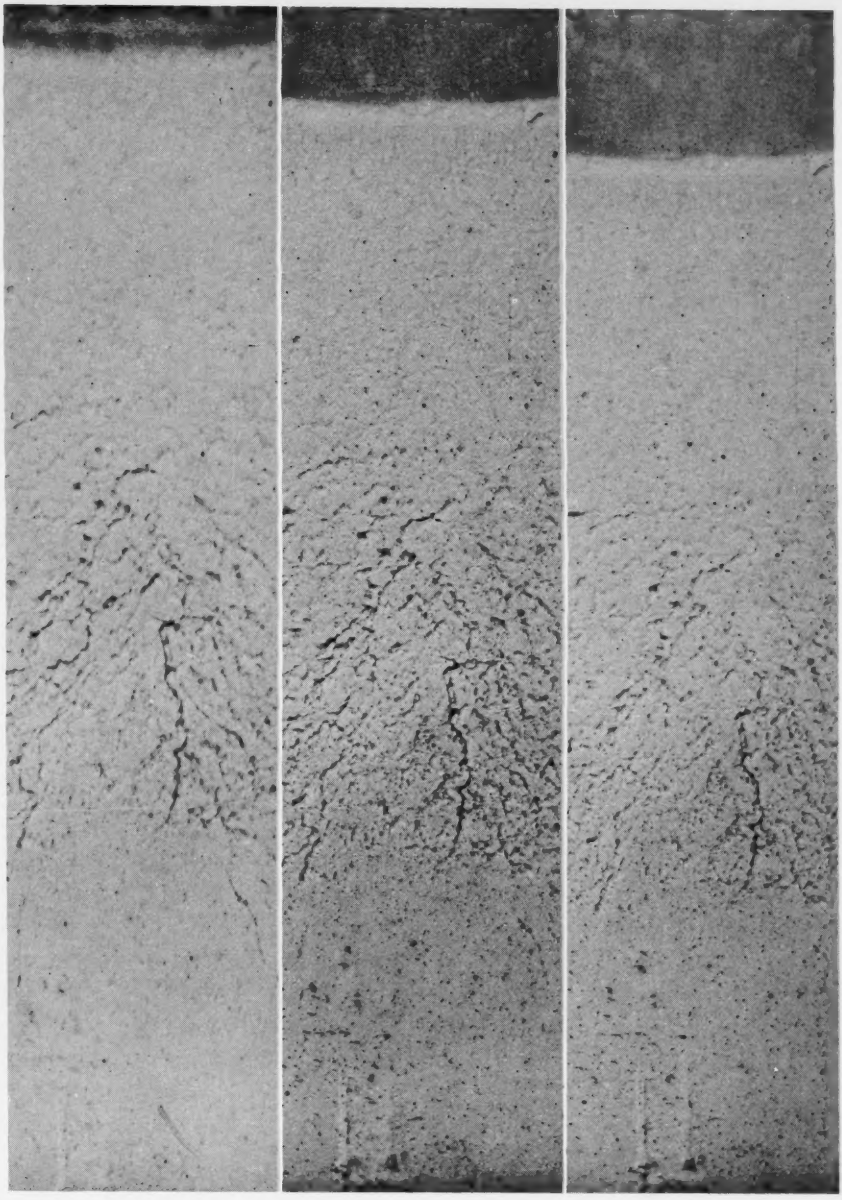

PLATE 2.—Showing synaeresis cracks in flocculated clay during sedimentation.

fine sand enter this tank per minute. The clay and sand, which settle to the bottom in the flocculated state, are pumped from the bottom of the tank as a thick slurry while the clear water containing electrolytes flows away at the top. Two plows, near the bottom of the tank, which make one revolution every minute, continually move the thick slurry to the center of the tank to be pumped out. The synaeresis cracks were able to form in this environment so that they were visible from the surface in spite of the agitation of the slurry being pumped in, slurry being pumped out, and the movement of the plows.

Observation in Natural Sediments

In natural sediments, argillaceous rocks with similar mineralogical composition vary widely in their physical properties. Experience has shown that when placed in water a fissile shale usually disintegrates very slowly, if at all, whereas shale with poor fissility disintegrates fairly rapidly. During drilling, usually very little of the core from a fissile shale is lost, but, if the shale has poor fissility, there may be considerable or total loss due to the rapid disintegration of the core in the presence of water. I have observed that fissile shales of the Paleozoic era usually have few slickensides, whereas shales with poor fissility usually have a large number of slickensides. In coal mines, the fissile shales make much better roofs than do the latter.

In order to study the orientation of the clay minerals in shales, sections were cut from cores of fissil shale and from shales with poor fissility, both parallel and perpendicular to the bedding. The sections were polished until smooth and then X-rayed. Figure 1 is representative of the fissile shales and figure 2 of the shales with poor fissility. In figure 1, the section cut parallel to the bedding gives only the *c*-axis reflections whereas the section cut perpendicular to the bedding gives strong 110, 202, and 060 reflections.

About 10 feet lower in the shale section, there is little difference in the X-ray traces for a thin section cut parallel to the bedding and one cut perpendicular to it. This part of the shale section had poor fissility. X-ray data indicate that as the degree of fissility decreased the orientation of the clay minerals became more random. When fissility was completely lacking, as in clays, the orientation of the clay minerals was also lacking or random. As the degree of fissility and orientation of the clay minerals decreases, the shale will not split along the bedding with the smooth even fracture that is characteristic of fissile shales and clay minerals that are highly oriented. The X-ray data also indicate that the mixed-lattice clay minerals are much less common in the fissile zone of the shale than in the zone of poor fissility.

Structures

The small internal structures that are commonly found in argillaceous sediments are fissility, slickensides, and fissures; a structure less commonly found is synaeresis cracks. Such structures are considered to indicate the chemical environment of deposition of the argillaceous sediments.

Fissility.—Students of sedimentary petrology generally recognize that fissility is not related to depth of burial. Rubey (1931, p. 39) has shown this in the Cretaceous shales of the Black Hills Region of South Dakota, and I have observed it in the Paleozoic shales of Illinois. Generally speaking, the clay minerals in calcareous shales are less likely to have good orientation, or fissility, than in the noncalcareous shales. The reasons for this are here postulated to be in the colloid-chemical environments of deposition.

If fissility resulted from compaction, we would expect that fissility would increase with increasing depth of burial, and thus the lower shales would be more fissile than the upper ones, but such is not everywhere the case. In drill cores, for example, shales a half mile or more in depth are no more fissile, and sometimes even less fissile, than those near the surface. Fissility is known also to vary within a shale member which may grade from fissile to nonfissile and back to fissile again within a short distance.

The differences in behavior of dispersed, semiflocculate, and flocculate clay suspensions in the laboratory would appear to show, on the other hand, that fissility can be related to the environment in which sedimentation took place. In a dispersed medium

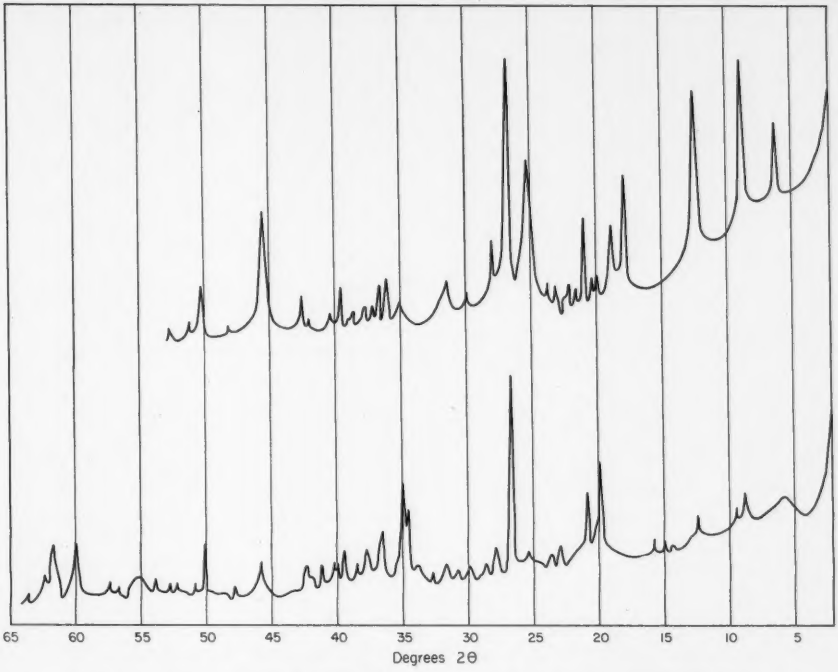

FIG. 1.—X-ray diagrams of shale sections cut parallel to the bedding (upper trace) and perpendicular to the bedding (lower trace).

the clay minerals will settle as individual particles, with all their *c*-axes parallel, and fissility will develop naturally in the mass as in the samples prepared in the laboratory. As calcium or other ions enter the system there will be a tendency for the system to flocculate and thus for the minerals to settle as flocs in which the clay minerals will be oriented randomly.

Within a sedimentary basin changes in the degree of fissility of the depositing material can come about because of changes in the salt concentration, changes in the type of salts present, or changes in the stream load, even though the salt concentration or type of salt remains constant. Rosenquist (1953, p. 199) points out "normal clays with a low sensitivity may either be deposited in fresh water where the clay-mineral grains adsorb thinner water-films, or it is possible that they may also be sedimented from so dilute a suspension that the clay mineral grains do not flocculate, but precipitate individually. This will result in a higher density of the sediment." Rosenquist (1955, p. 50) also has shown that it requires only 0.6% sodium chloride in a liter of water containing 3 grams of clay to give the same degree of flocculation that 3.2 percent sodium chloride will give with 0.3 gram of clay. If a stream does not bring enough clay into a basin for the salt to flocculate the clay, it will settle as individual particles, producing fissility. If during flood stages the stream brings in a more concentrated load, the clay may be flocculated by the salts in the water of the basin. When a stream is flooded it will have a diluting effect on the salts in the basin for a considerably greater distance than when the same stream is not in flood. Therefore, the water will allow a larger percentage of clay

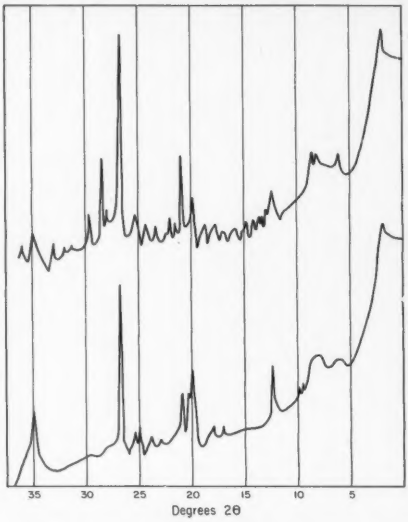

FIG. 2.—X-ray diagrams of shale sections cut parallel to bedding (upper trace) and perpendicular to the bedding (lower trace).

to remain dispersed than it would when the water is low. Whether a clay will settle in a dispersed or flocculated state will depend on both the concentration of clay and the concentration and kind of salts.

When a stream carries sediments into a body of water, and if the wave action is strong enough, the agitation from the waves may keep the flocs from forming and keep the clay particles in suspension until they are diluted enough to settle as individual particles over a very wide area. Under some conditions, part of the clay may floc and settle out whereas the remainder may be dispersed and may settle as individual particles.

It would appear that fissility in sediments owes its origin primarily to the chemical environment at the time of sedimentation, and that compaction and consolidation serve only to accent it by bringing the already oriented clay minerals closer together. Clay dispersed at the time of settlement will give rise to fissile shales, those that are flocculated will produce rocks with little fissility.

Synaeresis cracks.—It has been a popular belief that mud cracks in sediments have been formed entirely through drying. According to this theory, the original sediments were deposited under water, either the water was then drained off or evaporated, and the cracking developed as the sediments dried out on exposure to the atmosphere. Although most mud cracks may have formed in this way, others could have had a subaqueous origin as evidenced by this cracking of the clay suspensions discussed above.

Rich (1951, p. 14), who observed shrinkage cracks in shales and limestones of fondo origin, attributed their origin to subaqueous shrinkage; Pettijohn (1949, p. 144) suggested that mud cracks may form under water; and Paul Potter (personal communication) states that he has seen mud cracks in thin layers of shale between sandstone layers. Plates 3 and 4 are photographs of part of a sandstone bed above one of these thin shale beds containing synaeresis cracks. It is noted that the imprint of the cracks are on the surface of the sandstone which indicates that the cracks were present when the sandstone was being deposited. The loose sand filled the cracks during deposition of the sandstone above the shale, and when the sandstone was lithified, the sand in the cracks became part of the sandstone layer above. In some examples the sandstone layers above and below the shale layer are joined by the sand which had filled the cracks in the shale layer.

Fossil synaeresis cracks in the Tradewater Group in Fulton County, Illinois, give evidence, in my opinion, of subaqueous formation of this type. There is no evidence of curling at the surface, nor is there any gradation of the particle size from bottom to top of the layer containing the mud cracks. Further evidence to support a subaqueous rather than subaerial origin is that the cracks are not wedge-shaped but are of fairly uniform width from bottom to top, do not extend into the fissile shale beneath, and there are no clay aggregates in the sandstone above.

Synaeresis cracks are usually found in thin beds of clay between harder strata such as fissile shale, limestone, or sandstone. The clay minerals in the synaeresis cracked bed are not oriented as in shales. The

PLATE 3.—Chester sandstone showing sand that was deposited in synaeresis cracks in a thin shale layer between two sandstone layers.

synaeresis cracks are found in clays which appear to have been deposited in a flocculated state. The clay flocs when first formed usually contain large quantities of water between the individual clay particles. Owing to the larger quantity of water between the clay particles the flocs are, at first, larger and fluffy. After settling the flocs begin to lose water, even under their own weight, and their volume gradually decreases. This process continues until little clay islands begin to develop with cracks on all sides. The size of these islands will depend on the particle size of the sediment,

PLATE 4.—Chester sandstone showing sand that was deposited in synaeresis cracks in a thin shale layer between two sandstone layers.

the concentration and kind of cations present.

Fissures.—Engineers have noticed fissures in clays that have been consolidated to a moisture content near their liquid limit. Skempton (1953, p. 62) reports that a sample of clay remolded at its liquid limit and stored under water for a year developed fissures which he attributes to synaeresis. It appears that the electrochemical forces between the clay particles are sufficiently strong to cause a realignment of the clay particles so that physical structure of the clay mass would be nearer chemical equilibrium. In this readjustment, the fissures were developed.

Rosenquist (1955, p. 83–87), who has made a considerable study of Pleistocene clays of Norway, reports that the fissured clays are related to the electrolyte content of the clays, and the greater the polarizability of the cation the greater the tendency for the clay to produce fissures. A dispersed clay would have little tendency to develop fissures whereas a clay that has a concentration of soluble salts sufficient to cause the clay to flocculate would. The greater the polarizability of the flocculating cation the greater would be the tendency for fissure development.

The reason why we see these fissures in open cuts or outcrops may be that, when the pressure is released, a certain amount of swelling takes place. During this swelling, the clay particles may reorient themselves so that they are at equilibrium with their chemical environment.

In summary, synaeresis cracks or fissures may develop during sedimentation and remain as closed cracks during normal compaction, but will open again by rebound, when a fresh face is exposed. The clays may be sedimented in a chemical environment and compaction would squeeze out the water leaving the salts behind and causing the clay particles to be structurally out of equilibrium with their chemical environment. When the clay is exposed, the chemical environment will pull in more water, causing swelling or rebound, and in this environment the clay minerals will readjust to come into equilibrium with their chemical environment, which in turn causes the cracks.

Slickensides.—Slickensides occur in thicker argillaceous units than do the mudcrack type of synaeresis cracks. They also are more abundant in clay-shales and clays than in fissile shales. Because the clay minerals are randomly oriented, the clay minerals were most likely deposited in a flocculated state.

The slickensides probably have as their origin the same factors that produce synaeresis cracks. The unit concerned, however, is thicker, and slickensides are formed under continuous deposition and compaction of clay in a body of water. The flocculated clays would be subject not only to their own weight but also to that of the overlying sediments which are continually accumulating. This causes compaction of the clays, and as compaction continues the clay would probably reach a point where the cracks would begin to close by plastic flow, as one side of a crack would move against the other. The clay minerals would orient, giving the slick surface of the slickensides. With the increasing loss of water, and consequent compaction, and with increasing plastic flow the development of slickensides would also increase.

SUMMARY AND CONCLUSIONS

The structures in argillaceous rocks suggest a close relationship between the concentrations of clays and salts in a sedimentary basin. If for a given quantity of clay in sedimentary basin, the salt concentration were not large enough to flocculate the clay, the clay minerals would sediment as individual particles with parallel orientation which would produce good fissility in a shale. If the salt concentration were high enough to flocculate the clay, any one or more of several structures should occur, such as slickensides, synaeresis cracks, fissures, pits and mounds, and cones and craters.

REFERENCES

JÜNGST, H., 1934, Geological significance of synaeresis: Geologische Rundschau, vol. 25, pp. 321–325.

PETTIJOHN, F. J., 1949, Sedimentary rocks: Harper and Bros, New York, 526 p.

RICH, J. L., 1951, Three critical environments of deposition and criteria for recognition of rock deposited in each of them: Geol. Soc. America Bulletin, vol. 62, p. 1–20.

ROSENQUIST, I. T., 1953, Consideration on the sensitivity of Norwegian quick-clays: Geotechnique, vol. 3, p. 195–200.

———, 1955, Investigations in the clay-electrolyte-water system: Norwegian Géotechnical Institute Publication No. 9, Oslo, p. 125.

RUBEY, W. W., 1931, Lithologic studies of fine-grained Upper Cretaceous sedimentary rocks of the Black Hills region: U. S. Geol. Survey Professional Paper 165, p. 1–54.

SKEMPTON, A. W., 1953, Soil mechanics in relation to geology: Proc. Yorkshire Geol. Soc., vol. 29, p. 33–62.

WHITE, W. A., 1955, Water-sorption properties of homoionic clay minerals: Ph.D. Thesis, University of Illinois, 93 p.

JOURNAL OF SEDIMENTARY PETROLOGY, VOL. 31, NO. 4, PP. 571–585
FIGS. 1–9, DECEMBER, 1961

MECHANICAL ANALYSIS AND HEAVY MINERALS, MORRISON AND CLOVERLY FORMATIONS, SOUTHERN BIG HORN MOUNTAINS, WYOMING[1]

ARTHUR MIRSKY
Ohio State University, Columbus, Ohio

ABSTRACT

A mechanical analysis and heavy-mineral study were included as part of an investigation of the stratigraphy of the Morrison (late Jurassic) and Cloverly (early Cretaceous) rocks in the southern Big Horn Mountains, Wyoming. A total of 131 samples were mechanically analyzed and 34 slides were examined for heavy minerals. The heavy-mineral study was confined to the 62-micron fraction (very fine sand grade).

The results show that the Cloverly sandstones are somewhat coarser than those of the Morrison, but have essentially the same relatively high degree of sorting, roundness and sphericity.

The Morrison and Cloverly formations have approximately the same major heavy mineral assemblage, namely magnetite-ilmenite, leucoxene, hematite, pyrite, zircon, tourmaline, rutile, and garnet. They also contain many of the same minor minerals. However, of the 32 minerals and varieties identified, only colorless zircon and colorless garnet appear to be stratigraphically diagnostic. Specifically, it is suggested that a low zircon–high garnet content characterizes the Morrison whereas a high zircon–low garnet content characterizes the lower member of the Cloverly. If this distinction is real, the relationship should be useful in picking the contact between these two lithologically similar formations, especially in subsurface work.

The abundance of the stable heavy-mineral suite, zircon-tourmaline-rutile, and the high degree of rounding, indicate that both formations were derived largely from pre-existing sedimentary rocks.

INTRODUCTION

A stratigraphic study of the nonmarine upper Jurassic and lower Cretaceous rocks in the southern Big Horn Mountains, Wyoming, is summarized below. Mechanical analyses and heavy-mineral studies are given in some detail because the results are believed to be of special interest.

Nonmarine upper Jurassic and lower Cretaceous rocks crop out in a narrow belt along the eastern and western sides of the Big Horn Mountains (fig. 1). The nonmarine section, underlain by the marine Sundance Formation and overlain by the marine Thermopolis Shale is divisible into four mappable units. Unit 1, at the bottom, is a variegated mudstone, with gray-green predominating over shades of red. Unit 2 is a white to gray cross-bedded sandstone, which commonly is resistant and is conglomeratic at many places. Unit 3 is a variegated mudstone like unit 1, but shades of red predominate over green. Unit 4, at the top, is a black paper-thin shale, interbedded with thin lenticular tan cross-laminated siltstone and fine-grained sandstone. Both the lower and upper mudstones include siltstone, sandstone, and conglomeratic units.

The lower mudstone (unit 1) is referred to the Morrison Formation, the white sandstone (unit 2) and the overlying upper mudstone (unit 3) to the Cloverly Formation, and the black shale and siltstone (unit 4) to the basal Rusty Beds Member of the Thermopolis Shale (fig. 2). The Cloverly Formation is subdivided into the Otter Creek Sandstone Member (unit 2) and the Mudstone Member (unit 3). The age of the Morrison is very late Jurassic, and locally the upper part may be possibly early Cretaceous; the age of the Cloverly is early Cretaceous.

PROCEDURE

Collection of Samples

Two hundred and three samples, representing upper Sundance, Morrison, Cloverly, and lower Thermopolis rocks, were collected from 18 of 20 measured stratigraphic sections (fig. 1 and table 1). Because the sandy units were considered better suited for com-

[1] Manuscript received October 28, 1960.

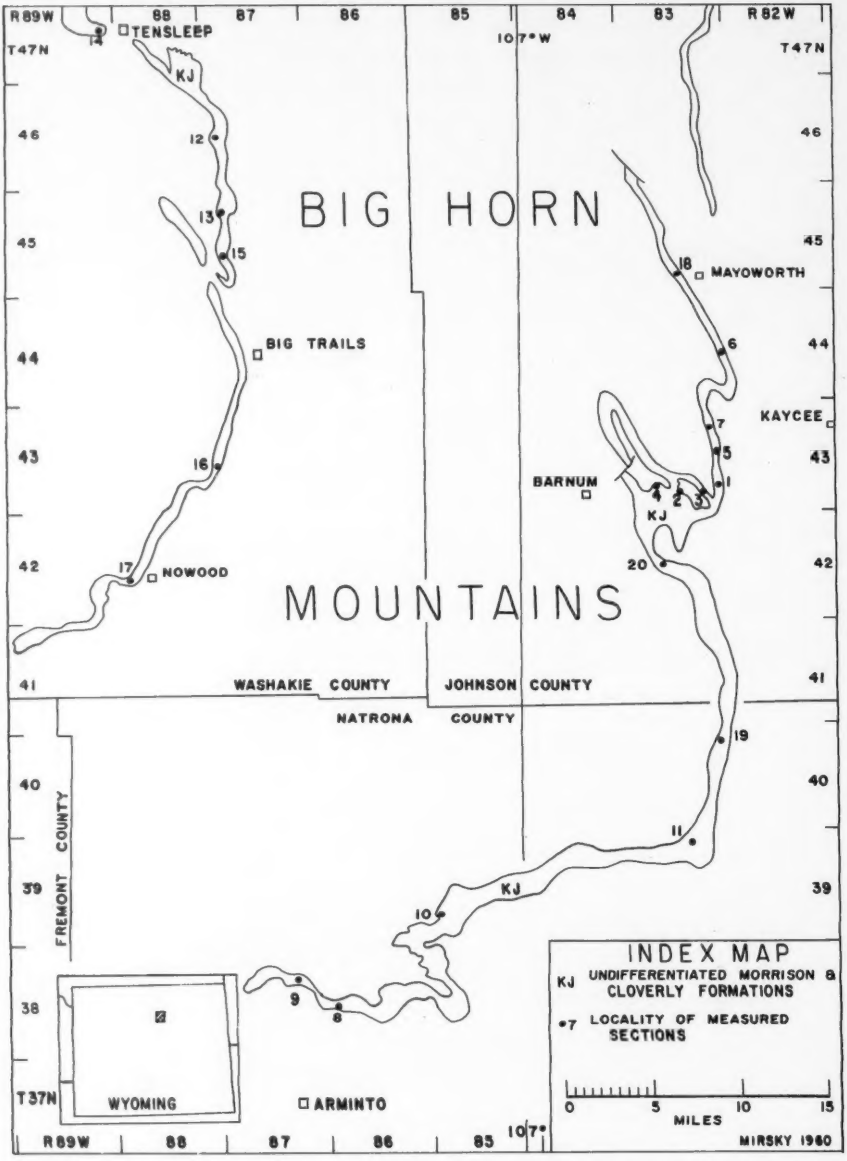

FIG. 1.—Index map showing Morrison-Cloverly outcrop around the southern Big Horn Mountains, Wyoming, and localities of measured sections.

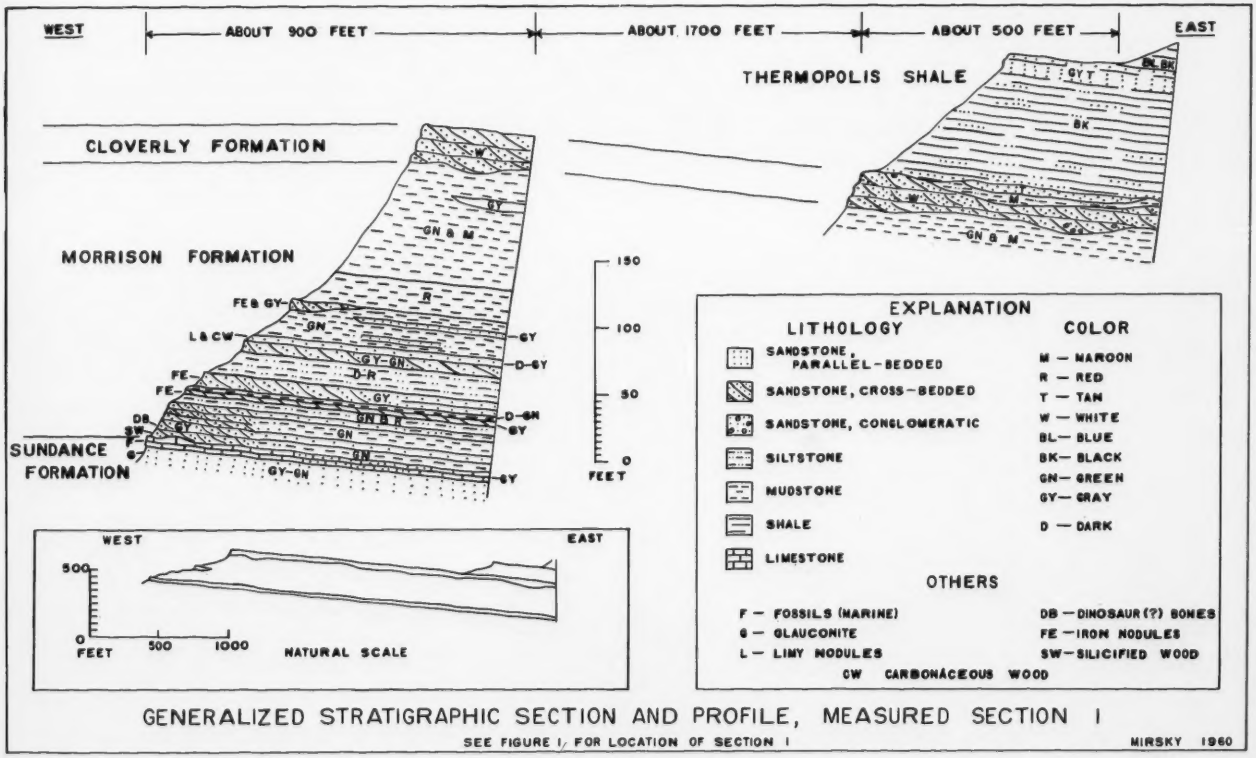

FIG. 2.—Generalized stratigraphic section and profile, typical of Morrison-Cloverly exposures on southeastern flank of Big Horn Mountains, Wyoming. Based on measured section 1.

parison, most of the samples were taken from sandstone or conglomerate, but some finer grained units were also analyzed.

Laboratory Work

Mechanical analysis.—After examination under a binocular microscope, 131 samples representing key units were selected for mechanical analysis. The following procedure was then used:

1. Approximately 50 grams of most samples were disaggregated, and each sample accurately weighed. As much as 100 grams of the coarser samples were used in order to have enough material for a heavy mineral separation.

2. If non-calcareous, the sample was sieved in a Tyler Ro-Tap sieve shaker for 10 minutes. If calcareous, the sample was first treated in 9 percent HCl until all reaction ceased; then the sample was washed three times, dried in filter paper, and again weighed to find the loss of solubles; after this, the sample was sieved through a set of Tyler screens with mesh openings of 2000, 1000, 500, 250, 125, and 62 microns.

3. Each sieve retent was weighed and the percentage of the total sample calculated.

4. Cumulative curves were drawn and analyzed according to the method employed by Inman (1952, p. 125–145).

5. The results of the mechanical analyses were tabulated (Mirsky, 1960, tables 2–5), and shown graphically; two of the graphs are reproduced as figure 3.

Heavy minerals.—The following procedure was used in the heavy-mineral study:

1. A 1 to 7 gm representative split of the very fine sand (125–62 μ grain diameter) was obtained with a micro-splitter.

2. The isolated representative sample was separated in tetrabromethane to obtain the heavy minerals.

3. Both heavy and light minerals were mounted on slides and examined for roundness, sphericity, and general mineral content.

4. The heavy minerals from 34 selected representative samples were examined in detail for types and percentages of minerals present. Each slide was first examined to ascertain the variety and approximate number of heavy minerals present. Then, by using a mechanical stage, each slide was methodically surveyed.

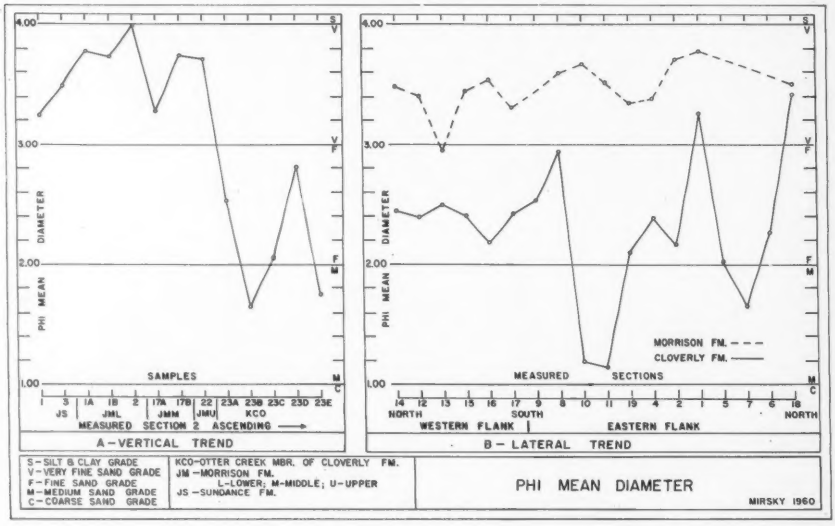

FIG. 3.—Graphs showing trends of phi mean diameter in the Morrison and Cloverly formations. A—Vertical trend in measured section 2. B—Lateral trend in the southern Big Horn Mountains.

A count of 300 grains was considered adequate for a representative percentage determination of the heavy minerals. In 10 slides, less than 300 grains were present, so every grain in the mount was counted. In two slides (samples 1-20a and 1-20f) considerably more than 300 grains were counted because a large percentage of the heavy-mineral suite was authigenic barite; therefore, enough grains were counted until 300 non-barite grains had been tabulated.

6. The results of the heavy-mineral examination are shown graphically in figures 4–9.

GRAIN SIZE DISTRIBUTION

Presentation of Statistical Data

The results of the mechanical analyses were computed according to the method employed by Inman (1952, p. 125–145). Inman used five descriptive measures in a phi notation. These descriptive measures, based on the $\phi 5$, $\phi 16$, $\phi 50$, $\phi 84$, and $\phi 95$ percentile diameters, are:

Measure	*Nomenclature*	
Central Tendency	1. Phi Median Diameter	$Md\phi = \phi 50$
	Phi Mean Diameter	$M\phi = \frac{1}{2}(\phi 16 + \phi 84)$
Dispersion (Sorting)	2. Phi Deviation Measure	$\sigma\phi = \frac{1}{2}(\phi 84 - \phi 16)$
Skewness	3. Phi Skewness Measure	$\alpha\phi = \frac{M\phi - Md\phi}{\sigma\phi}$
	4. 2nd Phi Skewness Measure	$\alpha 2\phi = \frac{\frac{1}{2}(\phi 95 + \phi 5) - Md\phi}{\sigma\phi}$
Kurtosis	5. Phi Kurtosis Measure	$\beta\phi = \frac{\frac{1}{2}(\phi 95 - \phi 5) - \sigma\phi}{\sigma\phi}$

Results of Statistical Data

Phi mean diameter.—For each section sampled, the phi mean diameters of the analyzed samples were plotted to note whether there are any vertical trends in a measured section. Figure 3a is the graph drawn for section 2, and illustrates the procedure. The abscissa represents the mechanically-analyzed samples in a section, ascending stratigraphically from left to right. The ordinate represents phi mean diameter, decreasing in size grade from bottom to top.

The graph for section 2 (fig. 3a) shows that the Morrison sandstones lie within the very fine sand grade, and those in the Cloverly lie within the fine to medium grades. This grade distinction is generally shown by the graphs for most of the other sections. The graph also shows that the base of the Cloverly is marked by an abrupt increase in mean diameter, a fact which is visible in the field and demonstrated in most of the other graphs. Finally, the variability of grain size in the Cloverly is suggested in figure 3a, although less so than in other graphs in which phi mean diameter varies between very fine and very coarse grades.

Average phi mean diameters were computed for the Morrison and Cloverly formations in each measured section. Then the average phi mean diameters were plotted to ascertain whether any lateral trends exists in each of these two units (fig. 3b). The abscissa represents the sampled sections. The sections are arranged in order, from left to right, from number 14 on the western flank, southward to number 17; then from number 9 on the eastern flank, northward to number 18. The ordinate represents average phi mean diameter, decreasing in grade (coarse to fine) from bottom to top.

As shown by figure 3b, no lateral trends are apparent. Although the curve for the Morrison seems to rise to the right, the change is insignificant. Rather, the graph shows the remarkable uniformity of the phi mean diameter of Morrison sandstones throughout the area of the study. Figure 3b also shows that the Cloverly sandstones are variable in grain size and always coarser than the Morrison. Thus, the graph of the lateral variation of phi mean diameter suggests that the vertical relationships illustrated by the graph for measured section 2 remain unchanged throughout the southern Big Horn Mountains.

Phi deviation measure.—The data concerning the phi deviation measure were analyzed

in much the same way as the phi mean diameter, although the graphs are not included in this paper. To facilitate comparison between samples, the following scale was used:

a spread of less than 0.50ϕ—very well sorted
0.50ϕ to 0.75ϕ—well sorted
0.75ϕ to 1.50ϕ—moderately sorted
1.50ϕ to 3.00ϕ—poorly sorted
a spread greater than 3.00ϕ—very poorly sorted

Fifty-nine samples from the Morrison Formation range in phi deviation measure from 0.28ϕ to 0.99ϕ (that is, very well sorted to moderately well sorted). However, 94 percent of the samples lie near the boundary between very well sorted (51 percent) and well sorted (41 percent), whereas only four samples (6 percent) lie within the moderately well sorted grade. This relationship is well shown when the average phi deviation measure for each section is plotted. The sorting values straddle the .50ϕ line, with 56 percent of the points lying within the very well sorted grade and 44 percent within the well sorted.

In contrast, 46 samples from the Cloverly Formation range in phi deviation measure from .24ϕ to 1.69ϕ (very well sorted to poorly sorted). The distribution is 33 percent within the very well sorted grade; 22 percent, well sorted; 37 percent, moderately sorted; and 9 percent poorly sorted. When the lateral trend of the average phi deviation measure is plotted, however, the distribution percentages noted above now have been changed respectively to 16, 42, 37, and 5 percent.

The generally poorer sorting of the Cloverly, as is evident above, reflects the much larger percentage of channel sandstones, and the more characteristically conglomeratic nature of these deposits.

Other significant measures.—The remaining significant measures, the two skewness and the kurtosis measures, were also analyzed. The graphs of the phi skewness measure show no definable relations within either the Morrison or the Cloverly, or between the two formations.

The same is true of the 2nd phi skewness measure and the phi kurtosis measure, both of which are most sensitive to the tails of the distribution. Because of the relatively good sorting of many of the samples, many of the cumulative curves had to be projected through the 5th and 95th percentiles. Therefore, the $\phi 5$ and $\phi 95$ figures needed in the computation of the 2nd phi skewness and phi kurtosis measures are not uniformly reliable. This may account in part for the erratic nature of the curves.

Roundness.—The roundness of a particle depends upon the angularity of the edges and corners, and is independent of the shape. The light minerals separated from the 62-micron sieve retent were examined for roundness by comparing the grains as seen under a binocular microscope with Powers' grain images (1953, fig. 1). Most of the samples in both formations lie within the angular to subangular roundness classes, although the spread is from very angular to subrounded. However, many quartz grains have secondary growths, and it is clear that the original grains were more rounded to subrounded. No lateral or vertical trends are apparent from the graphs, but the Cloverly has more samples with a higher degree of roundness than does the Morrison.

Sphericity.—Sphericity is the shape of a particle, as compared to a sphere. Sphericity was determined in the same manner as was roundness, except that the grains were compared with the sphericity chart prepared by Rittenhouse (1943, fig. 1). A sphericity value of 1.0 indicates that the particle is a true sphere. The sphericity for all samples ranged from .77 to .89. The average sphericity for the Morrison at each section ranged from .79 to 85, and that for the Cloverly from .80 to .85, indicating a fairly high degree of sphericity for both formations throughout the area of the study.

HEAVY MINERALS

Minerals Identified

The heavy minerals identified are divided into six major groups: opaques, zircon, tourmaline, rutile, garnet, and minor minerals. All occur as rounded to angular grains unless stated otherwise.

Opaques.—The opaque minerals include magnetite-ilmenite, leucoxene, hematite, and pyrite. Magnetite and ilmenite are considered together because no magnetic separation was made. The dominance of ilmenite over magnetite is suggested by the typical ilmenite form of most of the euhedral grains,

and the forms of many leucoxene grains.

Leucoxene is a prominent, if not the dominant, opaque mineral in every slide. Many grains identified as leucoxene are not the common variety that is white in reflected light. Leucoxene is an alteration product, primarily of rutile and ilmenite. Various stages in the alteration are discernible, and those grains of rutile and ilmenite which are only partly altered as well as the final alteration product were identified as leucoxene. Thus, leucoxene occurs as shades of brown, red, and yellow, in addition to the more usually described white color. A number of grains identified as leucoxene show the ilmenite crystal form; many others are translucent around the edges but opaque in the center, and if they had not behaved optically as opaque grains rather than anisotropic ones, they would have been identified as reddish-brown or honey-yellow rutile.

Hematite occurs as a minor constituent of most slides. Except in two samples, all the hematite is in angular grains and is mostly, if not entirely, authigenic. Some hematite-coated grains occur, but because they are obviously alteration products (such as from magnetite), they are included in the count of the original mineral. The two exceptions are the hematite in samples 14–16 and 8–17 in which the hematite appears to coat another mineral, much of which seems to be leucoxene; because the identity of the mineral was not certain, this type of grain was counted as hematite.

Pyrite is prominent in a few samples, present in minor amounts in many samples, and it is absent in some. Most of the pyrite grains are angular and irregular in shape; a few are euhedral; all are of authigenic origin. No rounded grains were identified. It is possible that some grains of marcasite have been included with the pyrite.

Zircon.—The zircon group is subdivided into colorless, pink, cloudy, and yellow varieties. The cloudy zircon owes its appearance primarily to fracturing, but a few altered or zoned grains (malacon?) are included. It is possible that some monazite is included with the zircon.

Tourmaline.—The tourmaline group is subdivided into colorless, tan, greenish-brown, pink, bluish-green, and blue varieties. Inclusions are common, and many grains show authigenic overgrowths.

Rutile.—The rutile group is subdivided into dark reddish-brown, light reddish-brown to yellowish-brown, and honey-yellow varieties. As noted above, many grains of rutile appear to be in varying stages of alteration to leucoxene. If alteration had not proceeded far enough so that the grain has lost its vitreous luster and anisotropic character, it was called rutile; otherwise, leucoxene.

Garnet.—The garnet group is subdivided into colorless without inclusions, colorless with inclusions, checkered (probably etched), and pink varieties. Some spinel may be included with the garnet.

Minor.—The minerals included in this group appear in fewer than half the slides, and generally as one or two grains only. They include apatite, biotite, barite, staurolite, hornblende, hypersthene, muscovite, aragonite, dolomite, epidote, and actinolite(?). Of these, no rounded grains were noted of barite, hornblende, aragonite, dolomite, epidote, and actinolite. Only the barite is clearly authigenic.

The identification of the actinolite is provisional. It occurs in only one sample, 2–23c, where it is present in the relatively significant amount of 13 percent. The mineral appears as an aggregate with a platy structure, and shows clear to yellow to yellowish-green pleochroism. It has a refractive index between about 1.60 and 1.68, and is length-slow. The edges of the aggregate-grain are jagged or sawtoothed. Extinction is parallel or slightly inclined. No figure is obtainable. The mineral appears to be an alteration product.

Results of Heavy-Mineral Study

A series of histograms was drawn in order to show graphically the relations between the major groups of heavy minerals, and between the various subdivisions within each group. The relations derived from a study of the graphs, and discussed below, may not be definitive because only 34 samples were analyzed from a relatively large area. Nevertheless, the results may be considered as strongly suggestive because of the essentially complete representation of units from the eastern, southern, and wes-

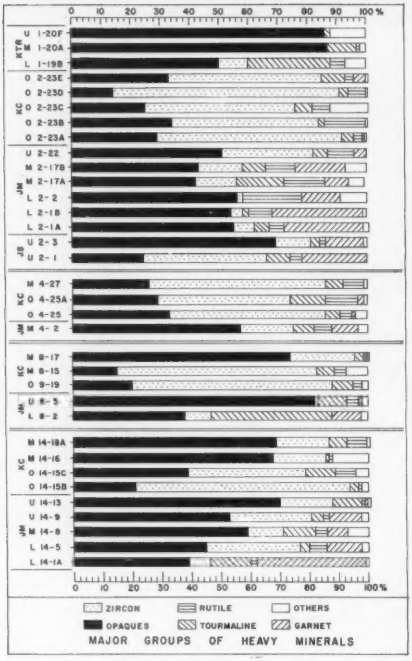

FIG. 4.—Percentage distribution of the major groups of heavy minerals. Samples on left side represent four sections or composite sections. Jm—Morrison Formation: L—Lower; M—Middle; U—Upper. Kc—Cloverly Formation; O—Otter Creek Sandstone Member; M—Mudstone Member. Ktr—Rusty Beds Member of Thermopolis Shale; L—Lower; M—Middle; U—Upper. Note relatively low percentage of zircon and high percentage of garnet in Jm, and the converse in Kco.

ern parts of the area, and the consistency of the relations.

General.—The graph of the six main groups of minerals clearly shows that the opaques and zircon, individually or in combination, make up the bulk of most slides (fig. 4). In general, the zircon increases as the opaques decrease, and the converse is true. Tourmaline and garnet are important locally, but usually they compose, together with rutile, less than 30 percent of the heavy minerals. The other minerals are of minor importance.

Figure 4 shows that in passing from the Morrison Formation to the Otter Creek Sandstone Member of the Cloverly Formation the percentage of zircon increases markedly, and the percentage of garnet decreases. These relationships are illustrated in more detail in figures 6 and 9, and are discussed below.

Opaques.—This group as a whole, and the individual minerals within it, occur randomly throughout the sections (fig. 5). The apparently lower percentage of opaques in the Otter Creek Member of the Cloverly is considered fortuitous because of the secondary origin of most of the constituent grains. Leucoxene is the dominant opaque mineral in most slides. In samples 8–17 and 14–16, hematite appears to be the chief opaque mineral, but as observed earlier, much of it occurs as a coating on other minerals.

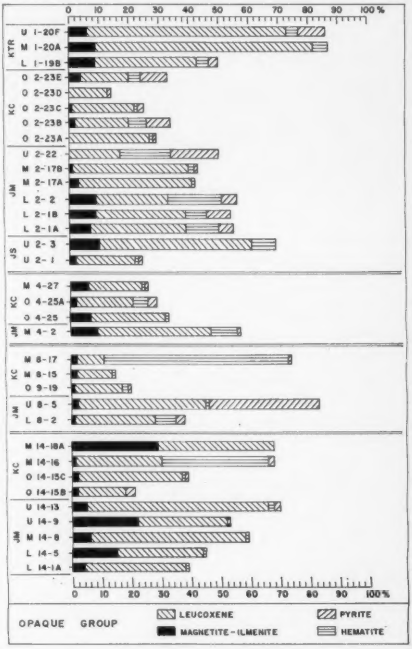

FIG. 5.—Percentage distribution of opaque heavy minerals. Samples are arranged in the same order as in figure 4. The distribution is random, and leucoxene is dominant. Individual minerals have not been plotted to a zero base because they are of little significance.

Throughout each of the four sections, the opaque minerals are slightly more angular to subangular (referred to as *A* for the remainder of this discussion) than rounded to subrounded (referred to as *R*). Some euhedral grains of magnetite-ilmenite are present at one section, and they are restricted to the upper Sundance, lower Morrison, and lower Rusty Bed units. A few euhedral pyrite grains occur at the same section, but are restricted to the lower Morrison.

Zircon.—The percentage of total zircon is significantly higher in the Otter Creek Sandstone Member of the Cloverly Formation than it is in either the Morrison Formation or the Rusty Beds Member of the Thermopolis Shale (fig. 6). The zircon content of the Mudstone Member of the Cloverly is variable.

It appears possible to pick the Morrison-Cloverly contact on the basis of the abrupt increase in zircon. An example of the feasibility of using this criterion is afforded by sample 14-13. The section from which this sample was collected is described below in condensed form.

Unit		*Feet*
14–15	Sandstone; white to gray, conglomeratic, cross-bedded; with white chert	62
14–14	Siltstone; dark olive-green; laterally restricted	3
14–13	Sandstone; gray, sparkly, resistant; bottom surface uneven; laterally restricted	2
14–12	Mudstone; dark gray	10
14–11	Mudstone; black, carbonaceous	9

This was one of the few localities where the Morrison-Cloverly contact was not clearly discernible in the field. Units 11 and 12 were typically upper Morrison in character, and Unit 15 unquestionably is the Otter Creek Sandstone Member of the Cloverly. Units 13 and 14, however, have features which could place them in either the Morrison or the Cloverly. In the field they were assigned to the Cloverly because unit 13 is the basal part of a hogback, and the bottom surface is uneven, both of which are features of the basal Cloverly elsewhere in the area. Although the lack of cross-bedding is not typical, and neither is the overlying olive-green siltstone typical, it seemed logical and convenient to include the

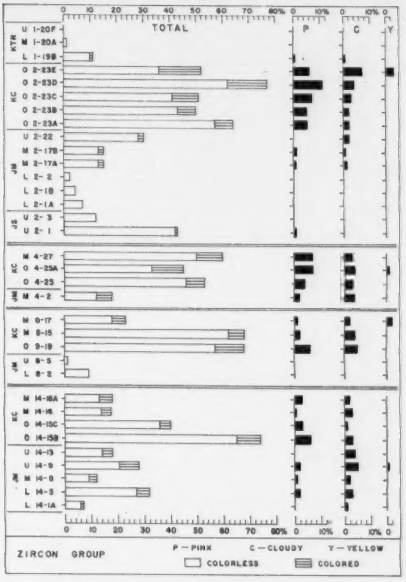

FIG. 6.—Percentage distribution of zircon group. Samples are arranged in the same order as in figure 4. Note that abrupt increase in total and colorless zircon marks the Morrison-Cloverly contact. Colored varieties are individually plotted in black to a zero base to emphasize distribution.

stratigraphically basal restricted sandstone (unit 13) with unit 15 above. The low zircon content of sample 14-13, however, suggests that the unit actually is part of the Morrison; accordingly, it has been reassigned to that formation.

Because colorless zircon occurs in much larger amounts than the other three varieties combined, the trend for colorless zircon parallels that for total zircon.

Although pink zircon is present in 22 samples, it never exceeds 11 percent, and normally is much lower. Fifteen occurrences are in Cloverly samples and range from a trace to 11 percent; six occurrences, ranging from trace to 2 percent, are in the Morrison; and a single grain was noted in a sample from the lower part of the Rusty Beds. Thus, pink zircon appears most characteristic of the Cloverly Formation.

Cloudy zircon is randomly distributed

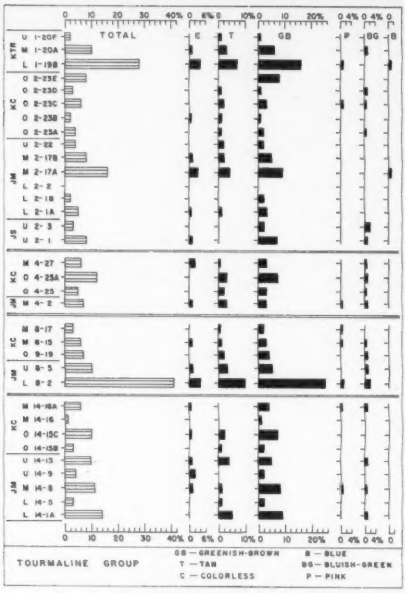

FIG. 7.—Percentage distribution of tourmaline group. Samples are arranged in the same order as in figure 4. The distribution is random. Total tourmaline is shown, and each variety is plotted in black to a zero base to emphasize distribution.

throughout the sections. Yellow zircon is too sparsely distributed to show a trend, although only a single grain occurs in the Morrison, whereas three Cloverly samples contain up to 2 percent. In the colorless variety of zircon, *R* grains are dominant over *A* grains. However, 14 samples contain from a trace to as much as 2 percent euhedral grains, and are representative of all formations. In the pink, cloudy, and yellow varieties, *R* grains are approximately equal to *A* grains in amount, but the percentage of grains involved is much too small to be really significant.

Tourmaline.—This group as a whole, and the individual varieties, are randomly distributed (fig. 7). Greenish-brown tourmaline is dominant, tan is secondary, and the other varieties are of little importance. In all the varieties of tourmaline, *R* grains exceed *A* grains, but because of the relatively small percentages, this fact could be of significance only for the greenish-brown and tan varieties.

Rutile.—The rutile group and the individual varieties are randomly distributed (fig. 8), similar to the opaques and tourmaline. The light reddish-brown and honey-yellow varieties are about equally prominent; the dark reddish-brown rutile is the least common of the three types. In all varieties of rutile, the number of *R* grains approximately equals the *A* grains, but there are relatively few grains.

Garnet.—The garnet group is either absent or nearly absent in the Cloverly, but it is a noteworthy, if at times minor, constituent of the Morrison (fig. 9). The percentage of garnet, in conjunction with that of zircon, appears to be a useful criterion for picking the Morrison-Cloverly contact in the area of this study. The colorless garnets, both with

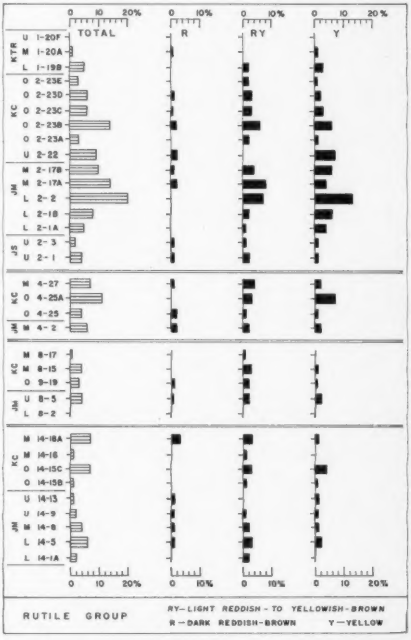

FIG. 8.—Percentage distribution of rutile group. Samples are arranged in the same order as in figure 4. The distribution is random. Total rutile is shown, and each variety is plotted in black to a zero base to emphasize distribution.

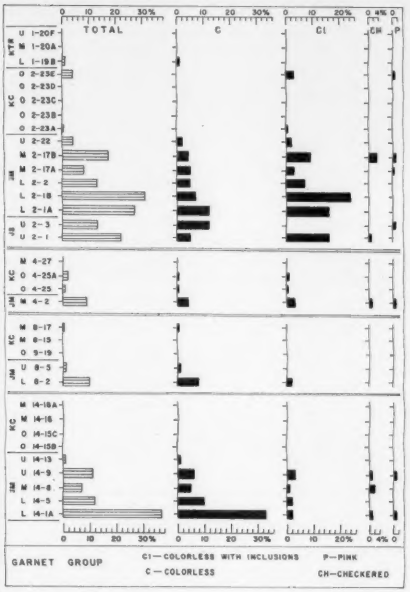

FIG. 9.—Percentage distribution of garnet group. Samples are arranged in the same order as in figure 4. Note the relative abundance of garnet in the Morrison Formation as compared with the Cloverly. Total garnet is shown, and each variety is plotted in black to a zero base to emphasize distribution.

and without inclusions, compose the bulk of the group. The checkered garnet is absent in the Cloverly, and occurs in only six samples. Also, of seven occurrences of pink garnet, only a few grains are present in one Cloverly slide. Thus, the apparent absence of checkered and pink garnet from the Cloverly follows the general garnet trend, but by itself may not be of significance, because of the small number of grains. In all varieties, *A* grains are dominant over *R* grains. It is interesting that in the chief varieties, the colorless garnets with and without inclusions, the difference in degree of rounding is greater in the lower part of the Morrison than in the upper part.

Minor.—In most slides, this group makes up a very minor part of the heavy mineral suite. The 11 minerals of this group are randomly distributed, or appear in only a few slides. No trend is observable. In all the minerals, *A* grains are more numerous than *R* grains.

DISCUSSION

The Morrison and Cloverly formations contain essentially the same major heavy-mineral assemblage, namely magnetite-ilmenite, leucoxene, hematite, pyrite, zircon, tourmaline, rutile, and garnet. In addition, they contain many of the same minor minerals.

Of the 32 minerals and varieties identified, however, only colorless garnet, both with and without inclusions, and colorless zircon, appear to be stratigraphically diagnostic. Specifically, it is suggested that in the area of this study, a low zircon–high garnet content characterizes the Morrison, whereas a high zircon–low garnet content characterizes the Otter Creek Sandstone Member of the Cloverly Formation. If this is a real distinction, then one need only note the relative percentages of garnet and zircon to determine whether a sample is from the Morrison or from the lower Cloverly. This would obviate the time-consuming labor of making careful grain counts and identifying all mineral types on a slide. It should be especially useful in subsurface work.

A seemingly excellent opportunity is afforded for checking the validity of the garnet–zircon relationship outside the area of this report. A heavy-mineral study was included in the stratigraphic work done on the northern and northeastern parts of the Big Horn Basin by Moberly (1956; 1960). In fact, the southernmost part of Moberly's area is only about 10 miles north of the area of the present investigation. The discussion of the comparison between the results of Moberly's heavy-mineral study and that of the present report refers only to Moberly's earlier work (1956) because the details given there are omitted or too much summarized in his later article (1960).

Moberly used the very fine sand grade and tetrabromethane for his heavy-mineral separation, as was done in this study. Unfortunately, a direct comparison between Moberly's heavy-mineral frequencies (1956, fig. 60) and the corresponding data for the area studied by the writer (Mirsky, 1960, tables 6–12; this report, figs. 4–9) is not

possible for the reasons that, (1) his percentages have been grouped into a logarithmic frequency distribution with nine grades, whereas the actual percentage is recorded by the writer, and (2) it is uncertain as to how the three members of Moberly's Cloverly are related to the two members of this report. One interpretation is as follows:

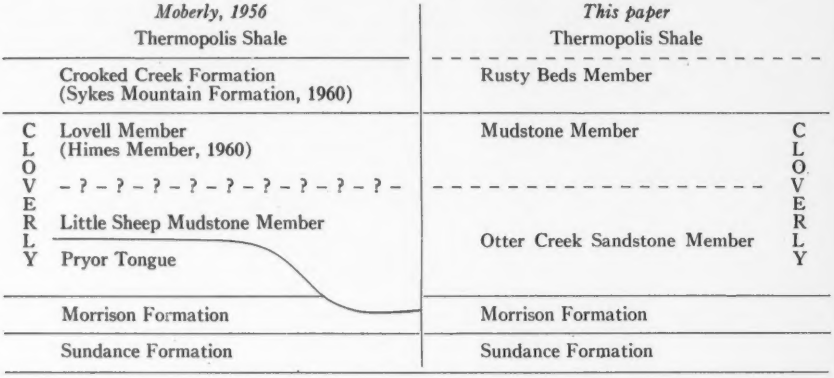

The tongue of Pryor Conglomerate is probably equivalent to the Otter Creek Sandstone Member; the Lovell Member is probably equivalent to the Mudstone Member; but the Little Sheep Member may be equivalent to parts of the Otter Creek and Mudstone members.

A third reason preventing a direct comparison is that Moberly's varietal subdivisons of garnet and zircon are not the same as those used in this study, so that only total percentages can be compared. Finally, his samples are geographically and stratigraphically identified only in a general way.

Although he does not make a special point of it, Moberly's data on heavy-mineral frequency show that the Pryor Tongue and the conglomeratic part of the Little Sheep Mudstone Member contain considerably more total zircon than does the Morrison. This appears to substantiate the suggestion of the present study that greatly increased zircon content marks the passage from the Morrison to the Cloverly. Moreover, frequency of zircon is more variable in Moberly's Lovell Member, and in the sandstone samples from the Little Sheep Mudstone Member. This agrees with the distribution of zircon in the Mudstone Member, the upper part of the Cloverly of this report.

Moberly's data for the distribution of total garnet does not agree with those of the present study, as he shows no significant difference in garnet content between the Morrison and the Cloverly. If the garnet relationship in each area is as indicated, the relationship must change somewhere in the unstudied region between the areas.

In the Black Hills, Bergenback *et al.* (1957, table 24, p. 406) found that high zircon—low garnet characterizes the Lakota-Fuson interval (equivalent to the Cloverly). Although low-zircon–high garnet occurs in the lower calcareous part of the Morrison, the percentages of these two minerals in the upper non-calcareous part of the Morrison are almost the same as those in the Lakota, rather than those in the lower part of the Morrison. Thus, in the Black Hills the change in the ratio of zircon to garnet takes place between the lower and upper parts of the Morrison rather than between the Morrison and Cloverly (Lakota), as is true in the southern Big Horn Mountains.

Mechanical analyses.—The Morrison sandstones are mostly in the very fine size grade. Mechanical analyses also show a fairly high degree of sorting, roundness and sphericity. As sorting is achieved quickly, whereas rounding is acquired slowly (Pettijohn, 1957, p. 555), the degree of roundness is the more critical factor in the history of the sediments. Long-continued abrasion,

TABLE 1.—*Names and locations of measured sections, southern Big Horn Mountains, Wyoming*

No.	Name	Location		
		Section	Twp.	Range
1	East Red Fork Powder River (J)*	S SE 26	43N	83W
2	Middle Fork Powder River (J)	S NE 33, NW SW 34	43N	83W
3	West Red Fork Powder River (J)	SW NE 34	43N	83W
4	East Barnum (J)	W NW 32	43N	83W
5	West Clark Ranch (J)	NW NE 23	43N	83W
6	Pass Creek (J)	NW 24	44N	83W
7	Northwest Clark Ranch (J)	S SW 11	43N	83W
8	Northeast Arminto (N)	NE NW 19	38N	86W
9	North Arminto (N)	S SE 10	38N	87W
10	Baker Cabin Road (N)	E NW, W NE, SE 25	39N	86W
11	Alkali Creek (N)	NE NE, NE SE 4	39N	83W
12	Spring Creek (W)	NE 19, NW 20	46N	87W
13	Otter Creek (W)	NE 7, NW 8	45N	87W
14	Tensleep (W)	SW 24	47N	89W
15	North Big Trails (W)	SE 19, S 20	45N	87W
16	South Big Trails (W)	NW 25	43N	88W
17	Nowood (W)	SE 19 (?)	42N	88W
18	Mayoworth (J)	NE 33, NW 34	45N	83W
19	Willow Creek (N)	SW 2, SE 3	40N	83W
20	Southeast Barnum (J)	NW 17	42N	83W

* (J)—Johnson County; (N)—Natrona County; (W)—Washakie County. *Note:* no samples were collected from sections 3 and 20.

and thus a long transport history, is denoted by rounded sand, although angular or subangular sand does not necessarily denote brief transport (Pettijohn, 1957, p. 554).

Two of the possible situations that could result in a long history of abrasion are (1) long transportation from a non-sedimentary rock or a sediment whose grains had a low degree of roundness, and (2) shorter transportation from an older sedimentary rock whose component grains were moderately to highly rounded because of a previous abrasion history. The mineralogical evidence suggests the second condition as the more probable.

The Cloverly sandstones are somewhat coarser than the Morrison, but have essentially the same degree of sorting, roundness, and sphericity. We can conclude that the depositional history is similar to that of the Morrison; but the coarser character of the Cloverly suggests that the source area (generally similar to that for the Morrison) either underwent renewed uplift or increased precipitation, or was closer. The last is very probable, and one or both of the other possibilities could have been accompanying factors.

Heavy minerals.—The heavy minerals in the Morrison and Cloverly formations suggest that these strata were derived chiefly from the erosion of pre-existing sedimentary rocks, possibly with some very minor direct contributions from both igneous and metamorphic rocks.

The authigenic minerals, and various alteration products (barite, aragonite, leucoxene, hematite, and pyrite) can be eliminated from a discussion of provenance. The remaining minerals can be considered in terms of original source, relative abundance, and degree of roundness.

Considering only the heavy minerals, without regard to relative abundance and roundness, it seems that the provenance was an igneous and metamorphic complex (table 2). However, the dominant minerals in the suite—zircon, tourmaline, and rutile—and the dominance of rounded to subrounded grains (table 3) indicate a mature sediment (Pettijohn, 1957, table 98, p. 513). This condition can be achieved by very long transportation of first-cycle detritus from a crystalline source, or by shorter transportation of detritus that has undergone several cycles of erosion. The overthrust belt of folded and faulted rocks in southeastern Idaho and southwestern Wyoming, about 200 miles

TABLE 2.—*Original sources of heavy minerals in the Morrison and Cloverly formations, southern Big Horn Mountains, Wyoming. The source rocks selected take into account the specific appearance, color, etc. of the heavy minerals examined. X—more probable; (X)—less probable (modified after Milner, 1940)*

		Igneous rocks	Acid igneous rocks	Intermediate igneous rocks	Basic igneous rocks	Ultrabasic igneous rocks	Pegmatites	Metamorphic rocks	Regionally metamorphosed rocks	Contact metamorphosed rocks	Acid volcanic rocks	Basic volcanic rocks	Alteration product	Authigenic
Magnetite	(1)	(X)	(X)	(X)	X	X	—	(X)	—	—	—	—	—	—
Ilmenite	(1)	—	—	—	X	(X)	—	—	—	—	—	—	—	—
Leucoxene	(1)	—	—	—	—	—	—	—	—	—	—	—	X	—
Hematite	(1)	—	—	—	—	—	—	—	—	—	—	—	X	X
Pyrite	(1)	—	—	—	—	—	—	—	—	—	—	—	—	X
Zircon	(1)	—	X	X	—	—	—	(X)	—	—	—	—	—	—
Tourmaline	(1)	—	X	—	—	—	X	X	—	—	—	—	—	—
Rutile	(1)	—	X	—	—	—	—	X	—	—	—	—	—	—
Garnet	(1)	(X)	—	—	—	—	—	X	—	—	—	—	—	—
Apatite	(2)	X	—	—	—	—	—	—	—	—	—	—	—	—
Hypersthene	(2)	—	—	(X)	X	X	—	—	—	—	—	(X)	—	—
Biotite	(3)	X	—	—	—	—	—	X	—	—	—	—	—	—
Barite	(3)	—	—	—	—	—	—	—	—	—	—	—	—	X
Staurolite	(3)	—	—	—	—	—	—	—	X	—	—	—	—	—
Hornblende	(4)	—	(X)	(X)	—	—	—	X	—	—	(X)	—	—	—
Muscovite	(4)	(X)	—	—	—	—	X	X	—	—	—	—	—	—
Aragonite	(4)	—	—	—	—	—	—	—	—	—	—	—	—	X
Epidote	(5)	X	—	—	—	—	—	X	—	—	—	—	—	—
Actinolite(?)	(6)	—	—	—	—	—	—	X	—	—	—	—	—	—

(1) present in Sundance, Morrison, Cloverly, and Thermopolis formations
(2) present only in Morrison and Thermopolis formations
(3) present in Morrison, Cloverly, and Thermopolis formations
(4) present only in Thermopolis shale
(5) present only in Morrison and Cloverly formations
(6) present only in Otter Creek sandstone member of Cloverly formation

westward of the area of this study, is believed to have been the probable source area for the Morrison and Otter Creek deposits. Thus, the immediate source rock for these units was probably a pre-existing sedimentary sequence. The presence of garnet in the Morrison and its virtual absence in the Cloverly, and the abrupt increase in zircon in passing from the Morrison to the Cloverly, indicate a longer sedimentation history for the Cloverly sediments. Finally, the presence of euhedral grains, especially of zircon, suggests that crystalline rocks possibly contributed some very minor amounts of material directly to the deposits.

A distinction between the formations appears practical on the basis of the heavy-mineral content, specifically that of zircon and garnet. Passage from the Morrison to the Cloverly is marked by an abrupt increase in zircon and a decrease in garnet. The change in amount of zircon seems also to occur outside the area of this study, along the flanks of the Big Horn Basin from Hyattville northward to Cody. In the Black Hills, where the Morrison is overlain by a Cloverly equivalent, the Lakota Formation, the change in percentage of zircon and garnet also occurs; however, the change takes place within the Morrison rather than between the Morrison and Lakota. Thus in the Big Horn area, the relative amounts of

TABLE 3.—*Comparison of relative abundance and degree of roundness of major heavy minerals in the Morrison and Cloverly formations, southern Big Horn Mountains, Wyoming. Jm—Morrison Formation; Kco—Otter Creek Sandstone Member of Cloverly Formation; Kcm—Mudstone Member of Cloverly Formation; Tr—trace; A—angular to subangular grains; R—rounded to subrounded grains.*

Mineral	Unit	Percent *A* grains			Percent *R* grains			Degree of Roundness
		Maximum	Minimum	Usual*	Maximum	Minimum	Usual*	
Magnetite-Ilmenite	Kcm	29	1	< 4	3	0	< 4	$R<A$
	Kco	4	0	< 3	6	0	< 3	$R\cong A$
	Jm	9	0	< 5	12	0	< 5	$R\cong A$
Zircon	Kcm	20	4	<11	58	7	<40	$R>A$
	Kco	22	10	<17	58	23	<50	$R>A$
	Jm	12	0	<10	20	0	< 9	$R\cong A$
Tourmaline	Kcm	4	0	< 2	5	1	< 4	$R>A$
	Kco	3	Tr	< 2	9	1	< 6	$R>A$
	Jm	7	0	< 4	39	0	< 9	$R>A$
Rutile	Kcm	5	0	< 4	5	Tr	< 4	$R\cong A$
	Kco	8	Tr	< 3	6	Tr	< 5	$R>A$
	Jm	12	0	< 6	8	0	< 5	$R\cong A$
Garnet	Kcm	Tr	0	0	0	0	0	— —
	Kco	4	0	0	1	0	0	— —
	Jm	33	0	<10	9	0	< 4	$R<A$

* The percentage occurring in about 70% of the samples.

zircon and/or garnet can be used either as a check on the more easily observed surface criteria, or perhaps as the only criterion for distinguishing between Morrison and Cloverly in subsurface work. In either case, it is unnecessary to spend time examining all the heavy minerals, because apparently only zircon and garnet are critical.

ACKNOWLEDGEMENTS

The writer gratefully acknowledges the helpful discussions with and criticisms given by Robert L. Bates, who suggested the stratigraphic problem and directed the investigation, to M. P. Weiss, and to G. E. Moore, Jr., who checked the heavy mineral identifications.

REFERENCES

BERGENBACK, R. E., CHISHOLM, W. A., AND MAPEL, W. J., 1957, Petrography of some sandstone beds in the Inyan Kara group and associated rocks: *in* Geologic investigations of radioactive deposits, Semiannual progress report for December 1, 1956 to May 31, 1957; U. S. Geol. Survey Traces Elements Invest. 690, Book 2, p. 398–413.

INMAN, D. L., 1952, Measures for describing the size distribution of sediments: Jour. Sedimentary Petrology, v. 22, p. 124–145.

MILNER, H. B., 1940, Sedimentary petrography, 3rd ed.: Thomas Murby and Company, London, 666 p.

MIRSKY, ARTHUR, 1960, Stratigraphy of the nonmarine upper Jurassic and lower Cretaceous rocks, southern Big Horn Mountains, Wyoming: Doctoral dissertation, Ohio State Univ., Columbus.

MOBERLY, RALPH, JR., 1956, Mesozoic Morrison, Cloverly, and Crooked Creek formations, Bighorn Basin, Wyoming and Montana: Doctoral dissertation, Princeton Univ.

———, 1960, Morrison, Cloverly, and Sykes Mountain formations, northern Bighorn Basin, Wyoming and Montana: Geol. Soc. America Bull., v. 71, p. 1137–1176.

PETTIJOHN, F. J., 1957, Sedimentary rocks, 2nd ed.: Harper and Brothers, New York, 718 p.

POWERS, M. C., 1953, A new roundness scale for sedimentary particles: Jour. Sedimentary Petrology, v. 23, p. 117–119.

RITTENHOUSE, GORDON, 1943, A visual method of estimating two-dimensional sphericity: Jour. Sedimentary Petrology, v. 13, p. 79–81.

JOURNAL OF SEDIMENTARY PETROLOGY, VOL. 31, NO. 4, PP. 586–593
FIGS. 1–10, DECEMBER, 1961

POST-SANGAMONIAN(?) CALCAREOUS SPRING DEPOSITS, WELLSVILLE AREA, COLORADO[1]

C. C. REEVES, JR.
Texas Technological College

ABSTRACT

Three closely associated travertine deposits that have been precipitated from hot springs occur near Wellsville, Colorado. Field relations suggest that hot waters dissolved carbonate from underlying Ordovician dolomites and migrated to the surface along faults that border each deposit. Conformity of the deposits to present topography plus several nearby tepid springs date the deposits as very recent. A post-Sangamonian(?) age is indicated by their occurrence on river gravels of Sangamonian(?) age.

INTRODUCTION

The occurrence of a large, well exposed hot spring deposit in Colorado is relatively rare, even though hot springs are found in many parts of the state. Hot springs are known in the Poncha Springs and Salida areas as well as along Cement Creek near Crested Butte. The hot springs at Mt. Princeton west of Nathrop and at Glenwood Springs have long been used by tourists as hot mineral baths. Because of this seeming ubiquity of hot springs, yet general absence of extensive, well exposed hot spring deposits, the occurrence of such a deposit in Colorado is a rarity worth geologic investigation.

LOCATION

The Wellsville community is located in Fremont County, Colorado, approximately 5 miles east of Salida and 45 miles west of Canon City on United States highway 50 (fig. 1). The hot spring deposits are located one-half mile north of Wellsville, in the W½ sec. 18, T. 49 N., R. 10 E. (fig. 2).

The northernmost of the three deposits occurs in the trough of the Wells Gulch Syncline, the other two deposits occur high on the northeastern flank of the much larger Wellsville Syncline (fig. 2). The hot spring deposits and the associated strata form a part of the eastern sedimentary outcrops of the northern Sangre de Cristo Mountains.

PREVIOUS WORK

Attention was first directed to the Wellsville area by Brainerd, Baldwin, and Keyte (1930) when they measured the Pennsylvanian outcrops near Badger Creek. Kirk (1931) designated the excellent Devonian outcrops of sec. 13, T. 49 N., R. 9 E., as the type section of his Chaffee Formation. Graduate theses by Coash (1949), Rold (1950), Siapno (1953), Bhutta (1954), Rahman (1954), and McLamore (1958), as well as professional papers by Brill (1952), Gableman (1952), and Litsey (1958), have dealt in varying degrees with the geology of the Wellsville area.

STRATIGRAPHY

Excellent exposures of a nearly complete Paleozoic stratigraphic section occur in the Wellsville area. The lower Paleozoic section has been measured by Rold (1950), and by McLamore (1958), the upper Paleozoic section by Brainerd, Baldwin, and Keyte (1930), and more recently by Brill (1952). For the purpose of this paper a detailed description of the strata closely related to the hot spring deposits is considered sufficient.

Devonian

Chaffee Formation.—The Chaffee Formation, named by Kirk (1931) for the excellent Devonian exposures one-half mile west of the hot spring deposits, consists of two members, the basal Parting Quartzite and the overlying Dyer Dolomite.

The basal Parting Quartzite Member, so named because of its position between the "White" and "Blue" limestones of the Leadville district (Emmons, 1882), is a unit of variable lithology in the Wellsville area. The lower part, which ranges in thickness

[1] Manuscript received October 7, 1960.

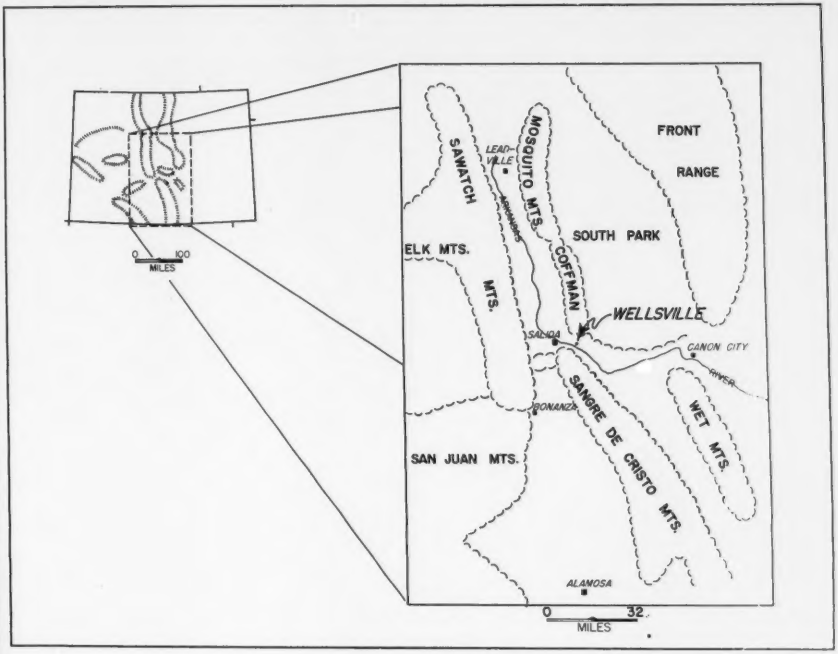

FIG. 1.—Index map of Wellsville area.

from a few feet to over 40 feet, consists of sandstone, poorly bedded, argillaceous, arenaceous dolomite, and green to light brown mottled shales that rest on a basal purple permanganate soil profile. This permanganate soil profile, designated by Rold (1950) as the lower unit of the Parting Member and by McLamore (1958) as reworked Fremont limestone, conspicuously marks the Ordovician-Devonian contact throughout the Wellsville area, especially along the south side of Arkansas River and along the western edge of Deposit B (fig. 2). The upper part of this lower unit of the Parting Member consists of a lenticular, arenaceous dolomite that weathers gray and grades upward into the vari-colored shales, siltstones, and mudstones that are conspicuous in outcrops on the south side of Arkansas River.

The upper part of the Parting Member forms a conspicuous brownish-red cliff and is approximately 30 feet thick. This unit generally is composed of cross-bedded, coarse-grained, brown to cream quartzite, but in many places lenses of sandstone and dolomite predominate.

The overlying Dyer Member is composed chiefly of buff to brownish-yellow, fine grained dolomite that contains numerous shale and limestone partings. The Dyer is characterized by well developed jointing that gives the unit a blocky appearance on weathered surfaces, and by highly irregular patterns of "wire-like" chert fillings that weather as irregular ridges to produce a pseudo pit and cusp surface. The unit has a variable thickness owing to erosion that preceded deposition of the overlying Mississippian limestone.

The contact with overlying Mississippian strata is represented by a weathered zone at the top of the Dyer that contains numerous angular Dyer Dolomite fragments. The basal Leadville Limestone (Mississippian) characteristically consists of a massively bedded, arenaceous, highly resistant limestone or sandstone breccia which both Rold (1950) and Siapno (1953) correlated with

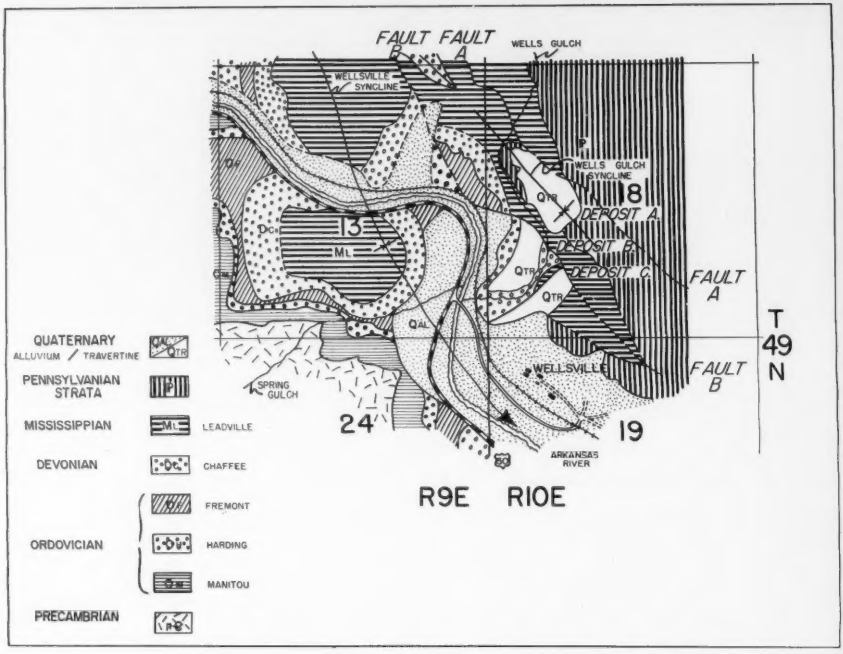

FIG. 2.—Geologic map of hot spring area (after Rold, 1950).

the Gilman Sandstone Member in the Leadville district.

Mississippian

Leadville Formation.—The Leadville Formation, named for the principal host rock for the ore in the Leadville mining area (Eldridge, 1894), can be divided into two units in the Wellsville area. The lower unit is 70 to 80 feet thick and consists of thin, evenly bedded blue-black limestone that contains several conspicuous intervals of limestone breccia. The upper unit is 80 to 170 feet thick and consists of irregularly bedded dark gray limestone that contains large black to gray chert fillings and nodules.

Because of a major unconformity that separates Mississippian and Pennsylvanian strata in this area, the upper unit of the Leadville Formation has a considerable range in thickness and contains numerous solution cavities and associated collapse structures. These features, and the characteristic yellow-brown to reddish-brown color of the weathered surface, make the Leadville the most conspicuous stratigraphic unit in the area. The contact between the Leadville Formation and the overlying Pennsylvanian strata is represented by an abrupt lithologic change to the carbonaceous, arenaceous, black illitic shales and coarse-grained sandstones and quartzites of the Kerber Formation.

Pennsylvanian

Kerber Formation.—Pennsylvanian terminology has been inconsistent, confusing, and unreliable for many years, especially in the Wellsville area. Brill's monumental work (1952) established the Kerber Formation as the basal Pennsylvanian unit in the Wellsville area. The Kerber Formation consists of nearly 200 feet of gray to black illitic shales and associated mudstones, coarse sandstone "grits," quartzite, and several thin coal-like beds. The lower part of the formation is

characterized by irregular and undulatory bedding and by abrupt lithologic changes. The top of the formation is in contact with andesite porphyry sills (Brill, 1952), one of which crops out around the northernmost travertine deposit. Work in progress by both the writer and D. W. Bolyard (personal communication) suggests that the top of the Kerber Formation should be redefined in the Wellsville area.

Quaternary Gravels

At least two prominent Quaternary gravel deposits are closely associated with the hot spring deposits in the Wells Gulch area. One of these lies beneath the travertine in Deposits B and C (fig. 2), and the other is the alluvium in the Arkansas River Valley and in Wells Gulch. Since deposition of extensive terrace deposits in the Arkansas River Valley north of Salida was closely related to the glacial and interglacial stages, preliminary correlation with these terraces suggests that the Wells Gulch gravels are of Recent age. Thus the overlying terrace gravels found beneath Deposits B and C, which were the source for the gravels in Wells Gulch, may be as young as Sangamonian. Deposits of this Sangamonian(?)[2] gravel occur on both sides of the Arkansas River Valley throughout the Wellsville area. The gravel in these deposits is well indurated and is composed dominantly of cannonball size boulders of the surrounding stratigraphic units bound together by a calcareous matrix. In many places the gravel contains lenses of fine to coarse-grained, cross-bedded sandstone (fig. 3).

HOT SPRING DEPOSITS

Location

Three separate hot spring deposits occur in the Wellsville area. For reference the northernmost is termed Deposit A, the westernmost Deposit B, and the southernmost Deposit C (fig. 2). Deposit A is best exposed in quarries owned by the American Crystal Sugar Company (fig. 4). Deposit B is best exposed along the steep sided valleys of the Arkansas River and Wells Gulch.

[2] Because of the preliminary nature of the correlation Sangamonian(?) instead of Sangamonian is used.

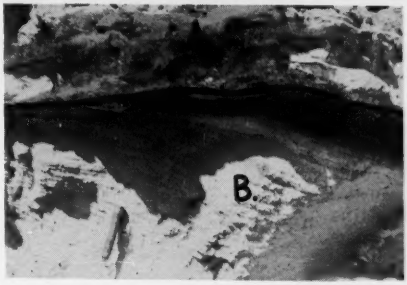

FIG. 3.—Travertine (A) overlying Quaternary sandstone (B), E½ NW¼ SW¼ sec. 18, T. 49 N., R. 10 E.

Deposit C is poorly exposed in most locations.

Description

For a general discussion of the origin, rate of deposition, and characteristics of hot spring deposits the reader is referred to a previous paper by the author and Harland Soper (1959).

The composition and other characteristics of the travertine show little variation between the three deposits. In the upper parts of the deposits the calcium carbonate content ranges from 97.7 to 98.9 percent (table 1), but the carbonate content decreases in the lower parts of the deposits owing to increased contamination by quartz and clay impurities. Bedding is not present everywhere. The thin, porous, tabular beds that characterize many hot spring deposits are

FIG. 4.—Quarried western side of Deposit A, looking to the northeast, E½ SW¼ NW¼ sec. 18, T. 49 N., R. 10 E.

TABLE 1.—*Insoluble residue analysis*

Specimen Location	Specimen Weight	Residue Weight	Percent $CaCO_3$	Percent Light Minerals	Percent Heavy Minerals
Deposit A	271.73	2.99	98.9	92.4	7.6
Deposit B	259.60	5.60	97.7	89.1	10.9
Deposit C	210.00	3.00	98.6	93.9	6.1

confined to the lower parts of the Wellsville deposits. The upper parts of the deposits generally are massive (fig. 5). The color varies from white to red or yellow on weathered surfaces, and fresh surfaces are cream to white.

The travertine in all three deposits contains abundant conglomeratic debris. Vertical pipes, which are interpreted as former hot water conduits, now contain travertine cemented conglomerates (fig. 6). Travertine cemented conglomerates also fill former channels within the deposits (fig. 7).

The basal portion of the travertine deposit, the characteristics of which vary from deposit to deposit and also within each deposit, generally is composed of pure, thin tabular masses on the north and west but on the south the masses are often interbedded with conglomeratic debris. In Deposit A the travertine rests on Mississippian and Pennsylvanian strata (fig. 8), but to the south and west the flows rest on the Devonian Chaffee Formation (fig. 9) and on Quaternary stream gravels and cross bedded sandstones (fig. 3).

Structural and Stratigraphic Relations

As shown in figure 2 the Wellsville hot spring deposits overlie strata of Devonian, Mississippian, Pennsylvanian and Quaternary ages. Deposit A lies on strata of Mississippian and Pennsylvanian ages, Deposit B on strata of Devonian and Quaternary ages, and Deposit C on strata of Devonian, Mississippian, Pennsylvanian (not apparent) and Quaternary ages.

As has been previously noted (Reeves and Soper, 1959), thermal water deposition is indicative of structural weakness. Figure 2 shows that all three deposits are bounded, on their up-dip side, by thrust faults. Southeast of the deposits, and along the strike of these faults, tepid springs flow into Arkansas

FIG. 6.—Edge of conglomerate filled conduit, $NW\frac{1}{4}$ $SW\frac{1}{4}$ $NW\frac{1}{4}$ sec. 18, T. 49 N., R. 10 E.

FIG. 5.—Massive flows in upper part of Deposit B.

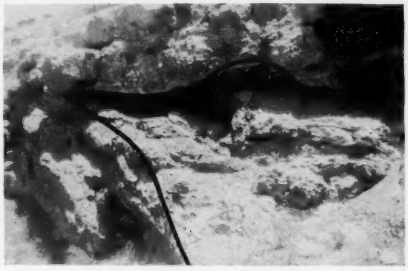

FIG. 7.—Drainage channel formed by escaping mineral waters, and now filled with travertine cemented conglomerate.

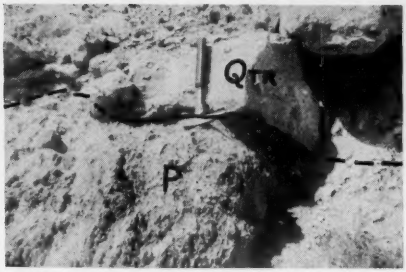

FIG. 8.—Basal flows of Deposit A overlying weathered Pennsylvanian Kerber Formation, SW¼ SE¼ NW¼ sec. 18, T. 49 N., R. 10 E.

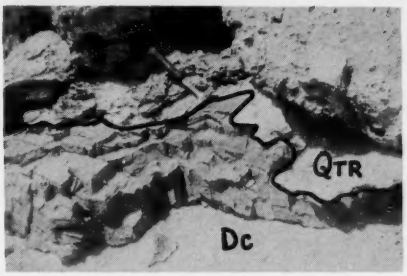

FIG. 9.—Basal flows of Deposit B overlying Recent erosion surface on Chaffee Formation, W½ NW¼ SW¼ sec. 18, T. 49 N., R. 10 E.

River. Since field investigation of the hot spring deposits shows the presence of several travertine lined and often conglomerate filled vertical conduits along these faults and in nearby areas, it is suspected that they were the avenues of escape for the rising mineral waters.

Sedimentary Analysis

Insoluble residue analyses of the upper and purest part of all three deposits show that the travertine is composed principally of calcium carbonate with only a trace of foreign material (table 1). The light mineral faction is composed primarily of fine grains of feldspar, quartz, mica, and clay minerals mixed with 1–2 mm aggregates of the surrounding country rock which includes fragments of Precambrian granite. The quartz, which may make up 90 percent of the light faction, is clear to rose to milky, and its angularity is inversely proportional to its grain size.

Virtually none of the heavy mineral faction, which averaged 8.2 percent, was highly magnetic, but distinction could be made by a Separator. The heavy minerals of all three deposits consist primarily of chlorite and contain small amounts of biotite, sphene, and rarely fluorite (personal communication, Rae L. Harris).

Origin and Age of the Hot Spring Deposits

Fluorite is considered a hydrothermal mineral (Bateman, 1956), therefore, its presence in all three deposits is indicttive of hydrothermal origin. Sporadically commercial Tertiary fluorite deposits are found in Precambrian rocks north and northwest of Wellsville and even as close as Poncha Springs.

Structural and stratigraphic relations indicate that the Wellsville hot spring deposits were produced by the escape of carbonate rich hydrothermal waters along thrust faults A and B (fig. 2). Thus the source of the excessive carbonate content of the hot springs must have been in rock units stratigraphically older than the Mississippian for Deposit A and Devonian for Deposits B and C. The thick Ordovician dolomites, the Manitou (200 feet) and the Fremont (230 feet) are likely sources, although the easily soluble upper Leadville Limestone could have contributed to a small degree to Deposit A.

The author considered a lacustrine hypothesis for the origin of the Wellsville hot spring deposits, but the following facts now make such an idea untenable:

1. Faults bound each deposit on the updip side.
2. Numerous vertical, travertine lined conduits near and along the fault planes.
3. Continued presence of tepid springs along the strike of the faults.
4. Varied base levels of the deposits.
5. Flowage of the travertine down-dip.
6. Intermittent character of the deposits.
7. Conformity of deposits to topography.
8. Deposits are thickest and purest near the bounding faults.

There were at least two separeate periods of hot spring deposition as shown by the occurrence of several large rounded travertine

FIG. 10.—(above) Contact of travertine boulder in younger travertine, NE¼ NW¼ SW¼ sec. 18, T. 49 N., R. 10 E. (below) Travertine boulder surrounded by younger travertine flows, NW¼ SW¼ NW¼ sec. 18, T. 49 N., R. 10 E.

boulders now surrounded by younger travertine flows (fig. 10). However, the intermittent nature of the springs is further emphasized by the numerous debris filled stream and drainage channels incorporated within the deposits. Although drainage channels characteristically develop on the surface of hot spring deposits they seldom exist for any considerable period of time, and certainly not long enough to be utilized by surrounding, well established drainage patterns. Enough time must have elapsed between periods of hot spring deposition to allow not only the weathering and movement of the large boulders, but also the adaptation of the drainage channels by the surrounding tributaries.

The sporadic presence of various fossil remains in the travertine is, in light of the preceeding evidence, not considered suggestive of lacustrine deposition. Rather it is suspected that the fossil debris was washed into the springs during periods of inclement weather, overrun by advancing travertine, or washed in by surrounding drainage during periods of spring inactivity.

The occurrence of fragments of Tertiary intrusive and extrusive rocks within the travertine deposits indicates that the deposits are post-Tertiary in age. That the deposits are of post-Sangamonian(?) age is indicated by their occurrence on Sangamonian(?) gravels. The flowage of the travertine over present topography (fig. 9) plus the tepid springs southeast of Wellsville further suggest a very recent age.

ACKNOWLEDGEMENTS

The author wishes to acknowledge several stimulating field sessions with John P. Brand and Wm. B. Arper, in particular those trips dealing with the Wellsville hot spring area. The fine cooperation of Mr. William Larson of the American Crystal Sugar Company was necessary for the successful completion of this investigation. Many thanks to Rae L. Harris for assistance with mineral identifications and critical review of the manuscript.

REFERENCES

BATEMAN, A. M., 1956, Economic Mineral Deposits: John Wiley and Sons, Inc., New York, p. 734–738.

BHUTTA, M. A., 1954, Geology of Salida area, Chaffee and Fremont Counties, Colorado: unpublished PhD thesis, Colorado School Mines, 173 p.

BRAINERD, A. E., BALDWIN, H. L., AND KEYTE, I. A., 1930, Badger Creek section Fremont County and Pre-Pennsylvanian formations along the Arkansas River south of Salida, Colorado: Fourth Ann. Field Conf., Kansas Geol. Soc., p. 74–96.

BRILL, K. G., JR., 1952, Stratigraphy in the Permo-Pennsylvanian zeugogeosyncline of Colorado and northern New Mexico: Geol. Soc. America Bull., v. 63, p. 809–880.

COASH, J. R., 1949, A sedimentary study of the Pennsylvanian-Permian section in the Howard-Wellsville area, Fremont County, Colorado: unpublished MS thesis, Univ. Colorado, 40 p.

ELDRIDGE, G. H., 1894, Description of the sedimentary formations, Anthracite and Crested Butte quadrangles, Colorado: U. S. Geol. Survey Folio no. 9, 19 p.

EMMONS, S. F., 1882, Geology and mining industry of Leadville, Lake County, Colorado: U. S. Geol. Survey Ann. Report 2, p. 215–230.

GABLEMAN, J. W., 1952, Structure and origin of northern Sangre de Cristo Range, Colorado: Am. Assoc. Petroleum Geologists Bull., v. 36, pp. 1574–1612.
KIRK, E., 1931, The Devonian of Colorado: Amer. Jour. Sci., 5th. Series, v. 22, p. 220–240.
LITSEY, L. R., 1958, Stratigraphy and structure of the northern Sangre de Cristo Mountains, Colorado: Geol. Soc. America Bull., v. 69, p. 1143–78.
MCLAMORE, V. R., 1958, Paleozoic geology of the Spring Gulch-Box Canyon area, Fremont County, Colorado: unpublished MS thesis, Texas Technological, 90 p.
RAHMAN, Y. H., 1954, Geology of the Wellsville-Calcite area: unpublished PhD thesis, Colorado School Mines, 146 p.
REEVES, C. C., JR., AND SOPER, H., 1959, Calcareous spring deposits, DuBois area, Wyoming: Jour. Sedimentary Petrology, v. 29, p. 436–446.
ROLD, J. W., 1950, Geology of the Wellsville area, north flank of the Sangre de Cristo Mountains, Colorado: The Compass, v. 27, pp. 159–178.
SIAPNO, W. D., 1953, Geology of part of northern Sangre de Cristo Mountains, Colorado: unpublished MS thesis, University of Colorado, 69 p.

JOURNAL OF SEDIMENTARY PETROLOGY, VOL. 31, NO. 4, PP. 594–602
FIGS. 1–3, DECEMBER, 1961

GENETIC RELATIONSHIP AMONG TERTIARY BLUE SANDSTONES IN CENTRAL CALIFORNIA[1]

J. F. LERBEKMO
University of Alberta, Edmonton, Alberta

ABSTRACT

Pliocene sandstones with a striking bluish hue are prominent along the western base of the Sierra Nevada Range in the Mehrten Formation, and in the Coastal ranges of central California in the Tehama, Neroly, Cierbo, Purisima, San Joaquin, and Etchegoin formations. The color has previously been shown to be due to a thin authigenic montmorillonoid coating on the dark-colored sand grains. These coated sandstones have in common a preponderance of andesitic detritus and a high degree of permeability. Interbedded coated and uncoated sandstones occur as a result of differing degrees of permeability, or, alternate derivation from andesitic and non-andesitic source rocks. Compositional and cross-stratification studies indicate that andesitic sandstones of the Mehrten, Etchegoin, and San Joaquin formations were derived from the Sierra Nevada; those of the Cierbo and Neroly formations, in addition to a major source in the Sierra Nevada, probably had some contribution from the Coast Ranges; the Tehama sediments were derived from the Coast Ranges; and the Purisima blue sandstones may have been derived from either Coast Range or Sierran effusive rocks to the east.

INTRODUCTION

Certain late Tertiary sandstones belonging to a number of formations in the Sierra Nevada and Coast ranges of California have a striking bluish hue which has attracted the attention of geologists since the latter part of the 19th century. The region in which they occur exceeds a length of 200 miles from north to south in central California, and extends from the Nevada border westward to the Pacific Coast.

The blue color of the sandstones was early recognized to be the result of coatings around individual detrital sand grains. The composition of the coating material has been variously suggested to be vivianite (Arnold and Anderson, 1910), opal or chalcedony (Anderson and Pack, 1915), and chlorite (Bramlette, 1934). The writer determined the coating to be an authigenic montmorillonoid derived from solution of volcanic detritus within the sandstone (Lerbekmo, 1957). The blue color results from light reflecting from dark-colored grains (which predominate in these sandstones) beneath the thin coating. Occasionally brown coated sandstones develop which are compositionally similar to the blue type, except that the coatings are too thick to allow the color of the underlying grains to show through.

[1] Manuscript received December 16, 1960.

This paper reports the areal, temporal, and compositional relationships among the principal blue sandstone occurrences in central California. The study was done under the direction of Professor C. M. Gilbert of the University of California.

DISTRIBUTION AND LITHOLOGY

Blue sandstones are common along the lower western slope of the central and northern Sierra Nevada, the western border of the central San Joaquin Valley, in the northern part of the Diablo Range east of San Francisco Bay, and in subsurface rocks in the San Joaquin and Sacramento valleys. The formations in which they are most abundant will be described briefly.

Mehrten Formation.—The writer has adopted Curtis's (1954) use of this name to apply to "all the deposits of clastic and pyroclastic material of predominantly andesitic composition deposited in the Sierra Nevada and contiguous terrain during the volcanic epoch."

At the base of the western slope of the Sierra Nevada the Mehrten Formation is a gently dipping unit a few hundred feet thick and predominantly composed of friable cross-stratified fluviatile sandstones, siltstones, and conglomerates interbedded with ill-sorted volcanic breccias which were probably deposited as mudflows. The sandstones are commonly well sorted, in which case they

have a conspicuous blue color. The formation underlies a belt of low rolling topography extending from east of Sacramento on the north to Merced in the south, and it dips below the later alluvium of the Sacramento and San Joaquin valleys to the west (fig. 1).

Northeastward, toward the summit of the Sierra Nevada, the formation becomes

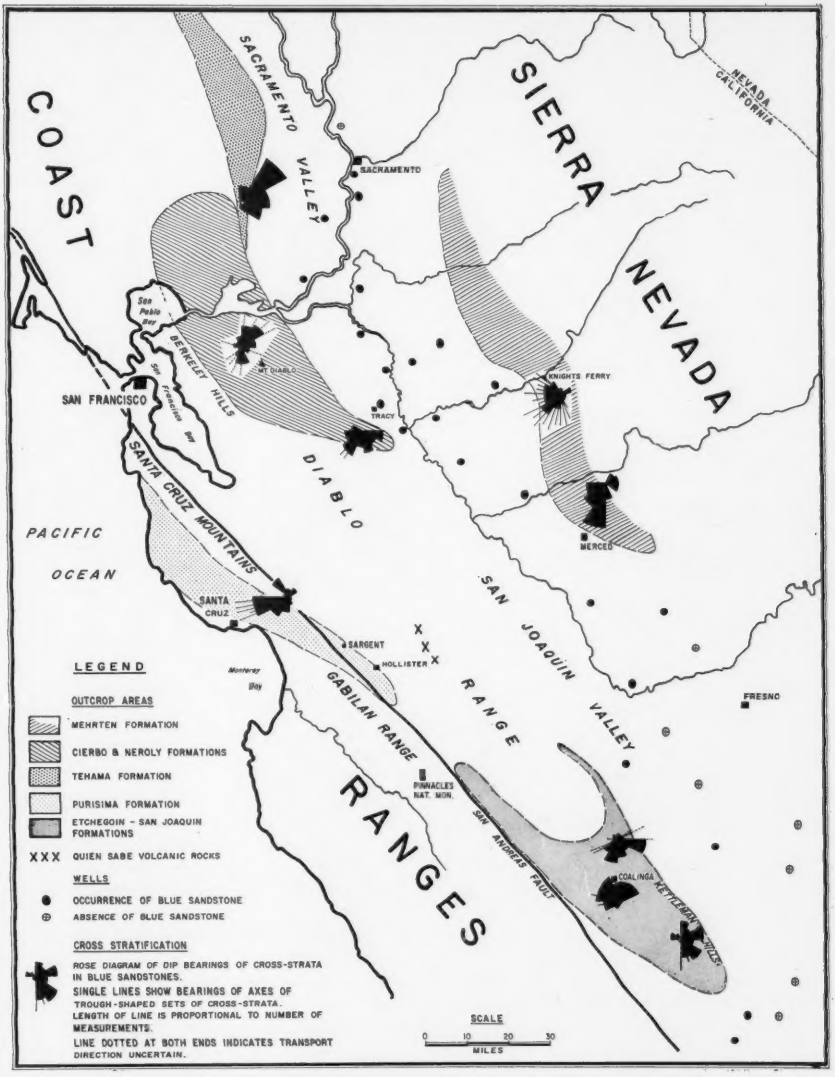

FIG. 1.—Distribution of blue sandstone formations in central California.

thicker, coarser and more poorly sorted. Blue sandstone continues to occur, though more sparingly, beyond the crest of the range and into Nevada.

Cierbo and Neroly Formations.—These formations are largely restricted to the northern Diablo Range, where they have been subjected to moderate to strong folding. The two formations are of comparable thickness in their typical development on the southeast shore of San Pablo Bay, where together they comprise about 2700 feet of rocks. The youngest, the Neroly Formation, crops out sporadically for about 30 miles north of the bay, and on the southeast extends a few miles beyond Tracy. The Cierbo Formation does not occur north of San Pablo Bay but has a distribution similar to the Neroly Formation to the south.

The Cierbo and Neroly formations are composed largely of medium- to coarse-grained sandstones except that the Neroly Formation thickens to the south by an increase of shale in the upper part. The sandstones of these formations are commonly blue only near their northern, eastern, and southern extremities where they are well sorted and have cross-stratification and organic remains indicative of a fluviatile or shoreline environment.

Tehama Formation.—Bordering the west side of the Sacramento Valley there is a series of slightly consolidated largely fluviatile volcanic gravels, pumiceous sandstones, and tuffs known as the Tehama Formation. Near their southern extremity the better sorted sandstones are coated and blue in color, and the coarser sediments are strongly cross-stratified.

Near its southern limit this formation unconformably overlies the Neroly Formation. Only a few hundred feet of these sediments are exposed here, before they dip below the alluvium of the Sacramento Valley. According to Taliaferro (1951), these sediments interdigitate to the west with the eastern edge of a group of volcanic flows and breccias called the "Sonoma volcanics."

Purisima Formation.—Blue sandstones occur in the Purisima Formation in the Santa Cruz Mountains in at least two localities, one north and another east of Monterey Bay. The most extensive outcrop area is northeast of Santa Cruz where perhaps 1000 feet of thick-bedded, commonly cross-stratified, nearly flat-lying, deeply dissected blue sandstones crop out. These grade down into 100 to 200 feet of light-colored tuffaceous sandy shales, which in turn conformably overlie the friable coarse white sandstones of the Santa Margarita Formation.

A 10,000-foot sequence of sediments has been mapped as Purisima Formation by Allen (1946) near the Sargent oil field a few miles northwest of Hollister. Blue sandstones are prominent in the lower part of the section (Jones, 1911), but also occur at intervals in the upper part.

The stratigraphic relationship between the two areas of blue sandstone in the Purisima Formation is uncertain. Both are largely unfossiliferous and appear to be dominantly continental beds.

Etchegoin and San Joaquin Formations.—The Etchegoin Formation occurs along the western edge of the central San Joaquin Valley and is principally a sequence of poorly consolidated thick-bedded medium- to coarse-grained blue sandstones and conglomerates. It is about 1500 feet thick near Coalinga and crops out for about 30 miles to the north and a similar distance to the southeast. This formation conformably overlies uncoated medium-grained argillaceous brown sandstones and shales of the Jacalitos Formation. The division is made on the basis of paleontology and usually closely approximates the lowest appearance of blue sandstone.

The San Joaquin Formation in turn rests unconformably on the Etchegoin. It is largely claystone and fine bluish sandstone with some conglomerate, is about 2000 feet thick near Coalinga, and has a distribution similar to that of the Etchegoin Formation.

Northwest of Coalinga, undivided lower and middle Pliocene sediments are preserved within the Diablo Range in a belt along the east side of the San Andreas fault. In this direction blue sandstones appear progressively higher but less frequently in the section, and lenses of rhyolitic tuff appear.

Subsurface Blue Sandstones.—Blue sandstones are present in the subsurface of the Sacramento and San Joaquin valleys. Occurrences identified by the writer from cores

and cuttings are shown in figure 1. In the southern part of the San Joaquin Valley these rocks are usually called Etchegoin; elsewhere they are most commonly simply referred to as "continental Miocene and Pliocene." Except occasionally in the extreme south, they are not reservoir rocks for petroleum, and therefore are seldom cored. Etchegoin-San Joaquin equivalents become finer grained to the southeast of the outcrop area beneath the San Joaquin Valley, and blue sandstones become more restricted.

AGE AND CORRELATION

The oldest of the blue sandstones lie stratigraphically near the Miocene-Pliocene boundary and are referred to as Mio-Pliocene. The youngest are near the Pliocene-Pleistocene boundary, and are called Plio-Pleistocene. Correlation and exact age determination are made difficult by the necessity of equating marine invertebrate with continental vertebrate faunas and floras. Nonetheless, the blue sandstones are essentially Pliocene if the extreme limits of this epoch be admitted. Approximate age relationships of the formations referred to are shown in table 1.

COMPOSITION

The blue sandstones have two properties which apparently are essential to the development of their coloration. First, they are moderately to well sorted with a high degree of permeability. Second, they have an abundance of volcanic debris in the form of fresh fragments of andesite (mostly porphyritic), intermediate plagioclase, hypersthene, augite, brown hornblende, and iron oxides. Andesitic rock fragments normally make up 40 to 70 percent of the sandstone, and the above ferromagnesian minerals 10 to 30 percent (table 2). These rocks are typical andesitic arenites (Williams, Turner and Gilbert, 1954) and the two samples of blue sandstones from the Mehrten may be taken as compositional representatives of pure andesitic sandstones. Other rock fragments, quartz, green hornblende, epidote-clinozoisite, glaucophane, andalusite, sphene, garnet, and tremolite-actinolite, all of which are rare or absent in the Mehrten samples, may be used as a measure of the contribution from non-andesitic sources, mainly Coast Range, to the other formations represented. Glaucophane is restricted to Coast Range source rocks (particularly the Franciscan Formation).

Lack of either of the two essential features of permeability and volcanic composition results in a normal non-coated sandstone. This is demonstrated by the following comparison of some sandstones whose compositions are given in table 2.

The amount of volcanic detritus in the lower part of the Cierbo Formation increases

TABLE 1.—*Correlation chart of blue sandstone formations in central California*

AGE	CENTRAL SIERRA NEVADA	SAN FRANCISCO BAY AREA	SANTA CRUZ AREA	COALINGA AREA
PLIO-PLEISTOCENE		Tehama Formation		San Joaquin Formation
PLIOCENE	Mehrten Formation		Purisima Formation	Etchegoin Formation
MIO-PLIOCENE		Neroly formation		
		Cierbo formation		

TABLE 2.—*Composition of some coated and associated uncoated sandstones*

Region	Sierra Nevada		North of Mt. Diablo				Tracy Area				Sargent Area		Coalinga Area						
Formation	Mehrten		Cierbo		Neroly		Cierbo		Neroly		Purisima		Jacalitos	Etchegoin				San Joaquin	
Sample No.	18*	20*	10	11*	4†	14*	76b	76e*	66†	76f*	108*	109	59	56a*	56c	58a*	58c	52a*	52c
	Percent		Percent				Percent				Percent		Percent	Percent				Percent	
Andesite fragments	50	54	38	48		67	40	52		53	43	8	27	43	45	45	23	51	22
Intermediate Plagioclase	21	20	15	13		8	24	14		26	7	13	14	14	9	17	13	11	12
Potash feldspar	4	3	14	6		5	9	8		4	6	11	12	8	5	3	12	2	6
Quartz	—	<1	18	11		6	19	8		3	14	27	23	17	19	7	17	12	30
Other rock fragments	—	<1	11	7		—	5	<1		<1	13	39	21	7	8	7	21	6	24
Total heavy minerals	25	23	4	15	13	14	3	18	22	14	17	2	3	11	14	21	14	18	6
Hypersthene	5	6	—	5	3		R	6	8	5	5	—	—	2	5	4	—	4	<1
Augite	6	6	≪1	3	3		—	6	8	5	4	≪1	—	2	3	4	2	4	<1
Hornblende (basaltic)	3	2	1	3	1		<1	<1	<1	<1	<1	≪1	—	<1	2	3	3	2	2
(brown)	3	1	1	3	<1		1	<1	<1	<1	<1	<1	—	1	1	3	3	2	1
(green)	<1	<1	1	<1	<1		2	<1	R	<1	3	<1	1	1	1	2	3	2	1
Iron oxides	8	7	<1	<1	6		≪1	5	5	3	3	<1	1	3	<1	4	2	4	1
Epidote-clinozoisite	R	1	1	<1	—		<1	—	—	—	1	<1	<1	<1	<1	1	1	—	<1
Glaucophane	—	—	≪1	<1	—		—	—	—	—	<1	R	≪1	R	—	R	R	—	≪1
Tremolite-actinolite	—	—	—	—	—		—	—	—	—	—	<1	≪1	—	—	—	<1	—	<1
Sphene	—	—	<1	<1	—		≪1	—	<1	—	—	—	≪1	—	—	<1	R	—	<1
Zircon	R	—	R	<1	—		R	<1	—	—	—	—	≪1	—	—	R	R	R	R
Biotite	—	—	—	—	<1		—	—	—	—	—	≪1	<1	<1	—	R	R	<1	—
Garnet	—	—	—	<1	—		R	—	—	—	—	—	≪1	—	—	—	—	—	—
Apatite	—	—	—	<1	—		R	—	—	—	—	—	—	—	—	<1	R	—	—
Andalusite	R	—	—	—	—		R	—	—	—	—	—	≪1	—	—	—	—	—	—

* Coated sandstones.
† Composite heavy mineral analysis of several spot samples taken over a considerable vertical interval.

rapidly upward, the change in composition being reflected by the change from uncoated to coated sandstones over a very short vertical interval at some apparently critical composition. Compare samples 10 and 11 which were taken only 5 feet apart stratigraphically, one below and the other above the lowest coated pebble conglomerate[2] in a section north of Mount Diablo. Sample 10 is a grey uncoated sandstone, sample 11 a light-blue coated sandstone. One might compare also samples 76b and 76e, taken approximately 100 feet apart stratigraphically from a section in the Tracy area. The first and lowest sample is a grey uncoated sandstone, the second a brown thick-coated sandstone. The most notable difference in composition between the coated and uncoated sandstones is the greater heavy mineral content (mostly hypersthene and augite) in the coated sandstones.

A similar abrupt compositional change is shown in the upper part of the Purisima Formation near the Sargent oil field where blue sandstone occasionally occurs interbedded with equally well sorted uncoated brown sandstones. The striking compositional difference between these two sandstone types is shown by samples 108 and 109 taken 30 feet apart stratigraphically. Here, there is a large difference in the quantity of volcanic rock fragments as well as a difference in the heavy mineral suites. An analogous situation occurs also in the Etchegoin Formation farther south, except that here the interbedded brown sandstones are the minor rock type. One might compare samples 58a and 58c taken a few feet apart stratigraphically from conformable beds: sample 58a is from a thick-bedded blue sandstone, sample 58c is from a thin-bedded to laminated uncoated brown sandstone.

The effect of sorting on the development of blue sandstone is illustrated in the Etchegoin Formation where coated and uncoated sandstones of similar composition occur interbedded. The coated sandstones are composed of sub-angular, medium to coarse sand grains which are well sorted ahd have high permeability. The uncoated sandstones are poorly sorted with considerable ashy matrix filling the pore spaces. The similar composition of two such adjacent sandstones is shown by samples 56a and 56c. A comparison of the particle-size distribution of these two samples with an adjacent thick-coated brown sandstone is shown in figure 2.

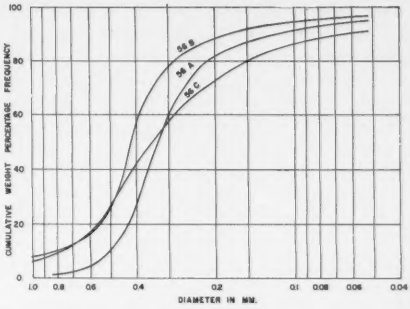

FIG. 2.—Particle-size distribution of three successive sandstones of similar composition from the Etchegoin Formation: 56A, blue sandstone; 56B, brown thick-coated sandstone; 56C, brown uncoated sandstone.

SPATIAL RELATIONSHIP OF POSSIBLE ANDESITIC SOURCE ROCKS TO PLIOCENE PALEOGEOGRAPHY

Although Mehrten breccias began to be deposited on the western slope of the ancestral Sierra Nevada in Mio-Pliocene time, and have since been exposed to erosion, Tertiary volcanic rocks, which may be only remnants of once larger bodies, also exist over limited areas in the Coast Ranges much nearer most of the blue sandstone occurrences.

In the Berkeley Hills the Mio-Pliocene subaerial Moraga andesites occur, the earliest of which may be as old as the upper part of the Neroly Formation, whereas north of San Pablo Bay well logs indicate several thousands of feet of subsurface andesites and basalts called the "Tolay volcanics," which are similar to the Moraga sequence and possibly include somewhat older strata. At approximately the time of

[2] The pebble composition of the conglomerate between these samples is one-half cherts, one-sixth aphanitic basic volcanic rocks, one-sixth medium to acid volcanic rocks, one-sixth quartzites. A count of 100 pebbles from a conglomerate near the top of the Neroly Formation (above) in the same section showed all but one to be intermediate volcanic rocks, one-half of which were hornblende-bearing.

this Coast Range volcanic activity, shallow-water Cierbo and Neroly sediments were deposited between the Coast Range and Sierran effusive regions in a marine embayment immediately east of the Berkeley Hills and extending eastward to perhaps the present confluence of the Sacramento and San Joaquin rivers, while farther east and southeast fluviatile and lacustrine sands and muds were being spread. Subaerial andesitic activity again occurred north of San Pablo Bay in the Pliocene with the deposition of at least 2000 feet of "Sonoma volcanics." At this time the Tehama continental sediments were being deposited along the inland flank of this volcanic coastal lineament.

Farther south, most of the Diablo Range was probably also undergoing erosion during the Pliocene, though a downwarp may have broken the range east of Monterey Bay (Allen, 1946). A continental sedimentary basin existed to the east in the central San Joaquin Valley while a marine Etchegoin embayment was present in the southern San Joaquin Valley connected to the open sea near Monterey Bay, where the Purisima sediments were being deposited, by a narrow channel between the Diablo and Gabilan ranges. A sizeable area of Tertiary volcanic rocks named the "Quien Sabe volcanics" occurs in the central Diablo Range about 15 miles to the east of Hollister. Ranging in composition from olivine basalt to rhyolite, and including hypersthene-augite andesite (Leith, 1949), they cover approximately 100 square miles and are up to 4000 feet thick. They lie conformably on Lower Miocene strata, and once may have been more extensive. Thirty miles to the south, a comparable area of volcanic rocks occurs in the Pinnacles National Monument area, but these are almost entirely rhyolitic in composition. Also, a few miles south of the Sargent oil field about 1000 feet of Miocene andesites cover a few square miles. According to Allen's (1946) descriptions, these are mostly acid andesites in which augite and hypersthene are rare.

CROSS-STRATIFICATION

Cross-stratification is present to some degree in all the formations containing blue sandstones. This fact prompted the writer to attempt a directional analysis of cross-stratification to aid in distinguishing between the possible sources of the andesitic debris in the blue sandstones.

The Mehrten Formation has yielded only a continental flora and bones of land vertebrates, and is believed to be entirely continental. Fluviatile cross-stratification appears to be prevalent in this formation, but exposures are few. Using the terminology of McKee and Weir (1953), it is mostly of medium-scale trough type, but medium- and large-scale simple cross-stratification also occurs. Since it is certain that the Mehrten sandstones have been derived from andesitic breccias higher on the western slope of the Sierra Nevada, study of available cross-stratification was made in one area of fairly good exposures near Knights Ferry to check the applicability of this method of directional analysis. The southwesterly pattern of transport indicated by the cross-stratification analysis here (fig. 1) was encouraging.

With the exception of the Tehama sediments, which like the Mehrten are entirely continental, cross-stratification is not as prevalent in the other formations studied. Marine or brackish-water invertebrate forms occur sporadically and show these rocks to be partly marine. Although cross-stratification of the types found in the Mehrten Formation, and judged to be fluviatile, was also found in some parts of the other formations, small-scale simple cross-stratification with poorly defined stratification planes of widely varying strike, interpreted as being developed in the littoral or inner sublittoral zone, is more common. A third type, large-scale low-angle simple cross-lamination with fossil echinoids present on the bedding planes, was found in one area of the San Joaquin Formation near Coalinga, and is believed to represent beach or bar accumulations.

The results of the analyses of dip directions of all cross-stratification measured and judged to be fluviatile are shown in figure 1. Dips were first plotted on a stereonet and corrected for formation attitude. With the exception of those from the Tehama Formation, which represent only about 100 feet stratigraphically, the cross-stratification measurements at each locality were taken from at least 300 feet of section and over an area of several square miles.

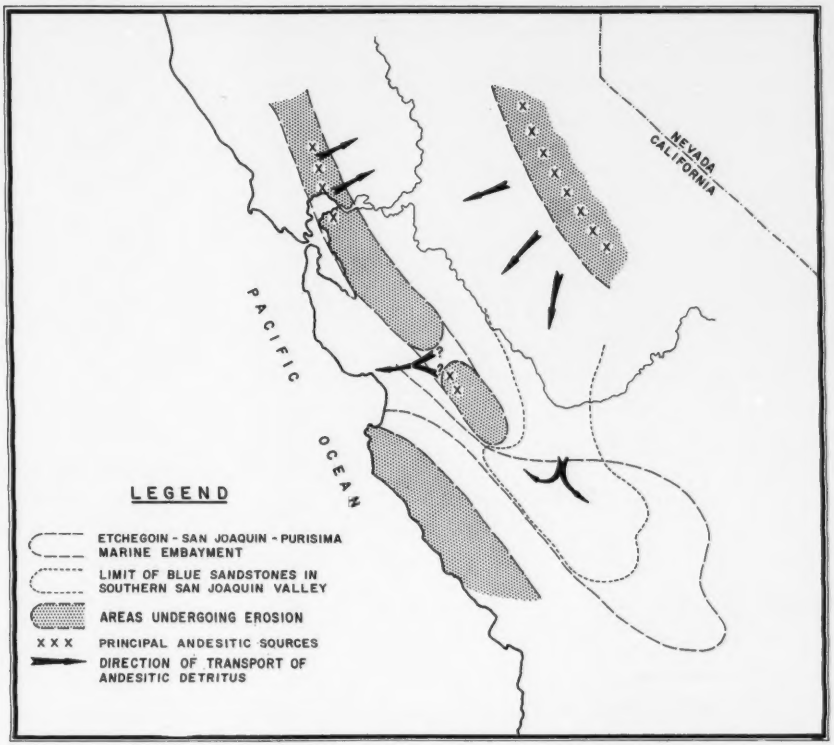

FIG. 3.—Etchegoin-San Joaquin-Purisima-Tehama depositional setting.

CONCLUSIONS

1. The blue sandstones (and coated brown sandstones) of central California were all derived from predominantly andesitic terrain. Montmorillonoid grain coating responsible for the blue coloration owes its origin to the andesitic composition of the sandstones and their high permeability. Interbedded coated and uncoated well-sorted sandstones are the result of derivation from andesitic and non-andesitic source areas respectively. Non-andesitic detritus in the blue sandstone formations is almost exclusively of Coast Range derivation.

2. A large part of the andesitic detritus in the Cierbo and Neroly formations east of San Pablo Bay was derived from the Mehrten Formation of the Sierra Nevada, but some may have come from the "Tolay volcanics" or equivalents of the Coast Range. This conclusion is based on the following evidence:

(a) There are appreciable and comparable amounts of basaltic and brown hornblende in the heavy mineral suites of the Cierbo, Neroly, and Mehrten formations; and half the pebbles from an upper Neroly conglomerate north of Mount Diablo were hornblende-andesite. This rock type is abundant in the Mehrten breccias, whereas samples from the most probable alternative source, the "Tolay volcanics" north of San Pablo Bay, are lacking in hornblende.

(b) The variation in direction of cross-bedding in this area and the presence of non-andesitic material in the sand-

stones shows a contribution from the Coast Range, part of which may well have been andesitic.

3. Cross-stratification shows the Tehama blue sandstones to have had their source in the "Sonoma volcanics" to the west.

4. The andesitic portion of the blue sandstones of the Etchegoin and San Joaquin formations is Mehrten detritus carried southward by streams across the San Joaquin Valley to the north shore of the Etchegoin sea. From here part of the distribution was to the southeast, part was to the northwest for a short distance around the southern end of the Diablo Range where rhyolitic tuffs were incorporated from explosive activity in the Pinnacles region (fig. 3).

5. Purisima blue sandstones were derived from the east, either from the Sierra Nevada through a gap in the Diablo Range east of Monterey Bay, or more locally from a former greater extension of the Quien Sabe volcanic rocks. The more local source is favored for the coarse blue sandstones interbedded in the Purisima near Sargent. The lack of blue sandstones for some distance southeast of Sargent argues against transportation of andesitic material into the Monterey Bay area from the southeast around the south end of the Diablo Range. The abundance of augite and hypersthene in the blue Purisima sandstones shows that the acid andesites immediately south of Sargent were not the major source of these sandstones.

REFERENCES

ALLEN, J. E., 1946, Geology of the San Juan Bautista quadrangle, California: Calif. State Div. Mines Bull., v. 133, 112 p.

ANDERSON, ROBERT, AND PACK, R. W., 1915, Geology and oil resources of the west border of the San Joaquin Valley north of Coalinga, California: U. S. Geol. Survey Bull., v. 603, 220 p.

ARNOLD, RALPH, AND ANDERSON, ROBERT, 1910, Geology and oil resources of the Coalinga district, Fresno and Kings Counties, California: U. S. Geol. Survey Bull., v. 398, 354 p.

BRAMLETTE, M. N., 1934, Heavy mineral studies on correlation of sands at Kettlemen Hills, California: Am. Assoc. Petroleum Geologists Bull., v. 18, p. 1559–1576.

CURTIS, G. H., 1954, Mode of origin of pyroclastic debris in the Mehrten Formation of the Sierra Nevada: Univ. Calif. Pub., Dept. Geol. Sci. Bull., v. 29, p. 453–502.

JONES, W. F., 1911, The geology of the Sargent Oil Field: Univ. of Calif. Pub., Dept. Geol. Sci. Bull., v. 1, p. 57–78.

LEITH, C. J., 1949, The geology of the Quien Sabe quadrangle, California: Calif. State Div. Mines Bull., v. 147, 60 p.

LERBEKMO, J. F., 1957, Authigenic montmorillonoid cement in andesitic sandstones of central California: Jour. Sedimentary Petrology, v. 27, p. 298–305.

MCKEE, E. D. AND WEIR, G. W., 1953, Terminology for stratification and cross-stratification in sedimentary rocks: Geol. Soc. America Bull., v. 64, p. 381–389.

TALIAFERRO, N. L., 1951, Geologic guidebook of the San Francisco Bay Counties: Calif. State Div. Mines Bull. v. 154. p. 117–150.

JOURNAL OF SEDIMENTARY PETROLOGY, VOL. 31, NO. 4, PP. 603–607
FIGS. 1–7, DECEMBER, 1961

BACKSET BEDS IN THE COSO FORMATION, INYO COUNTY, CALIFORNIA[1]

W. ROBERT POWER, JR.
The Georgia Marble Company, Tate, Georgia

ABSTRACT

Some cross-beds in coarse-grained sandstone and pebble conglomerate of the Coso Formation (lower Pleistocene) are inclined against the direction of flow of depositing currents. Textural gradation, mineralogical changes, and structural considerations show that the depositing currents flowed westward. About one half the cross-beds are inclined to the east, and the others are inclined to the west. The diametrically opposed directions do not fit the pattern expected of meandering streams. The eastward-inclined cross-beds are called backset beds.

Backset beds are the planar (inclined) type and make an angle of 25° or less with the normal bedding planes. Cross-laminations are long tapered wedges with the wide part of the wedge at the base. Material within the wedge is coarse near the bottom and grades to finer material at the top. Normal foreset laminations are either the inclined or festoon (trough) type, and material within each lamination is well sorted and not graded.

The backset beds are believed to have formed during the antidune phase of sediment transport described by G. K. Gilbert. The factors contributing to the antidune phase of sediment transport are high load, high velocity, high resistance, and shallow depth of water. Inasmuch as the deposits were probably deposited in a manner analogous to the heavily overloaded streams of the Basin and Range province today, all these factors could well have been present.

INTRODUCTION

A number of recent studies on paleocurrents have used the direction of inclination of cross-beds as one of the principal parameters in determining the direction of flow of ancient streams, on the assumption that cross-beds are inclined in the direction of flow (Kiersch, 1950; Schlee, 1957a; McDowell, 1957; Pettijohn, 1957; Pelletier, 1958; Potter and Glass, 1958). The cross laminations are called foresets. The purpose of this paper is to report the occurrence of cross-beds that are inclined against the direction of flow. These may be called backsets.

The writer does not doubt the validity of the conclusions reached in the paleocurrent studies cited above; all are supported by parameters other than cross-bedding. Backsets are rare and they probably form only under unusual circumstances. This paper emphasizes the need for using multiple parameters in paleocurrent studies.

LOCATION AND ACKNOWLEDGEMENTS

The backset beds occur in the early Pleistocene Coso Formation on the western flank of Haiwee Ridge, a northwestern spur of the Coso Mountains in Inyo County, California. Haiwee Ridge is on the eastern side of Owens Valley about eight miles south of Owens Lake and is located within the Haiwee Reservoir quadrangle (1:62,500), United States Geological Survey topographic map. The structures were first observed in the fall of 1956 when the author was studying uranium deposits on Haiwee Ridge for the United States Atomic Energy Commission. A report on these studies includes a geologic map of Haiwee Ridge (Power, 1958). The area was revisited during the summer of 1958 when measurements were made and additional examples found.

The author gratefully acknowledges the assistance of Arthur E. Granger, Chief, Salt Lake Branch, United States Atomic Energy Commission for support in the field work, and that of A. C. Waters, F. J. Pettijohn, and John S. Schlee for critical reading of parts of the manuscript.

GEOLOGIC SETTING

Figure 1 is a geologic section across Haiwee Ridge. The oldest rocks in the area are granite, which is exposed along the crest

[1] Manuscript received December 10, 1960.

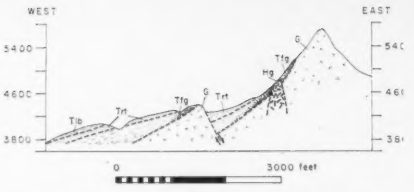

FIG. 1.—Geologic section—Haiwee Ridge. G, granite; Hg, hornblende gabbro; Tfg, fanglomerate; Trt, rhyolite tuff; Tlb, lake beds.

of the ridge, and hornblende gabbro which intrudes the granite. These are unconformably overlain by the Coso Formation which consists of three lithologic units: a fanglomerate, lake beds, and rhyolite tuff. The Coso Formation is in turn unconformably overlain by andesite tuff and flows (not shown in the cross-section, fig. 1).

The ridge is intensely faulted, the earliest faults cutting the granite, but not cutting the Coso Formation. Other faults cut the Coso Formation, but not the andesites. The youngest faults cut the andesite and are normal. Those with largest displacement dip to the east, but others dip to the west. It was impossible for the writer to determine the exact nature of the earliest faults, but clearly they resulted in the uplift of Haiwee Ridge relative to Owens Valley because sediments derived from granite exposed along the crest of the ridge were deposited in Owens Valley.

The Coso Formation includes fanglomerate, lake beds, and rhyolite tuff. The fanglomerate lies on the west flank of Haiwee Ridge; it grades into, interfingers with, and is overlain by lake beds that occupy Owens Valley. Rhyolite tuff is interbedded with the lake beds and fanglomerate.

Near the crest of the ridge, the fanglomerate is composed of coarse arkosic breccia that is derived from the underlying granite. The breccia grades westward through arkosic sandstone and pebble conglomerate into the lake beds which are composed of reworked tuff and fine arkosic sandstone. In Owens Valley the Coso Formation is essentially a conformably sequence of lake beds and tuff that dips about 10° west. On the flank of Haiwee Ridge the formation changes to fanglomerate, the dip becomes steeper, and unconformities are common. The Coso is thus a heterogeneous assemblage of rock types which records repeated volcanism, uplift, and erosion on Haiwee Ridge accompanied by almost continous deposition in Owens Valley.

CROSS-BEDS

The fanglomerate contains many cross-bedded units, about half of which are backsets. Figure 2 shows a typical exposure where both foreset and backset beds are exposed. The cross-bedded units range in thickness from a few inches to about one foot. Both backsets and foresets are commonly found within a single stratum. In such cases they are separated by a zone of no cross-beds. The maximum angle of inclination of cross-beds with true bedding is about 25°, but the angle typically changes along the stratum grading gradually into horizontal bedding.

Figure 3 is a circular histogram showing the direction of inclination of 54 cross-beds which were measured in a cliff exposing about 30 feet of section (NE¼ SW¼ sec 6, T. 21S., R38E). It shows two strong peaks, one to the west and the other to the east. The eastward inclined cross-beds are backsets; the westward inclined cross-beds, foresets. Although these are the only quantitative measurements made, similar relations can be clearly seen in most exposures of the fanglomerate.

Certain textural differences exist between foresets and backsets, but they are not

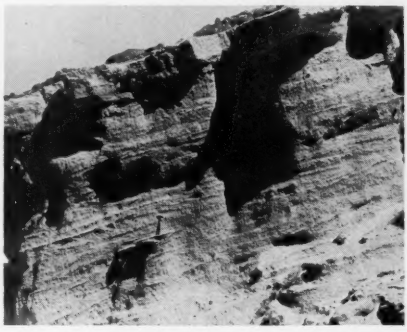

FIG. 2.—Typical exposure showing both backset and foreset beds. Current direction was toward the left. View is looking north. NW¼ NE¼ sec. 7, T. 21 S, R. 38 E.

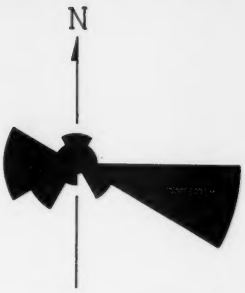

FIG. 3.—Circular histogram showing the direction of inclination of 54 cross-beds measured in a single cliff—NE¼ SW¼ sec. 6, T. 21 S, R. 38 E.

always so clear as to make possible a distinction on the basis of texture alone. Figure 4 is an idealized diagram drawn to show the differences. Foresets are of either the planar or trough type (McDowell, 1957). In the planar type the upper and lower bounding surfaces of the cross-bedded unit are essentially parallel planes. The foresets typically intersect the upper bounding surface at an angle, but they generally meet the lower bounding surface tangentially. When viewed in the direction of inclination these foresets appear parallel to true bedding. In the trough type, the upper surface is a plane, but the lower surface is an erosional trough with its long axis in the direction of current flow. When viewed at right angles to the direction of current flow the foresets are concave upward, and are tuncated by the upper bounding surface. Each foreset unit is thus a curved wedge. The material within each wedge is well sorted.

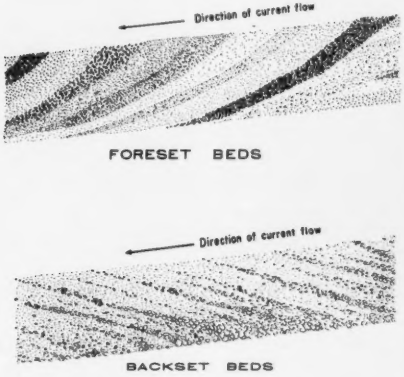

FIG. 4.—Idealized diagram showing textural differences between typical foreset and backset beds.

FIG. 5.—Backset beds. Current direction was to left (west). NE¼ SW¼ sec. 6, T. 21 S, R. 38 E.

Backsets are planar (figs. 5, 6). They are long tapered wedges with the wide part of the wedge at the base. The wedges strike the top and bottom of the cross-bedded unit at an angle. Within each wedge the material is graded, the coarsest material at the bottom grading upward into finer material at the top. Figures 5 and 6 show these relationships.

If one assumes that cross-beds are inclined in the direction of flow of depositing

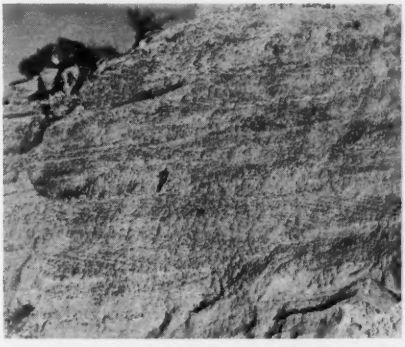

FIG. 6.—Backset beds. Current direction was to left (west). NE¼ SW¼ sec. 6, T. 21 S, R. 38 E.

streams one must conclude that streams were flowing in two opposing directions on Haiwee Ridge. The circular histogram does not fit a pattern of meandering streams which should give a fan-shaped diagram pointing in the down-valley direction (Schlee, 1957b).

The textural gradations and distribution of material in the fanglomerate do not, however, fit any pattern of east-flowing streams. The strata containing well developed backsets are pebble conglomerates and coarse arkoses that can be traced westward into fine-grained lake sands. There is no reversal of this textural change. Coarse arkosic breccia that can be traced westward into arkosic sandstone is found on the west side of once buried granite ledges now exposed on gully walls. Similar breccia is not found on the east side of these ledges.

At one place the fanglomerate covers a small body of gabbro that intrudes the granite. Fragments of the gabbro are found in sediments west of the gabbro outcrops, but not east. Finally there seems to be no mechanism by which both eastward and westward inclined foresets could be deposited in a single stratum by opposing streams. Nonetheless, about half of the cross-beds are inclined eastward; hence they are called backset beds.

ORIGIN

A clue to the origin of these back setbeds is found in the observations of G. K. Gilbert in his study of *The transportation of debris by running water* (1914), in which he found an "antidune" phase of transport in heavily overloaded streams. In Gilberts words (1914, p. 11):

"When the conditions are such that the bed load is small, the bed is molded into hills, called dunes, which travel downstream. Their mode of advance is like that of eolian dunes, the current eroding their upstream faces and depositing the eroded material on the downstream faces. With any progressive change of conditions tending to increase the load, the dunes eventually disappear and the debris surface becomes smooth. The smooth phase is in turn succeeded by a second rhythmic phase, in which a system of hills travel upstream. These are called antidunes, and their movement is accomplished by erosion on the downstream face and deposition on the upstream face. Both rhythms of debris movement are initiated by rhythms of water movement."

Inasmuch as foreset cross-beds have been explained by the downstream migration of ripple marks in aggrading streams (McDowell, 1957), it seems reasonable to suppose that backsets might be formed by the upstream migration of antidunes in aggrading streams. A necessary condition for aggradation is that deposition exceeds erosion. If during an antidune phase of transport more material is deposited on the upstream side of the antidune than is eroded on the downstream side, then a series of backsets might be formed and preserved. The textures within backsets may be easily explained by this mechanism of deposition. As Gilbert (1914, p. 34) points out, gravity aids transport on the lee or downstream side of dunes and retards transport on the upstream side. In the antidune phase the material is being deposited on the upstream side and it would be expected that finer material would be rolled further upslope than coarse material, thus producing the observed textural gradation.

The factors that Gilbert enumerated as contributing to the antidune phase are: high load, high velocity, high resistance, and shallow depth of water. Inasmuch as the Coso fanglomerates were probably deposited in a manner analogous to heavily overloaded streams of the Basin and Range province today, all of these factors could well have been present.

References to cross-beds inclined against the direction of flow are uncommon. Bucher (1919) called the antidune phase of transport "regressive sand waves" and implied that no geologic record of them could be left because they "could not exist at velocities other than those creating them" (1919, p. 181). Twenhofel (1939, p. 522) mentions antidunes and states that "such lamination as exists in inclined up-current and is made on the up-current slope." He further thought that there was "little chance of preservation, but they have been reported in Ordovician sandstone of Ireland." He gave no reference. Potter and Glass (1958, p. 19) claim to have found ripple marks due to antidunes in the Penn-

FIG. 7.—Backset beds at the base of a modern alluvial fan on the east slope of the Sierra Nevada just north of Cottonwood Canyon. View is looking north.

sylvanian sandstones of southern Illinois.

In order to find other examples of backset beds several modern alluvial fans on the east slope of the Sierra Nevada were examined. In one, just north of Cottonwood Canyon, cross beds inclined toward the mountain front were found (fig. 7). This is the only other example of possible backset beds known to the author.

CONCLUSIONS

The principle conclusion is that cross-beds inclined against the direction of current flow exist in water-laid sediments. Owing to the scarcity of reports of similar phenomena in the literature, it seems reasonable to infer that they are rare. The textural differences between backset and foreset beds observed on Haiwee Ridge may or may not be diagnostic. McDowell (1957, fig. 8, p. 21) says that graded cross-beds are fairly common, and by omission, implies that they are commonly foresets. Gilbert (1914) did not study textures or structures produced by the antidune phase of transport. Twenhofel (1939) is the only other author known to this writer who says that cross-beds inclined against the direction of current flow can or do exist in water-laid sediments.

REFERENCES

BUCHER, W. H., 1919, On ripples and related sedimentary surface forms and their paleogeographic interpretation: Am. Jour. Sci., v. 47, p. 241–269.

GILBERT, G. K., 1914, The transportation of debris by running water: United States Geol. Survey Prof. Paper, no. 86.

KIERSCH, G. A., 1950, Small-scale structures and other features of Navajo Sandstone, northern part of San Raphael Swell, Utah: Am. Assoc. Petroleum Geologists Bull., v. 34, p. 923–942.

MCDOWELL, J. P., 1957, The sedimentary petrology of the Mississagi Quartzite in the Blind River area: Ontario Dept. of Mines, Geological Circular, no. 6.

PELLETIER, B. R., 1958, Pocono paleocurrents in Pennsylvania and Maryland: Geol. Soc. America Bull., v. 68, p. 1033–1064.

PETTIJOHN, F. J., 1957, Paleocurrents of Lake Superior Pre-cambrian quartzites: Geol. Soc. America Bull., v. 68, p. 469–480.

POTTER, P. E., AND GLASS, H. D., 1958, Petrology and sedimentation of the Pennsylvanian sediments in southern Illinois: Illinois State Geol. Survey, Report of Investigations 204.

POWER, W. R., 1958, Preliminary report on the geology and uranium deposits of Haiwee Ridge, Inyo County, California: U. S. Atomic Energy Commission, RME-2066.

SCHLEE, JOHN S., 1957a, Upland gravels of southern Maryland: Geol. Soc. America Bull., v. 68, p. 1371–1410.

———, 1957b, Fluvial gravel fabric: Jour. Sedimentary Petrology, v. 27, p. 162–176.

TWENHOFEL, W. H., 1939, Principles of sedimentation, 1st ed.: McGraw-Hill, New York, 610 p.

JOURNAL OF SEDIMENTARY PETROLOGY, VOL. 31, NO. 4, PP. 608–636
FIGS. 1–21, DECEMBER, 1961

NOTES

NOTE ON MEASUREMENT OF GRAIN SIZE IN PHI UNITS[1]

G. C. GRENDER
Bakersfield, California

The use of phi units ($\phi = \log_2$ mm; Krumbein, 1936) in grain size measurement has become increasingly common. The purpose of this note is to call wider attention to the well known time-saving device of direct measurement in phi units.

A simplified phi-unit scale is shown in figure 1. The scale is constructed by first choosing the desired intervals in phi units, then determining the distance in millimeters of each interval mark from the ∞ mark by using a phi table (Page, 1955; Griffiths and McIntyre, 1958). If such a table is not readily available, the distances can be easily calculated by the formula:

$$\text{millimeters} = \text{antilog}_{10} \frac{-\phi}{3.322}.$$

For example, the -2ϕ mark is found to be $\text{antilog}_{10}\ 2/3.322 = 4$ mm from the ∞ mark.

It is desirable to measure enlargements of small grains rather than the grains themselves. When using millimeter scales the actual size is found by dividing the measurement of the enlargement by the magnification. When using the phi scale, the actual size is found by measuring the enlargement in phi units and adding

$$\log_2 (\text{magnification}) = 3.32 \log_{10} (\text{magnification}).$$

For example, suppose a $\frac{1}{8}$ mm (3ϕ) grain were enlarged 32 times to 4 mm. The measurement would be -2ϕ, and the actual size would be calculated as $-2+3.32 \log_{10} 32 = -2+5 = 3\phi$.

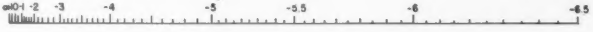

FIG. 1. Simplified scale in phi units.

Manuscript received September 9, 1960.

REFERENCES

GRIFFITHS, J. C., AND MCINTYRE, D. D., 1958, A table for the conversion of millimeters to phi units: Min. Ind. Exp. Sta., Penn. State Univ., University Park, Pennsylvania.

KRUMBEIN, W. C., 1936, Application of logarithmic moments to size frequency distributions of sediments: Jour. Sedimentary Petrology v, 6, p. 35–47.

PAGE, H. G., 1955, Phi-millimeter conversion table: Jour. Sedimentary Petrology, v. 25, p. 285–292.

A SIMPLE DRILLING TOOL FOR ORIENTING CORES AT SHALLOW DEPTH[1]

CARLTON R. JOHNSON AND OTHAR M. KIEL
Jersey Production Research Company, Tulsa, Oklahoma

Oriented cores have proved invaluable in studying the directional properties of the sedimentary structures of poorly exposed or buried rock units. Even where fresh exposures permit oriented sampling of a relatively unweathered rock surface, coring provides complete vertical sections that can be selected on a systematic three-dimensional grid. In reservoir studies, orientation of sedimentary structures such as cross-bedding and grain imbrication may be related to fluid flow properties, whose measurement from surface samples is probably neither reliable nor representative of reservoir conditions.

This note describes the construction and operation of a simple orienting device built for use with a light shot-hole type drilling machine. The tool, which can be built cheaply in any machine shop, is simpler and more dependable in operation than commercial orienting tools designed for the greater depth requirements of petroleum exploration. Also, the device offers advantages over the "drill-pipe" method reported by Johnson and Breston (1951) in that entire soft or friable horizontally-laminated cores can be confidently oriented without depending on the basal piece, which all too frequently is not recovered.

The orienting device (fig. 1) consists of a 20-ft length of heavy-gauge steel pipe, a, tipped with a $1\frac{3}{4}$-in insert-type drilling bit, b. Around the pipe is a 3-ft sleeve, c, slotted at its lower end. On the sleeve is mounted a lever-and-arm mechanism, d. A small projection, e, on the pipe fits into the slot, f, preventing the relative movement of the pipe and sleeve.

Before coring, the orienter is run into the hole and the sleeve rides on the projection, which is at the top of slot f. Each piece of drill pipe is marked so that the orientation of the tool is known after it has been lowered into the hole. On reaching the bottom of the hole, the lever-and-arm mechanism, which has been collapsed next to the sleeve, jams the sleeve and pipe to one side and the projection moves to the bottom of slot f. The entire drill string is raised 1 inch with the hoist and is then turned slightly by hand until the pipe projection reaches a second slot on the sleeve, g, allowing the bit to be lowered to the bottom of the hole. The

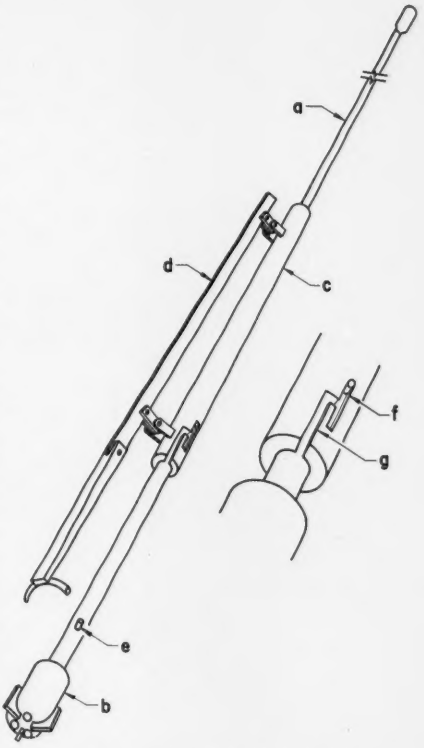

FIG. 1.—Diagram of orienting tool.

[1] Manuscript received July 5, 1960.

orienting hole is then drilled, the orienter is withdrawn, and the hole is cored with a conventional core barrel. Part of the small hole appears as a groove parallel to the length of the core (fig. 2). Because the orientation of the tool is known, the direction in which the grooved side of the core was oriented is known. This provides a positive means of orienting all of the core pieces.

The orienter worked successfully in more than 40 test holes in central Oklahoma, where oriented core samples were obtained from a friable late Pennsylvanian sandstone reservoir at a depth of 250 ft. Although the particular tool described here is designed for orienting 4-in cores, a scaled-down version should satisfactorily orient cores of smaller diameter.

REFERENCE

JOHNSON, W. E., AND BRESTON, J. N., 1951, Directional permeability measurements on oil sandstones from various states: Prod. Monthly, v. 15, no. 4, p. 10–19.

FIG. 2.—Offset hole of known orientation appears as a groove on these sandstone core samples.

REGENERATED ANHYDRITE REDEFINED[1]

MARCUS I. GOLDMAN
The Woodner, Apt. BG66, Washington 10, D. C.

The definition of "regenerated anhydrite" in the "Supplement to the Glossary of Geology and Related Sciences" (Amer. Geo. Inst., 1960, p. 55) has brought home to me that I have failed to define the term with the precision that a new term calls for.

The definition in the "Supplement" reads: "Anhydrite produced by the dehydration of gypsum." Redefined, it should read: Anhydrite produced by the dehydration of gypsum *that was itself formed by the hydration of anhydrite.*

The concept that the gypsum itself was derived from anhydrite is implied by the prefix re-, and in the original definition (Goldman, 1952, p. 60) the last part of the definition was intended to establish the connection between the use of *re-* and the conclusion that the gypsum in which regeneration takes place was itself derived from anhydrite. The derivation of the gypsum from anhydrite was also implied by the use of "reverted" in the first line of the last paragraph on page 2 (Goldman, 1952).

In my reply (Goldman, 1957, p. 196) to Ogniben's objection (1957, p. 68)—valid under the circumstances—to my use of regenerated, I clarified the meaning of the term.

But a single concise definition, as offered above, is still called for.

[1] Manuscript received February 1, 1961.

REFERENCES

AMERICAN GEOLOGICAL INSTITUTE, 1960, Supplement to the glossary of geology and related sciences: American Geological Institute, Washington, D. C., 72 p.

GOLDMAN, MARCUS I., 1952, Deformation, metamorphosis, and mineralization in gypsum-anhydrite cap rock, Sulphur Salt Dome, Louisiana: Geol. Soc. America Mem., 50, 169 p.

———, 1957, Relations of gypsum and anhydrite: Jour. Sedimentary Petrology, v. 27, p. 196–197.

OGNIBEN, LEO, 1957, Secondary gypsum of the sulphur series, Sicily, and the so-called integration: Jour. Sedimentary Petrology, v. 27, p. 64–79.

COMMENTS ON TEODOROVICH'S "STRUCTURAL CLASSIFICATION OF LIMESTONES AND DOLOMITES," AND SHVETSOV'S "GENETIC CLASSIFICATION OF LIMESTONES"[1]

HAROLD J. BISSELL AND GEORGE V. CHILINGAR
Brigham Young University, Provo, Utah, and University of Southern California, Los Angeles, California

Students of carbonate petrology and petrography throughout the world are cognizant of significant contributions by Russian geologists; among recent publications in this field are the important books by Teodorovich (1958) and Shvetsov (1958). Noteworthy in Teodorovich's comprehensive study on sedimentary rocks are two charts: the one on page 291 is a structural classification of limestones (fig. 1), and that on page 295 is a similar approach to classification of dolomites (fig. 2). Shvetsov has published an important text on sedimentary rocks, and of significance is his chart on pages 292–93 which presents a genetic classification of limestones based on predominating components (fig. 3). The writers of this review consider these charts of enough significance

[1] Manuscript received December 10, 1960.

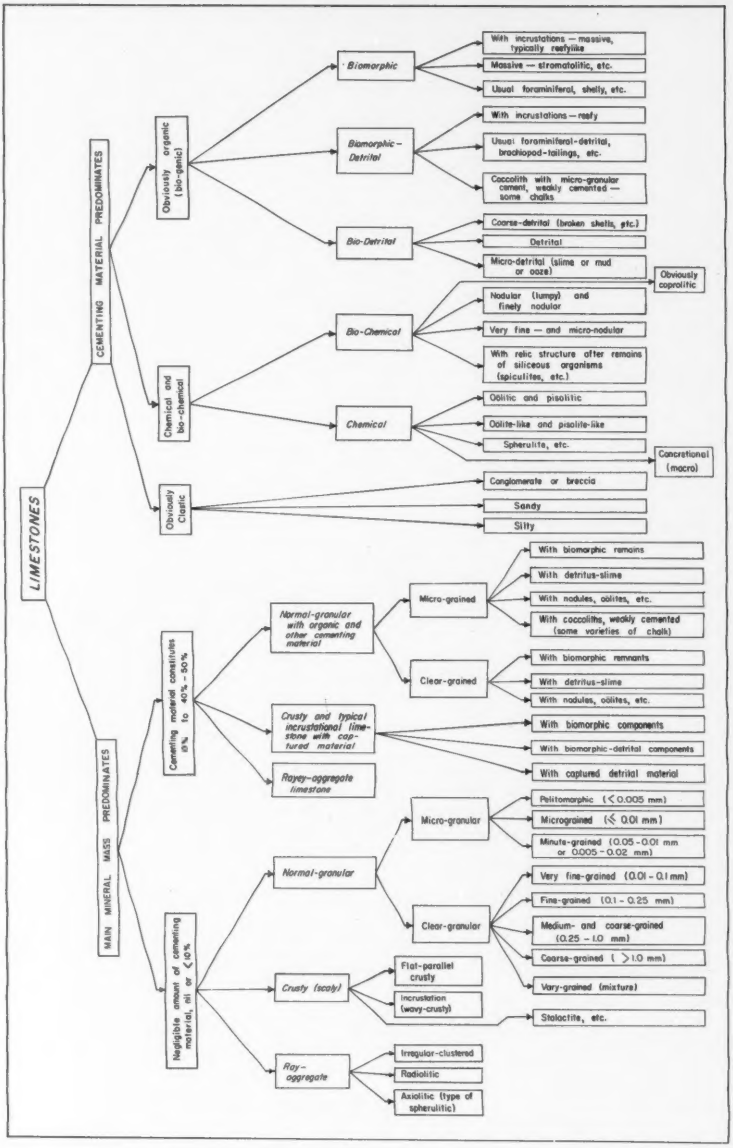

FIG. 1.—Structural classification of limestones (after G. I. Teodorovich, 1958, p. 291).

in the currently-accelerated study of carbonate rocks to merit making them available to other petrologists and petrographers.

Any attempt to classify limestones and dolomites on a structrual (i.e., textural) framework must of necessity relate concepts of genesis of the sediment. As a matter of fact, a detailed textural study elucidates the origin of carbonate rocks to a great extent. If not combined into an artificial and arbitrary classification, this method is utilitarian. Furthermore, it must prove of value in the field (petrologic) and also in the laboratory (petrographic) research, but not necessarily in equal emphasis. Thus, tangible concepts gained during the field investigations should lead to more scientific and useful synthesis during laboratory studies. It appears to the writers that Teodorovich has advanced a classificatory scheme which is not limited to a particular carbonate depocenter, nor is it adjusted to fit only limestones and dolomites of an arbitrarily-selected stratigraphic suite. It does indeed lend itself to multiplicity of carbonate types. Shvetsov is also to be complimented on his arrangement of limestones into two groups: (1) those which preserved the original composition thus permitting their division into primary genetic types; and (2) those which experienced considerable alteration of the original material and are therefore completely cryptogenic, that is, of unknown origin. Too often students of carbonate petrology and petrography overlook or minimize importance of alteration during diagenesis and epigenesis. Obviously, all students of carbonates will not find universal appeal in these classifications by Teodorovich, and by Shvetsov, but they will probably gain ideas and stimulus from these studies.

In their researches of a designated sedimentary realm, students of carbonate petrology and petrography realize at the outset that a sample or specimen under examination has a definitive fabric. Teodorovich makes his first subdivision (either of limestones or dolomites) on the basis of whether the cementing material predominates or whether the main mineral mass predominates. Experience teaches this to be a prudent practice, whether one deals with a granular or a crystalline texture. With no more than a ten-power hand lens, either in the field or in the laboratory, the sedimentologist ascertains the texture of carbonate rocks, and may apply terminology based on visually observed (or estimated) grain size or crystal size. Naturally, he thinks in terms of coarse-, medium-, or fine-crystalline (or-grained if not a crystalline rock), or aphanic (microcrystalline or cryptocrystalline), or micritic, or sparry. Perhaps he might use the name "matrix carbonate" if observable (or determinable) different size ranges of crystals or grains typify the rock. Or, he may view texture in terms of bioclastic, skeletal, skeletal-detrital, or other descriptive terms. Regardless, after allocating the carbonate under question to one of two categories in the Teodorovich scheme, the next subdivision should be founded on the type or ratio (or other relative component) of clastic, chemical, bio-chemical, or organic constituents to cementing material. If, as shown by Teodorovich, main mineral mass predominates in the carbonate rock, two readily determinable features of fabric can be made: these are shown as either abundant cementing material (subordinate however, to grains), or negligible (or small percentage) cementing material. For dolomites Teodorovich has a third category which relates to cavernous-porous dolomites with negative relic structure (that is, texture). Subdivisions in the classificatory scheme beyond these two (limestone) and three (dolomite) major divisions are self-explanatory, in large measure.

Teodorovich observes that in carbonate rocks in which cementing material predominates it is scientifically sound to allocate limestones to one of three categories, namely, (1) those which obviously are organic (biogenic), (2) those of chemical and bio-chemical make-up, and (3) those which are obviously clastic. Thus, a qualification of genesis and inference to the energy factor enters the classification; such an approach is desirable. In a limestone in which the main mineral mass predominates, it is believed by Teodorovich that a natural division and subdivision places these rocks in categories related to granularity or crystallinity, and whether or not the fabric is pelitomorphic, biomorphic, or micrograined, varigrained, etc. His scheme of further break-

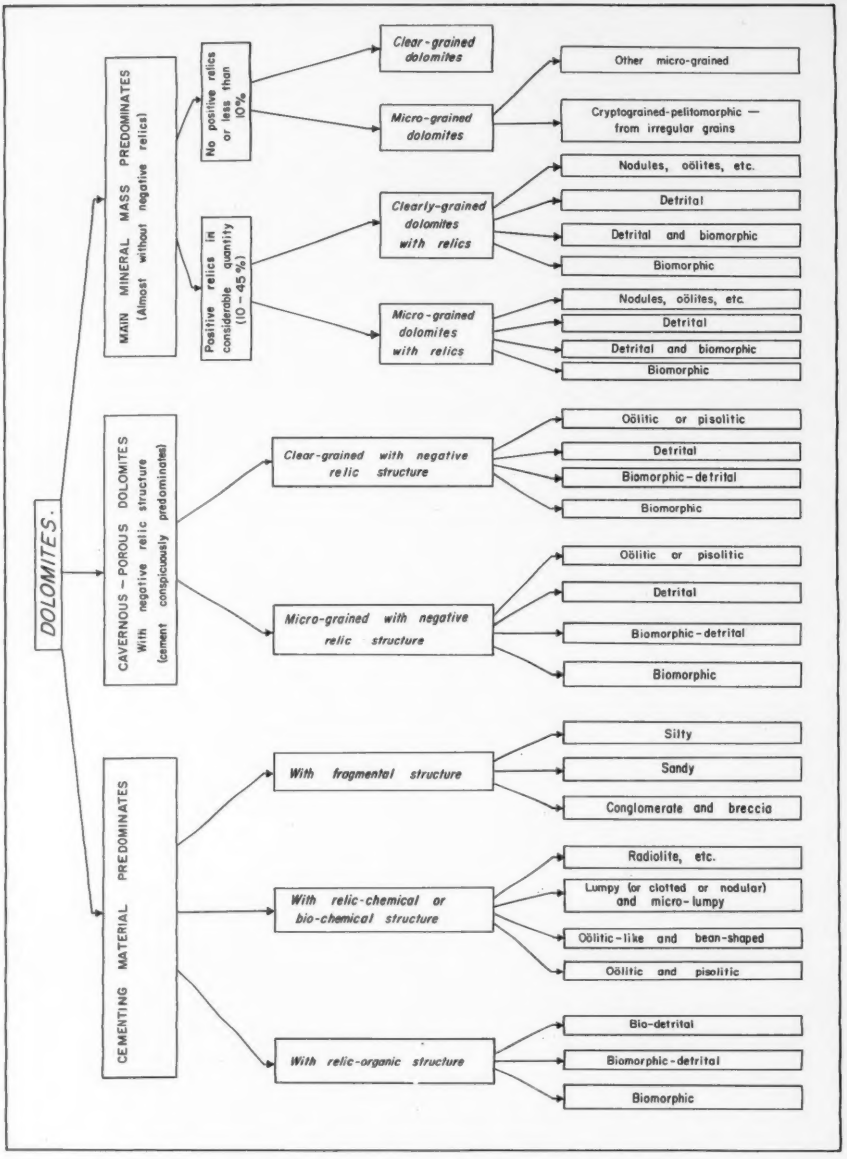

FIG. 2.—Structural classification of dolomites (after G. I. Teodorovich, 1958, p. 295).

MAIN GENETIC GROUPS OF LIMESTONES		MAIN STRUCTURAL-GENETIC VARIETIES	CHARACTERISTIC FEATURES, EXAMPLES, VARIETIES
GROUP I - LIMESTONES WHICH PRESERVED THE ORIGINAL COMPOSITION, THUS PERMITTING THEIR DIVISION INTO PRIMARY GENETIC TYPES	In major part obviously organic	Bioherms, stromatolites	Coralline, bryozoan, algal, etc.
		Whole-shelly (one piece shells)	Coarse-shell "coquina
			Fine-shell limestones (Foraminifera, etc.)
		Shelly-detrital	Coarse-detrital (detritus can be determined in thin section)
			Fine-detrital (detritus almost cannot be determined)
		Micro-grained (partly)	Chalk (largely), composed of coccoliths, fine Foraminifera, etc.
	In major part obviously primary chemical (including bacterial)	Calcareous tuffs	Coarsely-porous with plant impressions
		"Leakage" stalactites	Usually not porous; micro-layered with crystals, elongated across layering
		Oolitic and pisolitic	Rounded grains with concentric structure
		Micro-grained (partly)	Black Sea calcareous muds; rhizoid Carboniferous limestones of Russian Platform, etc.
GROUP II - LIMESTONES WITH CONSIDERABLE ALTERATION OF ORIGINAL MATERIAL, AND COMPLETELY CRYPTOGENIC (OF UNKNOWN ORIGIN)	Strongly altered, but preserving the vestiges of composition, structure, and origin of Primary material	Products of mechanical reworking — "Detrital" or "surf-accumulated"	Rolled-grained; fine-detrital, composed of rolled fragments of shells and limestones
			Coarse-fragmental, composed of vary-grained slightly-rounded limestone fragments
		Products of reworking by animals - coprogenic	Composed of rounded faeces of micrograined calcite
		Products of chemical replacement — Calcitization	Dedolomitized limestones. Usually coarse-grained, often brecciated
			Limestones — products of calcitization of sandstones. Granular with remnants of unreplaced sand grains
	Cryptogenic — reworked with clear vestiges of original composition, structure, and origin	Products of recrystallization with loss of primary structure	Recrystallized with obscure traces of original structure
			Fully recrystallized, vary-grained
			Recrystallized evenly-grained (marble)
		Micrograined (partly)	Some chalks, lithographic limestone, etc.
		Nodular (lumpy), ornamented — products of granulation and in part recrystallized	Ornamental (figured) micro-grained
			Pseudo-fragmental
			Complex structure with traces of repeated granulation and recrystallization

FIG. 3.—Genetic classification of limestones based on predominating components (after M. S. Shvetsov, 1958, p. 292).

down of obviously organic (that is, biogenic) carbonates into biomorphic, biomorphic-detrital, or bio-detrital is most useful. American geologists will recognize names which they apply to bioclastic and related carbonate sediments, such as skeletal, skeletal-detrital, skeletal-matrix, etc. Other divisions and subdivisions in Teodorovich's limestone classification chart (fig. 1) are obvious.

The reviewers believe that possibly many students of carbonates, in the past at least, have overlooked the importance of separating the dolomite and limestone classifications. Teodorovich has provided a scheme of dolomite identification (fig. 2) of unquestioned utility. In this chart (in verity a "flow-chart" scheme) the observer can readily determine the textural "pigeonhole." Relic texture (Teodorovich's "structure") is considered a key to at least part of a classification. In the field with no more than a ten-power hand lens it is normally easy to ascertain the type and arrangement of relics, whether fossil, detrital, or crystalline.

Shvetsov's arrangement of limestones may appear slightly less embracive than that of Teodorovich, but nonetheless his classification has merit. The reviewers consider it important that one attempts to ascertain whether limestones have been altered, or original fabric remains. For the most part this is a field (i.e., petrologic) problem and normally can be determined by moistening a freshly-fractured surface with water, lightweight oil, glycerin and water, or other suitable liquid that can be carried in the field in an eye-dropper bottle. With the aid of a hand lens one should experience little or no difficulty in making this determination; obviously, some samples and specimens require petrographic study before relics can be located and evaluated. Shvetsov further subdivides the first main group (fig. 3) into two genetic types: (a) readily determinable as obviously organic for the major part, and (b) obviously primary chemical (including bacterial). The second main group (namely, altered limestones) Shvetsov subdivides into (a) limestones which are strongly altered but preserve vestiges of composition, structure and origin of the primary material, and (b) those which are cryptogenic, that is, reworked sediment without clear vestiges of former fabric. Careful perusal of this chart shows that Shvetsov has provided a limestone classification worthy of rigid field test.

Perhaps some workers prefer a nomenclature of carbonate types based upon other textural and/or biomorphic entities; words (including some that are difficult to pronounce) are no more than stamps of identifications. Advantages of Teodorovich's two classifications certainly include utility in the field and laboratory, ease of identification, and advance of ideas as to genesis of the rock under study. The classification by Shvetsov perhaps has more value to the field worker (petrologist) than it does to the confined laboratory investigator (petrographer), but it does embody ideas of genesis. After all, concepts of genesis should still occupy a position of priority in the geologist's thinking during his researches in the carbonate realm. Both Teodorovich and Shvetsov are to be complimented for services rendered to carbonate researchers.

REFERENCES

SHVETSOV, M. S., 1958, Petrography of sedimentary rocks 3d ed., illus.: Gosgeoltekhizdat, Moscow, 416 p.

TEODOROVICH, G. I., 1958, Study of sedimentary rocks, illus.: Gostoptekhizdat, Leningrad, 572 p.

AXIOMETER—A MECHANICAL DEVICE FOR LOCATING AND MEASURING PEBBLE AND COBBLE AXES FOR MACROFABRIC STUDIES[1,2]

HENRY R. SCHMOLL AND RICHARD H. BENNETT
United States Geological Survey, Washington, D.C.

ABSTRACT

The axiometer is a mechanical device consisting of a clamp which holds a stone with its long axis vertical, and a track-mounted caliper, which, restricted in motion, locates and measures the two axes perpendicular to the long axis. Advantages of the axiometer over other methods tested by the authors are (1) axis locations determined by the axiometer are more accurate, so that the potential accuracy of the orientation goniometer may be realized, (2) less operator fatigue is induced by the procedure, and (3) less time is required.

INTRODUCTION

The mechanical device described in this paper, and referred to as an axiometer, was developed by the authors to locate and measure the two axes perpendicular to the longest axis of a stone. It is intended as a companion to the orientation goniometer described by Karlstrom (1952). While the longest axis can be found readily with a caliper, the other axes cannot be located accurately without some means of guidance. By the axiometer method, the stone is clamped with the long axis vertical, and a caliper is mounted to slide along and rotate about an axle which rolls captive on a track. Movement of the caliper is thus restricted so that the line between its jaw points is always horizontal and parallel to the same line.

Most early workers in stone orientation used only the long axis (e.g., Richter, 1932; Wadell, 1936), and did not encounter the problem of locating the other axes. To the authors' knowledge, Krumbein (1939a) was the first to point out the need for measuring two axes to determine the unique position of a stone in space; and his ingenious solution to the problem of locating the other axes by a photoelectric cell device (Krumbein, 1939b) is the only previously described systematic and precise method of locating these axes known to the writers. Krumbein (1941) also described a simplified means for locating these axes by visual estimate. If only the lengths of the axes are to be measured, visual estimates may be sufficiently accurate. For orientation work, however, they have proved unsatisfactory. The senior author of this paper, when first engaged in macrofabric studies of various diamicton[3] deposits in Alaska, experimented with several methods for making visual estimates with the aid of "guidelines," because the photo-cell equipment was not available. However, the accuracy achieved was not commensurate with the potential accuracy of the orientation goniometer. In addition, the use of the guiding devices improvised to aid the visual estimates was tedious and time-consuming. Dissatisfaction with such schemes led to the development of the axiometer.

As defined here, the A axis is the longest dimension of the stone, the B axis is the longest dimension of the stone perpendicular to the A axis, and the C axis is the longest dimension of the stone in a direction normal to the plane parallel to both the A and B axes. The three axes do not necessarily intersect at a point, and usually do not do so. These definitions are essentially those given by Cailleux (1945). They differ somewhat from the operational definitions of Krumbein (1939b) which apply in the use of the photo-cell method. In most cases,

[1] Publication authorized by the Director, U. S. Geological Survey.
[2] Manuscript received November 25, 1960.

[3] " . . . any nonsorted or poorly sorted terrigenous sediment that consists of sand and/or larger particles in a muddy matrix." (Flint, Sanders, and Rodgers, 1960a, 1960b)

however, the two sets of axes should very nearly coincide. Only in stones that have large concavities may there be a significant difference between the two sets of axes. Such stones generally have not been encountered in the deposits studied.

DESCRIPTION

The axiometer (fig. 1)[4] consists of two major parts, a vertical clamp and a horizontal caliper with its associated track, each mounted on a rectangular base (A).

The clamp consists of an upper and a lower assembly, each including a swivel so that the stone may rotate. The upper clamp assembly has two main parts: an inverted L-brace (B) bolted and welded to the base, and a vertical screw (C) threaded through the free end of the L-brace. The vertical screw is secured by a locknut (D) which tightens against the top of the L-brace. A cross-rod (E) through the top of the vertical screw serves as a handle for ease of turning. At the lower end of the vertical screw a housing (F) contains the upper swivel (G) mounted in a thrust bearing. The swivel tip (H), which holds the stone (I), is a rubber eraser of the type used in mechanical pencils, set in a cup-shaped recess in the lower end of the swivel. This tip wears out after a few hundred stones have been measured, and may be easily replaced.

The main part of the lower clamp assembly is a steel cylinder (J) bolted to the base on the same vertical axis as the vertical screw. The rubber tipped lower swivel (K) is bearing-mounted in the top of this cylinder, and a knurled setscrew (L) in the side of this cylinder contacts the swivel. A brass collar (M), in the shape of a truncated cone, is attached to the swivel. Lines engraved on this collar every ninety degrees permit one to rotate the swivel assembly exactly this amount.

The caliper (N) is a standard outside caliper, tension type, with screw adjustment. It is bolted to a brass collar (O) which has two needle bearings in the inner bore. This collar rotates about, and may slide along, a steel axle (P). Near each end of this main axle a steel plate (Q), normal to the axle, yokes two subsidiary axles (R). A steel wheel (S) with a V-groove as the tread is bearing-mounted on each subsidiary axle. These V-grooved wheels ride on rails (T) doubly bevelled to match the V-groove of the wheels. This groove arrangement and the tandem wheels keep the axle, and consequently the line between the points of the caliper, perpendicular to the rails at all times.

Two steel pressure bars (U), parallel to and a little higher than the rails at their outer sides, keep the caliper mounting firmly on the track. These pressure bars bear down upon bearings (V) pressed onto the ends of the main axle. The pressure bars are supported at each end by thin vertical rods (W) which are threaded into the base and which extend through the pressure bars. Pressure is adjusted by setting two nuts (X) which hold the pressure bar captive on each vertical rod.

A series of millimeter scales (Y) is taped to the base between the rails at the end near the clamp for a direct reading of axis length from the caliper opening. The scales are drawn with zero points at different places to accommodate different positions of the caliper along the axle.

The axiometer will clamp stones with a maximum A axis of 150 mm and a B axis of 130 mm. Stones of these extreme dimensions are rather difficult to handle, however, as are small pebbles. The ranges of axis length more easily handled are: A axis—32 to 128 mm; B axis—approximately 16 to 64 mm or somewhat larger. Corresponding C axes lengths are rarely less than 8 mm or larger than 64 mm.

PROCEDURE

Oriented stones to be measured in the axiometer are collected in the field by the method described by Karlstrom (1952), in which a cross is marked on each stone (while still in the outcrop face) with the aid of an orientation template. For ease in laboratory handling, the stones are washed to remove loose matrix particles, and the orientation cross is marked with India ink to assure permanence. Each stone is numbered in the lower left quadrant of the orientation cross, the number replacing Karlstrom's orientation dot. To minimize the amount of clamp

[4] Letters in parentheses in the following discussion refer to this figure.

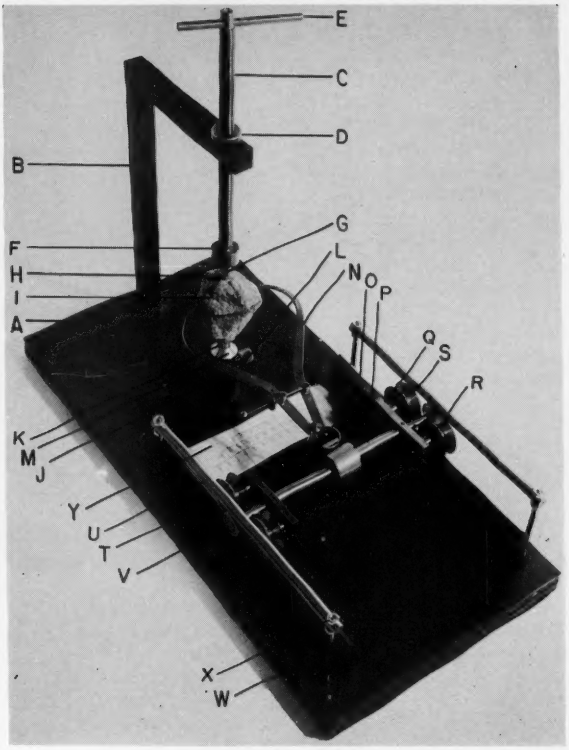

FIG. 1—Axiometer.

A	Base	$\frac{3}{16}$″ steel on $\frac{3}{4}$″ plywood, 10″×20″
B	L-brace	steel, $\frac{3}{4}$″ square, 10$\frac{3}{4}$″ high, 6$\frac{1}{4}$″ across
C	Vertical screw	steel, $\frac{1}{2}$″ diameter, 8″ long
D	Locknut	brass, 1″ diameter, $\frac{3}{16}$″ thick
E	Cross-rod	steel, $\frac{1}{4}$″ diameter, 4″ long
F	Upper swivel housing	steel, 1″ diameter, $\frac{3}{8}$″ high
G	Upper swivel	steel, $\frac{1}{2}$″ diameter, $\frac{3}{4}$″ high
H	Upper swivel tip	rubber, $\frac{5}{16}$″ diameter, $\frac{3}{8}$″ high
I	Stone	
J	Lower swivel housing	steel, 1″ diameter, 2″ high
K	Lower swivel and tip	(see G and H)
L	Setscrew	brass, $\frac{1}{4}$″ diameter with $\frac{1}{2}$″ diameter head; 1″ long
M	Swivel collar	brass, 1″ diameter, $\frac{1}{4}$″ high
N	Caliper	steel, 7″ long, maximum opening 5″
O	Caliper collar	brass, 1″ diameter, 1″ long
P	Main axle	steel, $\frac{3}{8}$″ diameter, 9″ long
Q	Axle yoke	steel, $\frac{1}{4}$″×$\frac{3}{4}$″×2$\frac{5}{8}$″
R	Subsidiary axle	steel, $\frac{3}{8}$″ diameter, 1$\frac{1}{4}$″ long
S	V-groove wheel	steel, 1$\frac{1}{2}$″ diameter with $\frac{1}{4}$″ groove, $\frac{1}{2}$″ wide
T	Rail	steel, $\frac{1}{2}$″ wide, 2$\frac{3}{4}$″ high with $\frac{1}{4}$″ bevel, 10″ long
U	Pressure bar	steel, $\frac{3}{8}$″ diameter, 10″ long
V	Axle bearing	steel, $\frac{7}{8}$″ diameter, $\frac{1}{4}$″ wide
W	Supporting rod	steel, $\frac{3}{16}$″ diameter, 3$\frac{1}{2}$″ high
X	Pressure adjustment nuts	steel
Y	Millimeter scale	paper, 2″×7″

adjustment between stones they are numbered in the order of approximate A axis length. The sample number is also added to each stone, conventionally at the base of the cross, to avoid possible misplacement.

The A axis is located first, with the aid of an unmounted caliper or other similar device (e.g., Krumbein and Pettijohn, 1938, p. 145; Krumbein, 1941, p. 65). The axial intercepts are marked with a quick-drying lacquer such as red fingernail polish. To allow the lacquer to dry before the stone is placed in the axiometer, the A axes are marked on all the stones of one sample—usually about one hundred—before proceeding to the next step.

The stone is mounted in the axiometer clamp with the A axis vertical by placing the red dots in the centers of the rubber swivel tips and tightening the vertical screw. The stone is then rotated until the approximate maximum dimension in the horizontal plane (B axis) is parallel to the caliper jaws. The mounted caliper is readily adjusted in its three directions of free movement (front to rear along the main axle; side to side on the track, and up and down rotating on the main axle) to roughly accommodate the approximate B axis. The precise location of the B axis is then determined by minor rotations of the stone and movements of the caliper. The swivel setscrew is tightened, the caliper jaws set, and the B axis intercepts marked on the stone in pencil. The axis length may then be obtained by lowering the caliper points to the millimeter scale.

To locate the C axis, the swivel assembly is rotated ninety degrees. The same procedure is followed as in locating the B axis, except that in this case the stone is fixed in position, and it is necessary only to find the largest dimension that the caliper will encounter.

When the stone is removed from the clamp, the penciled axial intercepts may be lacquered for greater visibility. The convention of using red fingernail polish for the A axis, blue for the B axis, and green for the C axis has been adopted for easy distinction among the three axes when the stone is mounted in the goniometer. When all of the stones of a sample have been measured and marked, they are ready to be mounted in the goniometer and measured according to the procedure described by Karlstrom (1952).

Although it is necessary to measure the orientation of only two of the axes (usually A and C), it is desirable to have the data for the third (B) axis, for example, for comparison with the work of Holmes (1941). Although the B axis data could be calculated from the A and C, it has been found more convenient to obtain them directly, inasmuch as the B axis has to be located for length measurment.

RESULTS

Ease of operation, accuracy of data, and saving of time are the principal advantages of the axiometer over previous "guide-line" methods. No comparisons have been made between either of these methods and that of Krumbein.

The advantage of the axiometer most apparent to the operator is the relative ease with which the work may be done compared to the "guide-line" procedures. The clamp serves as that necessary "third hand" and holds the stone firmly in place and the fixed guidance supplied to the mounted caliper obviates the continual need to align level bubbles or parallel lines simultaneously in three directions.

Although extensive studies of the comparative accuracy obtained with the axiometer and "guide-line" methods have not been made, a few random comparisons indicate that axiometer measurements result in considerably smaller errors. C axis orientations were calculated from measured A and B axis values and compared with the corresponding measured values. The mean differences between calculated and measured values for stones measured by the "guide-line" method averaged about 6 degrees and ranged as high as 12, whereas the same differences for a sample measured by the axiometer averaged about 3 degrees and in only one case were as high as 6. This 3-degree variation is probably close to the limit of accuracy of goniometer measurement, and certainly lies within the original error impressed upon the system while marking the orientation crosses on the stones in the field. The higher errors of the "guide-line" methods on the other hand

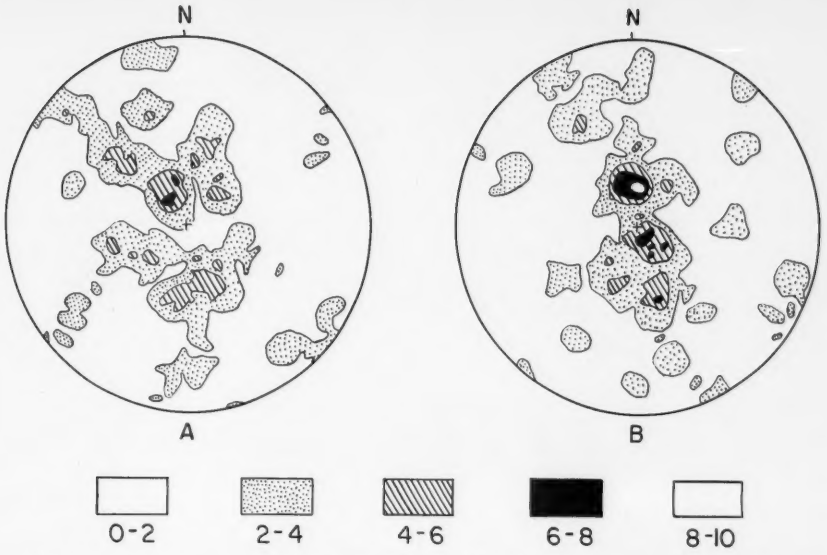

FIG. 2.—Contour diagrams of C axis distributions for the same 100-stone sample. Diagram A: axes located by visual estimate with the aid of guide lines. Diagram B: axes located by axiometer. Contour units in percent per one percent area.

may have been large enough to affect the result significantly.

Another means of comparison, perhaps more meaningful, is illustrated by two contour diagrams of C axis distributions of the same 100-stone sample (fig. 2). Diagram A is a plot of measurements obtained by the "guide-line" method, and diagram B, by the axiometer. Diagram B, in which the points are less scattered, shows a definite strengthening of the pattern. Since all errors involved are presumably random, and since the sum of goniometer measurement errors should be approximately the same in each case, diagram A is interpreted as resulting from larger axis location errors; diagram B therefore is a more accurate representation of the real C axis distribution. It is unlikely that the stronger pattern of diagram B would result from errors of equal or larger magnitude than diagram A or that diagram B is a less accurate representation of a true distribution less strongly oriented. Additional comparisons of this type have yielded similar results.

Although time consumption remains one of the principal shortcomings of detailed macrofabric work, a considerable reduction in time over the "guide-line" methods has been achieved. Axiometer analysis requires an average of about 3 minutes per stone, or about 5 hours per 100-stone sample. The work can be done faster than this for a few hours, but it has not been possible to maintain a faster pace over long periods of time. The "guide-line" method, when carefully done, required on the order of 5 minutes per stone, or between 8 and 9 hours per 100-stone sample.

Thus the use of the axiometer to locate and measure axes of stones for orientation studies requires less time to produce work of greater accuracy with much less operator fatigue than the earlier "guide-line" methods employed.

ACKNOWLEDGMENTS

The axiometer was developed during the study of macrofabrics of various diamicton deposits in the Copper River Basin, Alaska.

This work was an adjunct to areal geologic mapping in the area and is part of the U. S. Geological Survey program of terrain and permafrost investigations in Alaska sponsored largely by the Office of the Chief of Engineers, U. S. Army. The axiometer was constructed in the instrument shop of the U. S. Geological Survey from plans submitted by the authors. We are particularly indebted to Oscar J. Ferrians, Jr., in charge of mapping in the Northeastern Copper River Basin, and to Thor Karlstrom, for their support and encouragement.

REFERENCES

CAILLEUX, ANDRÉ, 1945, Distinction des gelats marins et fluviatiles: Soc. Geol. France, B. s. 5, t. 15, p. 375–404.

FLINT, R. F., SANDERS, J. E., AND RODGERS, JOHN, 1960a, Symmictite: A name for nonsorted terrigenous sedimentary rocks that contain a wide range of particle sizes: Geol. Soc. America Bull., v. 71, p. 507–510.

——— 1960b, Diamictite, a substitute term for symmictite: Geol. Soc. America Bull., v. 71, p. 1809–1810.

HOLMES, C. D., 1941, Till fabric: Geol. Soc. America Bull., v. 52, p. 1299–1354.

KARLSTROM, T. N. V., 1952, Improved equipment and techniques for orientation studies of large particles in sediments: Jour. Geology, v. 60, p. 489–493.

KRUMBEIN, W. C., 1939a, Preferred orientation of pebbles in sedimentary deposits: Jour. Geology, v. 47, p. 673–708.

——— 1939b, Application of the photo-electric cell to the measurement of pebble axes for orientation analyses: Jour. Sedimentary Petrology, v. 9, p. 122–130.

——— 1941, Measurement and geological significance of shape and roundness of sedimentary particles: Jour. Sedimentary Petrology, v. 11, p. 64–72.

KRUMBEIN, W. C., AND PETTIJOHN, F. J., 1938, Manual of sedimentary petrography: Appleton-Century-Crofts, New York, 549 p.

RICHTER, KONRAD, 1932, Die Bewegungsrichtung des Inlandeises rekonstruiert aus dem Kritzen und Längsachsen der Geschiebe: Zeitschrift für Geschiebeforschung, v. 8, p. 62–66.

WADELL, H. A., 1936, Volume, shape, and shape position of rock fragments in open work gravel: Geog. Annaler, Arg. 18, H. 1, p. 74–92.

METHOD OF SOLUTION OF CALCAREOUS MATERIALS USING THE COMPLEXING AGENT, EDTA[1]

EVERETT D. GLOVER

Socony Mobil Oil Company, Inc., Field Research Laboratory, Dallas, Texas

ABSTRACT

A method for removing calcareous material from sediments without destroying other minerals and polospores is described. This method is based upon the use of salts of ethylenedinitrilotetracetic acid (EDTA) to complex calcareous material and, thus, render it soluble. Data are given showing how EDTA concentration, pH, temperature, and particle size of calcium carbonate affect the solution rate.

This method is applicable to mineralogical analyses; recovery of pollen grains, insoluble residues, and ironbearing fossil casts; and to differentiate between calcite and dolomite.

INTRODUCTION

One of the most common cementing agents in sediments in calcite. To remove calcite is a simple matter of acid treatment, but to do this and at the same time avoid solution or alteration of other minerals, notably some clays, requires a control of the pH at not less than about 3.5 units. The use of strong acids, such as HCl, makes the treatment slow since they must be added intermittently. Buffered weak acids such as a lithium acetate-acetic acid mixture may

[1] Manuscript received November 7, 1960.

be used. Citric acid, a very soluble acid, the anion of which complexes calcium, would be a good choice except for the fact that the ciltrate salt of calcium is only sparingly soluble (<.25 g/100 ml).

The organic acid, ethylenediaminedinitrilotatracetic acid (EDTA), is an excellent complexing agent for calcium. When this material first became avaible in experimental quantities, it was reported to dissolve many water-insoluble metal salts, such as barium sulfate, by strongly complexing the cation. Although complexing of cations in solution by EDTA has been used for nearly a decade, its application to the solution of solid material has apparently been limited to the removal of scale from boilers and evaporators, the solution of calculi occuring inside the body, and the decalcification of bone sections in preparing them for microscopic examination.

Recently, a trial use of EDTA for solution of $CaCO_3$ in sediments showed an unexpectedly high solution rate, even for solid calcite particles as great as a few millimeters in diameter. As a result, a much more convenient and versatile way of removing calcareous material from sediments has been developed.

After this work was completed a note appeared on this subject (Hill and Runnels, 1960, p. 631). Since this note did not give details of the application of the method, this paper is presented to show interrelationship of pH, concentration of EDTA, temperature, time, and particle size of calcium carbonate in the solution process.

EDTA is a tetrabasic acid:

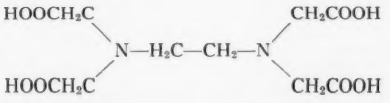

Its titration curves with several bases are shown in figure 1 reproduced from Schwarzenbach (in Martell and Calvin, 1952, p. 40). Curve A was obtained with the strong base, KOH, the K^+ forming no complex with EDTA. Curve B, with LiOH, shows a complexing effect at high pH and curve C, with $Ca(OH)_2$, shows strong complexing of Ca^{++}.

From curve A, equivalence points for 1, 2, 3, and 4 equivalents of base are at 3.5,

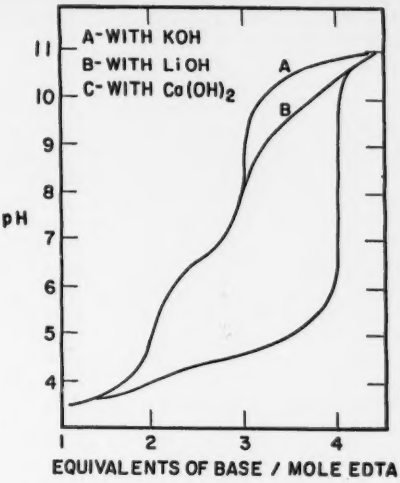

FIG. 1.—Titration of EDTA. After Martell & Calvin, *Chemistry of the Metal Chelate Compounds*, (C) 1952. Prentice-Hall, Inc.

5, 8.5, and 10.5 pH units. The neutralization of EDTA by $Ca(OH)_2$ forms mainly the calcium dihydrogen salt up to two equivalents. Beyond this point the additional calcium ion is complexed by the EDTA molecule so that at 4 equivalents/molecule of EDTA, the EDTA molecule is associated with two calcium atoms as shown in figure 2.

Thus, one Ca ion is complexed per molecule of EDTA and the theoretical amount of EDTA necessary to complex 1 gram of $CaCO_3$ is 2.923 grams.

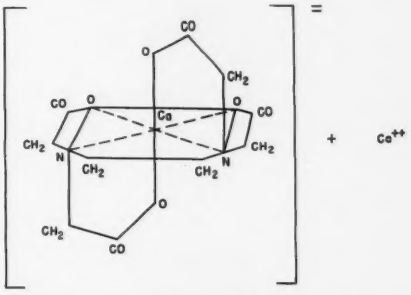

FIG. 2.—The association of EDTA with two calcium ions.

The free acid, the disodium dihydrogen salt, the trisodium hydrogen salt, and the tetrasodium salt are among the commercially available forms of EDTA. The free acid is only slightly soluble (<2 grams/liter). The disodium dihydrogen salt is available as an analytical reagent. Its solubility is about 10 grams/100 ml. The preparation used in this work had a pH of 4.4 in an approximately saturated solution. The trisodium hydrogen salt is available in technical grade with solubility >35 grams/100 ml and a pH of approximately 8.3. The tetrasodium form is still more soluble and should have a pH of about 10.5. This latter form is available but was not used in the present experiments.

EXPERIMENTAL PROCEDURE

Preliminary experiments were carried out with solutions of the disodium dihydrogen salt of EDTA and precipitated chalk (very fine $CaCO_3$). A solution of 5 grams of disodium dihydrogen EDTA in 55 ml of water (pH 4.4) dissolved a gram of the chalk in a few minutes at room temperature and in a few seconds at boiling temperature. Because the action was so fast, further solubility rate studies were made to determine the range of variation of the solubility rate with temperature, particle size, and pH of the EDTA solution.

The experiments were carried out in 50 and 100 ml beakers containing EDTA solution composed of 9 grams of the disodium dihydrogen salt of EDTA per 100 ml of water or its equivalent if other EDTA forms were used. In order to make the EDTA:$CaCO_3$ ratio relatively high, ½ gram amounts of $CaCO_3$ were used for every 5 grams of EDTA (disodium dihydrogen form) in most of the experiments. This made the EDTA quantity a little more than three times the $CaCO_3$ equivalent for the complexing reaction.

In the room temperature experiments, the solutions were stirred with a magnetic stirrer which rested on a small perforated stainless steel "platform" above the bottom of the beaker so as not to grind the calcite particles. In the experiments carried out at boiling temperature, the stirring was provided by the ebullition. The time for solution was recorded as the time interval necessary for disappearance of the solid phase.

RESULTS

The data are presented in figures 3, 4, and 5. In figure 3, the solution time for ½ gram of iceland spar is plotted against the average particle diameter for various EDTA solutions. For curve A, 5 grams of disodium dihydrogen EDTA/55 ml of water were used to produce a pH of 4.4. For curve B, a mixture of 2.5 grams of disodium dihydrogen EDTA and 2.65 grams trisodium hydrogen EDTA/55 ml of water gave a pH of 6.4, and for curve C, 5.3 grams of trisodium hydrogen EDTA/55 ml of water produced a pH of 8.3. The three curves represent results obtained from boiling solutions and illustrate how solution time changes with pH at constant EDTA concentration and temperature. Figure 4 shows the relationship between solution time and pH for given mesh sizes.

Curve D in figure 3 shows the effect of larger complexing ion concentration (22 grams trisodium hydrogen EDTA/55 ml) in the pH 8.3 system and may be compared to curve C where the EDTA solution con-

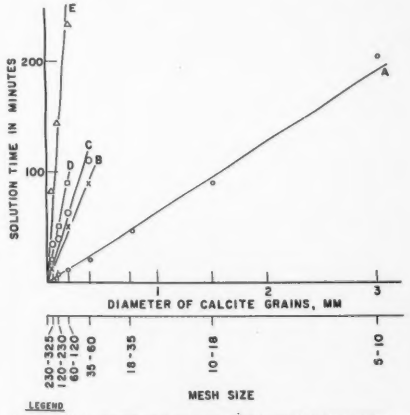
SOLUTION TIME IN MINUTES
200
100
E
A
C
B
D
1
2
3
DIAMETER OF CALCITE GRAINS, MM
230-325
120-230
60-120
35-60
18-35
10-18
5-10
MESH SIZE
LEGEND
A - 5.0 GRAMS OF DISODIUM EDTA PER 55 ML OF WATER - pH 4.4, SOLUTION BOILING.
B - 2.5 GRAMS OF DISODIUM EDTA AND 2.65 GRAMS OF TRISODIUM EDTA PER 55 ML OF WATER - pH 6.4, SOLUTION BOILING.
C - 5.3 GRAMS OF TRISODIUM EDTA PER 55 ML OF WATER - pH 8.3, SOLUTION BOILING.
D - 22 GRAMS OF TRISODIUM EDTA PER 55 ML OF WATER - pH ABOUT 8.3, SOLUTION BOILING.
E - 5.0 GRAMS OF DISODIUM EDTA PER 55 ML OF WATER - pH 4.4, TEMPERATURE 25°C.

FIG. 3.—Solution time for calcite in EDTA solutions under various conditions.

tained the standard amount of EDTA (5.3 grams trisodium hydrogen EDTA/55 ml = 9 grams disodium dihydrogen EDTA/100 ml). The lower solution rate may be due to the noticeably higher viscosity or to the lowered water activity of the more concentrated solution.

Curve E gives the solution times for the pH 4.4 system at room temperature. This curve and the related curve for the data at boiling temperature are shown more clearly in figure 5.

APPLICATIONS OF THE METHOD

Removal of Carbonate from Sediments in Preparing Sample for Mineralogical Analysis

The sample is suspended in a disodium dihydrogen or trisodium hydrogen EDTA solution (or, for intermediate pH values, a mixture of the two forms) having a ratio of $\frac{1}{2}$ to 1 gram of $CaCO_3$ to 5 grams EDTA in approximately 10 percent solution and boiled until a small portion of settled sediment gives no effervescence with 6N HCl. The suspension is in the flocculated state in the presence of the calcium complex and may be washed by centrifugation.

The choice of pH depends on the time allowed for solution and, also, on the importance of avoiding iron removal from the sample. Use of higher pH values favors the formation of the calcium complex over the iron complex.

The solution data above provide a guide to the time necessary for solution. However, the presence of coatings, such as organic matter, can lengthen the time interval considerably.

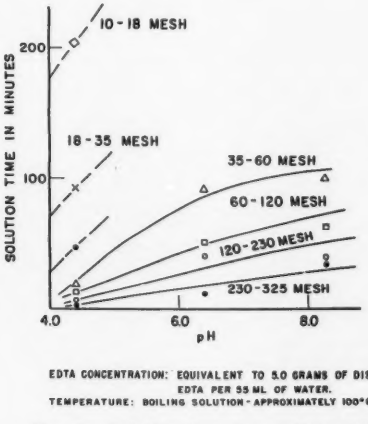

FIG. 4.—Solution time for calcite in EDTA solution as a function of pH for various mesh sizes.

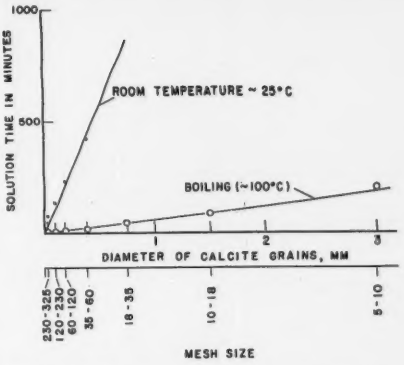

FIG. 5.—Solution time for calcite in EDTA as a function of mesh size for two temperatures, 25° C and 100° C.

Removal of Carbonate from Limestones to Recover "Insoluble" Residues

The method described can be used to recover "insoluble" residues. It may be used to dissolve either large pieces of fine-grained limestones, as mentioned above, or macrocrystalline limestones after grinding them to a desired mesh size. The mesh size depends on the nature of the insoluble residue. Clay residues are affected very little by grinding whereas larger grains of other insoluble minerals may be ground up.

Application to Pollen Extraction Problems

Many limestones give poor pollen recovery. When material is recovered it may consist of broken and damaged grains. This may be due to mechanical disruption on acid treatment or it may be due to forces produced in recrystallization of the limestone. This point can be investigated by dissolving carbonate samples with EDTA solution, pH 8.3, at temperatures just under boiling. Under these conditions the bicarbo-

nate ion rather than CO_2 is present, and thus there is no CO_2 or vapor bubbles to cause mechanical disruption of the pollen. If mechanical disruption in acid treatment is found to be the cause of poor pollen material in some cases, the EDTA method could be adapted to the routine procedure for extraction of pollen from sediments.

Removal of Iron-Containing Minerals, Fossils, or Replicas from Carbonate Rocks

By carrying out EDTA treatment in the alkaline range of pH it is possible to remove iron-containing entities from carbonates without dissolving the iron. This procedure is especially applicable to the recovery of fragile material where either mechanical comminution before magnetic separation or solution of the carbonates by dilute acids may destroy the material. An example of this application is the removal of fragile glauconite-replaced or coated sponge spicules which occur in the Wapanuka Limestone.

Differentiation of Calcite and Dolomite

A method of differentiating calcite from dolomite by a colorimetric test using EDTA has been previously described (Weissman and Diehl, 1953, p. 433).

Experiments to determine the feasibility of differentiating calcite from dolomite by means of their solubility in EDTA solution showed that the maximum differentiation between the two minerals is brought about with a solution of pH 6.3. Knife scrapings of a rock sample were treated with a drop or two of the pH 6.3 solution. Calcite produced a prompt evolution of gas bubbles as observed with a hand lens, whereas dolomite produced either a delayed evolution of bubbles or none at all. In the writer's opinion this reagent is superior to dilute strong acid; however, as with the use of acids, use of this reagent requires considerable care and experience on the part of the user.

This reagent is made by mixing 10 grams ($\frac{1}{3}$ ounce) of disodium EDTA, approximately 5 pellets of sodium hydroxide and 85 cc of water (3 fluid ounces.) For precise control of the pH the amount of sodium hydroxide necessary may be determined by the use of a pH meter. At present EDTA is not generally available in drug stores, but may be obtained from chemical supply houses.

ACKNOWLEDGMENTS

The author wishes to express his gratitude to the Socony Mobil Oil Company for permission to publish this work. Acknowledgment is made of the assistance of Andy A. Bufford with the experimental part of this work.

REFERENCES

Hill, W. R., Jr. and Runnels, R. T., 1960, Versene, new tool for study of carbonate rocks: Am. Assoc. Petroleum Geologists Bull., v. 44, p. 631–632.

Martell, A. E., and Calvin, M., 1952, The chemistry of the metal chelate compounds: Prentice-Hall, Inc., New York, 613 p.

Weissmann, R. C., and Diehl, A., 1935, A new method utilizing Versene for determination of the calcite-dolomite ratio in carbonate rocks: Proc. Iowa Acad. Science, v. 60, p. 433–437.

OCCURRENCE OF *RANGIA CUNEATA* GRAY AND *CRASSOSTREA VIRGINICA* (GMELIN) IN SABINE LAKE, TEXAS-LOUISIANA[1]

HENRY E. KANE
Ball State Teachers College, Muncie, Indiana

Sabine Lake, a lake estuary (Kane, 1959), is situated in the extreme southeastern corner of Texas and the southwestern corner of Louisiana. The northern boundary of the lake is approximately at lat. 29° 59′ N.; the southern at lat. 29° 45′ N.; the eastern at long. 93° 45′ W.; the western at long. 93° 57′ W.

Field observations and cores to a maximum depth of 9 feet indicate that *Rangia cuneata* Gray, an estuarine genus (Ladd, 1951), occurs in Sabine Lake, mainly north of lat 29° 50′ N. This species apparently occupies the fresher water portion of Sabine Lake and could serve as an index type to this part of the lake. *Rangia* shells are usually scattered throughout the sediments and do not necessarily show any tendency to form reeflike masses. The pattern of core-spacing, however, was too widespread to delineate the geometry of *Rangia* occurrence.

The same data indicate that *Crassostrea virginica* (Gmelin), the common edible oyster, occurs singly or as reefs in Sabine Lake south of lat. 29° 50′ N. This species which apparently is typical of the more saline part of the lake could serve as an index type to this portion of the lake. One large reef of *Crassostrea virginica* (Gmelin) is located along the Louisiana shoreline between Blue Buck Point and Garrison Ridge and another along the Texas shoreline approximately opposite Blue Buck Point. The pattern of core-spacing did not permit delineation of the reef geometry.

Acknowledgements.—The writer is grateful to Shell Development Company for its financial grant toward this project.

[1] Manuscript received November 28, 1960.

REFERENCES

KANE, H. E., 1959, Late Quaternary geology of Sabine Lake and vicinity, Texas and Louisiana: Trans., Assoc. of Gulf Coast Geological Societies, Houston, Texas, v. 9, p. 225–235.

LADD, H. S., 1951, Brackish-water and marine assemblages of the Texas coast, with special reference to mollusks: Pubs. of the Inst. of Marine Sci., Texas Univ., v. 2, no. 1, p. 136.

THE FREE-CORER: SEDIMENT SAMPLING WITHOUT WIRE AND WINCH[1]

DAVID G. MOORE
Sea-Floor Studies Section, U. S. Navy Electronics Laboratory, San Diego, California

The free-corer is a simple, inexpensive bottom sediment coring device intended to eliminate the necessity of wire line lowering of gravity corers. The free-corer consists of two basic assemblies: (1) a recoverable core barrel, check valve, buoyant chamber assembly, and (2) an expendable weight and casing assembly. When these two assemblies are combined, the core barrel fits loosely inside of the casing. Operation of the free-corer is accomplished by dropping the device from the ship and allowing it to fall free through the water column to the sea floor. A simple release-delay timer then releases the core barrel and its buoyant float from the weight-casing assembly; the barrel is then lifted up out of the casing and back to the surface by its attached float while the expendable weight-casing remains embedded in the sediments (fig. 1).

[1] Manuscript received November 7, 1960.

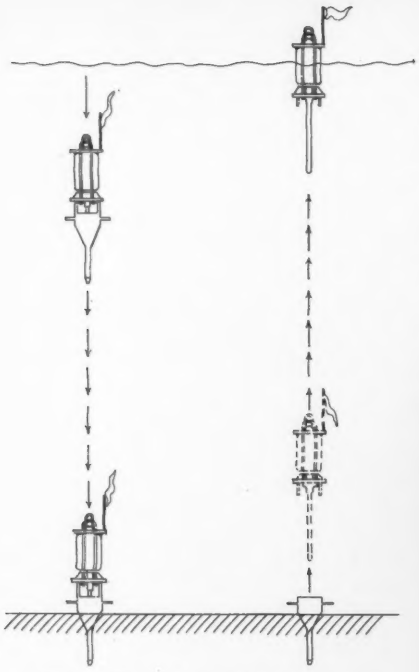

FIG. 1.—Stages in operation of free-corer.

The potential usefulness of a free-coring instrument has long been apparent and the use of recoverable free instrument vehicles (Isaacs and Schick, 1960) has recently been demonstrated as a reliable technique. However, no practical method of extracting a core barrel after it has become firmly embedded in bottom sediment has previously been suggested. This paper is intended to introduce a practical system of overcoming the extraction problem. The system consists of abandoning a casing and weight in the bottom and thereby allowing the encased sediment filled core barrel to break free at its tip and float up out of the embedded casing with only a small excess buoyancy. This process requires no complicated working parts or large buoyant tanks; therefore the entire assembly can be relatively small, easy to handle, and inexpensive.

The free-corer system has been tested at sea with three operational drops using a prototype corer which was assembled mainly to test the effectiveness of the expendable casing idea and was not engineered for optimum core recovery. Two drops were made in San Diego Bay in ten fathoms of water so that divers could observe the attitude of the embedded corer and note any possible flaws in the release process. These shallow drops recovered short silty sand cores, 18 and 60 cm in length. The inherent hydrodynamic stability of the free-corer was well demonstrated in these tests in which the corer was rolled off the edge of the boat on its side and was able to right itself and fall vertically true almost within

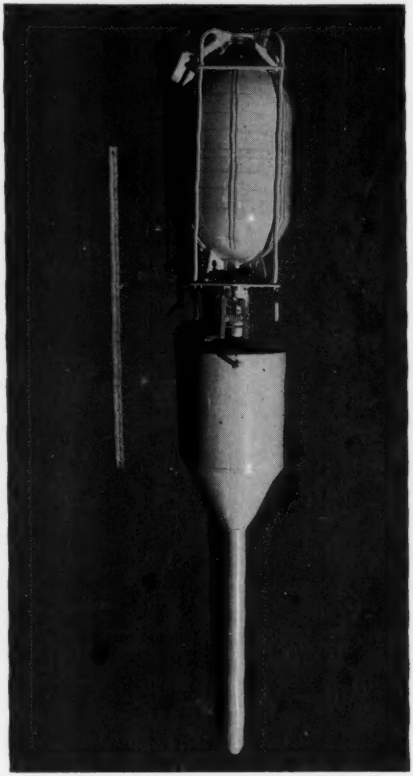

FIG. 2.—Prototype of free-corer for shallow water testing. In this photograph delay-release timer is open and core barrel is partially removed from casing. Yardstick shows scale.

its own length. This stability, which is necessary to insure a vertical attitude on bottom contact, is the result of the forces of the buoyant tank pulling upward while the weight-casing unit exerts a stronger downward force.

The prototype free-corer used in these tests was made from the valve, barrel, and plastic barrel liner of a standard 1-$\frac{3}{8}$ inch gravity corer. An air-filled low pressure oxygen bottle was attached to serve as a buoyant tank (fig. 2). The weight-casing

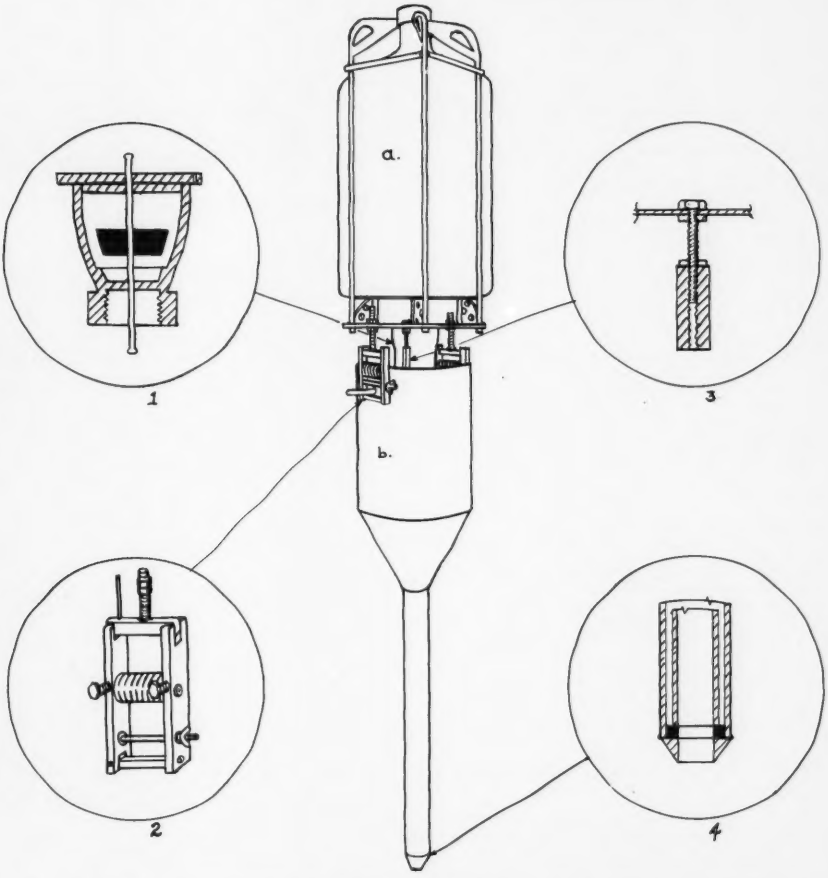

FIG. 3.—Diagram of free-corer with polyethylene bottle (a) which, when filled with gasoline, acts as pressure-proof buoyant chamber. Core barrel attached to buoyant chamber fits loosely inside of expendable weight-casing (b). Circles show details of corer parts: 1. check valve helps prevent loss of core; 2. Van Dorn release-delay timer; magnesium rod, inside of spring coils, holds spring compressed. Wing nut is backed off before lowering to allow latch on lower end of timer to fall open when magnesium rod snaps at prearranged time as a result of galvanic action. Size of rod determines time delay; 3. three spacer nuts, as shown here, are adjusted against concrete weight to give rigidity to corer; 4. detail of casing shoe which is tack-welded to bottom of casing; inside diameter of shoe is like that of core barrel shown seated on rubber washer.

unit was a heavy gauge steel pipe with a concrete weight cast around it. Clearance between the barrel and casing, when the two units were combined, was about $\frac{3}{16}$ in. A machined casing shoe was tack-welded to the base of the casing to act as a core cutter and to seat the core barrel inside the casing. A Van Dorn (1953) marine release-delay timer was used to secure the two units together. Threaded spacers were attached to the base plate of the buoyant chamber which were adjustable to seat against the concrete weight and give rigidity to the assembled corer for handling (fig. 3).

The last of the initial test drops was made in 700 fathoms of water off San Diego. The free-corer dropped at a rate of about two fathoms per second, as determined by echo sounder readings, and returned to the surface 18 minutes after drop time with a sandy silt core about 50 cm long. For this deep test, the air filled tank was replaced with a 13 gallon polyethylene bottle filled with gasoline. This gave an ample excess buoyancy of about 30 pounds to the recoverable unit of the corer. In the greatest depths of the oceans the gasoline filled bottle would lose only about 10 percent of its buoyancy as a result of compression and contraction of the gasoline from pressure and cold. The compliancy of the polyethylene bottle easily tolerates this volume change. Thus there is no depth limitation to the use of the free-corer.

The principal problem associated with the use of the free-corer will be the location and recovery of the returned floating core. In water 5000 fathoms deep, for example, the travel time of the corer to the bottom and back will be about two hours. This will allow the ship to drift off the release point for what might be a considerable distance and also permit the corer to be exposed to current action for this period of time. For this reason a small drogue or dye marker is needed to mark the drop position and minimize the effect of wind drift. A flag of high visibility fabric which was attached to the free-corer in the 700 fathom drop off San Diego made the float visible as soon as it surfaced. A small Navy liferaft radar reflector used by Isaacs and Schick (1960) on their free instrument vehicle provided contact to 4 miles by radar.

Operational use of a free-corer is planned for the near future in geological studies to be made by the Sea Floor Studies Section of the Navy Electronics Laboratory. The corer will be used from surface vessels to obtain closely spaced deep-sea cores in which the distance between cores will be accurately known from drop positions. With the free-coring technique it is practical to take a series rather than a single deep-sea core inasmuch as the travel time of any individual core will be great compared to the drop time of the series. It is impossible to obtain a series of closely spaced cores of known relative positions from abyssal depths using wire line lowering.

It is planned to use the free-corer as a sampling system in connection with bathyscaph operations to be conducted by this Laboratory. The corer will be released magnetically and will return to the surface after the submerged bathyscaph has moved to another location. The floating barrel will then be recovered by the surface tender.

Because the free-corer does not require a winch and heavy cable, it can be used from almost any type of boat. It is believed that this will prove to be exceptionally valuable to smaller marine institutions which are unable to afford oceanographic vessels equipped with large deep-sea winches. With the introduction of the free-corer the way is open for a more detailed areal study of deep-sea sediments, and a wider participation of small institutions in deep-sea programs.

REFERENCES

ISAACS, J. D. AND SCHICK, G. B., 1960, Deep-sea free instrument vehicle: Deep-Sea Research, v. 7, p. 61–67.

VAN DORN, W. G., 1953, The marine release delay timer: Oceanographic Equipment Report No. 2, Scripps Institution of Oceanography Reference 53–23, 10 p., 7 figs.

FIELD METHOD FOR SIEVE ANALYSIS OF SAND

EMANUEL AZMON[1]
Marine Geology Consulting, Los Angeles, California

ABSTRACT

A field method for the mechanical analysis of sand is attained by using a sieve and cylinder combination. The sand is passed through a nest of sieves, and the fraction remaining on each is measured in a graduate cylinder. This method is simple and rapid, and the results obtained are comparable with the settling tube analyses.

INTRODUCTION

Two fundamental techniques are available for the mechanical analysis of sand grains, the sieve method and settling tube method. In the sieve method (Krumbein and Pettijohn, 1938) the grains are sorted according to their diameters, and the frequency of each fraction is determined according to its weight. This is a well standardized procedure, but it requires heavy and expensive equipment, and many time consuming weighings. In the settling tube method (Emery, 1938) the grains are grouped according to their settling velocities and the cumulative frequencies of the fractions are measured by volume. This too is a well standardized procedure requiring only relatively simple equipment, being more rapid than the first.

FIELD METHOD

During an investigation of beaches in southern California in connection with some beach engineering problems, a need developed for a rapid field method for the mechanical analysis of sand. A simple apparatus was set up for this purpose, consisting of a sand sorting unit and a sand frequency measuring unit. The sorting unit (fig. 1) was made of five brass sieves having a frame diameter of three inches, pore openings of 1000, 500, 250, 125, and 62 microns, and a total height of 6.5 inches. The measuring unit (fig. 2) was made of a stand, a funnel, and a 10 cc graduate cylinder.

The sieves were arranged in order of pore opening so that the coarsest sieve was on top and a pan was on the bottom below the finest sieve. A small amount of sand, less than 10 cc, was dumped into the top sieve and covered with a metal cover. The unit was then vibrated by hand for one minute, tapping it lightly against the other hand with each vibration. Then, the contents of each sieve were poured into the cylinder through the funnel, beginning with the coarsest fraction, and the cumulative heights of the column of sand recorded. The cylinder

FIG. 1.—A sorting unit consisting of five brass sieves having a frame diameter of 3 inches and a total height of 6.5 inches.

[1] Manuscript received November 15, 1960.

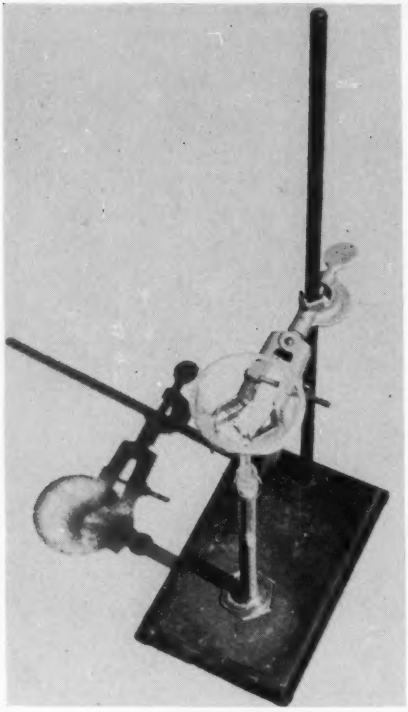

FIG. 2.—A measuring unit consisting of a 10 cc graduate cylinder, a funnel, and a stand.

was tapped lightly before each reading to assure proper compaction of the sand.

When the sand was wet or partly dried, a wet sieving procedure was followed, and sea water was used to wash the sand through the screens and into the graduate cylinder. The sand settled immediately to the bottom of the cylinder, and the excess water was then decanted.

RESULTS

Twenty sand samples were selected to demonstrate the similarity of results obtained by the sieve and cylinder method to those obtained by the settling tube. These samples have a grain size distribution covering the total sand fraction, and some samples contain as much as 40 percent carbonates (soluble in dilute HCl). Each sample was analyzed both by the settling tube and by the sieve and cylinder, and the median diameter (Md), the first quartile (Q_1), and the third quartile (Q_3) computed (fig. 3). The results obtained by the two methods are closely related through the entire range from very fine sand to very coarse sand. Under certain circumstances, however, this relationship does not hold. If for example, a sand sample is high in shell material, these shells will float in the settling tube and settle with the very fine fraction in spite of their size. The same shells, when sieved, will be retained by the coarser screen. Consequently, the numerical value of the first quartile (Q_1) diameter, obtained by sieve and cylinder, will be larger than the one obtained by settling. The high shell content may be easily detected, and taken into consideration when evaluating the sedimentary history of the sample.

On the other hand, if the sand is high in heavy mineral grains, these grains will settle with the coarser fraction in spite of their smaller size. The same heavy mineral grains, when sieved, will go through the coarser screen and will be retained with the finer

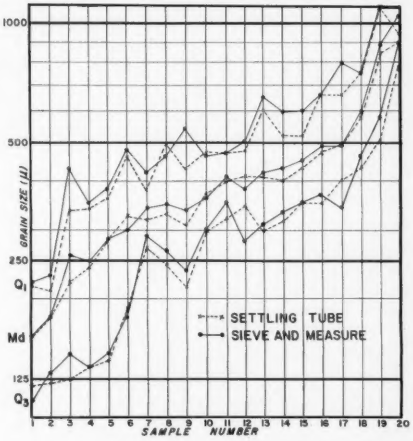

FIG. 3.—Grain size distribution of twenty samples, obtained by two methods: settling tube, and sieve and cylinder. Samples range from very fine sand (finer than 125 microns) to very coarse sand (coarser than 1000 microns). Md = median diameter; Q_1 = first quartile diameter; Q_3 = third quartile diameter; μ = micron.

fraction. Consequently, the numerical value of the third quartile (Q_3) diameter, obtained by sieve and cylinder, will be larger than the one obtained by settling. This distribution of the heavy minerals according to their grain size rather than settling velocities may be regarded as an advantage as will be explained below.

EVALUATION

Comparing this method of measuring sand in a graduate cylinder with that of accurately weighing the sample on an analytical balance may give an erroneous impression that the latter method is more accurate than the former. But, considering the inherent errors due to collecting and splitting the sample (Krumbein, 1934) and additional errors due to extrapolating a continuous cumulative curve on the basis of five or six points, it follows that the accuracy of reading the graduate cylinder is satisfactory. If a greater accuracy is desired it may be achieved statistically by collecting more samples rather than by refining the methods of collecting, splitting or graphing.

The two main advantages of the sieve and cylinder method, and the reason for resorting to it, are its simplicity of procedure and portability of equipment. It can be executed right on the beach or in the trunk of the car, and may be used with either dry or wet sand. There is no need for a preliminary elimination of silt, as the silt is collected directly in the pan. If individual fractions must be examined, in order to determine carbonates, glauconite grains, or heavy mineral grains for example, this can easily be done by keeping the fractions separated. The fractions are sorted according to their grain size and not according to their hydraulic equivalents (Azmon, 1960), thus the frequency of heavy mineral grains in any fraction is primarily a function of the original crystal sizes and may be characteristic of the source rock. Lastly, in the sieve and cylinder method both the sorting of the grains and the measuring of the fractions are based on one criterion—grain dimensions.

APPENDIX

No.	Method	Q_1 μ	Q_3 μ	Md μ	%HCl soluble
1	Settling	215	120	160	8.0
	Sieve	220	110	160	8.0
2	Settling	210	155	180	
	Sieve	230	155	180	
3	Settling	335	150	220	40.0
	Sieve	430	170	260	40.0
4	Settling	340	160	240	30.1
	Sieve	350	160	250	30.1
5	Settling	360	165	285	26.7
	Sieve	380	170	285	26.7
6	Settling	460	190	325	29.7
	Sieve	480	180	300	29.7
7	Settling	380	270	320	
	Sieve	420	290	340	
8	Settling	495	245	330	
	Sieve	460	265	350	
9	Settling	430	215	310	
	Sieve	540	236	340	
10	Settling	470	295	370	
	Sieve	460	300	360	
11	Settling	470	350	410	0.0
	Sieve	470	320	400	0.0
12	Settling	475	345	410	
	Sieve	500	280	380	
13	Settling	600	300	410	
	Sieve	650	310	420	
14	Settling	520	315	400	
	Sieve	600	330	430	
15	Settling	560	350	430	
	Sieve	620	350	450	
16	Settling	660	365	470	
	Sieve	660	350	490	
17	Settling	660	400	500	
	Sieve	790	340	490	
18	Settling	745	430	580	19.7
	Sieve	750	460	600	19.7
19	Settling	1100	500	840	12.1
	Sieve	1100	580	890	12.1
20	Settling	950	780	900	
	Sieve	1100	890	1050	

μ = micron; Q_1 = first quartile; Q_3 = third quartile; Md = median diameter.

REFERENCES

AZMON, EMANUAL, 1960, Heavy minerals in sediments of southern California: Ph.D. Dissertation, Univ. Southern Calif., 148 p.

EMERY, K. O., 1938, A rapid method of mechanical analysis of sands: Jour. Sedimentary Petrology, v. 8, p. 105–111.

KRUMBEIN, W. C., 1934, The probable error of sampling sediments for mechanical analysis: Am. Jour. Sci., v. 27, p. 204–214.

KRUMBEIN, W. C. AND PETTIJOHN, F. J., 1938, Manual of Sedimentary Petrography: D. Appleton-Century Co., New York, 549 pages.

CLAY AND PEAT BOULDERS[1]

WILLIAM F. TANNER
Department of Geology, Florida State University, Tallahassee, Florida

ABSTRACT

Soft-particle conglomerates contain pebbles, cobbles, and even large boulders of clay, peat, or other materials which were more or less plastic at the time of deposition. A Tertiary example in Alabama and a Pennsylvanian example in Arkansas are cited. A study of modern coasts reveals that rounded boulders of clay and peat are produced along the seaward edge of the chenier plain. Although other mechanisms are available to account for such conglomerates, it is thought that most of the lithified examples represent coastal deposits. Beachrock is a member of the same class of sediments.

INTRODUCTION

Soft-particle conglomerates are coarse detrital rocks containing individual fragments which were quite soft at deposition. Particle lithologies may have been calcium carbonate, clay, peat, or other soft material. These particles were not indurated until the surrounding matrix was also lithified.

Soft pebbles of calcium carbonate are deposited in beachrock (Ginsburg, 1953; Tanner, 1956) and in travertine (Tanner, 1954); perhaps other deposition environments are common. Less well described in the literature are similar beds where the pebbles were laid down as clay or as peat. It is the purpose of this article to mention examples of the latter, and to point out a possible mode of accumulation.

ANCIENT EXAMPLES

Toulmin, La Moreaux and Lanphere (1951) have described an example of the accumulation of clay fragments in the Eocene Tuscahoma Formation of Choctaw County, Alabama. The matrix is largely an uncemented sandstone, although silty clay is present. The boulders, up to 50 cm in diameter, include some sandstone, but chiefly are gray silty clay. It is clear that very little transportation is involved, perhaps not more than a few meters.

A more spectacular example occurs in vertical Pennsylvanian rocks above the Narrows dam, north of Murfreesboro, Arkansas. The Pennsylvanian Jackfork formation is beautifully exposed in clean cuts in a parking lot on the hill east of the dam. Shales, sandstones and conglomerates are present. The latter contain pebbles of quartz, and pebbles, cobbles and boulders of black shale.

In at least one thick bed, the black shale boulders and the black shale matrix are almost indistinguishable; in other beds, the shale boulders occur in a matrix of siltstone or sandstone. The general appearance of these beds is one of tectonic deformation. However, more competent layers both above and below have not been similarly crumpled. Closer inspection reveals that the black shale unit is a very coarse conglomerate.

In other exposures, black shale boulders occur as isolated masses in typical Jackfork sandstone. Field relationships indicate that the boulders were laid down on a wet layer of unconsolidated quartz sand. In some places the boulders are as much as 80 cm across.

It is obvious that a soft boulder of such size, though well-rounded, was not transported a great distance. Since ordinary black shales occur nearby, in the same stratigraphic interval, one can infer that the boulders are penecontemporaneous. Locally sharp edges and corners are common on pebbles. The distance of transport to such sites must have been negligible.

The writer has visited many widely-scattered localities, where details differ but the situation is generally as described above. The large shale "erratics" of the Ouachita Mountains of Oklahoma (Kramer, 1933; Cline, 1956) pose a different problem, and are not considered here.

[1] Manuscript received November 25, 1960.

MODERN EXAMPLES

The chenier is a fairly common coastal feature (Price, 1955; Russell, and Howe, 1953). It consists of a ridge of clastic materials resting on a soft base such as clay or peat. Cheniers are known at various places along the Atlantic and Gulf coasts. Good examples occur in New Jersey (fig. 1), Florida, and Louisiana. In nearly every case, the seaward toe of the chenier is covered with younger clay or peat, or a small wave-cut nip is developed in the older clay or peat underlying the chenier.

In many examples the soft layer is neither strictly clay nor peat, but is a dark tough material having a high content of plant fibres. Small cliffs or nips cut in this material stand essentially vertically.

Where the bedding is not too thick, blocks of clay are torn loose and moved slightly seaward or landward (fig. 2). If the blocks are rather large, this short transport may be the work of storm waves. Blocks which were moved landward generally rest on the surface of the clay or peat bed, or on top of firm dry sand. Blocks which moved seaward commonly sink part-way into loose, wet sand or soft mud.

In either case the sand-blast effect of wave action may round part or all of each block.

FIG. 1.—Nip in peaty layer exposed at low tide, Cold Springs inlet, about 3 miles north of Cape May, New Jersey. To the right is a chenier of quartz sand and shell debris. Blocks of peaty material are broken off by wave action; some are moved seaward short distances, where they may be buried, whereas others are moved to the top of the peaty layer.

FIG. 2. Peaty boulder torn from an ocean-facing nip north of Cape May, New Jersey, and moved high up on the beach. Pocket knife for scale.

The total transport distance may have been a matter of only a few tens of centimeters.

Preservation of such blocks is not to be expected along consistently emergent coasts. Where submergence is great, suitable parent beds are probably not exposed for cliffing and production of blocks. Oscillating coasts having a net downward trend could provide the soft parent layer and quick burial for the blocks produced by destruction of that layer. The result would be essentially what can be seen in the Pennsylvanian exposures of Arkansas.

Clearly, an oscillating shore is not the only possible mechanism for producing a soft-particle conglomerate. The Montana earthquake of August 17, 1959, left peaty boulders up to two meters across on the remains of the black-topped highway north of Lake Hebgen. These blocks had been torn from nearby marshes by violent wave action and thrown at least 10 feet above normal lake level. Travertine pebbles are formed in a different manner, clay pebbles can be cut on the banks of tidal flat channels, and yet other agencies may be responsible for depositing soft particles (Shepard, 1959).

However, it appears likely that many such soft particle conglomerates were formed along or close to a shore line. A careful study of the peats or clays involved should, in general, yield enough faunal data to either refute or confirm this idea.

REFERENCES

BYRNE, J. V., LEROY, D. O., AND RILEY, C. M., 1959, Chenier plain and its stratigraphy, southwestern Louisiana: Bull. Amer. Assoc. Petroleum Geologists, v. 43, p. 2520.

CLINE, L. M., 1956, Regional stratigraphy and history of Ouachita Mountain area: Bull. Amer. Assoc. Petroleum Geologists, v. 40, p. 427.

GINSBURG, R. N., 1953, Beachrock in south Florida: Jour. Sedimentary Petrology, v. 23, p. 85–92.

KRAMER, W. B., 1933, Boulders from Bengalia: Jour. Geology, v. 41, p. 590–621.

MCKEE, E. D., 1957, Primary structures in some recent sediments: Bull. Amer. Assoc. Petroleum Geologists, v. 41, p. 1704–1747.

PRICE, W. A., 1955, Environment and formation of the chenier plain: Quarternaria, v. 2, p. 75–86.

RUSSELL, R. J., AND HOWE, H. V., 1953, Cheniers of southwestern Louisiana: Geogr. Review, v. 25, p. 449–461.

SHEPARD, F. P., 1959, Marine sediments: Science, v. 130 (17 July), p. 141–149.

TANNER, W. F., 1954, The Brush Hollow Limestone in the Canon City reentrant, Colorado: Proc. Okla. Acad. Science, v. 35, p. 95.

———, 1956, Examples of probable lithified beachrock: Jour. Sedimentary Petrology, v. 26, p. 307–312.

TOULMIN, L. D., LA MOREAUX, P. E., AND LANPHERE, C. R., 1951, Geology and groundwater resources of Choctaw County, Alabama: Geol. Survey of Ala., Special Report 21, County Report 2, 197 p.

JOURNAL OF SEDIMENTARY PETROLOGY, VOL. 31, NO. 4, PP. 637–640
SEPTEMBER, 1961

REVIEWS

Salt Marshes and Salt Deserts of the World, by V. J. Chapman, 1960. Pp. xvi+392, 102 figures, 45 plates. Leonard Hill, London; Interscience, New York. $14.50.

This book is an excellent synthesis of existing information on the salt marsh environment. Although the author is primarily a botanist and his approach to salt marshes is vegetational, there is a wealth of information that should be of interest to coastal geomorphologists, ecologists, and workers in recent sediments. Pertinent topics include marsh physiography, biogeography of marshes, and a thorough treatment of the "soil factor."

The purpose of the volume, according to Chapman, "is to present, so far as possible a general picture of salt marshes and related tracts throughout the world." In an effort to achieve this aim a large portion of the book is devoted to accounts of various marshes around the world and elaborations on the British marshes where detailed studies have been accomplished. These discussions emphasize schematic successional relationships in the marsh vegetation but physiology and ecology are also included. It would have been good to have a treatment of the salt marsh in its entirety as an ecosystem embracing fauna as well as flora. Of biogeographic interest in the world survey is the fact that 20 to 30 percent of local species are similar in their global occurrence. In addition, Chapman's synthesis points toward the origin of most halophytes in the Northern Hemisphere.

Little information is present on salt deserts but this is due to a general lack of studies on this environment. There is no discussion of evaporites in the geologic sense.

The book has abundant illustrations and most appear to be well selected, but local situations are frequently poorly indexed cartographically. A world map summarizing the distribution of salt marshes would have been useful for reference and orientation.

In general, *Salt Marshes and Salt Deserts of the World* is welcomed as the first comprehensive scientific treatise of its kind. Forthcoming companion volumes covering mangrove swamps and another on sand dunes are awaited with interest.

MAYNARD M. NICHOLS
University of California
Los Angeles, Calif.

Petrology of the Fountain and Lyons Formations, Front Range, Colorado, by John F. Hubert. Quat. Colo. Sch. Mines, vol. 55, No. 1, Jan., 1960, 242 pp., 71 figs., 40 tables. $3.00 Colorado School of Mines, Golden, Colorado.

This exhaustive monograph on the petrology of the redbed sequence bordering the eastern margin of the Ancestral Rocky Mountain Front Range element is based on a Ph.D. thesis completed under the direction of P. D. Krynine; the treatment conforms to the philosophic framework established by Krynine and his students.

Field data were gathered at three measured sections of the Glen Eyrie Shale Member of the Fountain Formation and from four measured stratigraphic sections of the Fountain Arkose and Lyons Sandstone located between Colorado Springs and Boulder. For purposes of analysis, field descriptions and sampling were related to a relatively few, readily identified basic rock types within each formation. Sampling of the Glen Eyrie Member and the Lyons Sandstone was dependent upon the occurrence of the basic rock types. In the much thicker Fountain Arkose, however, the irregular occurrence of the three basic rocks required collection of a very large number of samples or collection according to a rigorous and sophisticated statistical plan. Hubert, therefore, divided each section into five equal "levels" or "statistical strata" which were then sampled at random in order to provide a basis for comparisons between different parts of the same measured section as well as between sections. By means of these devices Hubert was able to come to grips with the forest without significant interference from the trees—no mean accomplishment in dealing with such a large and diverse mass of rocks.

On page 23, Hubert states his objectives in the form of questions requiring answers.

A summary of these questions and their answers as gleaned from reading his paper follows and will serve to illustrate the significance, strong points, and shortcomings of his paper:

"1. Did the ancestral Front Range highland undergo a single or several upward movements? Was the highland a single tectonically integrated highland or did it undergo differential movements at different places? Where was the eastern margin of the highland located?" Study of the change in grain size and the proportion of channel, flood plain, and leltaic-lacustrine sediments from the base to the top of the Fountain Arkose leads Hubert to conclude that the highland acted as a unit and was lifted once. These conclusions are well supported and represent a significant contribution to our ideas concerning the Ancestral Rockies. Provenance studies suggest that the eastern margin of the highland was near the present mountain front.

"2. What specific environments are involved in deposition of the Fountain and Lyons sediments?" Fountain environments are predominantly fluvial and are represented by channel arkose, floodplain redstone, and deltaic-lacustrine feldspathic sandstone. The Lyons Sandstone is composed of arkose deposited on rocky beaches and feldspathic quartzite deposited as beaches, bars, and dunes. These conclusions reinforce generally held ideas regarding the formations.

"3. What are the differences, in terms of field structures, mineral composition, and texture among the coexisting phases, and corresponding rock types, of the fluvial Fountain and shoreline Lyons sedimentary systems on an arkosic background?" Extensive and detailed rock descriptions provide an answer to this question and probably constitute the major contribution of this paper.

"4. What was the climate during Fountain and Lyons time, both in the source area highland and area of deposition?" Hubert concludes that the area was warm and humid and seasonally dry with slightly more arid conditions possibly occurring during deposition of the Lyons Sandstone. His findings coincide with generally held modern opinion concerning these deposits.

"5. What are the petrographic characteristics of the relatively unexplored transition from arkose to orthoquartzite rock types as seen in the Lyons sandstones?" Hubert describes these rocks thoroughly and incorporates his findings in a new scheme of classification. Although some may object to yet another classification designed to accommodate a relatively scarce group of rocks, this reviewer is of the opinion that, if a classification serves a useful purpose within the context in which it is proposed, such a classification is justified. Hubert's classification qualifies on these grounds, but this does not mean that it must be adopted into a classification scheme designed for all sedimentary rocks.

"6. Are the Lyons feldspathic quartzites first cycle derived, or second cycle, sandstones?" Hubert concludes, on the basis of a significant lack of reworked Fountain pebbles within the Lyons, that the Lyons is "first cycle derived." This finding is a new contribution to a currently unsettled debate.

"7. Does a single tectonic cycle control the Fountain, Lyons, and Lykins sequence of redbeds?" Hubert's answer of, "yes," is in harmony with the best and most widespread current opinion.

"8. What is the interaction of tectonism, systems and phases of sedimentation and resulting rock types in the Fountain and Lyons Formations?" This question is never specifically considered, but the reader can assemble his own answer from the great mass of data and piece-meal interpretation presented by Hubert.

Hubert and the School of Mines are to be commended for presenting such a thorough and significant study to the reading public. There are far too few outlets for monographic works in geology. On the other hand, more rigorous editing to eliminate repetition, unnecessary review of old material, and uneconomical expression would have improved this paper. This reader was disappointed to find that detailed descriptions of columnar sections had been omitted to save space when he found that page 58 was devoted to a diagram illustrating Mc-

Kee and Wier's (1953) terminology of cross-stratification and that page 233 was devoted to a full account of the four types of quartzose sandstone generally recognized in the literature. Tabulated data may be of limited interest, but would seem to be of more value than reiteration of widely known, already published material. It also seems likely that statements such as, "Until criteria for distinguishing these loci of deposition become more diagnostic, it is difficult to derive operational field definitions to differentiate them. However, certain polar types of cross-stratification, often intercalated at a given outcrop, are suggestive of specific loci," (p. 95) could be repharsed to save space and increase understanding. Also, about one fourth of the photographic illustrations are of little value because the screen employed does not adequately resolve the detail and contrast in the original prints.

In short this is a significant contribution to regional geology and to sedimentary petrology, but it is a bit difficult to read.

R. L. LANGENHEIM, JR.
University of Illinois

The Sea Off Southern California, A Modern Habitat of Petroleum, by K. O. Emery, 1960. Pp. xi+366, 248 figs., 31 tables, one 27×31 in map inside back cover, list of references, author index, and subject index; 7.00×10.25 in., cloth. John Wiley & Sons, Inc., New York and London. Price $12.50.

The Sea Off Southern California represents a compilation of work from many sources, including the author's own researches, concerning the present day geologic processes and their effects on the sea floor off that coast. The book goes into some detail to show how they operate and to indicate how they must have operated in the past. The book is well written and easy to understand for the geologist who is not particularly familiar with this area. The author has brought together a vast amount of information about a region where data are both difficult and expensive to obtain, and has synthesized it into general concepts that a geologist can use. The author summarizes in detail the physiography, lithology, structure, water, life, sediments, and economic aspects of the region. The writing is well documented for those who wish to pursue specific points, and the list of references of over 800 entries will be a welcome aid to anyone interested in the area. Almost 300 figures and tables illustrate and illuminate the text.

The present day environs off the coast of southern California are complex and encompass many processes. The multitude of variables and parameters transcend almost every phase of geology. The book will be especially interesting to persons who must interpret the past from the evidence seen in the rock column of that region. The petroleum geologist in particular might well digest all that is presented. The stratigrapher would do well to review and note the documented methods of transportation, types, origins, and rates of accumulation of the sediments. The controversial turbidity current is apparently an important mechanism for the transportation of material to the basins that lie offshore. The paleontologist should note the ecological controls imposed on the environment by the various oceanographic conditions. In addition, the evidence of both reworked and redeposited sediments and fossils should be a reminder to all that this process has been operative, though not always recognized, in the past.

In the exploration of the geologic facets of this region, man's effect on the natural processes are discussed, hence bringing forth the problems of the ground water geologist, engineering geologist, geographer, oceanographer, and others. A summary of the problems involved with ground water, slumpage, sewerage, radioactive material disposal, subsea mining and drilling is discussed. Even man's contribution of artifacts to the sediments of that area is presented, and a map of the location of sunken ships is provided for the armchair geologist adventurer to ponder.

One very minor criticism that the reviewer has is the occasional lack of continuity in the units of measure. For example, the depth of water is not consistently given in meters.

This volume is heartily endorsed as a requisite for both students and professionals alike. Its perspective on current geologic processes should provide a better understanding of what we see in the rock column. It should provide excellent supplemental reading material for statigraphy and sedimentation courses in our universities and colleges. Professor Emery's approach has been one that certainly further entrenches the Huttonian concept.

The task of the geologist is to study and unravel earth history. While many are capable of assembling small bits of information and studying specific problems, Professor Emery has gone further and brought together all the material of a region and presented a well organized, coordinated, and lucid chapter in our earth history. *The Sea Off Southern California* is an excellent example of compilation, workmanship, and synthesis. It should be an example and goal for all other geologists.

ELLIOTT A. RIGGS
University of Illinois

Journal of Sedimentary Petrology

INDEX TO VOLUME 31

A non-laminated miniature sample splitter 471
A note on the replacement in joints 478
A simplified method for determining relative energies of deposition of stratigraphic units 291
"A Traverse of Post-Avis Cisco Rocks, Brazos Valley, North Central Texas," review of 485
Acid, use in separation of clay minerals from carbonate rocks 123
Adams, John K., Groot, Johan J., and Hiller, N. William, Jr., article by 546
Alberta, Canada, reef petrography of Beaverhill Lake Formation, Upper Devonian, Swan Hills area 497
Allen, J. R. L., article by 325
Alluviation, mineral and chemical, in a unique pedologic example 80
Aluminum, iron, magnesium, and calcium in carbonate rocks, analysis for with EDTA 113
Analcime–Montmorillonite, association in the series of Stanleyville, Congo 293
Analysis of carbonate rocks for calcium, magnesium, iron, and aluminum with EDTA 113
Analysis of carbonate rocks for calcium, magnesium, iron, and aluminum with EDTA, errata 486
Anhydrite, genesis of primary structures 553
Anhydrite, regenerated, redefined 611
Announcements 492
Argillaceous rocks, colloid phenomena in sedimentation of 560
Authigenic tourmaline and zircon in the Vindhyan formations of Sone Valley, Mirzapur District, Uttar Pradesh, India 482
Awasthi, Nirja (Miss), note by 482
Axiometer—a mechanical device for locating and measuring pebble and cobble axes for macrofabric studies 617
Azmon, Emanuel, note by 631

Backset beds in the Coso Formation, Inyo County, California 603
Bahamas, Inagua, early diagenetic dolomite associated with salt extraction 473
Beach and dune sands, distinguishing between 196
Beach, dune, and river sands, distinction by textural characteristics 514
"Beaches and Coasts," review of 133
Beaverhill Lake Formation, Upper Devonian, Swan Hills area, Alberta, Canada, reef petrography of 497
Bedding, cyclic, in carbonate rocks, France 453
Bennett, Richard H., and Schmoll, Henry R., note by 617
Best paper award 492
Big Horn Mountains, Wyoming, Morrison and Cloverly Formations, mechanical analysis and heavy minerals of 571
Bihar, India, pattern of Talchir sedimentation in Burhai Gondwana Basin 63
Bisque, Ramon E., article by 113
Bisque, Ramon E., errata in article by 486
Bissell, Harold J., and Chilingar, George V., note by 611
Blue sandstones, Tertiary, central California, genetic relationship among 594
Bottom sediments of Georges Bank 165
Bottom sediments of Lake Michigan, petrography of 402
Boulders, clay and peat 634
Breccia and Pennsylvanian cave filling in Mississippian St. Louis Limestone, Putnam County, Indiana 275
Breccias, evaporite solution, Mississippian, southwest Montana 189
Brightseat Formation, Maryland, phosphatic pebbles from 546
Burhai Gondwana Basin, Bihar, India, sedimentation pattern in Talchir series 63
By-passing and sorting process, the flotation phenomenon 476
Byrne, John V., and Riley, Charles M., article by 553

Calcareous material, solution of, by EDTA 622
Calcareous spring deposits, post-Sangamonian(?), Wellsville area, Colorado 586
Calcite-dolomite ratios in sedimentary rocks, rapid determination of 130
Calcium, magnesium, iron, and aluminum analysis with EDTA 113
Calcium-strontium ratios and magnesium contents in Recent carbonate sediments, Florida Keys, variations of 336
California, Inyo County, Coso Formation, backset beds in 603
California, Tertiary, genetic relationships among blue sandstones of 594
Cambrian, Potsdam Sandstone of New York, composition, grain size, roundness, and sphericity 5
Canada, Alberta, reef petrography of Beaverhill Lake Formation, Upper Devonion, Swan Hills area 497
Cape of Good Hope, South Africa, size distribution characteristics of shallow marine sands 256
Carbon isotope distribution and limestone petrology, late Pennsylvanian and early Permian, Glass Mountains, Texas 231
Carbonate rocks, analysis for calcium, magnesium, iron, and aluminum with EDTA 113
Carbonate rocks, separation of clay minerals by using acid 123
Carbonate rocks, South-Central France, cyclic bedding in 453
Carbonate sedimentation on the Heron Island Reef, Great Barrier Reef 215
Carbonate sediments, Florida Keys, variations of strontium-calcium ratios and magnesium contents in 336
Carbonate sediments, mineralogy and early diagenesis 358
Carozzi, Albert V., articles by 262, 497
Carozzi, Albert V., "Microscopic Sedimentary Petrography," review of 135
Cave filling and breccia, Pennsylvania, in Mississippian St. Louis Limestone, Putnam County, Indiana 275

Channel sands, South Canadian River, New Mexico, Texas, and Oklahoma, compositional and textural properties, significance of 15
Chapman, V. J., "Salt Marshes and Salt Deserts of the World," review of 637
Chemical and mineral alluviation in a unique pedologic example 80
Chilingar, George V., and Bissell, Harold J., note by 611
Clay and peat boulders 634
Clay and shale, thin sections of 131
Clay dunes, marine and lagoonal deposits, Gulf Coast, Texas 245
Clay mineralogy of Cretaceous-Tertiary of Upper Mississippi Embayment 38
Clay minerals, separation from carbonate rocks by using acid 123
Clay pebbles, Johore, Malaya, occurrence and origin of 437
Cloverly and Morrison Formations, Big Horn Mountains, Wyoming, mechanical analysis and heavy minerals of ... 571
Colloid phenomena in sedimentation of argillaceous rocks 560
Colorado, Wellsville area, post-Sangamonian(?) calcareous spring deposits 586
Comments on Teodorovich's "Structural Classification of limestones and dolomites" and Shvetsov's "Genetic classification of limestones" 611
Comparative efficiencies of size analysis by hydrometer and pipette methods 96
Composition, grain size, roundness, and sphericity of the Potsdam Sandstone (Cambrian) in northeastern New York 5
Compositional and textural properties of channel sands, South Canadian River, New Mexico, Texas, and Oklahoma, significance of 15
Concerning the association montmorillonite–analcime in the series of Stanleyville, Congo 293
Congo, montmorillonite–analcime association in Stanleyville series 293
Cores at shallow depth, a simple drilling tool for orienting 609
Coso Formation, Inyo County, California, backset beds in 603
Crassostrea virginica (Gmelin) and *Rangia cuneata* Gray, occurrence in Sabine Lake, Texas-Louisiana 627
Creager, Joe S., and Sternberg, R. W., article by 96
Cretaceous-Tertiary clay mineralogy of the Upper Mississippi Embayment ... 38
Cross-lamination, micro, in upper Keweenawan sediments of northern Michigan 390
Cyclic bedding in pure carbonate rocks from South-Central France 453

Day, R. W., Fleming, P. J. G., and Maxwell, W. G. H., article by 215
Dean, John R., and Yedlosky, Robert J., article by 372
Devonian, Beaverhill Lake Formation, Swan Hills area, Alberta, Canada, reef petrography of 497
Diagenesis and mineralogy of carbonate sediments 358
Diagenetic dolomite associated with salt extraction process, Inagua, Bahamas. 473
Discriminating between refractory and nonrefractory quartzite by quantitative petrography 530
Distinction between dune, beach, and river sands from their textural characteristics 514
Distinguishing between beach and dune sands 196
Distorted oolites and pseudoolites 262
Dolomite-calcite ratios in sedimentary rocks, rapid determination of 130
Dolomite, diagenetic, associated with salt extraction process, Inagua, Bahamas. 473
Dolomites, comments on Teodorovich's "Structural classification of limestones and dolomites" and Shvetsov's "Genetic classification of limestones" 611
Domes, spring, developed in limestone 288
Drilling tool for orienting cores at shallow depth 609
Dune and beach sands, distinguishing between 196
Dune, beach, and river sands, distinction by textural characteristics 514
Dunes, clay, marine and lagoonal deposits, Gulf Coast, Texas 245

Early diagenetic dolomite associated with salt extraction process, Inagua, Bahamas 473
EDTA, analysis of carbonate rocks for calcium, magnesium, iron, and aluminum with 113
EDTA, method of solution of calcareous material 622
Emery, K. O., "The Sea Off Southern California, A Modern Habitat of Petroleum," review of 639
Energy deficit, offshore shoals in area of .. 87
Energy, relative depositional, simplified method for determining in stratigraphic units 291
England, sandstone-plugged pipes, Lower Old Red Sandstone, Shropshire 325
Errata, "Analysis of carbonate rocks for calcium, magnesium, iron, and aluminum with EDTA" 486
Evaporite solution breccias from the Mississippian of southwest Montana 189

Ferric oxides in red beds as paleomagnetic data 296
Field method for sieve analysis of sand ... 631
Fleming, P. J. G., Day, R. W., and Maxwell, W. G. H., article by 215
Florida Keys, Recent carbonate sediments, variations of strontium-calcium ratios and magnesium contents in 336
Flotation phenomenon—a by-passing and sorting process 476
France, cyclic bedding in carbonate rocks. 453
Friedman, Gerald M., article by 514
Fuller, A. O., article by 256

Genesis of primary structures in anhydrite 553
Genetic relationship among Tertiary blue sandstones in central California 594
Geology of the submarine Santa Rosa-Cortes ridge 534
Georges Bank, bottom sediments 165
Glass, H. D., and Pryor, W. A., article by. 38
Glass Mountains, Texas, limestone petrology, carbon isotope distribution, late Pennsylvanian and early Permian 231
Glover, Everett D., note by 622
Goldman, Marcus I., note by 611
Gondwana Basin, Bihar, India, pattern of

Talchir sedimentation in 63
Grain size in Phi units, measurement of .. 608
Grain size, roundness, sphericity, and composition of Potsdam Sandstone, New York 5
Great Barrier Reef, Heron Island Reef, carbonate sedimentation on 215
Grender, G. C., note by 608
Groot, Johan J., Adams, John K., and Hiller, N. William, Jr., article by 546
Gulf Coast, Texas, marine and lagoonal deposits, clay dunes 245

Hamblin, Wm. Kenneth, article by 390
Hansen, Bernold M., review by 485
Harrison Formation, Miocene of Nebraska, heavy minerals of 52
Harrison, W., and Terasmae, J., article by. 448
Head, William B., and Rogers, John J. W., article by 467
Heavy minerals and mechanical analysis, Morrison and Cloverly Formations, Big Horn Mountains, Wyoming 571
Heavy minerals of the Miocene Harrison Formation in northwestern Nebraska. 52
Heron Island Reef, Great Barrier Reef, carbonate sedimentation on 215
Hiller, N. William, Jr., Adams, John K., and Groot, Johan J., article by 546
Hower, John, and Stehli, Francis G., article by 358
Hubert, John F., "Petrology of the Fountain and Lyons Formations, Front Range, Colorado," review of 637
Hulsey, J. D., article by 101
Humphries, D. W., note by 471
Hydrometer and pipette methods, comparative efficiencies of size analysis by 96

Inagua, Bahamas, diagenetic dolomite associated with salt extraction process .. 473
India, authigenic tourmaline and zircon in the Vindhyan formations of Sone Valley, Mirzapur District, Uttar Pradesh 482
India, Bihar, pattern of Talchir sedimentation in Burhai Gondwana Basin 63
Indiana, Putnam County, breccia and Pennsylvanian cave fillings in Mississippian St. Louis Limestone 275
Indiana, Wabash Valley, variation in pebble composition of Wisconsin outwash sediments in the 73
Inyo County, California, Coso Formation, backset beds in 603
Iron, calcium, magnesium, and aluminum analysis with EDTA 113

Johnson, Carlton R., and Kiel, Othar M., note by 609
Johore, Malaya, clay pebbles, occurrence and origin of 437
Joints, replacement in 478

Kane, Henry E., note by 627
Keller, W. D., article by 80
Keweenawan sediments, northern Michigan, micro-cross-lamination in 390
Kiel, Othar M., and Johnson, Carlton R., note by 609
King, Cuchlaine A. M., "Beaches and Coasts," review of 133
Kolář, Václav, "Spiral motion of fluids," review of 134
Kornicker, Louis S., and Price, W. Armstrong, article by 245

Lagoonal and marine deposits, clay dunes, Gulf Coast, Texas 245
Lake Michigan bottom sediments, petrography of 402
Langenheim, R. L., Jr., review by 637
Late Pennsylvanian and early Permian limestone petrology and carbon isotope distribution, Glass Mountains, Texas 231
Lerbekmo, J. F., article by 594
Limestone, breccia and Pennsylvanian cave fillings in Mississippian St. Louis Formation, Indiana 275
Limestone petrology and carbon isotope distribution, late Pennsylvanian and early Permian, Glass Mountains, Texas 231
Limestone, spring domes developed in 288
Limestones, comments on Teodorovich's "Structural classification of limestones and dolomites" and Shvetsov's "Genetic classification of limestones" 611
Louisiana-Texas, Sabine Lake, occurrence of *Rangia cuneata* Gray and *Crassostrea virginica* (Gmelin) in 627

McCammon, Richard B., article by 73
Macrofabric studies, measurement of pebble and cobble axes, axiometer 617
Magnesium, calcium, iron, and aluminum analysis with EDTA 113
Magnesium contents and strontium-calcium ratios in Recent carbonate sediments, Florida Keys, variations of .. 336
Magnetism, remanent, in Pleistocene silts, North America 448
Malaya, Johore, clay pebbles, occurrence and origin of 437
Manos, Constantine, article by 456
Marine and lagoonal deposits in clay dunes, Gulf Coast, Texas 245
Marine sands, shallow, size distribution characteristics, Cape of Good Hope, South Africa 256
Maryland, phosphatic pebbles from Brightseat Formation 546
Maxwell, W. G. H., Day, R. W., and Fleming, P. J. G., article by 215
Measurement of grain size in Phi units ... 608
Mechanical analysis and heavy minerals, Morrison and Cloverly Formations, southern Big Horn Mountains, Wyoming 571
Mechanical device for locating and measuring pebble and cobble axes for macrofabric studies, the axiometer 617
Median size and sorting coefficients of synthetic sands, relationships between ... 467
Melhorn, Wilton N., Smith, Ned M., and Sunderman, Jack A., articles by 275
Membership list, S.E.P.M. 137
Method of solution of calcareous material using the complexing agent, EDTA ... 622
Michigan, Keweenawan sediments, micro-cross-lamination in 390
Micro-cross-lamination in upper Keweenawan sediments of northern Michigan .. 390
"Microscopic Sedimentary Petrography," review of 135
Middleton, Gerald V., article by 189
Miller, D. N., Jr., note by 473
Mineral and chemical alluviation in a

unique pedologic example 80
Mineralogy and early diagenesis of carbonate sediments 358
Mineralogy of clays of Cretaceous-Tertiary of Upper Mississippi Embayment 38
Minerals, clay, separation from carbonate rocks by using acid 123
Minerals, Miocene Harrison Formation of Nebraska, heavy minerals of 52
Miocene Harrison Formation, Nebraska, heavy minerals of 52
Mirsky, Arthur, article by 571
Mirzapur District, Uttar Pradesh, India, authigenic tourmaline and zircon in Vindhyan formations of Sone Valley. 482
Mississippi Embayment, Cretaceous-Tertiary clay mineralogy of the 38
Mississippian, Montana, evaporite solution breccias, of 189
Mississippian St. Louis Limestone, Putnam County, Indiana, breccia and Pennsylvanian cave filling in 275
Montana, evaporite solution breccias, Mississippian 189
Montmorillonite–Analcime, association in the series of Stanleyville, Congo 293
Moore, David G., article by 343
Moore, David G., note by 627
Moore, John Ezra, article by 402
Morrison and Cloverly Formations, Big Horn Mountains, Wyoming, mechanical analysis and heavy minerals of ... 571

Nebraska, Miocene Harrison Formation, heavy minerals of 52
New Mexico, South Canadian River channel sands, significance of compositional and textural properties of 15
New York, Potsdam Sandstone, composition, grain size, roundness, and sphericity 5
Nichols, Maynard M., review by 637
Nitecki, Matthew H., note by 478
Niyogi, Dipankar, article by 63
North America, remanent magnetism in Pleistocene silts 448
Nossin, J. J., article by 437
Note on measurement of grain size in Phi units 608

Oana, Shinya, and Ross, Charles A., article by 231
Occurrence and origin of clay pebbles on the east coast of Johore, Malaya 437
Occurrence of *Rangia cuneata* Gray and *Crassostrea virginicia* (Gmelin) in Sabine Lake, Texas-Louisiana 627
Offshore shoals in area of energy deficit ... 87
Oklahoma, South Canadian River channel sands, significance of compositional and textural properties of 15
Old Red Sandstone, Lower, sandstone-plugged pipes, Shropshire, England ... 325
Oolites and pseudoolites, distorted 262
Orienting cores at shallow depth, a simple drilling tool for 609
Origin and occurrence, clay pebbles, east coast Johore, Malaya 437
Ostrom, Meredith E., article by 123
Outwash sediments, variation in pebble composition of Wisconsin outwash, Wabash Valley, Indiana 73

Paleomagnetic data, ferric oxides in red beds 296
Pattern of Talchir sedimentation in Burhai Gondwana Basin, Bihar, India 63
Peat and clay boulders 634
Pebble and cobble axes, the axiometer, a device for locating and measuring 617
Pebble composition of Wisconsin outwash sediments in Wabash Valley, Indiana, variation in 73
Pebbles, clay, Johore, Malaya, occurrence and origin of 437
Pebbles, phosphatic, from Brightseat Formation, Maryland 546
Peckham, Alan E., article by 52
Pennsylvanian cave filling and breccia in Mississippian St. Louis Limestone, Putnam County, Indiana 275
Pennsylvanian, late, and early Permian, Glass Mountains, Texas, limestone petrology, carbon isotope distribution 231
Permian, early, and late Pennsylvanian, Glass Mountains, Texas, limestone petrology, carbon isotope distribution ... 231
Petrographic features of sandstone that affect their suitability for road material 372
Petrography, discriminating between refractory and non-refractory quartzite. 530
Petrography of northeastern Lake Michigan bottom sediments 402
Petrography of reef, Beaverhill Lake Formation, Upper Devonian, Swan Hills area, Alberta, Canada 497
Petrography of the Teays-Mohomet Valley deposits 456
"Petrology of the Fountain and Lyons Formations, Front Range, Colorado," review of 637
Phenomena, colloid, in sedimentation of argillaceous rocks 560
Phi units, measurements of grain size 608
Phosphatic pebbles from the Brightseat Formation of Maryland 546
Pipes, sandstone-plugged, Lower Old Red Sandstone, Shropshire, England 325
Pipette and hydrometer methods, comparative efficiencies of size analysis by 96
Pleistocene, remanent magnetism in silts from North America 448
Pollack, Jerome M., article by 15
Porosity, median size, and sorting coefficients of synthetic sands, relationships between 467
Porosity, synthetic sands, median size, sorting coefficients, relationships between. 467
Post-Sangamonian(?) calcareous spring deposits, Wellsville area, Colorado 586
Potsdam Sandstone (Cambrian) of New York, composition, grain size, roundness, and sphericity of the 5
Power, W. Robert, Jr., article by 603
Price, W. Armstrong, and Kornicker, Louis S., article by 245
Primary structures in anhydrite, genesis of 553
Pryor, W. A., and Glass, H. D., article by. 38
Pseudoolites and oolites, distorted 262
Putnam County, Indiana, Mississippian St. Louis Limestone, breccia and Pennsylvanian cave filling in 275

Quartzite, discriminating between refractory and non-refractory types by quantitative petrography 530

Rangia cuneata Gray and *Crassostrea virginica* (Gmelin), occurrence in Sabine Lake, Texas-Louisiana 627
Rapid determination of calcite-dolomite ratios in sedimentary rocks 130
Recent carbonate sediments, Florida Keys, variations of strontium-calcium ratios and magnesium contents in 336
Records and activities, S.E.P.M. 301, 487
Red beds, ferric oxides as paleomagnetic data 296
Reef, Great Barrier, Heron Island Reef, carbonate sedimentation on 215
Reef petrography in the Beaverhill Lake Formation, Upper Devonian, Swan Hills area, Alberta, Canada 497
Reeves, C. C., Jr., article by 586
Refractory and non-refractory quartzite, discrimination by quantitative petrography 530
Regenerated anhydrite redefined 611
Relations of settling velocity of sand sized spheres and sample weight 101
Relationships between porosity, median size, and sorting coefficients of synthetic sands 467
Remanent magnetism in silts of Pleistocene age from North America 448
Replacement in joints 478
Riggs, Elliott A., review by 639
Riley, Charles M., and Byrne, John V., article by 553
River channel sands, South Canadian River, New Mexico, Texas, and Oklahoma, significance of compositional and textural properties of 15
River, dune, and beach sands, distinction by textural characteristics 514
Road material, sandstones, petrographic features affecting their suitability 372
Rocks, argillaceous, colloid phenomena in sedimentation of 560
Rocks, carbonate, analysis for calcium, magnesium, iron, and aluminum with EDTA 113
Rocks, carbonate, separation of clay minerals, by using acid 123
Rocks, carbonates, cyclic bedding, South-Central France 453
Rocks, cyclic bedding in carbonate, South-Central France 453
Rocks, sedimentary, calcite-dolomite ratios, rapid determination of 130
Rogers, John J. W., and Head, William B., article by 467
Ross, Charles A. and Oana, Shinya, article by 231
Roundness, grain size, sphericity, and composition of Potsdam Sandstone, New York 5

S.E.P.M., "A Traverse of Post-Avis Cisco Rocks, Brazos Valley, North Central Texas," review of 485
S.E.P.M., membership list 137
S.E.P.M., records and activities 301, 487
Sabine Lake, Texas-Louisiana, occurrence of *Rangia cuneata* Gray and *Crassostrea virginica* (Gmelin) in Sabine Lake, Texas-Louisiana 627
St. Louis Limestone, Mississippian of Indiana, breccia and Pennsylvanian cave fillings in 275
Salt extraction process, Inagua, Bahamas, early diagenetic dolomite associated with 473
"Salt Marshes and Salt Deserts of the World," review of 637
Sample splitter, a non-laminated miniature 471
Sampling of sediment without wire and winch, the free-corer 627
Sand, field method for sieve analysis 631
Sand sized spheres and sample weight, relations of settling velocity of 101
Sanders, John E., review by 135
Sands, beach and dune, distinguishing between 196
Sands, dune, beach, and river, distinction by textural characteristics 514
Sands, shallow marine, size distribution characteristics, Cape of Good Hope, South Africa 256
Sandstone-plugged pipes in the Lower Old Red Sandstone on Stropshire, England 325
Sandstone, Potsdam (Cambrian) of New York, composition, grain size, roundness, and sphericity of the 5
Sandstones, central California, genetic relationship among Tertiary blue sandstones in 594
Sandstones, petrographic features affecting suitability for road material 372
Santa Rosa-Cortes ridge, submarine geology of 534
Schmoll, Henry R., and Bennett, Richard H., note by 617
Sediment sampling without wire and winch, the free-corer 627
Sedimentary rocks, calcite-dolomite ratios, rapid determination of 130
Sedimentation, argillaceous rocks, colloid phenomena in 560
Sedimentation, carbonate, Heron Island Reef, Great Barrier Reef 215
Sedimentation pattern of Talchir series, Burhai Gondwana Basin, Bihar, India 63
Sediments, carbonate, mineralogy and early diagenesis 358
Sediments, lake, petrography of bottom sediments, Lake Michigan 402
Separation of clay minerals from carbonate rocks by using acid 123
Settling velocity of sand sized spheres and sample weight, relations of 101
Shale and clay, thin sections of 131
Shepard, Francis P., and Young, Ruth, article by 196
Shoals, offshore, in area of energy deficit 87
Shropshire, England, sandstone-plugged pipes in Lower Old Red Sandstone 325
Shvetsov's "Genetic classification of limestones" and Teodorovich's "Structural classification of limestones and dolomites," comments on 611
Siegel, Frederic R., article by 336
Sieve analysis of sand, field method for 631
Significance of compositional and textural properties of South Canadian River channel sands, New Mexico, Texas and Oklahoma 15
Silts, Pleistocene North America, remanent magnetism in 448
Silts, remanent magnetism, in Pleistocene North America 448
Size analysis by hydrometer and pipette methods, comparative efficiencies of 96
Size distribution characteristics of shallow

marine sands from the Cape of Good Hope, South Africa 256
Slumps, submarine 343
Smith, F. G., and Weber, J. N., note by ... 130
Smith, Ned M., Sunderman, Jack A., and Melhorn, Wilton N., article by 275
Society records and activities: see S.E.P.M.
Solution breccias, evaporite, Mississippian, southwest Montana 189
Sone Valley, Mirzapur District, Uttar Pradesh, India, authigenic tourmaline and zircon in Vindhyan formations 482
Sorting and by-passing process, a flotation phenomenon 476
Sorting coefficients of synthetic sands, relationships between porosity, median size, and 467
South Africa, Cape of Good Hope, size distribution characteristics of shallow marine sands 256
South Canadian River channel sands, New Mexico, Texas, and Oklahoma, significance of compositional and textural properties of 15
South-Central France, cyclic bedding in *carbonate rocks* 453
Sphericity, grain size, roundness, and composition of Potsdam Sandstone, New *York* 5
"Spiral motion of fluids," review of 134
Spring deposits, calcareous, post-Sangamonian(?), Wellsville area, Colorado. 586
Spring domes developed in limestone 288
Stanleyville, Congo, montmorillonite–analcime association in Stanleyville series 293
Stehli, Francis G., and Hower, John, article by 358
Sternberg, R. W., and Creager, Joe S., *article by* 96
Stewart, John C., article by 453
Stratigraphic units, simplified method for determining relative energies of deposition 291
Strontium-calcium ratios and magnesium contents in Recent carbonate sediments, Florida Keys, variations of ... 336
Structures in anhydrite, genesis of primary 553
Submarine geology of the Santa Rosa-Cortes ridge 534
Submarine slumps 343
Sunderman, Jack A., Melhorn, Wilton N., and Smith, Ned M., articles by 275
Swan Hills area, Alberta, Canada, reef petrography of Beaverhill Lake Formation, Upper Devonian 497
Synthetic sands, relationships between porosity, median size, and sorting coefficients 467

Talchir sedimentation in Burhai Gondwana *Basin, Bihar, India*, pattern of 63
Tanner, William F., article by 87
Tanner, William F., note by 634
Tanner, William F., reviews by 133, 134
Teays-Mohomet Valley deposits, petrography of 456
Teodorovich's "Structural classification of limestones and dolomites" and Shvetsov's "Genetic classification of limestones," comments on 611
Terasmae, J., and Harrison, W., article by 448
Tertiary blue sandstones in central California, genetic relationship among 594
Tertiary-Cretaceous clay mineralogy of Upper Mississippi Embayment 38
Texas, Glass Mountains, limestone petrology, carbon isotope distribution, late Pennsylvanian and early Permian 231
Texas, Gulf Coast, marine and lagoonal deposits, clay dunes 245
Texas-Louisiana, Sabine Lake, occurrence of *Rangia cuneata* Gray and *Crassostrea virginica* (Gmelin) in 627
Texas, South Canadian River channel sands, significance of compositional and textural properties of 15
Textural and compositional properties of *channel sands, South Canadian River*, New Mexico, Texas, and Oklahoma, significance of 15
Textural characteristics of dune, beach, and river sands 514
The flotation phenomenon—a by-passing and sorting process 476
The free-corer: sediment sampling without wire and winch 627
"The Sea Off Southern California, A Modern Habitat of Petroleum," review of. 639
Thin sections of clay and shale 131
Tourmaline and zircon, authigenic, Vindhyan formations of Sone Valley, Mirzapur *District, Uttar Pradesh, India*. 482
Tourtelot, Harry A., note by 131

Uchupi, E., article by 534
Uttar Pradesh, India, authigenic tourmaline and zircon in the Vindhyan formations of Sone Valley, Mirzapur District 482

Valley, Teays-Mohomet, petrography of deposits 456
Van Houten, Franklyn B., note by 296
Variation in pebble composition of Wisconsin outwash sediments in the Wabash Valley, Indiana 73
Variations of Sr/Ca ratios and Mg contents in Recent carbonate sediments of the *northern Florida Keys area* 336
Vernet, Jean-Pierre, note by 293
Vindhyan formations of Zone Valley, Mirzapur *District, Uttar Pradesh, India*, authigenic tourmaline and zircon in .. 482
Visher, Glenn S., note by 291

Wabash Valley, Indiana, variation in pebble composition of Wisconsin outwash sediments in the 73
Weber, J. N., and Smith, F. G., note by ... 130
Wellsville area, Colorado, post-Sangamonian(?) calcareous spring deposits. 586
White, W. Arthur, article by 560
Wiesnet, Donald R., article by 5
Wigley, Roland L., article by 165
Williamson, Iain, note by 288
Wisconsin outwash sediments in the Wabash Valley, Indiana, variation in pebble composition of 73
Wolf, Karl H., note by 476
Wood, G. V., article by 530
Wyoming, Big Horn Mountains, mechanical analysis and heavy minerals, Morrison and Cloverly Formations .. 571

Yedlosky, Robert J., and Dean, John R., article by 372
Young, Ruth, and Shepard, Francis P., article by 196

PUBLICATIONS OF
THE SOCIETY OF ECONOMIC PALEONTOLOGISTS AND MINERALOGISTS

A Division of
The American Association of Petroleum Geologists

JOURNAL OF PALEONTOLOGY (published jointly with the Paleontological Society).

Price list of available issues on request.

JOURNAL OF SEDIMENTARY PETROLOGY

Price list of available issues on request.

SPECIAL PUBLICATION NO. 1: BIBLIOGRAPHY OF OTOLITHS (Out of print.)

SPECIAL PUBLICATION NO. 2: TURBIDITY CURRENTS AND THE TRANSPORTATION OF COARSE SEDIMENTS TO DEEP WATER. (Out of print.)

A symposium. October, 1951. Pp. iv-107; figs. 60. Price, $2.75 ($2.25 to members of S.E.P.M.).

SPECIAL PUBLICATION NO. 3: FINDING ANCIENT SHORELINES

A symposium with discussions. December, 1955. Pp. iv-129; figs. 57. Price, $3.00 ($2.50 to members of S.E.P.M. and A.A.P.G.). Out of print.

SPECIAL PUBLICATION NO. 4: RECENT MARINE SEDIMENTS

A reprint with addition. September, 1955. Pp. i-lvi and 1-736; figs. 139. Index. Price, $5.00 ($4.00 to members of S.E.P.M. and A.A.P.G.). Out of print.

SPECIAL PUBLICATION NO. 5: REGIONAL ASPECTS OF CARBONATE DEPOSITION

A symposium with discussions, February, 1957. Pp. iv-188; figs. 66; 22 full tone plates. Price, $4.50 ($3.50 to members of S.E.P.M. and A.A.P.G.). Out of print.

SPECIAL PUBLICATION NO. 6: INDEX TO THE JOURNAL OF SEDIMENTARY PETROLOGY

Volumes 1-26 (1931-1956), 1958. Price, $1.50 ($1.25 to members of S.E.P.M.).

SPECIAL PUBLICATION NO. 7: SILICA IN SEDIMENTS

A symposium with discussions, March 1959. Pp. v-185. Price, $5.00 ($4.00 to members of S.E.P.M. and A.A.P.G.).

SPECIAL PUBLICATION NO. 8: INDEX TO THE JOURNAL OF PALEONTOLOGY

Volumes 1-25 (1927-1951), 1961. Price, $8.00 ($6.50 to members of S.E.P.M., A.A.P.G., and P.S.).

SPECIAL PUBLICATION NO. 9: TAXONOMIC NOTES ON BRADY'S FORAMINIFERAL PLATES, CHALLENGER REPORT

1960, 238 pp. including 115 pls. Price, $8.50 ($7.00 to members of S.E.P.M., A.A.P.G., and P.S.).

Please send orders to:

S.E.P.M. Box 979, Tulsa 1, Oklahoma

Ex-British Government GEOLOGICAL INSTRUMENTS, ETC.

LIQUID PRISMATIC COMPASS

(SERVICE PATTERN MARK III)

Precision pocket instrument engraved 0-360° in one degree divisions. The mother-of-pearl dial is suspended in non-freezing liquid. Adjustable magnifying prism. Well-made hinged case of 2 in. diameter. Net Weight 11 oz. Current cost approx. $36.40.
With Web Case.
Post and Packing 50 cents **$11**

SIGHTING PLANE TABLE ALIDADES

An extremely well-made instrument constructed of Phosphor Bronze fitted with sighting vanes and parallel rule attachment. Length 18 in. Net weight 2½ lb. In polished wood container, all in new condition. Fraction of cost.
Post and Packing $1.75 **$5**

EX-M.O.S. SURVEYING RANGEFINDERS

Coincidence type. Base 80 cm. Range 250-10,000 yards. Good serviceable condition. Current cost approx. $420.08. Tripod can be supplied as an extra. Freight Forward **$34**

ANY ITEM ON
14 DAYS' APPROVAL

INDIAN CLINOMETERS

Base 9½ in. Ministry release at fraction of cost. New and unused. With Leather Case. Post and Packing $1.75 **$10.50**

Ex-Govt. 6 X 30 PRISMATIC BINOCULARS by Taylor Hobson. Guaranteed 5 years.
$21.70
Post & Packing $1.60

CHARLES FRANK LTD.

67-75 SALTMARKET,
GLASGOW, C.I.
SCOTLAND

ESTABLISHED 1907 *SEND FOR ILLUSTRATED CATALOGUE*

7680-8-2

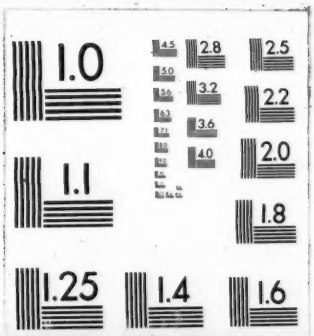
1.0
1.1
1.25
1.4
1.6
2.8
3.2
3.6
4.0
2.5
2.2
2.0
1.8